UNIVERSIDAD COMPLUTENSE DE MADRID

FACULTAD DE MEDICINA

DEPARTAMENTO DE FISIOLOGÍA

TESIS DOCTORAL

Functional study about the circuits underlying emotional processing of the visual scene in humans

MEMORIA PARA OPTAR AL GRADO DE DOCTOR

PRESENTADA POR

Constantino Méndez-Bértolo

DIRECTORES

Bryan Strange
Stephan Moratti

Madrid, 2017

UNIVERSIDAD COMPLUTENSE DE MADRID

FACULTY OF MEDICINE
DEPARTAMENT OF PHYSIOLOGY

Functional study about the circuits underlying emotional processing of the visual scene in humans

PhD Thesis

Constantino Méndez-Bértolo

Advisors

Bryan Strange y **Stephan Moratti**

MADRID
2015

UNIVERSIDAD COMPLUTENSE DE MADRID

FACULTAD DE MEDICINA
DEPARTAMENTO DE FISIOLOGÍA

Estudio funcional de los circuitos para el procesamiento emocional de la escena visual en humanos

Trabajo de investigación que presenta
Constantino Méndez-Bértolo
Para la obtención del Grado de Doctor

Bajo la dirección de los doctores
Bryan Strange y **Stephan Moratti**

MADRID
2015

Con todo mi amor, a mi familia

Resumen

En la introducción de este trabajo se expone el conocimiento actual acerca de las proyecciones visuales talámicas subcorticales ('Low Road") y corticales ("High Road") con énfasis en los debates sobre la facilitación para el procesamiento de estímulos emocionalmente relevantes de la primera vía ("Low Road Hypothesis") y la participación integrada de áreas de alto y bajo nivel jerárquico para la construcción de representaciones mentales ("cierre perceptivo") en la segunda. Asimismo, se explica el interés de esta tesis dado que actualmente no existe evidencia funcional directa en humanos que respalde la hipótesis de que la información obtenida por la amígdala a través del núcleo pulvinar sea suficiente para generar una señal de alarma en ausencia de inputs corticales a la par que hay una carencia de evidencias matemáticas basadas en datos fisiológicos a favor de modelos corticales de procesamiento visual recurrente en oposición a los modelos clásicos de procesamiento jerárquico serial.

Los objetivos del presente texto serán tratar de arrojar luz sobre ambas cuestiones e hipótesis. Para ello emplearemos metodologías propias de la fisiología y la psicología. Para responder a la primera pregunta (Experimentos 1 y 2) como unidad de medida emplearemos registros con electrodos intracraneales implantados en la amígdala y el giro fusiforme de pacientes epilépticos (Experimento 1) y registros magnetoencefalográficos (Experimento 2). La tarea principal de ambos experimentos será un juicio de género ("hombre vs. mujer") empleando retratos de caras con expresiones emocionales neutras, de alegría y de miedo. La manipulación crítica experimental consistirá en presentar dichas imágenes de manera naturalista o mediante filtros que excluyan sus componentes espaciales

de alta o baja frecuencia, sirviéndonos para responder a nuestra hipótesis de la particularidad diferencial de las neuronas magnocelulares que componen la vía talámica subcortical ya que no transportan información de alta frecuencia. En el Experimento 1 también emplearemos una tarea secundaria de discriminación "interior-exterior" con imágenes de escenas visualmente complejas neutrales y extremadamente desagradables. Para responder a la segunda cuestión (Experimento 3) utilizaremos de nuevo registros magnetoencefalográficos y una tarea de discriminación de "cara-no cara" usando estímulos bidimensionales ambiguos ("Mooney faces")

Los resultados recogidos en esta tesis se pueden resumir de la siguiente manera. Los potenciales de acción local (Experimento 1) registrados en la amígdala muestran una respuesta emocional entre 70-110 ms específica para las caras de miedo y dependiente de la presencia de componentes de baja frecuencia espacial en la imagen. Dicha respuesta temprana no se encuentra para las imágenes visuales complejas de escenas desagradables ni en la actividad del giro fusiforme, aunque tanto la amígdala como éste muestran respuestas emocionales independientes de la frecuencia espacial en ventanas de tiempo posteriores. Estos datos, que apoyan la hipótesis de la "Low Road" suponen una aportación novel a la literatura y como tal son discutidos en la discusión. En el Experimento 2 encontramos una modulación con la misma especificidad y similarmente temprana (~80 ms) en la corteza parietal y el cuneus. Ésta observación también es novel y en la discusión sugerimos que puede tratarse del efecto indirecto de la activación de la vía subcortical dado que ambas regiones reciben proyecciones magnocelulares de la amígdala. En dicho experimento, también localizamos las fuentes neurales responsables del procesamiento de una cara en cada una de las etapas caracterizadas por los campos magnéticos evocados: corteza estriada y extraestriada seguida del cortex laterooccipital y cortex ventrotemporal. En el Experimento 3 localizamos las fuentes responsables del fenómeno de cierre perceptivo ("perceptual closure") en las cortezas occipital y parietal así como el giro fusiforme mediante el análisis de la actividad gamma, que refleja actividad síncrona y comunicación a larga distancia. Mediante modelado dinámico causal, demostramos que el modelo que explica con mayor probabilidad la comunicación entre las tres áreas es aquel que incluye proyecciones bidireccionales entre la corteza visual y ambas estructuras jerárquicamente superiores.

Por tanto, concluimos existe evidencia a favor de la hipótesis de la "Low Road" en humanos así como a favor de la necesidad de comunicación bidireccional entre áreas visuales de alto y bajo nivel jerárquico para mantener la representación perceptiva. Además del interés para la neurociencia básica de ambas conclusiones, la primera observación es de especial importancia clínica para nuestra comprensión de diversas patologías afectivas como la ansiedad o el estrés postraumático así como para la explicación de modulaciones emocionales en fenómenos como la visión ciega o el síndrome de heminegligencia.

Abstract

In this work's introduction we detail the current knowledge about the subcortical ("Low Road") and cortical ("High Road") thalamic projections with special focus on the current controversies about the facilitation for processing of biologically relevant along the first route ("Low Road Hypothesis") and the integrated participation of hierarchically high- and low- level structures for the elaboration of mental representations ("perceptual closure"). It is also explained the interest of this thesis given that there is currently no direct functional evidence in humans that supports the hypothesis that the information obtained by the amygdala through the pulvinar nucleus is enough to trigger an alert mechanism in absence of cortical inputs while at the same time there is a lack of mathematical evidence based on physiological data that supports recursive models of visual processing as opposed to serial hierarchical feedforward push of classic models.

The objectives of the present work are shed ding light over both issues and Hypothesis. We will employ for that methodologies pertaining to physiology and psychology. To answer the first question (experiments 1 and 2) we will employ as measure unit intracranial recordings of patients implanted with electrodes in the amygdala and the fusiform gyrus (Experiment 1) and magnetoencephalographic recordings (Experiment 2). The main task of both experiments will be a gender judgment task ("man vs. woman") employing face portraits with fearful, happy or emotionally neutral facial expressions. A critical experimental manipulation will consist on presenting said pictures in naturalistic from (broadband) or filtered to exclude either their low or high spatial frequency components, taking advantage of the differential properties of the magnocellullar neurons

that compose the subcortical pathway and cannot carry high spatial frequency components. In Experiment 1 we will also employ a secondary task of indoor-outdoor judgment with complex visual scenes of neutral or extremely unpleasant contents. To answer the second question (Experiment 3) we will employ again magnetoencephalographic recordings and a face-non face discrimination task with bidimensional ambiguous stimuli ("Mooney faces")

The results gathered in this thesis can be summarized the following way. The local field potentials (Experiment 1) recorded at the amygdala show an early emotional response between 70-100 ms specific for fearful faces and dependent on the presence of low spatial frequency components in the picture. Such an early response is not found for complex visual scenes of unpleasant nature or in the fusiform gyrus, albeit the amygdalae as well as the later show emotional responses independent of the spatial frequency in following time windows. These data, supporting the Low Road hypothesis, represent a novel contribution to the literature and as such they are discussed in the conclusions. In Experiment 3 we found a modulation with a similar specificity and latency (~80 ms) at parietal cortex and cuneus. This is also a novel observation and we suggest in the discussion that it may be an indirect effect cause f the activation of the subcortical pathway, given that both structures receive magnocellullar inputs from the amygdala. In said experiment, we localize the neural sources sustaining the processing of a face at each stage characterized by the evoked magnetic fields: striate and extrastriaste cortex, laterooccipital cortex and fusiform gyrus. In Experiment 3 we localize the neural sources related with the perceptual closure process at the fusiform gyrus and the occipital and parietal cortex via analysis of the power in the gamma band that indexes synchronous activity and long-range communication. Employing dynamic causal modelling, we show that the model that best explains the nature of the communication between those three areas is the one that included feedback as well as forward projection between the visual cortex and hierarchically higher structures.

Therefore, we conclude there is evidence supporting the hypothesis of the "low Road" in humans as much as the necessity of bidirectional communication between hierarchically high- and low- level areas to sustain the percept. Besides the interest of these conclusions for basic neuroscience, the first one pose special clinical interest for our comprehension of several affective pathologies such anxiety or posttraumatic stress disorder as much as the explanation of emotional modulations observed in phenomenon such as blindsight of neglect.

Content Index

Index of Figures

Index of Tables

Acronyms

ANOVA	Analysis of Variance
BSF	Broadband Spatial Frequency
BOLD	Blood Oxygen Level Dependent
CT	Computerized Tomography
CM	Centimeter
DCM	Dynamic Causal Modelling
EEG	Electroencephalography
eRMF	Event-Related Magnetic Field
Exp	Experiment
fT	Fentotesla
FFA	Fusiform Face Area
GHQ	General Health Questionnaire
HSF	High Spatial frequency
HARS	Hamilton Anxiety Rating Scale
HDRS	Hamilton Depression Rating Scale
HR	Hour
IAPS	International Affective Picture Set
iEEG	Intracranial Electroencephalography
iERP	Intracranial Event-Related Potential
IQ	Intelligence Quotient
fMRI	Functional Magnetic Resonance
ISI	Inter Stimulus Interval
LCMV	Linearly Constrained Minimum Variance
LFP	Local Field Potential
LOC	Lateral Occipital Cortex
LSF	Low Spatial Frequency
MANOVA	Multivariate Analysis of Variance
MEG	Magnetoencephalography
MNI	Montreal Neurological Institute
MRI	Magnetic Resonance
MS	Millisecond
μυ	Microvolt
OFA	Occipital Face Area
P	Probability
pAm	Picoamperometer
PLV	Phase-Locking Values
pT	Picotesla
SC	Superior Colliculus
sEEG	Stereotactic Electroencephalography
SEM	Standard Error Mean
SF	Spatial Frequency
STS	Superior Temporal Sulcus
V-EEG	Video Electroencephalography
VEP	Visual Evoked Potential
WAIS	Wechsler Adult Intelligence Scale

Resumen extendido

El presente trabajo pertenece al área de la neurociencia del procesamiento visual humano. Describiremos tres estudios experimentales que aportan nuevos datos con los que trataremos de responder dos preguntas principales: ¿permite la vía subcortical tálamo-amygdalar la rápida detección de señales indicadoras de peligro en la escena visual? y, ¿necesita el proceso de creación de perceptos ("cierre perceptivo") de la participación conjunta de áreas visuales de alto y bajo nivel jerárquicos?

Las neurociencias tratan de explicar el funcionamiento del cerebro. Es una rama joven y creciente de la medicina que se beneficia de la unión de conocimientos científicos interdisciplinarios. Hemos recabado datos en forma de actividad electro (EEG) y magnetoencefalográfica (MEG) proveniente de pacientes epilépticos y sujetos sanos realizando tareas visuales diseñadas para indagar en dichas cuestiones. Por tanto, navegaremos por las aguas de la fisiología y la psicología, así como de la física y las matemáticas en última estancia (para procesar y analizar la señal).

Ambas preguntas tienen que ver con como nosotros (o mejor dicho, el cerebro) damos sentido al mundo. La primera pregunta forma parte de un largo debate todavía vigente principalmente a causa de la falta de evidencia directa en humanos. Consideremos cómo el cerebro ha evolucionado: el neocortex, una estructura reciente en términos filogenéticos, es donde la mayoría de nuestras habilidades cognitivas superiores residen. Por ejemplo, el lóbulo occipital es excelente a la hora de procesar detalles de la escena visual (hoy por hoy ningún algoritmo desarrollado por humanos puede igualar la capacidad para

reconocer patrones del cerebro humano). Sus inputs visuales provienen de los núcleos del tálamo en el prosencéfalo, prácticamente en el centro del cerebro, desde donde los impulsos eléctricos generados en los conos y bastones viajando a lo largo del quiasma óptico son transmitidos sobre todo a través de la subdivisión del núcleo geniculado lateral. Pero ese no es el único camino que la información visual puede recorrer. Existe una vía neural filogenéticamente más antigua que se separa en el núcleo pulvinar (otra subdivisión del tálamo) e inerva estructuras subcorticales menos recientes que el cortex, principalmente la amígdala

La literatura ha dado a las proyecciones tálamo-amigdalar y tálamo-cortical los folclóricos términos del "camino de *abajo"* y el "camino de *arriba"* (LeDoux, 1996). Éste último (cortical) contribuye a la percepción consciente de los objetos que percibimos mientras que, basándose inicialmente en estudios animales, existe la hipótesis de que la anterior (subcortical) es responsable de incrementar automáticamente la respuesta emocional (ej. en el condicionamiento aversivo) y como el mecanismo subyacente que explicaría fenómenos como la visión ciega. Ambos caminos están activos simultáneamente en individuos sanos (por ejemplo, el condicionamiento aversivo depende de ambos caminos para operar) pero hoy por hoy falta evidencia directa que apoye la "hipótesis del camino de abajo" en humanos.

Abordaremos esta controversia adquiriendo directamente actividad eléctrica intracraneal de la amígdala y el giro fusiforme de pacientes epilépticos que fueron implantados con electrodos estereotácticos mientras observan estímulos neutros y emocionales (Experimento 1). Usaremos tareas implícitas. El procedimiento experimental principal será una tarea de juicio de género empleando varios retratos de actores y actrices posando expresiones faciales de miedo, alegría y neutrales. Como manipulación experimental crítica, filtraremos con filtros pasa-baja o pasa-alta dos tercios de las imágenes con el objeto de mantener o quitar los componentes espaciales de alta (HSF) o baja (LSF) frecuencia (esto es, los cambios de luz rápidos o lentos presentes en la escena) bajo la asunción de que las células magnocelulares que componen la fibra del camino de abajo no pueden transportar la información perteneciente a las altas frecuencias espaciales. La tarea secundaria será un juicio de interior-exterior presentando imágenes de escenas complejas neutrales o extremadamente desagradables (ej. gore).

Nuestros datos aportan evidencia nueva a favor de la hipótesis del camino de abajo. Los potenciales de acción local (LFP) de las caras de miedo adquiridos en nueve amígdalas presentan un incremento temprano (~70 milisegundos; ms) que no está presente en el caso de las caras felices o neutrales. De manera crítica, esta respuesta depende de la presencia en la imagen de componentes de baja frecuencia espacial (las imágenes de caras de miedo con sólo frecuencias espaciales altas no provocaron esta respuesta); asimismo también está ausente en el caso de las imágenes de escenas complejas desagradables. Adicionalmente, las caras de miedo y de felicidad (independientemente de sus frecuencias espaciales) así como las imágenes de escenas desagradables aumentaron la actividad de la amígdala en posteriores ventanas temporales. Más aún, los LFPs registrados en siete electrodos en el giro fusiforme no mostraron actividad significativa dentro de la ventana temporal de la respuesta temprana amigdalar y la primera modulación emocional se encontró alrededor de la marca de los 170 ms.

Con el objetivo de observar la actividad cerebral a un nivel macroscópico superior repetimos la tarea de las caras con sujetos sanos registrando actividad magnetoencefalográfica (MEG; Experimento 2). Dentro de la ventana temporal de la respuesta de la amígdala (~80 ms) encontramos un incremento de la actividad específico para las caras de miedo de baja frecuencia en el córtex parietal posterior y el cúneo. No encortamos evidencia directa a favor de la hipótesis del camino de abajo en este contexto experimental (como podíamos parcialmente esperar dado que los sensores MEG son relativamente ciegos a las señales provenientes de estructuras profundas) pero especulamos que este efecto sea el resultado de inputs magnocelulares provenientes de la amígdala y por tanto consecuencia indirecta de ella.

Mientras que la primera pregunta nos situaba en los dominios de la neurociencia afectiva, la segunda cuestión está más asentada en la neurociencia cognitiva dado que se refiere a la percepción y a los procesos perceptivos per se. El procesamiento de la información visual a lo largo de la vía cortical (el camino de arriba) ha sido ampliamente estudiado. Tradicionalmente, se considera que la información viaja desde el cortex visual temprano (ej. el cortex estriado) hacia áreas multisensoriales de alto nivel (ej. el giro fusiforme) incrementándose su complejidad conforme avanza hacia delante por la jerarquía del sistema visual. Sin embargo, crear y mantener una representación mental del objeto percibido puede requerir la actividad simultánea de varias áreas distantes a lo largo del

recorrido visual. Más aún, puede ser que áreas de bajo nivel que codifican aspectos particulares de la información visual contribuyan junto con menos específicas áreas superiores de la escalera cortical tal y como los precursores de las teorías gestálticas sugirieron. Percibir "desde lo local a lo global" versus percibir "de lo global a lo local" constituye un debate todavía a día de hoy. Esto último requeriría de la existencia de vías neurales para el procesamiento en feed-back (hacia-atrás), opuesto a lo que los modelos jerárquicos tradicionales de las vías visuales proponen.

En el Experimento 2, además del efecto mencionado, también exploramos las etapas tempranas en el procesamiento visual de las caras desde el primer componente hasta la M170 (que señala el paso del procesamiento visual en el que se codifica la forma) porque podría darnos importante información sobre el mecanismo a través del cual componemos la representación de un objeto. Reconstruimos la señal MEG para encontrar sus fuentes y confirmamos que los primeros pasos del procesamiento tienen lugar en el cortex estriado del lóbulo occipital y que hay una participación del cortex latero-occipital y ventro-temporal alrededor de 90 ms similar a la que ocurre alrededor de 170 ms. De manera más interesante, encontramos que las caras de alta frecuencia espacial provocaron una M170 más extensa en el tiempo que parece tener dos fuentes -una occipital y otra extraoccipital- que ocurren consecutivamente en vez de simultáneamente como en el caso de las caras naturalistas y las de baja frecuencia espacial. A pesar de que encontramos grandes diferencias de amplitud alrededor de 120 ms que podrían haber afectado a la latencia de los siguientes componentes, también presentamos evidencia de modulación emocional del M170, lo que se suma a la controvertida literatura al respecto. Más específicamente, sólo las caras con componentes espaciales de alta frecuencia modularon la amplitud de la M170, lo que sugiere como causa el diferente tipo de información que contiene cada banda de frecuencia. Nótese que los componentes de baja frecuencia espacial forman imágenes borrosas cuyo significado puede sin embargo extraerse de manera holística mientras que las imágenes de alta frecuencia son ricas en detalles y la información está distribuida muy localmente.

Para enfrentarnos directamente a la segunda pregunta empleamos una tarea de discriminación cara-no cara usando versiones control y versiones descompuestas de un tipo de estímulos ambiguos llamados caras Mooney (Experimento 3). Se trata de imágenes bi-dimensionales (ej. en blanco y negro) donde diferentes formas son dispuestas para asemejar

una cara aunque normalmente carentes de algunos elementos. Al igual que en el Experimento 2, adquirimos datos MEG de sujetos sanos. Centramos nuestros análisis en el dominio espectral de la señal, a diferencia de los anteriores experimentos en los que exploramos los cambios de amplitud debido a nuestro interés en la dimensión temporal de los datos. Específicamente, buscamos los cambios de intensidad en la banda gamma con respecto a la línea base en el espacio sensor para posteriormente identificar el origen neural subyacente mediante reconstrucción de fuentes. Nótese que la actividad gamma se ha relacionado con el proceso de cierre perceptivo en previos experimentos y que también se sugiere que marca comunicación de largo alcance entre áreas cerebrales distantes. De acuerdo con la literatura, encontramos una respuesta en la banda gamma comenzando alrededor de 200 ms post-estímulo y sostenida durante más tiempo para las caras Mooney intactas en comparación con las caras Mooney descompuestas. De manera interesante, localizamos la red neural responsable del efecto gamma en el cortex visual temprano, el giro fusiforme y el cortex parietal. Además de la participación síncrona de áreas de bajo y alto nivel durante el proceso de cierre perceptivo proveemos más evidencia acerca de la naturaleza de la conectividad funcional de la relación entre las tres áreas. Recurriendo al modelado dinámico de causas (DCM) demostramos que junto con proyecciones hacia-delante muy probablemente tienen lugar proyecciones hacia-atrás desde el giro fusiforme y la corteza parietal hacia el cortex visual.

Extended abstract

The current work belongs to the neuroscience of human visual processing. We will summarize three experimental studies reporting novel data where we will address two main questions: ¿does the subcortical thalamo-amygdalar visual neural pathway permit the rapid detection of threat related cues in the visual scene? And, ¿does the creation of percepts (perceptual completion) require the integrated engagement of hierarchically low- and high-level visual areas?

Neurosciences try to explain brain functioning. It is a young and growing branch of medicine that benefits from the marriage of interdisciplinary expert knowledge. We gathered physiological data in the form of electro- (EEG) and magneto- encephalographic (MEG) activity of clinical epileptic patients and healthy subjects performing visual tasks designed to deep into the aforementioned questions. Therefore, we will delve into the fields of physiology and psychology and ultimately physics and mathematics – to process and analyze the signal.

Both questions have to do with how do *we* -or rather the brain, give meaning to the world. The first question is part of a long debate going on at present day mostly because of the lack of direct evidence in humans. Let's consider how the brain has evolved: the neocortex, a recent structure in phylogenetic terms, is where most of our superior cognitive abilities lay. For example, the occipital lobe excels at processing the details of the visual scene (no man-made algorithm developed yet can match the pattern recognition skill of the human brain). Its visual inputs come from the thalamic nuclei of the forebrain, almost in the center of the brain, where electrical impulses originated at the rods and cones travelling along the optic chiasm are relied mostly through the lateral geniculate nuclei subdivision.

But that is not the only *road* that visual information can traverse. There is a philogenetically older neural pathway that detours at the pulvinar nuclei (another subdivision of the thalamus) and innervates less-recent-than-cortex subcortical structures, particularly the amygdala.

Literature has given the thalamo-amygdalar and the thalamo-cortical projections the folkloric terms of the *Low* and *High* roads (LeDoux, 1996). The later (cortical) contributes to a conscious perception of the objects we perceive while, initially based on animal studies, the former (subcortical) has been hypothesized to be responsible of automatic enhancement of the emotional response (e.g. fear conditioning) and the mechanism underlying phenomenon like blindsight. Both are active simultaneously in healthy individuals (e.g. fear conditioning relies on both pathways to operate) but up-to-date direct evidence supporting the Low Road hypothesis in humans is lacking.

We will address this controversy by directly recording intracranial electrical activity of the amygdala and the fusiform gyrus of epileptic patients implanted with stereotactic electrodes watching emotional and neutral stimuli (Experiment 1). We will use indirect tasks. The main experimental procedure will be a gender judgment task employing several different portraits of actors/actresses posing fearful, happy or neutral facial expressions. As a critical experimental manipulation, we will high- or low-pass filter two thirds of the pictures to either keep or remove their high (HSF) or low (LSF) spatial frequency components (this is, fast or slow light changes present in the scene) under the assumption that the magnocellullar neurons composing the low road pathway fibers cannot carry the information pertaining to the high spatial frequencies. Our secondary task will be an indoor/outdoor judgment presenting neutral and extremely unpleasant (e.g. gore) pictures of complex scenes.

Our data provides novel support for the Low Road hypothesis. Local field potentials (LFP) to fearful faces recorded from nine amygdalae present an early (~70 milliseconds; ms) enhancement that is not present for happy or neutral faces. Critically, this response is dependent on the presence of LSF components in the picture (high spatial frequency fearful faces did not provoke an early modulation); and is absent in the case of unpleasant complex visual scenes. In addition, fearful and happy faces (independently of their spatial frequencies) as well as unpleasant scenes increased amygdala activity at later stages. Furthermore, LFP recorded at seven electrodes within the fusiform gyrus showed

no significant changes within the time window of the early amygdala response and the first emotional modulations were found in the range of ~170 ms.

In order to observe the brain activity at a more macroscopic level we repeated the face task with healthy subjects acquiring MEG data (Experiment 2). Within the time window of the amygdala response (~80 ms) we found enhanced activity specific for LSF fearful faces at posterior parietal cortex and cuneus. We did not find any direct evidence for the Low Road hypothesis with this experimental frame (as we partly expected given the relative blindness of MEG sensors to signal coming from deep structures) but we speculate this effect may be the result of magnocellullar inputs coming from the amygdala and thus indirect consequence of it.

While the first question placed us in the domains of affective neuroscience the second question is more cognitive neuroscience based as it refers to perception and perceptual processing per se. Visual processing along the cortical pathway (high road) has been widely studied. Traditionally, it is considered that the information travels from early visual cortex (e.g. striate cortex) towards multisensory high level areas (e.g. the fusiform gyrus) increasing its complexity as it pushes feed-forward into the visual system hierarchy. However, creating and maintaining a mental representation of the perceived object may require the simultaneous activity of several distant areas along the visual stream. Moreover, hierarchically lower areas that code precise aspects of visual information may be involved along with more unspecific areas higher in the cortical stairs just like early gestalt researchers suggested. From local-to-global versus from global-to-local perception constitutes a debate still nowadays. The later would require the existence of feedback processing streams unlike traditional hierarchical stream models propose.

In addition to the mentioned effect, we explored the early stages of face visual processing in Experiment 2 from the first component to the M170 (that indexes a step where structural encoding of the visual information is achieved) because it could give us valuable insights about the mechanism which we compose the representation of an object. We source localized the MEG signal and confirmed that initial processing happens at occipital striate cortex and there is an involvement of lateraoccipital and ventrotemporal cortices at around 90 ms similar to the one that occurs at ~170 ms. More interestingly, we found that HSF faces elicited longer in time M170 component that seemed to have occipital and extraoccipital sources consecutively as opposed to concomitantly like in the case of LSF and BSF faces. Although we found big amplitude differences at around 120 ms

that could have affected the latency of following components, we present evidence of emotional modulation of the M170, which sums to the controversial literature on the subject. More specifically, only faces with HSF components modulated the amplitude of the M170, suggestive of the different type of information that is conveyed for each spatial frequency band. Note that LSF components form blurry pictures whose meaning can albeit be extracted holistically while HSF pictures are rich in details and the information is locally arranged.

To specifically tackle the second question we employed a face-non face discrimination task using control and scrambled versions of ambiguous stimuli called Mooney faces (Experiment 3). These are two-dimensional (e.g. black and white) pictures where different shapes are arranged to resemble a face but commonly lacking some elements. Like in Experiment 2, we acquired MEG data from healthy subjects. We focused our analysis on the spectral domain of the signal, unlike previous experiments where we explored amplitude changes due to our interest in the temporal dimension of the data. Specifically, we explored for changes in gamma power with respect to the baseline across the scalp for later identification of the underlying neural sources via source reconstruction. Note that gamma activity has been linked with the process of perceptual completion in previous experiments and is also supposed to index long range communication between distant brain areas. In accordance with the literature we found a gamma band response starting around 200 ms post stimulus and longer sustained for Mooney faces as compared to scrambled Mooney faces. Interestingly, we localized the neural network responsible of the gamma effect at early visual cortex, fusiform gyrus and parietal cortex. In addition to the synchronous engagement of low- and high-level areas at the time of perceptual completion we provide further evidence about the functional connectivity nature of the relationship between the three areas. Recurring to dynamic causal modelling we demonstrate that feed-back projections to visual cortex from fusiform and parietal cortex do take place along with feed-forward projections.

"Oh, ye'll take the high road and I'll take the low road,
And I'll be in Scotland afore ye."

The Bonnie Banks o' Loch Lomond
Traditional Scottish song.

1 Introduction

Affective neuroscience's field of study is vast; its interlacement with cognitive neuroscience perhaps infinite. Partly due to historical reasons (Cacioppo and Gardner, 1999a) emotion has been treated like a fundamental process separate from traditional processes: memory, attention, language, perception, action, etc. However, emotion permeates these so-called *cognitive* processes. While some of them, or some of their stages at least, can be attributed to distinctive neural substrates, emotional involvement can affect processing at many neural levels. This is illustrated by the abundance of literature that focuses on emotion and its many interactions with cognitive processes (Cohen, 2005). It is like a mesh that connects perception and action; there are brains structures considered eminently emotional (e.g.: the amygdala) albeit with large connectivity patterns (Pessoa, 2008) that link anterior, posterior and subcortical areas globally. There are multiple direct connections from and to the amygdala (and extended amygdala; Alheid, 2003) with cortical and subcortical structures (Aggleton, Burton, Passingham, 1980; Porrino, Crane and Goldman-Rakic, 1981; Mufson, Mesulam and Pandya, 1981; Aggleton, 1986; Suzuki, 1996; GhashghaeiI and Barbas, 2002; Amaral and Behniea, 2003; Morecraft et al., 2007).

Therefore, to define affective neuroscience without leading into reductionist overkill can leave us with a rather ambiguous description: the branch of neuroscience that tries to explain the interplay between emotions and the brain mechanisms that give meaning to the world and articulate a response. But there are no –it seems, platonical emotions waiting to modulate *perceptions* and *responses*. Emotion itself is the perception, and the response. Indeed, the word emotion means "move out", as it derives from the Latin forms *movere* (-"to move") and *ex* (-"outside"). At the same time, reacting towards a certain event efficiently in Darwinist terms requires the processing of outside and inside

information. Emotions are ingrained in the very mechanism that give meaning to the world we create as much as it is part of the subjective experience that may come along the response.

The theory of evolution states that every aspect of the organisms, be it physical or behavioral, adapts to the environment through natural selection. Hence, affective *processing* as much as affective *responses* had changed according to evolutionary laws of adaptation along a species evolution. Therefore, emotion per se was been a subject of study since the foundation of the still current evolutionary paradigm. However, the behavioral component of emotion was the only thing that could be studied until the coming of modern neuroimaging techniques. This shift facilitated the collection of observations about the underlying mechanisms of emotion as a neurocognitive process that relates with most brain mechanism from perception to response in operative form.

One of the main aspects of the emotional response is its expression. Events cause a cascade of autonomous reactions that ideally prepare the organism to offer the best reaction. Classic fight-or-flight behavior (Cannon, 1932) that is present across species illustrates the relationship between emotion and bodily changes. In the present example, the latter are originated due to the release of adrenalin that induces a pattern of activity of the sympathetic system. For social beings, those changes perform a secondary communicative function; alerting of dangers and informing the other members of the group about the inner state and motivations. The idea that these automatic physiological responses and bodily changes are adaptive and serve both a motivational and a communicative function was already present in Darwin's work, who dedicated a single book to the subject (Darwin, 1872; see Darwin, 2002 for a re-edition; Figure 1.1).

Figure 1.1. Darwin's illustration of animal/human emotional expressions.

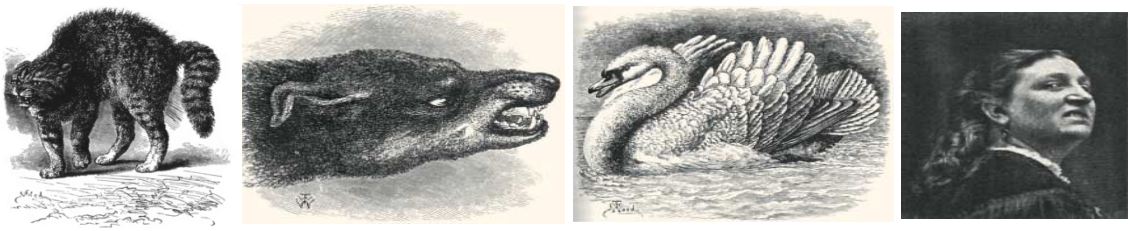

Darwin dedicated part of his efforts to ellucidate the relationship between inner state expressions and evolution. Illustration taken from "*The Expression of the Emotions in Man and Animals"* (Darwin, C., 1872)

Darwin though that emotional expressions were part of an adaption that evolved not only to prepare the organism for action but also to outwardly manifest the inner state. Hence emotional expressions were hereditary and evolved by natural selection (Hess and Thibault, 2009). As much of his work, he based his assumptions about emotional expression on observations. He thought facial expressions were spontaneous. He established parallelisms between emotion expressions in animals and his ancestors, including humans; describing correlates of facial expressions that seemed to be consistent across species, like frowning and showing the teeth similarly correspond to rage across species. He speculated about an inherent relationship between emotion and facial expression and stated that differences in facial musculature are the only source of differences in facial expression across species. By observing infant children and humans of different cultures, he also anticipated the notion of universality on emotion facial expression in humans.

Of course, his scientific study of facial expression of emotion was focused on its function, as he studied the response and could say little about the mechanism underlying such processes: when and how emotional expressions are created. But current models of emotion expression and cognition are still influenced by his work (Ekman, 2006). One of the initial aims of such models of emotion was to describe the simple variants of it, the basic emotions, which would represent a precise set of reactions serving a specific motivational and informative function. Since then, much research has been done focusing on facial muscular activation and facial expression recognition transculturally, and six (Figure 1.2) are the emotions considered basic: fear, anger, disgust, sadness, happiness and surprise (Ekman, 1976, 1992).

They are called *basic* not only in the sense of being unique but also because they arise from fundamental life tasks and thus they are at some level innate and have evolved along with organism adaptations to the environment (Ekman, 1971). Note that four out of the six basic emotions are negative emotions. We have seen how emotions can be considered reactions that are adjusted to specific environmental stimuli. Without lessening the importance of positive emotions, from an evolutionary point of view it seems fairly more adaptive to react efficiently to events that menace individual's integrity like threats. Thus, thread-related cues such as fearful expression convey vital information and organism may have evolved to referentially process them. In humans, it has been described that

negative emotions receive increased attentional resources and generate enhanced responses in comparison with other emotionally laden stimuli (Peeters and Czapinski, 1990; Taylor, 1991), a feature called negativity bias (Cacioppo and Berntson, 1999b; Rozin and Royzman. 2001) that has been highlighted in physiological (Carretié et al., 2001; Huang and Luo, 2006) and psychological studies (Vaish et al., 2008; Williams et al., 2009) within and outside the frame of basic emotions.

Figure 1.2. Facial expressions of the six basic emotions.

From left to right: top row (anger, fear and disgust), bottom row (surprise, happiness and sadness) © Paul Ekman 1975

No doubt such a mechanism, enabling fast detection of threat related or salient enough cues, would have supposed a great evolutionary advantage. Also, it would have evolved along a species development. Hence a precursor neural network may have specialized long before we became anatomically modern though later it may overlap its functions with other systems or other areas may perform the same function in a more efficient manner. In mammals, the neocortex is phylogenetically the newest part of the brain. Assuming a certain degree of reductionism, it is best descripted using the functional wise division between posterior and anterior (Luria, 1966), that respectively are in charge of processing the inputs and organizing the output. Human perception is predominantly visual. A single lobe of the posterior brain, the occipital lobe, is fundamentally dedicated to vision, though high level cognitive representations –percepts, require further processing at other lobes and most probably the integrated collaboration of many single areas sparsely distributed. Anyhow, pattern recognition is probably the best perk of human's brain

perceptual skills and at the same time one the biggest unsolved problems in computational neuroscience.

But the refined cortical visual system is a newcomer, it coexists with older subcortical areas capable of perceptual processing to some extent that may nowadays overlap and share its function as much as continue to operate independently (even if already surpassed in performance by the newer systems). Architectonically the brain has been built from within-outwards, the cortex warped around the limbic system and the limbic system warped around the diencephalon. In regard to emotions, most of the activity related with emotion relies on the participation of medial subcortical structures. Needless to say current perspectives regard many structures of the neocortex like the insula, the cingulum or the orbitofrontal cortex as fundamental for emotional processing but the earliest models gave much importance to the medial and subcortical structures. They all attributed a great importance to the ventral regions of the brain from Cannon and Bard (Bard, 1928) to Papez (Papez, 1937) and MacLean (MacLean, 1949) that invented the term limbic system and attributed a key role in emotion regulation to the amygdala.

Presently, the theories purporting the existence of a functional system capable of fast detection of threat related cues propose that the mechanism that renders this possible depends on the phylogenetically older connection between medial structures of the brain such as the amygdala and the sensory nucleus like the pulvinar (in the thalamus) that directly innervate it. The articulation of this theory, namely the Low Road theory, corresponds to Ledoux (Ledoux, 1996: Figure 1.3).

It has been based on several animal and human evidences but so far no direct evidence in human had been shown. This mechanism is purportedly automatic and hence unconscious. At the same time, criticism and alternative theories of visual processing pathways that may as well coexist in human had been proposed, specially remarking the fact that visual processing in the cortical pathway is extremely fine and also fast (Pessoa 2013). Ultimately, visual cortical processing addresses the question of how the brain gives meaning to the world, how percepts or cognitive representations, are created and carried into awareness.

Figure 1.3. Cortical and subcortical pathways.

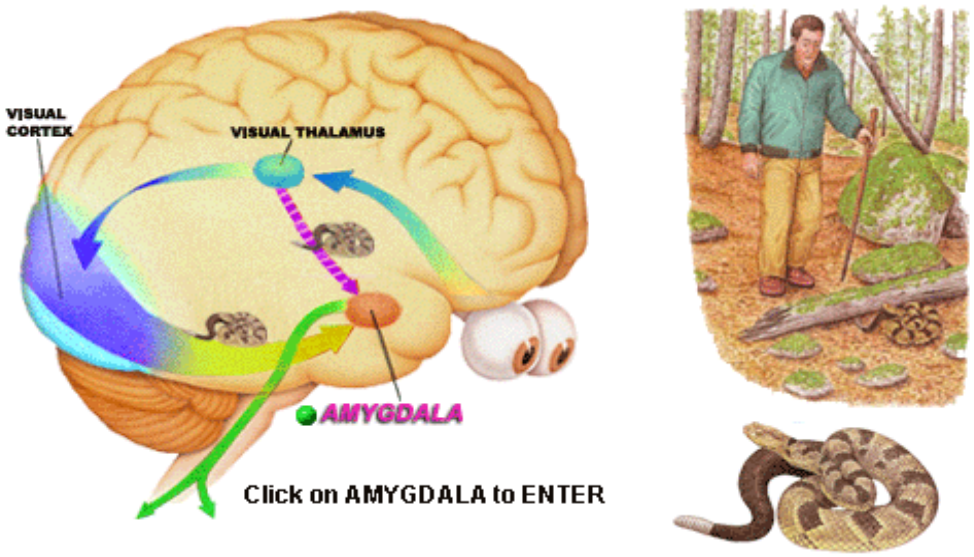

Illustration depicting the two (cortical and subcortical) pathways. Coming from the eye, information commonly travels from the nuclei of the thalamus, in the center of the brain, information travels to the occipital cortex (blue route) and it is subsequently relied to the amygdala. The subcortical pathway (red dashed route) detours at the thalamus to the amygdala bypassing cortical processing. In both cases, processing at the amygdala enables autonomous bodily reactions (green route) like the fight or flight response. Illustration based on LeDouc, J. E., 1994.

In this introduction, we will first take a look at two of the most important structures in the low road theory – the amygdala and the pulvinar nucleus of the thalamus. Then, we will discuss the feasibility and criticism around this account of emotional processing. Later, we will remember the function and organization of the cortical pathway responsible for object recognition, namely the ventral stream, focusing from the hierarchical assumptions of visual processing to the controversy around domain-general versus domain-specific characteristics. Lastly, we will speculate about the mechanism underlying the creation of percepts in conscious perception, a process so called perceptual completion, in relation with accounts of visual parallel and recursive processing alternate to classic feedforward visual processing.

1. 1 The amygdala

The amygdala is an almond shaped structure that can be found bilaterally deep inside the brain. It is composed of several different nuclei of neurons with functional and anatomical differences divided spatially, namely: cortical, medial, central and basolateral, that is as well divided into lateral and basal nuclei (Solano-Castiella et al., 2010, Carlson, 2012). One of its main defining characteristics is the extended degree up to which the amygdala is interconnected with others regions of the brain. It receives inputs from medial and cortical brain regions. For instance, information arrives from all the sensory systems to the lateral nuclei while the medial nuclei receive projections from the olfactory bulb and olfactory cortex. Within the amygdala the central nuclei main inputs come from the basolateral nuclei, that had been linked to several arousal behaviors. It is considered that memories of emotional experiences imprinted in the lateral nuclei activate specific reactions involving specific behaviors as well as autonomous changes through the connections of the central nuclei with the rest of the brain (Blair, 2001). It innervates several regions involved in somatic and autonomous functions: there are efferent projection to the hypothalamus, the dorsomedial thalamus, the thalamic reticular nucleus, the nuclei of the trigeminal nerve and the facial nerve, the ventral tegmental area, the locus coeruleus and the laterodorsal tegmental nucleus.

In its privileged sit deep inside the brain side by side with the hippocampus, it has been linked to several cognitive functions, especially the ones related with emotional (Zald, 2003, Phelps and Ledoux, 2005) and social behavior, but not only. Its role in emotional learning and memory formation has been highlighted (LeDoux, 2002) and in particular the subject of fear conditioning (LeDoux et al., 1990; Miserendino et al., 1990; Philips and LeDoux, 1992). It is considered necessary for the acquisition of fear conditioning and the mechanism proposed the long term potentiation (Maren, 1999). It has been linked to several emotional memory processes. Its activity during codification of events correlates with the level of posterior recall (Hamann et al., 1999a) enhancing the consolidation of emotionally relevant events in particular (Cahill et al., 1996) given its role in the noradrenergic system (Strange and Dolan, 2004) and its relationships with the hippocampal circuit (Richardson, Strange and Dolan, 2004) and the temporal lobe (Dolcos, LaBar and Cabeza, 2004). It has been proposed to take part in other anomaly memory issues like the recursive and intrusive memory enhancement patients with PSTD suffer (Debiec and

Ledoux, 2006) and its role in memory reconsolidation modulates the decay/sustain of the memory traces, influencing the reconsolidations or recalling of emotional events (Strange et al., 2010)

On the other hand, it has been linked to many other social functions. Critically, its role in facial expression recognition had been highlighted (Adolphs et al., 1994, Gur et al., 2002). Neuroimaging studies show its activity increases when subjects either passively see emotional faces (Whalen et al., 2001), perform an implicit task or had been explicitly asked to recognize the emotional expressions (Critchley et al., 2000, Habel et al., 2007). Masked presentation of emotional faces activates the amygdala (Whalen et al., 1998). The amygdala also shows activity when making social judgments (Bzdok et al., 2010) and it has been linked to the perception of the personal space as fMRI studies show that it is activated when subjects feel that other people are close to them (Kennedy et al., 2009).

Due to its preferential access to the information coming from the autonomous nervous system and frontal structures, its link with emotional behaviors and pathologies such as anxiety are noteworthy besides emotional learning and emotional processing. The amygdala activates when fear or negative emotions are experienced or recognized and the central nuclei of the amygdala directly innervate the hypothalamus and the brainstem, that can induce fear or anxiety related bodily reactions.

The amygdala is part of the limbic system, the medial part of the brain around which the cortex has evolved warped around. Since the very first model of emotion and cognition, it has been considered a key structure in emotional processing. It is McLean's triune model of the brain, elaborated upon Cannon-Bard (Bard, 1928) and Papez (Papez, 1937) previous models, the first to attribute a key role to it in emotional processing. MacLean's (MacLean, 1949) architectural model of the brain divides it into three subdivisions according to their evolutionary onset and function: two 'brains', the most recent neo-mammalian brain (composed by the neocortex) and the phylogenetically older old mammalian brain -that later he will call 'limbic system'- composed by the thalamus, hypothalamus, hippocampus, cingulate cortex (already considered key parts of an emotional circuit by Papez) and the amygdala both sit on the evolutionary oldest so-called 'reptilian brain' (striatal complex and basal ganglia).

Affective neuroscience's fathers suspected that the medial and inferior parts of the temporal lobe were fundamental for emotional processing thanks to mostly behavioral observations and study of clinical lesion cases. In particular, the Kluver-Bucy syndrome, where among visual agnosia and memory deficits the animals presented altered emotional behaviors like sexual hiperorality, indiscriminated hyperfagia, hypersexuality, etc. First studies completely removed the temporal lobe (Kluver and Bucy, 1937) but Weiskrantz work narrowed the damage to the amygdaloid area (Weiskrantz, 1956). These works were crucial to highlight the relationship of the amygdala with emotion, memory and learning. Nowadays, even if McLean's subdivision of the brain are helpful in understanding brain dynamics and had penetrated to a cultural level sociologically, cognitive models of emotion actually propose networks composed of several areas more or less far away in evolutionary terms as well as inside the brain. Medial and temporal structures such as the amygdala are included with phylogenetically younger areas such as the prefrontal cortex. However, lesion cases are still being used to shed light over the different roles of this multifaceted structure in emotion and cognition: emotional regulation, fear conditioning, social interaction…

In present days, there is a female *patient* known as S.M. (Adolphs et al., 1994) who's been known as the "woman *with no* fear". She presents a unique case of very local amygdalectomy (Figure 1.4). Consequently she is left unmoved by aversive stimuli like pictures of snakes or spiders, horror film clips or even real life experiences (Feinstein et al., 2011). Her ability to recognize emotional facial expressions in others (Adolphs et al., 1994) as well as social clues (Adolphs et al., 1998) is impaired. She does not have either memory consolidation facilitation for emotionally arousal material (Adolphs et al., 1997). She doesn't have a sense of personal space (Kennedy et al., 2009). However, S.M. experienced fear when inhaling carbon dioxide yet again another study simulating the subjective experience of suffocating.

Figure 1.4. SM amygdala damage.

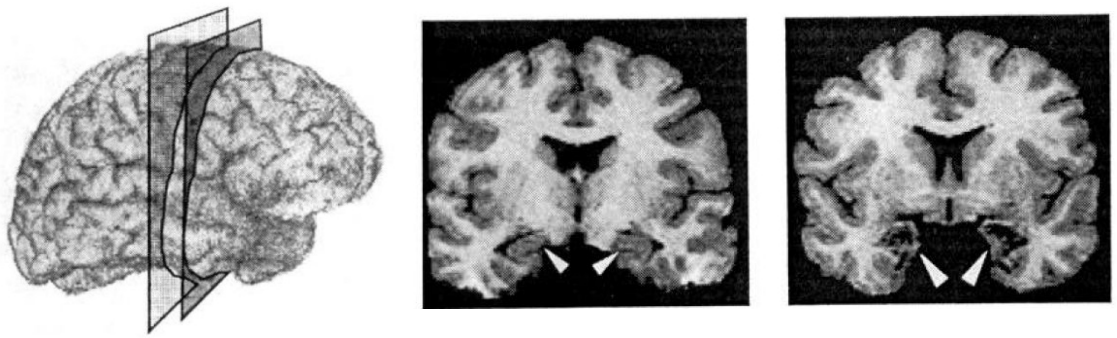

Magnetic resonance images of patient SM's brain at two planes section. Transverse planes are represented at the left. Middle and right brains show the bilateral but secluded extension of the damage, that spares cortex and hippocampus. Adolphs et al., 1994.

S.M. and other patients with bilateral and unilateral amygdala damage had been subject of numerous experiments that highlighted the role of the amygdala in experiencing emotion, specially fear, even when listening to music (Gosselin et al., 2007) as much as minimized its status as a key structure for some processes such as emotion recognition (Hamann and Adolphs, 1999b). Adolph's group showed that most subjects with amygdala damage present impaired recognition of fear and fear related emotional face expression, but not happy expressions (Adolphs et al., 1999). S.M. and a few other subjects participated in several studies. This is understandable given that this type of isolated lesions occur sparsely. But studies of lesions can only shed light on the function of a structure indirectly. The amygdala is localized deep inside the brain and hence, it is very difficult to obtain a measure of its activity with a minimum temporal certainty. While neuroimaging techniques such as fMRI or PET can detect the activity of such a deep-in structure the only way we can obtain a temporal measure of it is by implanted intracranial electrodes.

There are few studies that had localized activity in the amygdala using noninvasive MEG and source localisation algorithms but localizing activity of medial structures with above the scalp electric or magnetic measures still remains a complicated matter due to the distance to the sensors, the structures that lay between (EEG and MEG both best measure the activity of the pyramidal neurons of the cortex) and the very same constitution of the amygdala – a collection of nuclei of differently oriented neurons. We were able to overcome this fundamental problem in the present work by recording the activity from several epileptic patients implanted with intracranial stereotactic electrodes for pre surgery clinical evaluation purposes.

1.2 Thalamus and pulvinar nucleus

In primates, there are cortical and subcortical projections from the thalamus to the striatum and the amygdala (Day-Brown, 2010) respectively. This is, besides the primary visual pathway from the retina to V1 (striate cortex) through the lateral geniculate nucleus of the thalamus, associated with conscious perception, there is a philogenetically older projection that goes from the superior colliculus (SC) to the pulvinar nuclei of the thalamus (Stepniewska and Kaas, 2000) relying information to several structures cortical and subcortically, being its connection to the nuclei of the amygdala (Linke at al., 1999; Shi and

Davis, 2001) of great interest for the current work. Actually, pulvinar nuclei project as well to the striatum (Takada, 1985; Harting and Updyke, 2006; Kunzle, 2006), temporal (Berman and Wurtz, 2008; Wong et al., 2009) and parietal cortex (Stepniewska and Kaas, 1999; Lyon et al, 2010). It is noteworthy that this information comes from anatomical and physiological studies with primates like the tree shrew monkey (Day-Brown, 2010) or the macaque (Lyon et al., 2010) but also cats and even hedgehogs (Kunzle, 2006).

There are several evidences like blindsight that have lead researchers to think this subcortical thalamoamygdaloid pathway may still be functional in humans, and responsible for automatic, unconscious physiological changes and behaviors (Ledoux, 1996). Blindsight (Cowey, 2010) is the phenomenon of guided visual movements in the absence of conscious perception. It can happen when there is damage in V1. Patients are left cortically blind, but nonetheless they may show behaviors and physiological reactions stimuli related (Morris ta al., 1999). Another phenomenon called 'unseen fear' refers to the elicitation of emotional responses to normally fearful faces presented subliminally (Liddell et al., 2004, Williams et al., 2006). The mechanism underlying this effect has been attributed to this thalamo-amygdalar shortcut too (Liddell et al., 2005). Neuroimaging studies employing fMRI show that SC, pulvinar and amygdala are engaged when processing masked fearful faces (Morris et al., 1999). Yet from lesion studies, it has been seen that damage to the pulvinar nuclei impairs recognition of threatening images (Ward et al., 2005)

One of the main interests of the anatomical studies is the relationship between SC and pulvinar nucleus with oculomotor control (*e*.g. Harting et al., 2001). Pulvinar nucleus functionality still remains not well known (Day-Brown, 2010) but it has in fact been associated with spatial attention guidance and context-specific visomotor responses (Grieve et al., 2000). Again, evidence from lesional studies support this association, as damage to the pulvinar results in an impairment to coordinate movements with visual signals (Snow et al., 2009; Wilke, 2010). Also, spatial neglect, a syndrome where patients are unaware of the corresponding field of view (Vallar, 2001) may happen when there is damage at the pulvinar's target areas in parietal and temporal cortices (Verdon et al., 2010).

The pulvinar receives both a topographic and a diffuse projection from the retina via superior colliculus, but the later arrives only at the dorsal nuclei (Chomsung et al., 2008, see Figure 1.5). Moreover, it has been shown (Day-Brown et al., 2010) that both dorsal and

central nuclei project to caudate and putamen but only *dorsal* nuclei actually projects to the amygdala. This discovery led authors to outline the existence of two types of efferences from the pulvinar nucleus, different in their functionality and the type of information they carry. Assuming that pulvinar acts as a rely bypassing the information coming from the superior colliculus to striate and subcortical structures, authors propose that there is an 'specific pathway' leading to the striate areas -conveying information necessary to guide attention- and a 'diffuse pathway' innervating the amygdala carrying non topographic information useful to 'recognize' or at least able to provoke alert signals to potentially dangerous threats.

Figure 1.5. Pulvinar dorsal and ventral nuclei.

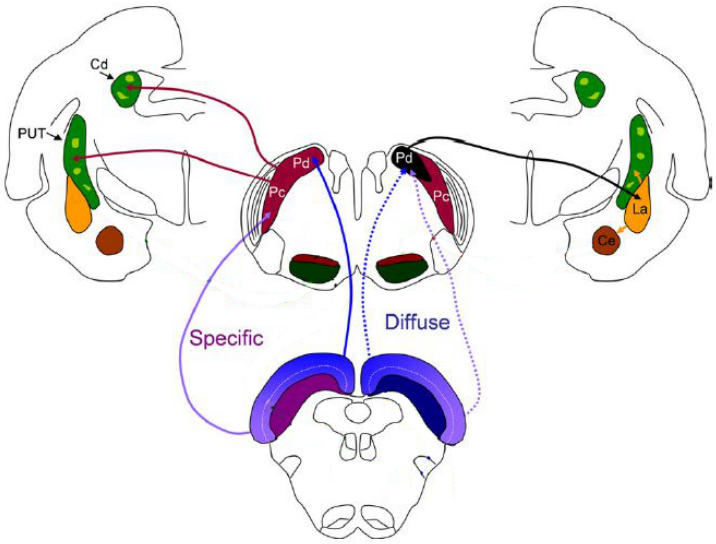

Pulvinar dorsal and ventral nuclei diferentially project to medial structures. Dorsal (Pd) and central (Pc) pulvinar nuclei receive topographic ("specific") inputs from the superior colliculus and project to Putamen (PUT) and Caudate Nucleus (Cd) but importantly, the dorsal pulvinar nuclei receive additional non-topographic ("diffuse") projections from the superior colliculus that are directed to the lateral nuclei of the amygdala (La) which ultimately projects to the central nuclei of the amygdala (Ce) enabling body changes. Adapted from Day-Brown et al., 2010.

1.3 The low road

The term low road was coined by Joseph Ledoux in its book "The Emotional Brain. The mysterious underpinnings of Emotional Life" (Ledoux, 1996). The author summarizes a brain model of emotion where emotion and cognition are conceived as interacting but separate processes and brain systems. Among other subjects he focuses on conscious versus unconscious cognition (and emotion) and pinpoints to the amygdala as the key part of the brain responsible of fear responses. He states that information arrives there earlier than the visual cortex and suggests that the amygdala operates limited pattern recognition capabilities that may trigger emotional responses before the information arrives

to the visual cortex. Later on, more sophisticated analysis in the cortex would help generate a more complex response to the stimulus. The existence of a subcortical pathway rendering the amygdala able to react to emotionally relevant stimuli in absence of cortical processing has only been indirectly inferred (Vuilleumier et al., 2003; Garrido et al., 2012; Johnson, 2005; Reinders et al., 2006). As we have seen, anatomical evidence comes mainly from studies working with primates and other mammals while functional evidence of it keeps restrained to a classical fear conditioning model using rodents (Ledoux, 1996). Out of human lesion studies involving blindsight patients (Morris et al, 2001; Tamietto et al., 2012), only few studies with control subjects employing subliminal presentation of emotional cues like faces and low temporal resolution neuroimaging techniques like fMRI (Morris et al., 1998; Pasley et al., 2004) offer support to this theory in human.

Among the few research with humans with non-clinical subjects, there is a study by Vuilleumier and colleagues (Vuilleumier et al., 2003) that is especially relevant for the current work. They presented fearful and neutral emotional face expressions. Subjects had to perform an implicit task (gender judgment) while laying inside the fMRI. The critical manipulation involved spatially filtered pictures. For each broadband -naturalistic- picture, a spatially filtered version of it where either its low or high spatial frequency components were preserved was elaborated (see Figure 1.6 for clarification on frequencies in space)

Figure 1.6. Spatial frequencies illustrated

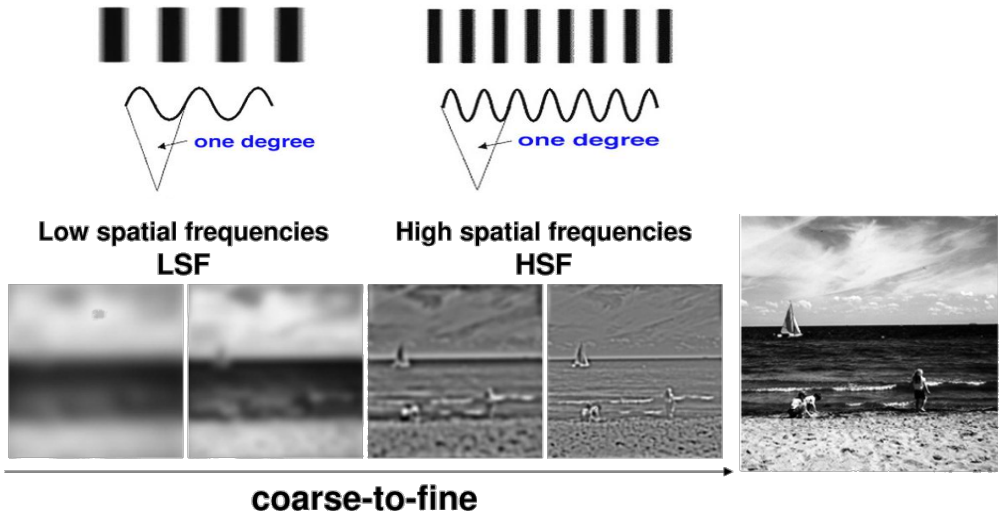

The patches and sine waves at the top represent how there are frequencies in the spatial domain (patches) like in the temporal domain (waves) only that instead of the degree of changes during a certain period of time it refers to the number of changes inside a certain area (in the case of a picture, the changes in light). Bottom pictures represent the effect of filtering (removing) the high (two most left pictures) or low spatial frequencies (middle pictures) from an original, broadband picture (right most). The tag coarse to fine reveals the nature of the information conveyed by low or high frequency bands. The former are still honest to the picture at a global (coarse grained) shape level while the former rely detailed (fine grained) information. Adapted from Peyrin and Musel, 2012.

This is a clever line of research, the assumption being that the subcortical tectopulvinar pathway that innervates the amygdala carries only low spatial frequency components of the visual scene. The work showed that amygdala BOLD responses were greater to either broadband (BSF) or low spatial frequency filtered (LSF) faces; while responses in higher order temporal object recognition areas like the fusiform were greater for either BSF or high spatial frequency (HSF) filtered pictures. Furthermore, activation of pulvinar and superior colliculus was present specifically for LSF fearful faces. Nonetheless, this is additional evidence suggesting that the coarse information that is carried to the amygdala through the subcortical pathway may provide the necessary input to elicit threat related responses. Unfortunately, fMRI lacks the temporal resolution that neuroimaging techniques possess, and we cannot tell about the activation differences at early stages of processing before object recognition stages are achieved via classical forward cortical visual processing.

In addition evolutionary theories support the low road hypothesis. From an evolutionary perspective, stimuli associated with recurrent survival threats, such as fearful faces, require minimal neural processing for identification, a notion referred to as "preparedness" (Seligman, 1971). Being dexterous at rapid detection of threat would result in an adptative advantage. For a system evolved to enable coarse object recognition and start recruiting the necessary physiological changes the amygdala would be the perfect headquarter due to its privileged efferent and afferent connections. Such a system would be able to detect patterns using the lowest level information available. While low level cortical visual areas manipulate the information with greater complexity, identification of highly biologically relevant cues may be possible at the amygdala at this level of processing via magnocellullar talamo-pulvino-amygdalar input that as we have seen carries non topographic, diffuse, low spatial frequency visual information. This processing of salient emotional signals in amygdala may be automatic in the sense that it occurs fast, efficiently, and not necessarily under voluntary control (Moors and De Houwer, 2006), hence directly elicited by presentation of the specific stimulus. However, fast amygdala responses to stimuli representing survival threats for our ancestors, such as potentially deadly predators, remains to be tested and it is still a matter of debate whether there is a fast amygdala response to simple, biologically relevant stimuli such as snakes (Seligman, 1971).

1.4 The case for faces

The case of faces is somehow particular. In the extensive debate (Pessoa, 2013) that links automaticity, emotion and perception, the amygdala plays a crucial role in the *rapid*, *automatic* and *non-conscious* processing of emotional stimuli (Tamietto and De Gelder, 2010). Evolutionary theories purpose that social cues can convey or communicate emotional relevant events. Amygdala's preference to social threat signals had been already shown (Öhman, 2002, Anderson et al., 2003). Moreover, the emergence of social communities and social signals of emotions during evolution presumably contributed to making amygdala-centered circuits particularly responsive to threat cues communicated by other conspecifics, such as facial expressions and perhaps other social signals (Öhman, 2002, Kling and Brothers 1992). If our congener's facial expression can communicate the presence, the location or even the nature of a threat, we are able to react and focus our attention on the particular danger. So this socially evolved alarm system relies on efficient recognition of facial expressions (Vuilleumier, 2005a). Indeed damage to the amygdala results in impaired fear facial expression recognition (Adolphs et al., 2002). Furthermore than the acquisition of conditioned paulovian fear by direct exposure, the amygdala mediates the vicarious acquisition of fear responses too, as it has been shown in rat and human studies involving fear transmission through peer observing (Knapska et al., 2006; Olsson et al., 2007).

How does the amygdala accomplish rapid recognition of social signals like facial expressions that involve great unpredictability than fear conditioned stimuli? Amygdala's preference for emotion does not necessarily imply an innate response; it could be a learnt one. Monkey studies had shown that captivity grown animals do not exhibit fear responses to biologically relevant stimuli like snakes unless they had been exposed to them and watched their peers reaction in their first years of life (Mineka et al., 1984; Cook and Mineka, 1989). The role of the amygdala may go further than fear perception as such and studies now show that it may rather be crucial for detecting saliency and biological relevance in general terms. With bilateral presentations, neglect patient's attentional failure to the hemifield is less aggravated when the stimuli presented is a face, and further less if it is expressing an emotion (Vuilleumier and Schwartz, 2001), which suggests some degree of object recognition in absence of complete cortical input. In addition to face expressions, studies had found attentional blink modulations by visual complex aversive pictures after previous fear conditioning (Smith et al., 2006). Moreover, another study found attentional

blink modulations to strongly affective words (Anderson and Phelps, 2001) that correlated with amygdala damage too, which means even stimuli whose relationship between its low level physical features and their emotional relevance is idiosyncratic are processed at some degree by the amygdala. However, the literature linking amygdala and facial emotion recognition is humongous and its evolutionary role well established. But amygdala shows preference not just for threat related signals as such but for learnt stimuli. In the case of faces, an fMRI study found two independent modulations of amygdala activation by emotional faces, to the mere exposure and after learning (Hooker et al., 2006).

Emotion recognition wise, the most informative area in a picture of a face is the eyes. In fact, amygdala lesions impair the ability to seek out and make use of the eye region of faces, resulting in impaired fear perception. We have already seen the relationship between pulvino-amygdalar connections spatial attention and eye movement guidance. In a study with temporal resolution exploring the discrimination of facial expressions using 'bubbles' to occlude parts of the faces and ERPs, the first emotion modulated responses that appeared correlated with the information conveyed at the eye region, that was enough to recognize the expression as a fearful expression (Schyns et al., 2007). The eye region has shown to activate the amygdala in more degree than other regions of the face also using fMRI (Morris et al., 2002). It seem that impairment of fear recognition in amygdala damage patients depends on the loss of ability to naturally fixate spatial attention to the region of the eyes as has been shown experimentally (Adolphs et al., 2005) and in real social context (Speziom et al., 2007). Indeed, S.M. inability to detect fearful expressions almost turned into normal recognition when she was explicitly asked to fixate in the eye region (Adolphs et al., 2005).

Whether threat recognition process at the amygdala are just triggered by threat related cues or dependent up to some degree on the analysis of the low level features of the stimuli can only be tested experimentally by effectively disentangling high and low spatial frequency visual information.

1.5 Main criticisms to the Low Road hypothesis

There is a lot of debate about the low road hypothesis because it ultimately raises questions about human cognition that had been at the heart of some deep debates for decades. For instance, how do we assign attributes to our perceptions, this is: how does object recognition work? is it the end of a feedforward hierarchical process (be it subcortical or cortical) or does it involve top-down feedback and parallel pathways? On the other hand, the question of modularity versus connexionism lays. It also addresses the debate of automaticity. How is this achieved? is there, or are there, largely independent systems that operate outside of consciousness or does it involve recursive processing between higher-level and specific systems? In sum: the debates of modularity versus connexionism and conscious versus unconscious (automatic) processing. Furthermore, its purported automaticity makes us question what its need then for awareness experience to encompass object recognition and when does this subjective experience start.

The main criticism to the low road hypothesis is the lack of direct evidence by electrophysiological studies in human. While it has been proved with rats and a fear condition paradigm that a projection that goes from the auditory nucleus of the thalamus, the medial geniculate nucleus, to the amygdala does exist and its functional, and homologous direct measure of a functional pathway from the visual nuclei of the thalamus, the lateral geniculate nucleus, is lacking. Also, is important not to forget the fact that pulvino-cortical projections are extremely abundant in the brain as if the whole cortex was warped around it (Ships, 2003). Almost every visual related area in occipital cortex receives projections from the pulvinar (Stepniewska, 2004) as does the rest of the brain: parietal, temporal, frontal and cingulate cortex; all receive projection from the pulvinar.

There are also evidences coming from electrophysiology studies that should be taken into account to put into context the idea of a unique and independent mechanism for threat detection that the low road hypothesis purports. First of all cortical responses to visual stimuli are not as 'slow' as the theory supposes, and faster than cortical emotional modulations has not been recorded yet at subcortical structures like the amygdala (Pessoa and Adolphs, 2002). Recorded latency response to visual stimulation at cortical sites can be also extremely fast as has been recorded with macaques (Schmolesky et al., 1998; Lamme and Roelfsema, 2000) and cats (Ouellette and Casanova, 2006). While pulvinar activation

by visual stimulation is recorded around 50-60 ms post stimulus onset, simultaneous responses had been observed at visual cortical areas corresponding to V1 and V2 in the cat. Visual response latencies in the inferotemporal cortex, supposedly a late processing cortical area, had been recorded as early as 60-85 ms and as short as 40-70 ms at the frontal eye fields, a more anterior region in the cortex. Overall these findings indicate that responses in the cortex can be really fast.

However, the earliest responses recorded intracranially in the monkey amygdala range in between the 100 to 250 ms post stimulus window as measured with monkeys (Nakamura et al., 1992; Leonard et al., 1985; Gothard et al., 2007) with the earliest differences between emotional and neutral stimuli recorded as early as 120ms (Gothard et al., 2007). There are some human studies measuring the activity at the amygdala with intracranial electrode recordings employing emotional stimuli and they report rather late (130-200 ms) amygdala emotion modulated responses. Most of them presented complex scenes or standard photographs including (Sato et al., 2011; Pourtois et al., 2010) or not (Oya et al., 2002; Brázdil et al., 2009) fearful faces, which may have obscured a fast amygdala response under the assumptions that emotional scenes need a higher level of processing for threat related information to initiate a response and that scenes may not be as biologically relevant as faces are. The fastest response previously reported was around ~130 ms when they also included fearful faces. Needless to say, this is not fast enough to justify the low road hypothesis. In a study presenting only faces (Krolak-Salmon, 2004) the emotional modulation in the amygdala onset at ~200 ms, though it is noteworthy that they employed eight different stimuli that were presented 30 times in two tasks and the amygdala has shown to be sensitive to habituation (Breiter et al., 1996; Wright et al., 2001; Fischer et al., 2003).

Secondly, it may well be possible that a different network other than the pulvino-amygdalar pathway is responsible of rapid threat detection. Indeed, as proposed by the low road hypothesis, fast processing of coarse information is what an organism most need to gain evolutionary advantage. Alternative models wouldn't consider the amygdala a 'necessary' piece of the mechanism. There are neurophysiological evidences that could support the existence of a broader subcortico-cortical mechanism that would perform the function of fast threat detection. Pessoa and Adolphs, propose an alternative to the low road hypothesis, which they call 'multiple waves theory' (Pessoa and Adolphs, 2010; figure

1.7). This model takes into account evidence from neurophysiological studies in both human and animals and suggests that recursive processing and parallel computation in visual areas enabling the detection of biologically relevant stimuli can occur very fast within the human brain.

Figure 1.7. Low road and multiple wave theories

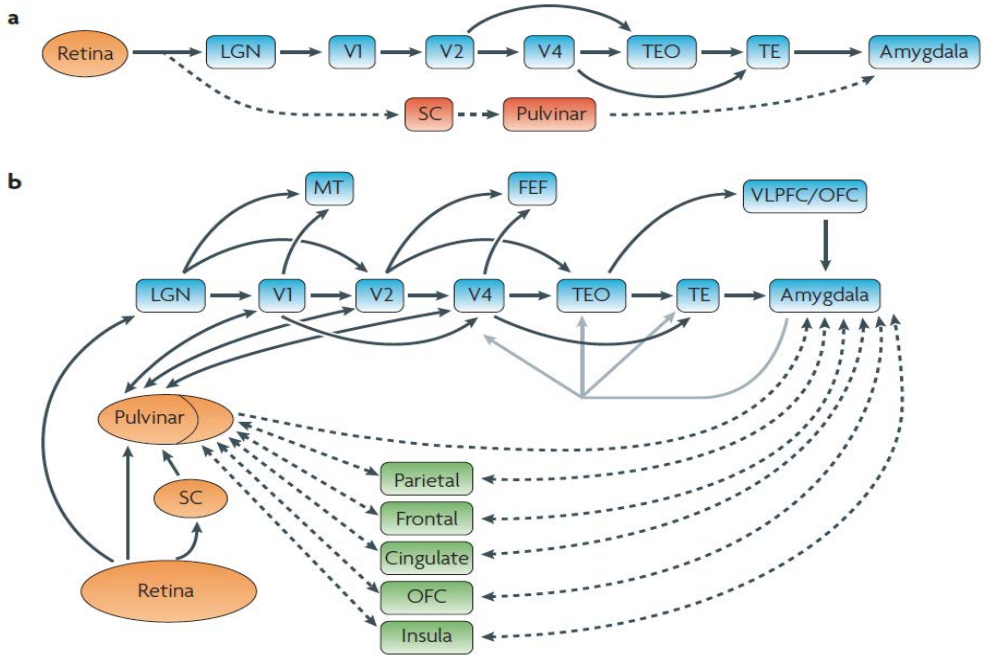

Panel a illustrates the high and low roads this is, the proposed theory that, besides hierarchical processing from early visual areas into temporal cortex, an alternate route detours before the lateral geniculate nucleus (LGN) through the pulvinar and arrives to the amygdala bypassing cortical processing. Panel b depicts the proposal by author's Pessoa and Adolphs based on several electrophysiological evidence that more than two neural pathways may coexist given the extensive amount of shortcuts as well as parallel and feedback-projections between strictly visual and less modular regions (like the orbitofrontal (OFC) or ventrolateral prefrontal (VLPFC) cortex. LGN: lateral geniculate nucleus. SC: superior colliculus. TEO: inferior occipital area; TE: inferior temporal area; MT: medial temporal cortex; FEF: frontal eye fields. Pessoa and Adolphs, 2010.

Pessoa and Adolphs do not state this just because responses in the cortex may occur before the ~70 ms mark (though in many of the studies with animals the latencies reported reflects only a visual response, not affective discrimination) but also because visual cortex may contribute to rapid affective processing more than previously thought. The nature of the connectivy within 'early' and 'late' visual cortical areas needs to be further taken into account. There may be multiple pathways: there are bottom-up shortcuts between V1 and V4, from V2 to the posterior inferior temporal cortex and from V4 to the anterior temporal gyrus (Shipp, 2003), so the inferotemporal cortex may be provided with information from visual pathways quite fast (Pessoa et al., 2010). There are also connection

from the LGN that go directly to extraestriate regions such as V2 (Yukie and Iwai, 1981) and V4 (Bullier and Kennedy, 1983) bypassing striate processing at V1.

But there are also long-range short-cuts, and they may be able to rely coarse information to parietal, temporal and frontal cortices (Bar, 2003). Magnocellullar fibers do arrive to the early visual cortex that may provide temporal and parietal cortex, more involved into spatial attention and perceptual integration (Kveraga et al., 2007), with coarse information. Ventral visual cortex does project to the prefrontal region too, including the orbitofrontal region (Bar, 2003). So there are many roads, not one road, and it is said that each step adds 10 ms to the processing time. But the question would be: would those alternative pathways be functional for emotions? A lesion study with fMRI showing visual dependent activation in areas V2, V3, V4 and V5/MT in macaques with intact LGN and cortical lesion restricted to V1 corroborates the ability of this short-cuts to perceive color and orientation (Schmid, 2009), suggesting a different explanation for some aspects of the blindsight phenomenon.

In short, there are multiple parallel routes and connections that information can follow during visual processing towards recognition at higher-level areas. A new model has to explain how fast emotion modulated responses in electrophysiological components within the 100-200 ms window occur. Overall, these evidences go against the assumption that visual processing, ending with object recognition, occurs in a hierarchical feedforward flow, and support the idea that it may depend on more than one route, and non-local neighbor areas working in conjunction. This leads us to question how information coming from different systems or nodes, is integrated (a process called biding) to create an unique perception with attributes that may trigger certain responses; and ultimately what is need for this percept to come into awareness.

1.6 The High Road

We may as well refer to the thalamo-cortical projection as the 'high road' in contraposition with the thalamo-subcortical visual pathway nick - low road. Visual

processing is considered to be carried out in striate and extrastriate visual areas in a push forward manner: starting from highly-specialized, stimulus-dependent occipital regions, acquiring degrees of complexity on its way through the laterooccipital regions (LO) to the invariant-domain visual areas in the inferotemporal cortex. The terms low-level and high-level areas appeal to the hierarchical nature of this mechanism.

The thalamo-cortical projections are divided into two functionally different pathways (Goodale and Milner, 1992) that converge, the dorsal -occipitotemporal- and ventral -occipitoparietal- streams, traditionally known as the "where" and "what" routes given the former's relevance for spatial attention and the latter's importance for object recognition. Both streams originate at the primary visual cortex but the ventral stream extends along the surface of the ventral brain into inferotemporal cortex while the dorsal stream keeps going up towards parietal cortex. It is thought that the dorsal stream extracts information about features like movement and location, and it has been linked with visual guidance and spatial attention (Desimone and Duncan, 1995; Glickstein, 2000). The ventral stream on the other hand performs the discrimination of objects based on information about the shape and other features of the stimuli (Serre et al., 2005). But one should not forget that both streams are interconnected; interaction between both types of knowledge is on demand. The final stages of processing occur at high-order associative areas, which should be selective but invariant to low level feature changes of the stimulus (Cauchoix and Crouzet, 2013).

Primary visual areas, corresponding anatomically to the striate cortex, represent the lowest level in the hierarchy of visual processing and thus are called V1. V2 corresponds anatomically to the prestriate cortex while V3-V5/MT are extrastriate regions. V1 receives magno and parvocellullar projections from the LGN. Indeed, the name striate is given due to the fibers of axons that go from the later to the former (visible to the naked eye). It is cytoarchitectonically divided into six layers. It is supposed to perform the first step of visual analysis. Its neurons are dependent of low level features like changes in ligth and stimulus variance. They are highly dependent to stimulus changes in size and orientation – a feature called tuning properties. Its functional organization seems to be relatively independent of the level of awareness (Vincent et al., 2007). Moreover, neurons in V1 are organized retinotopically, resembling the image in the retina in a very precise manner (Tootell et al., 1998). A certain patch of neurons codifies the information corresponding to

a certain portion of the contralateral hemifield of view - the upper-right lip of the calcarine fissure codifies the lower part of the left hemifield and viceversa (Engel et al., 1997).

Retinotopy is not equally proportional though, a bigger portion of V1 cells process information from the central area of the visual field (Grill-Spector and Malach, 2004a). These neurons are particularly sensible to changes in orientation but they are able to detect small changes in color and spatial frequency too. This particular sensitivity to spatial frequency, which have been extensively studied with Gabor patches and its currently a hot topic of research, has led researchers to think that the way the visual primary cortex codifies the topographical input is not so much based on spatial cues but also in edge detection, as it has been seen that neurons are spatially grouped in different columns depending on the particular feature (orientation, spatial frequency) they are tuned to (Nauhaus et al., 2012). There more neurons involved in codifying light changes than light invariances, as it has been shown that neuronal fire increases accordingly with spatial frequency (Movshon et al, 1978). As information is relayed from here into higher visual areas, the local spatial information gets lost stepwise, though it remains encoded in the retinotopical layers of V1.

From here, the high road bifurcates into the dorsal and ventral streams in V2. V1 and V2 are intricately connected via feedforward/feedback projections and direct/indirect connections (Bullier et al., 2001a). V2 receives inputs from V1 directly and indirectly via pulvinar and also projects feedback to V1 again. V2 can be subdivided into dorsal and ventral areas bilaterally regarding its functional properties. Its cells do tune to color, orientation and spatial frequency of the stimulus like in V1 but they are sensible to attentional modulation (Friston and Büchel, 2000) and able to detect more complex patterns (Hegdé and Van Essen, 2000). Indeed, V2 has shown sensitivity to abstract visual features like illusory contours (Zeki, 1998). It has also shown ability to disentangle the figures from the background (Qiu and Von Der Heydt, 2005).

The regions comprised by the ventral stream extend from V2 out of the occipital lobe ventrally into the lateroоccipital cortex through V4. V4 would be the third stage of the ventral stream feedforward route, still in the extrastriate cortex. It shows greater dependence to attention than V2, in fact, it was the first region of the occipital cortex where differences between attended and unattended stimuli were found (Moran and

Desimone, 1985). Its cytoarchitectonical subdivision in human cortex is less clear than previous areas, and it occupies the inferotemporal portion of the occipital lobe. In the hierarchical model, V4 receives mainly parvocellullar inputs from V2 and projects extensively to the inferotemporal gyrus (Felleman et al., 1997). But as we have already seen, V1 projects to V4 as well (Zeki et al., 1991; Van Essoni and Mcclendoni, 1994) and there are back and forth connection between V4 and V5 (Zeki et al, 1991).

Into the inferotemporal cortex, the ventral stream goes from posterior to anterior, acquiring bigger complexity, higher selectivity and greater stimulus invariance gradually. Specialization becomes bigger and bigger to the point that certain portions in the ventral temporal gyrus react preferentially to certain object categories. One of the most well known of such high-order visual areas is the face area in the fusiform gyrus. There is a debate about the specificity vs. selectivity of the fusiform face area though it seems that patches on the anterior and posterior fusiform do present a response bias towards faces, exhibiting greater responses to faces as compared to visual stimuli of other categories (Sergent et al., 1992a; Kanwisher et al., 1997). However, the search for identifying object-specific portions of the fusiform gyrus has led to the proposal of areas as specific as the visual word form area generating some debate (Cohen and Dehaene, 2004).

1.7 Lateral occipital and inferotemporal cortex

The ventral stream leads from cuneus and lingual into the lateral occipital cortex where object recognition, or at least an essential part of the processes involved in it, take place. Actually, the extension of the visual area associated with object recognition goes far beyond the lateral occipital sulcus deep into the temporal cortex, flowing ventrally into lingual and parahippocampal gyri and from the most posterior to the most anterior part of the fusiform gyrus.

The term lateral occipital complex (LOC) refers strictly to the bank of the fusiform gyrus, in the junction between the occipital and temporal cortex, extending ventral and dorsally (Grill-Spector et al., 2001). It was first shown to respond preferentially to

perceived visual objects in an fMRI study (Malach et al, 1995) that demonstrated higher level of activity when subject passively viewed natural photos of common objects, whether familiar or unfamiliar, as compared to stimuli without identifiable shapes –visual textures. A later study (Kanwisher et al, 1996) found that this enhancement persisted when the stimuli employed were contour lines depicting a 3d object (also familiar and unfamiliar) and randomly arranged similar lines. Furthermore, a study (Allison et al, 1994) involving patients with surface electrodes found an increased activation present for various objects of different categories like faces, cars or butterflies (as compared to scrambled pictures) and later localized to face-specific and letter-specific regions within the medial and anterior fusiform gyrus (Allison et al., 1999; part of a series entitled *Electrophysiological studies of human face perception*). In addition, other studies had found that this response is not modulated by transformation of the object's shape in size, orientation or lightning of the shapes, a property called cue-invariance (Grill-Spector et al., 1999; Tong et al., 2000), which had been previously shown in animal studies recording size and position invariant responses in macaque inferior temporal cortex (Ito et al., 1995).

Therefore, the relevance of the ventrolateral occipitotemporal cortex in object recognition is a well-established matter, along with the fact it somehow deals with higher-order cognitive representations, relatively independent of low-level changes in the visual input; real-life perception of objects would require a system able to operate unaltered by the constant changes in light, size or orientation. It is widely admitted that, even if not sufficient, it is at least necessary for object recognition to take place. In fact, patients with damage to different areas of the fusiform gyrus suffer from a variety of visual recognition deficits (visual agnosia) that may be specific to a certain category of stimuli (Farah et al., 1991; Feinberg et al., 1994; Moscovitch et al., 1999) like prosopagnosia, the selective inability to identify individuals by their facial features (Damasio et al., 1982). Hence, the debate has moved from its cue invariance processing capabilities to its degree of specificity in object recognition, as there are areas in the fusiform gyrus that seem to exhibit some selectivity for certain categories of stimuli. The fusiform face area (FFA, Sergent et al., 1992a) does not only increase its activity when presented with any visual object but it increases it even more when this object is a face. In a first fmri study (Kanwisher et al., 1997) comparing intact two-tone drawings of full-front faces with similar scrambled two-tone drawings, full-front photos of faces versus full front photos of houses and partially occluded photos of faces with photos of hands found an increase of the activity linearly

related with the level of accuracy (Kanwisher et al., 1997). Since then, there is still controversy about whether this response is selective just for faces or extensible to other types of stimulus (Tarr and Gauthier, 2000; Grill-Spector, Knouf and Kanwisher, 2004b). This touches the issue of domain specificity in visual system. Recently, it has been suggested that it may be composed of smaller nodes at a local scale that fine-tune to certain category specific features (Weiner and Grill-Spector, 2010) and are sparsely distributed in the fusiform gyrus (beyond the FFA in the case of faces too).

Besides imaging research, studies employing event-related time resolution techniques had associated object specific modulated responses with a negative deflection (N170; Bötzel et al., 1995; Bentin et al., 1996) recorded in EEG studies around the 150-200ms time window and source localized to the fusiform gyrus (Itier and Taylor 2004a). It is linked to the correct recognition of the object (Kanwisher, 2000; Tanaka, 2001) and it is enhanced to human faces as compared to other objects (Kanwisher et al., 1999; Rossion et al., 2000a; Grill-Spector, 2003). It also has been shown that this potential evoked by faces and objects shifts ventrally from the bank to the anterior part of the fusiform (Bötzel et al., 1995; Bar et al., 2001). The face sensitive nature of the component has been challenged (Thierry et al., 2007) and supported (Rossion and Jacques, 2008, Eimer, 2011). Today its face selective nature is generally assumed although some studies (Grill-Spector, Knouf and Kanwisher, 2004b; Rossion et al., 2003a; Rossion and Jacques, 2004) even employing with intracranial electrodes (Dering et al., 2009) still makes this assumption questionable.

Most scientists may agree that the fusiform region is related to face processing in particular but may not be the solely area in charge of it. Part of the relevance of this area in discrimination tasks may be related with visual expertise. It has been proposed that the object-specific modulations of the N170 may rely more on the visual expertise of the viewer within the stimulus category than the specific category per se, as it has been shown that the amplitude of the component is enhanced when subjects discriminate between categories they are experts with as compared to a category of objects to whom they are relatively novel (Gauthier et al., 1999; Tanaka and Curran, 2001). Given the biological relevance of faces for us humans and some primates as social species and the relevance of the information they convey, it is logical to assume that our brain had become an expert at identifying/discriminating faces; be that expertise achieved philogenetically or acquired in our lifetime. Critically, it has been found that emotional face expressions modulate the

amplitude of the N170 (Pizzagalli t al., 2002; Batty and Taylor, 2003; Caharel et al., 2005; Blau et al., 2007) though there are as well studies that did not find modulations (Pourtois et al., 2005; Ashley et al., 2004; Rellecke et al., 2013). Also face-selective responses had been found at earlier latencies (Linkenkaer-Hansen et al., 1994; Itier and Taylor, 2004b; Dering et al., 2009).

In somma, the fusiform gyrus is related with object discrimination and the FFA shows a preference for face processing; it is possible that face-specific processes may coincide with face-unspecific and domain-general ones (Palermo and Rhodes, 2007) but what seems crucial is that the N170 reflects a process in the fusiform gyrus through which it renders a somehow holistic representation relatively independent of stimulus variance that is carried on for later processing (Eimer et al., 2011) but most probably the integrated representation of the face/object is carried out at more places than the fusiform gyrus (Ishai, 2008).

1.8 Then how are integrated representation achieved? Perceptual closure

We have seen how the classical model of object recognition assumes a hierarchy in the visual system. Within the ventral visual stream, low order visual cortex process simple geometric lines and shapes that are submitted to higher order areas that code invariant object and category information (Mishkin et al., 1983; Hochstein and Ahissar, 2002). Visual processing starts with tiny bits, fragments of information. Indeed, the bases of visual processing are truly modular: examples we have seen include the automatic processing of biologically relevant stimuli or the retinotopical nature in the cytoarchitectonical arrange of the layers in V1. There are simple cells in the striate cortex that are only excited when a line with a certain orientation in their point of the visual field, otherwise they are inhibit (Hubel and Wiesel, 1977). But for conscious perception, incomplete or overlapping visual forms must be integrated, creating a representation, and ultimately the subjective experience of awareness (Ernst and Bülthoff, 2004). The latter is of course impossible to measure operatively, but there is almost a century of psychology literature discussing how the visual

features may be integrated into a percept, starting from the school of Gestalt (Wagemans et al., 2012a, 2012b).

On one side, Gestalt refers to the creation of a meaningful, coherent percept as *perceptual completion* (Wertheimer, 1923, 2012). The Gestalt school considers perceptuial completion arises from processing a stimulus as a whole, choosing the easiest of the possible interpretations from the interaction of the stimulus parts, rather than the summation of the single parts themselves. On the other hand, there is the *binding* problem (Treisman, 1998). In order to create this meaningful percept, different types of information coming from different processing modules need to be integrated, a process called *perceptual binding*. To sum up, this proposal claims for the existence of interaction between distinct regions in the brain as much as the collaboration of local and distant modules in the brain as an integrated network.

Global to local and distributed processing is not consistent with the local-to-global hierarchical classic model commented above. Perceptual completion may not be a stream that goes from start to end collecting the bits of the future percept until the entire puzzle is figured out. There shall exist guidance from higher order to low order visual areas, a sort of feedback or top-down mechanism. Of course, gestalt theories did not provide any clue on the brain mechanism linking global with local processing.

Within the neurophysiology field, some studies regarding visual perception had explored the interaction between brain areas and support the existence of top-down regulation and recursive processing from high to low order visual areas as well as the synchronous collaboration of distant regions in order to achieve the *illusion* of the percept. Furthermore, gamma power oscillations had been used in event-related studies as an index to assess local and long-range common processing between regions of the brain forming a network (Tallon-Baudry and Bertrand, 1999; Fries, Nikolic, Singer, 2007; Gruber et al., 2008).

Some studies had employed different stimuli to address this matter, mainly ambiguous figures like bi-stable stimuli (figure 1.8). Bi-stable stimuli are interesting because they generate conflicting percepts that may spontaneously alternate to solve the rivalry problem, while there are no real changes in the image per se. An fMRI (Andrews et al.,

2002) study employing Rubin's Vase-Face illusion found that subject's BOLD signal from the fusiform correlated with their perception of a face as compared to a vase, suggesting that the extrastriate areas in charge of processing particular categories of objects play a role in the conscious perception of a representation. Another fMRI study (Kleinschmidt et al., 1998) employing various bi-stable ambiguous figures shows that distant and specialized areas work together to maintain a stable perception. Transient changes were apparent in the pulvinar nuclei, striate and ventral visual cortex, and higher-order visual areas of the intraparietal cortex, supporting the idea that it is a set of neural structures that are responsible for the creation of a perceived representation rather than a single area on top of the processing stream.

Figure 1.8. Bi-stable stimuli

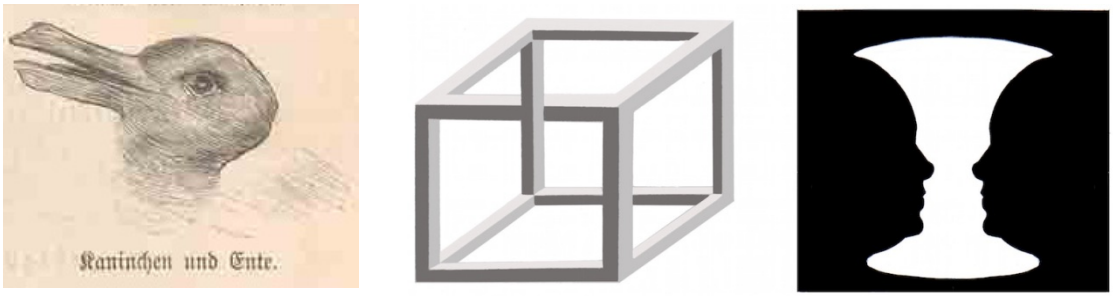

Three examples of bi-stable stimuli employed to study perceptual closure. Two confronting representations coexist in such ambiguous stimuli but only one is perceived after the rivalry problem is solved. Left: "Kaninchen und Ente" ("Rabbit and Duck") from the 23 October 1892 issue of *Fliegende Blätter*. Middle: Necker cube. Right: Rubin's vase.

The areas implicated in that network extend beyond the ventral visual stream including parietal and associative areas. Another study (Dolan et al., 1997) exposing subjects to consecutively less degraded versions of the same image revealed that medial and lateral parietal regions implicated in attention and visual imagery were involved in correct recognition besides inferotemporal regions, linking distant areas belonging to specialized modules in a network responsible of binding and perceptual completion. Object recognition is just a part of conscious perception, and attentional networks had always been related to the later (Corbetta et al., 1998). Parietal and frontal cortex rather than early sensory areas modulate covert recruiting of attentional resource to visual locations. This mechanism requires that the mentioned frontoparietal network interact somehow with extrastriate regions in the ventral visual system to enhance processing (Fernandez-Duque

and Posner, 2001) and these regions are consistently found to be active in perceptual completion tasks like the cited above

Functional MRI lacks temporal resolution to disentangle between the different stages of a cognitive process. Doniger and colleagues (Doniger et al., 2000) identified an occipitotemporal component of the event related response related to perceptual completion after the N170 window, with onset at around 230 ms and peaking at 290 ms. In another study (Sehatpour et al., 2006) corregistered fMRI and EEG was employed while subjects viewed partially occluded objects, another method derived from the gestalt that ensures perceptual closure is necessary to correctly recognize the stimuli. ERP differences between occluded figures and scrambled control pictures were evident in the time frame between 230-400 ms, consistent with previous observation, in a negative component that was localized to the laterooccipital complex.

These timings imply that object recognition starts at the top of the *automatic* forward hierarchical processing. How can this be achieved? There are descriptions of models of visual processing that include backward connections from higher to lower order visual cortical areas supposed to carry predictions calculated from the information arriving through the forward sweep (Rao and Ballard, 1999; Friston, 2003a). The reverse hierarchy theory (Hochstein and Ahissar, 2002) proposes that a generalized description of the scene is first generated for later vision scrutiny, via attentional modulation of the low level areas. that then will incorporate detailed information into the conscious perception. There is a lot of discussion on how top-down feedback carries global information to local processing units in early visual cortex. As we have seen, magnocellullar cells of the lateral geniculate nucleus project to parietal cortex sending information very rapidly; the result of this first coarse computation, may then be passed to V1 and V2 and it is used to guide further processing in the inferotemporal cortex (Bullier, 2001b). Whether initial visual subjective experience arises at fusiform gyrus object specific visual areas or in an integrated manner, it is a coarse experience, encoded in a general manner. On a secondary, attention dependent visual processing, information may be added to enrich conscious percept with details, (Campana and Tallon-Baudry, 2013) via top-down fine tuning of low level visual areas. With the information conveyed in the first forward sweep the early visual areas can rapidly group certain feature *constellations*, perhaps incapable of yielding awareness but that may trigger efficient responses hardwired into the visual system. But recursive processing

and/or horizontal connections are needed to account for the tuning capabilities of the visual system (Lame and Roelfsema, 2000), even if the processing is automatic.

However, the neuroimaging studies of perceptual completion described above do not report engagement of lower order visual cortex. Nonetheless, one event-related fMRI study (Altmann et al., 2003) reported both primary and higher order visual cortex activity activation during global shape integration of collinear contours although a measure of interaction between these levels of hierarchy was not provided. Interrupting communication between early and higher visual cortices with TMS impairs perception of natural scenes (Koivisto et al., 2011) and perceptual completion of illusionary Kanizsa-type figures (Wokke et al., 2013). But although these recent evidences suggests that coherent perception relies on feedback from higher to lower order visual cortex, paralleling the global-to-local concept of Gestalt psychology, a characterization of this process in terms of effective connectivity is currently lacking.

How to measure local and long range communication between distant areas? Electrophysiological studies had related certain power bands with specific types of brain processing. Gamma band activity is considered a fundamental activity mode for information processing (Fries et al., 2007) and more importantly, not only for perception but also for higher cognitive functions such as attention and memory (Jensen et al., 2007). One physiological interpretation of gamma is that the amount of activation in the pyramidal cortical cells is re-coded based on the time of occurrence of the spikes relative to the gamma cycle (Olufsen et al., 2003). Within this framework, gamma has been conceived as a temporal reference frame for sharing spike-phase coded information between nodes that are working in conjunction – hence constituting a neuronal network (Singer and Gray, 1995). This way, distant areas can share a temporal code and be able to tune accordingly. Once located the sources of interest (by comparing the amount of gamma changes with respect to the baseline) a network responsible of maintaining the stimulus representation can be defined, which in this case would result in an operational definition of perceptual closure at the brain level. Furthermore, hypothesis about the forward, backward and bidirectional nature of such network can be tested with Bayesian inference models like Dynamic Causal Modeling (DCM).

1.9 Our road

That will be the last part of this thesis and the application of this mathematical instrument will be explained in Experiment 3. First, we will come back along the lines of this introduction and get deep inside the brain employing intracranial recordings of the amygdala and the fusiform to explore human evidence of the so called Low Road. We will hopefully be able to establish some mechanics of the subcortical pathway. Then we will magnify our looking glass by repeating the same experiment with magnetoencephalographic recordings. It will help us learn more about the visual pathways at the cortical level and perhaps support or expand the observations made in Experiment 1. Finally, in Experiment 3, we will climb the ladder of visual processing hierarchy to the top and optimistically we will be able to take a look at how perceptual closure is achieved, whether bidirectional or backwards connectivity between areas of the visual stream is need; and whether high- as much as low-level visual areas are involved in perceptual closure - like the early *gestaltische psychologische* proposed.

2 Objectives

The main objective of the present work involves addressing the current controversy surrounding the so- called 'Low Road' theory (Ledoux, 1996). This theory states that highly biologically relevant stimuli may trigger attentional and perceptual bias at very early stages of visual processing via thalamo-amygdala-cortical projection relying on low-level features analysis of the scene. This analysis would take place in the amygdala before cortical visual processing is achieved via thalamo-cortico-amygdalar ('High Road') classic feedforward push (Mishkin et al., 1983), considered to proceed in hierarchical fashion with the integrated representation of the stimulus -percept- at the top. It is important to note that while the two proposed pathways -thalamoamygdalar and thalamocortical- represent visual processing circuits developed at earlier and later eras of the evolution of the animal brain in phylogenetic terms human perception in its more complex form is usually achieved by the integrated work of several neural areas/circuits rather than the work of single neural nodes/circuits (Hochstein and Ahissar, 2002). Also, cortical processing may be achieved in a seemingly fast manner and shortcuts as much as feedback projections between low- and high-level regions in the visual hierarchical scheme are common (Pessoa and Adolphs, 2010). However, as fast as cortical processing may be there is a time window (~100 ms poststimulus) where the amygdala may be able to process low level features of the stimulus conveyed via magnocellullar neural projections in absence of more *sophisticated* cortical inputs whose first efferences to the amygdala are assumed to occur via fusiform later than 100 ms poststimulus.

Direct evidence in humans supporting the Low Road hypothesis is currently lacking. For the reasons explained above it would require temporal assessment of amygdalar as well as cortical activity within the same task. We will do so by recording in situ

electrophysiological activity from the amygdala and fusiform gyrus of epilepsy patients with implanted stereotactic electrodes undergoing clinical assessment. Two main experimental manipulations will be performed. First, we will use neutral and emotionally laden stimuli. Furthermore, we will use stimuli of different complexity grades: faces and complex visual scenes. Human faces are stimuli to which the human brain has evolved adaptive processing strategies given the relevant biological and social information they convey. This facilitation is a notion termed *preparedness* (Seligman, 1971) that postulates that that certain stimuli can modulate perception assuming there are configural presets along human perception that may trigger attentional mechanisms given enough simplicity in the amount of information that enters the system. Thus, on the other side, complete pictures of visual scenes, as informative as they may be, would require a more in-depth analysis. Secondly, we will manipulate the spatial complexity of the *prepared* stimuli, faces, so that only low or high spatial frequency components are present in the image. In this fashion we intend to tag the properties of the magno- and parvo-cellullar neurons constituting most of the neural population present in both the thalamo-amygdalar and thalamo-cortical projections. Note that with this experimental manipulation we do not imply that magnocellullar neurons, which are assumed unable to carry high spatial frequency information, are absent in the thalamo-cortical route. Rather, we will also use naturalistic images (or broadband, conveying all the spatial frequencies) so as to compare the modulations that may arise. In soma, we will try to elucidate whether a fast emotional modulation, as compared to the fusiform gyrus, occurs in the amygdala by relying low spatial frequency emotional expression based on the 'Low Road' theory suggestions.

As mentioned before, while visual processing may be represented as a feedforward push, there are many shortcuts and recurrent processing projections involved overall during the creation of a visual representation, or *percept*. Thus, manipulations of the spatial frequency components of a stimulus may affect different areas other than the amygdala or the fusiform gyrus and different stages of visual processing other than the ones occurring before 100 ms poststimulus. Hence, we will repeat the paradigm involving faces employed with the epilepsy patients while acquiring over the scalp magnetoencephalographic activity of healthy control subjects. This technique provides a temporal resolution as good as intracranial electroencephalogram (iEEG) with the difference that activity from all the brain can be acquired, offering a more less focal albeit more exhaustive image in spatial terms of the whole brain processes taking place at the expense of lowering the spatial

resolution. However, we expect to perform source reconstruction on the event related magnetic fields (eRMF) that will help establishing a locus for the early effects that we may observe. It is important to note though that MEG sensor are much more sensible to the activity coming from the cortex than medial and deeper structures such as the amygdala.

Also mentioned above, faces and emotional expressions are of special relevance for the human visual processing. Another objective of this work will be describing the early stages of human face visual perception in terms of magnetic field responses divided by components and their respective source localisation. Lastly, and as anticipated in the first paragraph, it is interesting to study the later stages of visual processing where a representation or percept of the stimuli is created. The study of such processing, where the *synchronous* activity of distant areas may be required, can be addressed by manipulating the subject's interpretation of initially ambiguous stimuli that may or may not resemble actual objects in a different degree such as the *Mooney* faces. By acquiring MEG data during a face- non-face discrimination task we intend to tag the stage -perceptual completion- at which the percept is integrated via *biding* and integrative processes. This event is assumed to take place at high-level areas in the visual processing hierarchical scheme, such as the fusiform gyrus. It is assumed that perceptual completion requires the integrated contribution of a network of neural patches rather than a single node. Thus, we will focus on the frequency component of the eRMF with special emphasis on the Gamma band power and coherence between different regions, given that such a measurement will describe the extent of activity integration within the temporal window identified for perceptual completion. Furthermore, given that gestaltische theories (Wertheimer, 1923; Wagemans et al., 2012) and different evidences (Bullier, 2001b; Friston, 2003a) point towards the existence of top-down regulations from high- to low-level visual areas that would be required to achieve perceptual completion of the stimulus as a whole we will perform dynamic causal modelling (DCM) on the different feasible directionalities of the projections between the localized areas of interest to test the probability that high- to low-level top-down neural circuits are relevant at this *final* stage of visual processing.

Already stated the objectives of the current work, we would like to add as a corollary that this thesis pertains to the field of affective neuroscience as much as to the field of visual perception. The main interest is exploring the emotional biases that may exist in early visual stages. As a secondary object we are interested in visual processing per se and

hence the third experiment does not address affective aspects of the visual processing but the integrated perception of a neutral but biologically relevant stimulus – a face. In order to achieve good comprehension of affective processes it is important to draw the best possible knowledge about the processes with which they intermingle. Emotion is not just a lineal process like perception, language or memory may be accounted for when observed in solitaire. Though we will address the controversy of whether a supposedly automatic activation of brain mechanisms takes place as the result of an isolated process involving the thalamus and the amygdala we consider Emotion to be a transversal process that stains most cognitive processing in a global manner. Hence, shedding light on how issues such as the neural nodes and pathways through which information is conveyed or/and integrated will help understanding interesting affective issues such as phobias, unexplained emotional modulations like blindsight or fast emotional responses recorded between 100 and 200 ms. Lastly, putting this into perspective with current emotional and perceptual models, we can state that the third interest behind this work is testing traditional versus alternate views of visual processing like whether subcortical processing as opposed to classic cortical visual processing may be enough to identify emotional cues in the scene or whether cortical visual processing is achieved in a feedforward fashion or there are, otherwise, recurrent circuits and/or backward projections.

3 Experiment 1

3.1 Introduction

A classical model of emotional responses in the brain (Ledoux, 1996) holds that the amygdala receives direct subcortical inputs through the superior colliculus and pulvinar (Day-Brown, 2010), which enables crude but rapidly processed information about fear-related cues to bypass detailed cortical processing in visual pathways (Tamietto and De Gelder, 2010). This "low-road" model for fear processing is based primarily on rodent data (Ledoux, 1996). Evidence for a fast pathway in humans has only been inferred indirectly from neuroimaging studies in healthy individuals (Garrido et al., 2012; Johnson, 2005; Reinders et al., 2006), using sub-conscious emotional stimulus presentation during functional magnetic resonance imaging (Morris et al., 1998; Pasley et al., 2004; Whalen et al., 1998), and in cortically blind patients who show preserved processing of unseen visual fear-related stimuli (Morris et al, 2001), possibly mediated by intact fiber connections between pulvinar, superior colliculus and amygdala (Tamietto et al., 2012), after damage to visual occipital areas. However, given a lack of direct electrophysiological evidence for short latency fear-related responses in human amygdala (Krolak-Salmon, 2004; Naccache et al., 2005; Brázdil et al., 2009; Oya et al., 2002), an alternative to the low-road model suggests that some cortical regions may be equally fast at processing fear as the amygdala (Vuilleumier, 2005b; Pessoa and Adolphs, 2010).

We addressed this controversy by presenting emotional (fearful, happy) and neutral faces (Exp. 1a: faces) as well as unpleasant and neutral complex visual scenes (Exp. 1b: scenes) to patients with medication-resistant epilepsy in whom stereotactic electrodes had

been implanted in the amygdala for pre-surgical evaluation. A critical experimental manipulation was that faces were presented either as normal photographs (broad spatial frequency, BSF) or were spatially filtered such that only their low (LSF) or high (HSF) spatial frequency components were displayed.

3.2 Objectives

The main objective of this experiment is shedding light over the low road hypothesis controversial lack of evidence in humans. Thus, one of the primary objects is detecting or not a fast modulation of the activity at the amygdala depending on the emotional content of the stimuli. Thus, in order to elicit such a response, we utilized facial expressions – because of the biological relevance inherent to them as social stimuli; low- and high- spatial frequency filtered versions of the stimuli –to disentangle the so called low road by inhibiting or potentiating the amount of information transmitted from the pulvinar nuclei to the amygdala; intracranial electrophysiological recordings with stereotactic electrodes at the amygdala and along the fusiform -both relevant areas when dealing with visual representation and emotional processing; and cluster based permutation statistics that offer great temporal resolution -best suited to detect fast changes like the one we want to study while effectively correcting for multiple comparison

Our first objective is therefore studying the signal from human amygdalii to explore for emotional modulations and interactions with spatial frequency. Secondary objectives, but not least important, are: confirming within the same design that such a fast emotional modulation, if any, does not occur at the same or earlier latencies in cortical regions of the visual pathway were that information may be integrated, such as the fusiform; and comparing the visual processing of emotional facial expression with more complex scenes of arousing unpleasant scenes.

3.3 Hypothesis

Because subcortical pathways are thought to carry only crude (LSF) visual input to the amygdala via magnocellular neurons (Berson, 1988; Carretié et al., 2007; Inagaki and Fujita, 2011; Schiller et al., 1979; Vuilleumier et al, 2003), we hypothesized that rapid amygdala responses to emotional faces would be restricted to those containing LSF information (*i.e.* LSF and BSF faces). Secondly, given that the low road is proposed to be a fast, automatic process requiring only the participation of subcortical structures, we anticipated that emotional modulation at cortical electrodes (fusiform) may be found at later time windows. We also expected that fast amygdala responses would occur for phylogenetically "prepared" stimuli (Seligman, 1971), such as faces, and not for more complex emotional stimuli such as arousing scenes.

3.4 Methods

3.4.1 Subjects

Participants were medication-resistant epilepsy patients (see Table 3.1) with depth electrodes surgically implanted at the Ruber International Hospital. The purpose of the procedure is solely clinical: identifying the ictal foci and addressing the risks of removing/cauterizing the targeted tissue. Implantation sites were chosen solely on the basis of clinical criteria. After surgery, patients are given rest for around ~24 hrs. The common risks of the surgical procedure are the infection of the area where the electrodes were implanted and hemorrhages, neither of which occurred. The patients remain in the Video-EEG (V-EEG) room around 4-5 days being monitored day and night by the clinical team of the V-EEG unit. During these days, we asked them to perform a battery of experimental designs we had previously designed, including memory and spatial tasks among the two tasks (Exp. 1a: faces and Exp. 1b: scenes) included in the current manuscript.

Demographics of the sample are presented in Table 3.1 including sex, handiness, level of completed studies along with etiology of the epilepsy, locus, age at onset, type of

Table 3.1. Patient demographic and clinical data. The first column indicates patient participation in Exp 1 only (no shading), Exp 2 only (grey shading) or both (black shading)

Patient	Sex	Hand-edness	Age (years)	Age (years) at onset of epilepsy	Aetiology	Lesion location	Seizure type (frequency per months)	Drugs and dose (mg)	VIQ	PIQ	Education completed	% trials with epileptic spikes in amygdala (Exp 1)	% trials with epileptic spikes in amygdala (Exp 2)
02	F	R	38	21	Hippocampal sclerosis plus focal dysplasia	Right hippocampal sclerosis plus porencephalic cyst over the parieto-occipital junction	Weekly CPS	LCS 400 LEV 3000	103	91	Tertiary	NA	0.3%
03	M	R	55	21	Focal dysplasia	Right temporal neocortex	Monthly CPS	PHT 200	132	125	Tertiary	10.6 %	NA
04	F	R	21	12	Focal dysplasia	Extensive lesion over the left frontal region involving dorsolateral and orbitofrontal cortex and anterior border of the cingulum	Daily CPS Daily SPS	CBZ 600 CNZ 3.5 LEV 1500 TOP 400	86	80	Tertiary	0.7 %	21.7%
05	M	R	29	16	Periventricular heterotopia plus focal cortical dysplasia	Bilateral occipital horn heterotopia plus focal dysplasia over the left occipital cortex	Weekly CPS Daily SPS	CBZ 1000 TOP 400	64	73	Secondary	2.6 %	0.3 %
06	M	R	49	14	Hippocampal sclerosis	Left hippocampal sclerosis	Weekly CPS Monthly SG TCS	LGT 200 CLB 30 LCS 300	115	86	Tertiary	Left 0% Right 0%	Left 0% Right 0%
08	F	R	29	8 months	Focal dysplasia	Extensive right posterior dysplasia involving the convexity and medial aspect of parietal, occipital and posterior temporal lobes	Monthly CPS	LEV 2000 LTG 500	67	71	Secondary	NA	10.6 %
10	M	R	59	26	Encephalocele plus focal cortical dysplasia	Right anterior temporal pole and basal area. Encephalocele confirmed at surgery.	Weekly CPS Monthly SG TCS	PGL 375 ECZ 1600	105	102	Tertiary	3 %	NA
13	F	R	42	16	Focal dysplasia	Right basal temporal cortex	Monthly CPS	PGL 450 LCS 400	87	88	Secondary	NA	10.6 %
15	F	R	35	16	Focal dysplasia	Left temporal pole	Daily CPS Weekly SG TCS	OXC 1200 PHT 150	97	98	Tertiary	0.4%	0%
16	M	R	30	14	Reactive gliosis, diffuse microglia activation and small vessel vasculopathy	Medial wall of the left parietal region (precuneus and posterior cingulum)	Daily CPS 4 SG TCS yearly	LCS 400 ECZ 800 LTG 300 VAL 300 CLB 20 ESC 20	102	93	Tertiary	Left 1.5% Right 1.1%	Left 0.8% Right 0%

Abbreviations: CBZ = carbamazepine; CLB = clobazam; CNZ = clonazepam; CPS = complex partial seizure; ECZ = eslicarbazepine; ESC = escitalopram; LCS = lacosamide; LEV = levetiracetam; LTG = lamotrigine; NA = Not applicable; OXC = oxcarbazepine; PGL = pregabalin; PHT = phenytoin; PIQ/VIQ = Procedural/Verbal Intelligence Quotient of the Wechsler Adult Intelligence Scale, version III (WAIS-III); SG TCS = secondary generalized tonic clonic seizure; SPS = simple partial seizure; TOP = topiramate; VAL = valproate.

crisis and drugs that had been administered lately. Note that medication was halted after the surgery for the whole stay of the patient in the V-EEG room. All the patients had completed the Wechsler Adult Intelligence Scale (WAIS) and Verbal and Perceptual Intelligence Quotients are included. In the two most right columns, the percentage of trials including spikes in the amygdala electrodes is offered for those subjects that performed Exp. 1a: faces and / or Exp. 1b: scenes.

All the patients signed informed consent and were made note that the objective of these tasks were purely experimental and it was not meant to help them with their clinical issues. The study had full approval from the Hospital Ruber Internacional Ethics Committee. Patients had normal or corrected-to-normal vision and had no history of head trauma or encephalitis. Their amygdalae were radiologically normal on pre-operative MRI. For all the patients, axial and coronal views centered on the amygdala can be seen in Figure 3.1.

Figure 3.1 Patient's coronal and transverse preoperative images

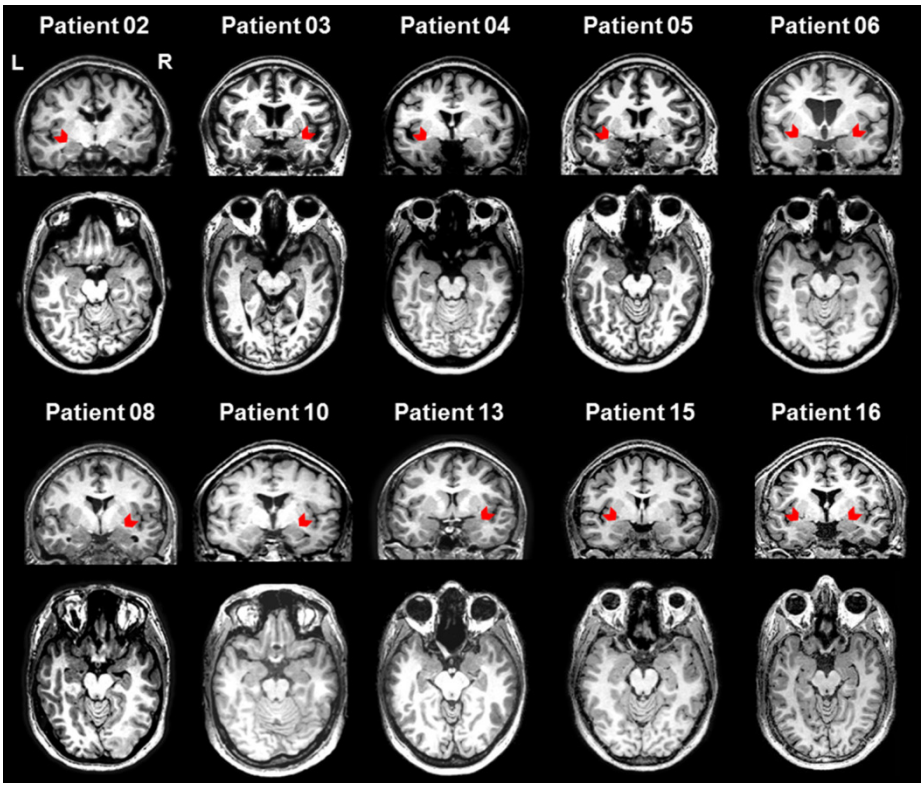

Structural magnetic resonance imaging (coronal and transverse sections) of pre-electrode insertion T1 weighted MRIs, illustrating radiologically normal amygdala in the 10 patients for which iERPs are presented. Red arrows indicate the amygdala in which stereotactic electrodes were inserted. L: left; R: right.

Some patients concurred with depression, attention deficits or alterations of the level of awareness; few were unable to perform the task satisfactorily or understand it. Only patients included in one of the two experiments are included in Table 3.1. Our inclusion criteria were physiological and behavioral. First, the V-SEEG evaluation had to find the locus of the epilepsy outside the amygdala. The amygdala electrodes had to show a normal physiological signal and be spike-free or almost spike-free (more than 75% spike-free trials). Finally, behavioral performance in the task had to be between some limits: most of the responses between 200 and 2200 ms, one button press per trial and few omissions, altogether demonstrating task engagement.

In Exp. 1a: faces, we tested 14 patients with amygdala electrodes, of whom 7 satisfied our inclusion criteria (3 right, 2 left, 2 bilateral). Of 10 patients with amygdala electrodes who met inclusion criteria on the basis of performance on the gender judgment task, 7 also had electrodes in visual areas; of whom 5 also had amygdala electrodes and met all inclusion criteria. In Exp. 1b: scenes, 12 patients with amygdala electrodes completed this task, of whom 8 satisfied our inclusion criteria (3 right, 3 left, 2 bilateral).

3.4.2 Electrodes and localisation

Stereotactic surgery or stereotaxy is a minimally invasive form of surgical intervention that makes use of a three dimensional coordinate system to locate small targets inside the brain to perform actions such as implantation.

Figure 3.2 Preoperative + postoperative image (example)

Electrode contacts in the amygdala. Coronal (left) and transverse (right) sections of pre-operative MRI from a representative patient (Patient 10). Post-operative CT images from each patient were coregistered with their corresponding pre-operative MRI scan. Insets show these coregistered images superimposed to display amygdala contacts.

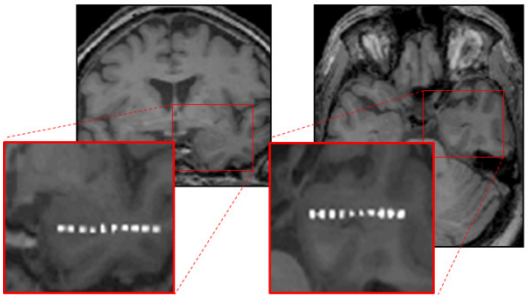

Figure 3.3 Patients preoperative + postoperative image

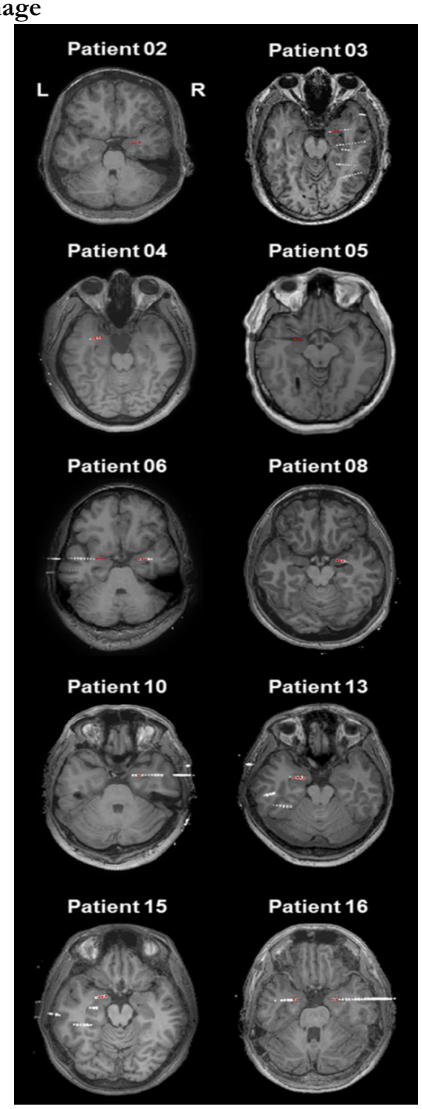

Post-operative CT images from each patient have been corregistered with their corresponding pre-operative MRI scan and superimposed to display amygdala contacts in transverse section. In the case of bilateral amygdala implantation, transverse sections are slightly rotated to enable viewing of both left and right contacts in the same cut. Electrode contacts included in each patient's averaged iERP are indicated in red. Note that post-operative CT quality for Patient 05 precluded adequate corregistration, thus for this patient electrode contacts were localised on post-operative MRI scan (electrode trajectory is visible in the left temporal lobe and correctly targets the amygdala on that side).

A contrast enhanced MRI was performed pre-operatively under stereotactic conditions to map vascular structures prior to electrode implantation and to calculate stereotactic coordinates for trajectories using the Neuroplan system (Integra Radionics, Burlington, USA). DIXI Medical (Besancon, France) Microdeep depth electrodes (multicontact, semi rigid, diameter 0.8mm, contact length 2mm, inter-contact isolator length 1.5mm) were implanted based on the stereotactic Leksell method. This method uses a polar coordinates system (also called spherical) instead of a Cartesian coordinate system (also called translational) and it is easier to use and calibrate in the surgery room. Electrode localisation was performed by comparing pre and post- operative pictures. Figure 3.2 shows the output of a representative subject for illustration.

To take advantage of the visibility of individual electrode contacts on computed tomography (CT) images, for each patient we co-registered the pre-electrode placement T1-weighted magnetic resonance images (pre-MRI) to post-electrode placement CT (post-CT) whole-brain volumes. MRIs were acquired on a 3 Tesla Signa HDx GE scanner (GE Healthcare, Waukesha, WI,

USA). To optimise this co-registration, both brain images were first skull-stripped (removed from the skull and other non-brain tissue like dura and eyes). For CTs this was done by filtering out all voxels with signal intensities between 100 and 1300HU. Skull stripping of the pre-MRI proceeded by first spatially normalising the image to MNI space employing the "New Segment" algorithm in SPM8 (http://www.fil.ion.ucl.ac.uk/spm). The resultant inverse normalisation parameters were then applied to the brain mask supplied in SPM8 (a volume that is used to weight the spatial normalization so that the final solution is not influenced by voxels outside the brain) to transform the brain mask into the native space of the pre-MRI. All voxels in pre-MRI lying outside the brain mask and possessing a signal value in the highest 15th percentile were filtered out. The skull-stripped pre-MRI was then co-registered and re-sliced to the skull-stripped post-CT. Next, the pre-MRI was affine normalized to the post-CT, thus transforming the pre-MRI image into native post-CT space. The two images were then overlaid, with the post-CT thresholded such that only electrode contacts were visible. Figure 3.3 shows the electrodes of each subject over CT images.

3.4.3 Stimuli.

3.4.3.1 Experiment 1a: faces

We compiled faces of 139 different actors (70 female) posing fearful, happy, and neutral expressions from three databases: the Karolinska Directed Emotional Faces database (KDEF; Karolinska, Lundqvist, Flykt and Öhman, 1998; 35 females and 35 males), the Radboud Faces database (RaFD; Langner et. al., 2010; 19 females and 20 males) and the Warsaw Set of Emotional Facial Expression Pictures (WSEFEP; Olszanowski et. al., 2015; 16 females and 14 males). Eye gaze of all face stimuli was directed forward. Images were grey-scaled and enclosed in a rectangular frame (198×251 pixels) excluding most hair and background and cropped. Spatial frequency content in the original stimuli (BSF) was filtered using a high-pass cut-off of >24 cycles/image for HSF stimuli, and a low-pass cut-off of <6 cycles/image for LSF stimuli (using Matlab, The Mathworks, Inc., Natick, Massachusetts). Figure 3.4 represents the nine types of stimuli arranged for all the

levels of our two factors - emotion: fearful, happy and neutral; and frequency: BSF; HSF and LSF.

Figure 3.4 Experiment 1a: faces; stimuli

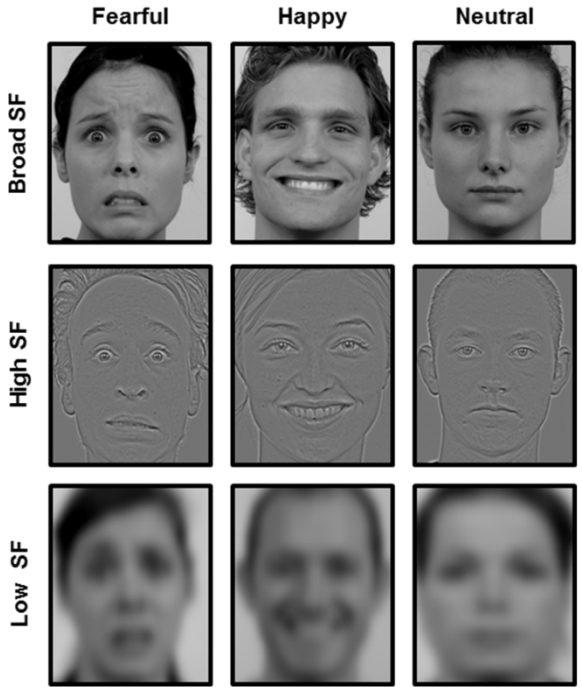

Examples of broad, low, and high SF faces with neutral, fearful, or happy expressions presented in Exp 1. Note that each stimulus was identity-unique (*i.e.*, a different actor for each of the 135 faces presented).

Presented faces subtended a visual angle of 7.4º, resulting in spatial frequency cut-offs of 3.24 and 0.81 cycles/degree for HSF and LSF, respectively. Lastly, overall luminance was equated across different spatial frequencies. For each patient, 135 different identities (out of the 139 that composed the whole set) were randomly selected for presentation. Each of the 135 identities was pseudorandomly assigned to one of the nine possible conditions: BSF fearful, HSF fearful, LSF fearful, BSF happy, HSF happy, LSF happy, BSF neutral, HSF neutral and LSF neutral faces. Thus, each condition was composed of 15 different identities, unique to that condition. Pseudo-randomisation proceeded such that either 8 or 7 identities shared gender within each condition. Once the 135 faces were selected, their order of presentation was randomized. The task was repeated twice. In the second block, performed ten minutes after the first, the same stimuli as the first block were presented but in a different pseudo-random order.

3.4.3.2 Experiment 1b: scenes

Patients were presented with 40 emotional and 80 neutral color pictures. These were drawn at random from a pool of 80 high-arousing unpleasant (mutilations and attack) scenes selected from the International Affective Picture System (IAPS; Lang, Bradley and Cuthbert, 2005), and 160 low-arousing neutral pictures: 149 taken from the IAPS (household scenes and neutral persons) and eleven neutral landscape pictures taken from the world-wide web. Figure 3.5 shows two sample pictures for each of the emotional categories. Mean normative IAPS picture ratings on a 9-point scale for valence were 5.05 (s.e.m. = 0.05) for neutral, and 2.04 (s.e.m. = 0.05) for unpleasant pictures. Mean arousal ratings were 3.29 (s.e.m. = 0.06), and 6.3 (s.e.m. = 0.07) for neutral and unpleasant pictures, respectively. Note that in both Exp. 1a and Exp. 1b, the ratio of negative emotional to non-negative stimuli is 1:2.

Figure 3.5 Experiment 1b: scenes; stimuli

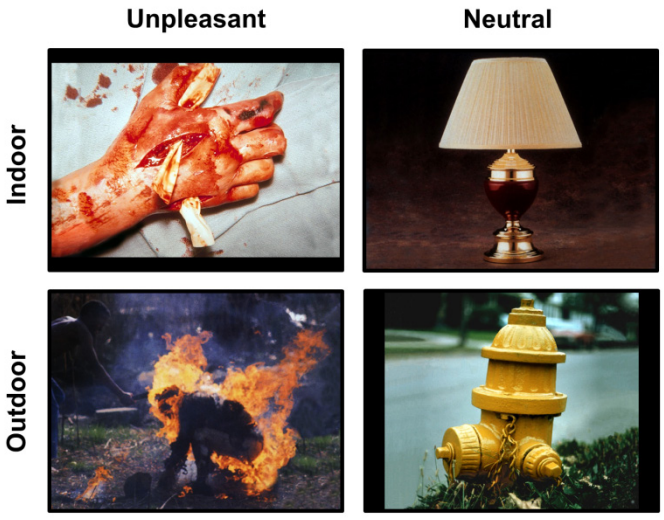

Examples of unpleasant and neutral complex visual scenes presented in Exp 1b. Top- and bottom-row correspond to expected indoor and outdoor responses.

3.4.4 Procedure

3.4.4.1 Experiment 1a: Faces

Experiments were conducted during the second post-operative day. All patients were seizure free for the previous 12h. In each of 2 experimental blocks, faces were centrally displayed on an LCD computer screen (using Matlab with Cogent2000 toolbox; http://www.vislab.ucl.ac.uk/cogent_2000.php) for 500 ms followed by a fixation cross for 3500 ms. Patients were required to make a gender judgment, via button press, for each face. Patients remained as still as possible attending to the center of the screen while avoiding verbalizations and minimizing eye-blinks A visual representation of the experimental procedure can be seen in Figure 3.6, panel A.

Figure 3.6 Experiment 1b: scenes; stimuli

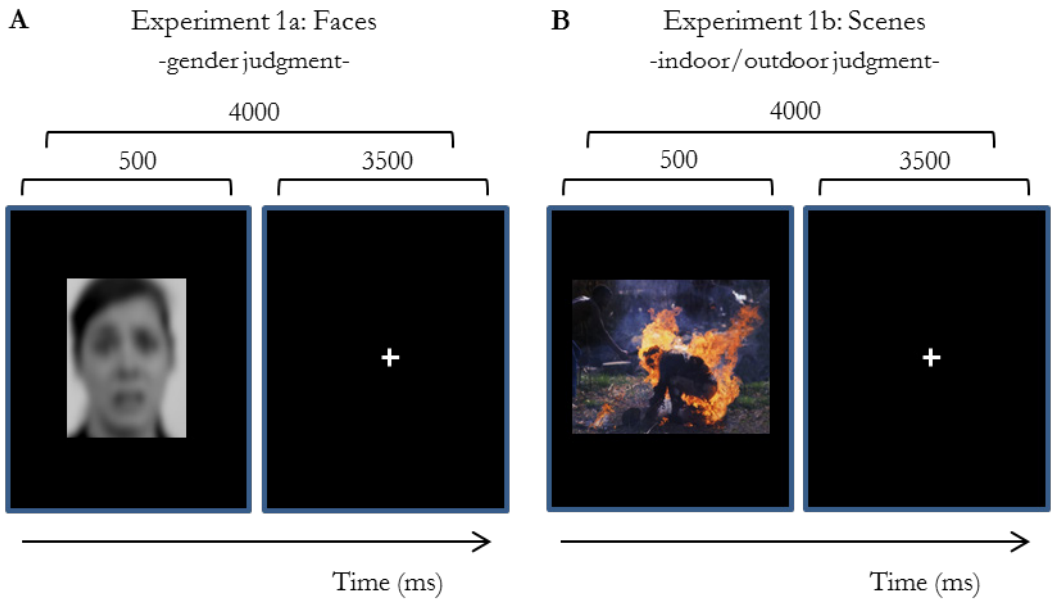

Each panel shows one typical trial for one of the experimental tasks. Panel A: illustration of the experimental procedure for Experiment 1a (task: gender judgment). Panel B: illustration of the experimental procedure for Experiment 1b (task: outdoor/indoor judgment).

3.4.4.2 Experiment 1b: Scenes

This experiment was conducted during the third post-operative day. Emotional and neutral pictures were presented pseudo-randomly (presentation time 500 ms; ISI 3500 ms) with the constraint that emotional pictures were separated by at least one neutral picture. Patients were required to make an indoor-outdoor judgment to each picture via button-press. Prior to signing informed consent, patients were shown one example of an unpleasant IAPS picture and instructed that they would see similar pictures both on that day and the next (patients saw the same pictures again the next day during a recognition memory test, the results of which will be reported elsewhere). A visual representation of the experimental procedure can be seen in Figure 3.6, panel B.

3.4.5 Acquisition and preprocessing

Ongoing intracranial EEG (iEEG) activity was acquired using an XLTEK EMU128FS amplifier (XLTEK, Oakville, Ontario, Canada). iEEG data were recorded at each electrode contact site at a 500 Hz sampling rate (online bandpass filter 0.1-150 Hz) and referenced to linked mastoid electrodes. The accuracy of stimulus onset latencies was first measured with a photo-diode and a light-to-voltage converter (TKK Brain Research Unit), and latency uncertainty found to be in the range of 2 ms.

3.4.6 Behavioral task analysis.

3.4.6.1 Experiment 1a: faces

As long as gender judgment is an implicit task we were interested in the emotional and/or spatial frequency modulations rather than the performance. In addition, we had a somewhat low number of stimuli per condition. Hence, in order to increase our signal-to-noise ratio, all the trials on which subjects gave one and only one answer were considered valid and their epochs included in the electrophysiological analysis. We report the mean reaction times for both the valid trials (those on which subjects pressed *any* one of the two buttons once and only once between 200 ms and 2200 ms) and the correct trials (those on which subjects pressed the *correct* button once and only once between 200 and 2200 ms). Table 3.2 shows the average reaction time of all the valid trials and the number of not valid trials (none or more than one button press). Tables 3.3 and 3.4 show respectively the average reaction time and accuracy ratings of the correct trials. The results were

analyzed statistically by means of a repeated measures ANOVA with factors emotion (three levels: fearful, happy and neutral) and frequency (three levels: BSF, HSF and LSF) and post-hoc t-tests were conducted were necessary

Table 3.2: Experiment 1a: faces reaction times (valid trials)

Patient	BSF Fearful	HSF Fearful	LSF Fearful	BSF Happy	HSF Happy	LSF Happy	BSF Neutral	HSF Neutral	LSF Neutral	# Missed Responses
03	604 (22)	651 (37)	649 (48)	656 (55)	616 (29)	613 (29)	604 (30)	676 (31)	623 (27)	6
04	821 (88)	788 (50)	897 (82)	738 (44)	978 (109)	863 (85)	777 (53)	888 (71)	749 (48)	1
05	674 (56)	694 (27)	705 (53)	667 (46)	684 (45)	652 (28)	676 (48)	624 (24)	674 (30)	3
06	724 (56)	918 (93)	921 (110)	703 (72)	962 (118)	1057 (155)	688 (33)	780 (61)	811 (87)	2
10	1453 (71)	1540 (59)	1416 (67)	1392 (55)	1516 (64)	1387 (53)	1424 (99)	1563 (80)	1452 (85)	1
15	783 (56)	859 (55)	817 (53)	844 (40)	903 (51)	922 (57)	776 (62)	915 (71)	898 (71)	2
16	814 (71)	922 (88)	892 (78)	974 (133)	891 (68)	949 (97)	794 (56)	910 (88)	926 (100)	1
Mean	839 (107)	910 (112)	900 (95)	853 (99)	936 (110)	920 (98)	820 (104)	908 (118)	876 (105)	2.3 (0.7)

Experiment 1a: faces *valid* trials behavioural data. Valid trials were those on which the patient answered just once within a certain poststimulus time frame. Reaction times are shown in milliseconds (standard error means in parenthesis). Rows: patients; columns: condition. Bottom row: patient's average reaction time in milliseconds per condition (standard error means in parenthesis). Right most column: absolute number of *non*-valid responses (misses: patient did not succeed in pressing either just any button or any button at all within 200 – 2200 ms

Table 3.3: Experiment 1a: faces reaction times (correct trials)

Patient	BSF Fearful	HSF Fearful	LSF Fearful	BSF Happy	HSF Happy	LSF Happy	BSF Neutral	HSF Neutral	LSF Neutral
03	604 (22)	657 (39)	639 (43)	656 (55)	628 (28)	615 (31)	603 (29)	675 (34)	626 (28)
04	821 (88)	788 (50)	822 (62)	738 (44)	978 (109)	851 (85)	770 (53)	888 (72)	765 (49)
05	674 (56)	694 (27)	679 (37)	667 (46)	690 (48)	654 (29)	694 (49)	613 (22)	677 (31)
06	727 (58)	935 (100)	961 (128)	671 (33)	942 (139)	1055 (173)	691 (34)	823 (60)	765 (59)
10	1437 (72)	1531 (60)	1415 (72)	1393 (60)	1473 (52)	1346 (44)	1432 (103)	1556 (84)	1408 (82)
15	783 (56)	866 (56)	826 (58)	844 (40)	898 (53)	932 (61)	780 (63)	915 (74)	881 (71)
16	812 (75)	914 (93)	905 (83)	974 (133)	907 (71)	954 (101)	794 (56)	886 (92)	937 (104)
Mean	837 (104)	912 (111)	892 (97)	848 (101)	930 (103)	916 (94)	823 (105)	908 (116)	865 (99)

Experiment 1a: faces *correct* trials average reaction times in milliseconds (standard error means in parenthesis). Correct trials were those valid trials on which the performance on the gender judgment task was accurate. Rows: patients; columns: condition. Bottom row: patient's average reaction time per condition

Table 3.4: Experiment 1a: faces; error rates (correct trials)

Patient	BSF Fearful	HSF Fearful	LSF Fearful	BSF Happy	HSF Happy	LSF Happy	BSF Neutral	HSF Neutral	LSF Neutral
03	0	3	4	0	4	2	4	4	1
04	1	0	4	0	0	1	2	1	2
05	0	1	3	0	4	2	4	2	1
06	3	4	5	3	7	3	2	4	6
10	5	4	2	3	5	8	1	3	8
15	0	2	6	0	2	5	1	3	4
16	2	3	2	0	4	1	0	3	1
Mean	1.57 (0.63)	2.43 (0.5)	3.71 (0.50)	0.86 (0.49)	3.71 (0.74)	3.14 (0.85)	2 (0.51)	2.86 (0.36)	3.29 (0.94)

Experiment 1a: faces *correct* trials number of errors per condition. Correct trials were those valid trials on which the performance on the gender judgment task was accurate. Rows: patients; columns: condition. Bottom row: patient's absolute number of errors (standard error means in parenthesis).

3.4.6.2 Experiment 1b: scenes

Exp. 1b was at the same the study session of a 2-day memory experiment of whom the test session, that patients were not aware off, was performed after 24 hours (not included in this manuscript). Thus, we did not analyze the accuracy in the task – indoor/outdoor judgments. Same as Exp. 1a: faces, those trials including one and only one button press between 200 and 2200 ms were considered valid and included in the behavioral and electrophysiological analysis. Average reaction times for all the valid trials are included in Table 3.6. Difference between conditions (unpleasant and neutral) was analyzed by means of a t-student statistical test.

Table 3.5: Experiment 1b: scenes; reaction times (valid trials)

Patient	Unpleasant	Neutral	# Missed Responses
02	1587 (77)	1564 (52)	2
04	1543 (93)	1361 (53)	0
05	1394 (119)	1396 (71)	1
06	1236 (102)	1147 (58)	0
08	837 (49)	802 (25)	4
13	1237 (78)	1025 (45)	1
15	733 (23)	783 (25)	2
16	1615 (99)	1349 (53)	1
Mean	1273 (119)	1178 (102)	1.4 (0.5)

Experiment 1b: scenes *valid* trials average reaction times in milliseconds (standard error means in parenthesis). Rows: patients; columns: condition. Bottom row: patient's average reaction time in milliseconds per condition (standard error means in parenthesis). Right most column: absolute number of *non*-valid responses (misses: patient did not succeed in pressing either just any button or any button at all within 200 – 2200 ms poststimulus

3.4.7 Electrophysiological statistical analysis

3.4.7.1 Experiment 1a: faces

Of 14 patients with amygdala electrodes who completed the task, two patients did not meet our criteria for spike-free trials (75%) and were thus excluded. A further two patients were excluded due to poor task engagement (12% and 38% trials in which responses were omitted respectively, compared to an average 0.96% across all other patients). One patient was excluded due to the presence of large amplitude slow oscillations during recording. Lastly, electrophysiological responses from one patient did not demonstrate any discernible stimulus-evoked components during the 640 ms post-onset interval. Data from this patient were also excluded. Thus, we analyzed iERPs from nine amygdalae from seven patients (3 left-sided, 2 right-sided and two bilaterally implanted). As mentioned before, patient demographics and clinical details are given in Table 3.1. Although Patient 05 has procedural and verbal IQ in the borderline and extremely low range, respectively, this patient's gender judgment performance is comparable to that of other patients (Tables 3.2-3.4).

The preprocessing steps were the following. For each amygdala contact, experimental condition, and patient, epochs from -200 to 640 ms peri-stimulus time were extracted from continuous iEEG data. Epochs containing epileptiform activity or artifacts (large amplitude slow wave drifts or high frequency activity) were rejected by trial-by-trial visual inspection, as were epochs corresponding to absent or multiple behavioral responses. Epochs were then detrended, baseline corrected (100 ms pre-stimulus baseline) and no filter was applied. We did not filter the data to avoid filter effects that may distort waveforms and hence introduce latency artifacts. For each experimental condition, data were then averaged across the two blocks. In the case that there was more than one contact within the amygdala, data from all contacts were averaged within trial for that amygdala.

To analyze the amygdala iERPS, we applied a cluster-based non-parametric permutation statistic (explained in the next paragraph), based on MANOVA *F* values with within-subject factors of emotion (fear, happy, neutral) and spatial frequency (BSF, LSF, HSF), to determine the time points of significant interaction between emotion and spatial frequency with respect to iERP amplitude. Next, to explore the differences in each

significant time cluster (for main effects and interaction), the mean amplitude values for each subject and each condition across the significant clusters were computed for each effect and tested with post-hoc *t*-tests. Finally, we applied cluster-based permutation statistics on the iERP to each of the 9 face stimulus types separately, to test a null hypothesis of deflections being equal to zero for the entire post-stimulus period.

The cluster-based permutation approach effectively corrects the family-wise error rate in the context of multiple comparisons of latency bins (Maris and Oostenveld, 2007). Under the null hypothesis of no differences between levels of each test (main effects of emotion or spatial frequency, and their interaction), the amplitude values can be permuted between conditions. After a permutation step, a MANOVA is calculated at each dataset (in this case, time bin) and clusters of correspondingly changing time-points are created. In the current case significant time-clusters were formed by temporal adjacency of supra-threshold effects (a cluster contained at least two significant neighbors along the time dimension). We did two analyses with different cluster threshold levels ($P < 0.01$ and $P < 0.05$). For each cluster, the MANOVA *F*-values (Wilk's lambda) of the corresponding test are summed and the greatest sum among all clusters entered into the permutation distribution. Note that as the permutation distribution is a data driven non-parametric distribution, no degrees of freedom are given. Permutation steps were repeated 1000 times and permutation distributions for main effects and interactions created. Initially, empirical cluster sums of MANOVA *F*-values that were greater than the 99th centile within the permutation distribution were considered as significant temporal clusters of emotion/spatial frequency main effects or interaction. We next applied a less conservative cluster threshold of $P < 0.05$ and repeated the permutation testing. All pre-processing steps and permutation statistics were done using the Fieldtrip toolbox (http://fieldtrip.fcdonders.nl/) and R software for statistical computing (the MANOVA with two within-subject factors was calculated using R; http://R-project.org; Code).

Further exploring of repetition effects and laterality differences in the amygdala iERPs was conducted as following. To specifically verify whether amygdala iERPs are modulated by repetition in our paradigm, we performed an additional MANOVA for the mean amplitude across the time windows indicated by the cluster based permutation analysis, including a within-subject factor 'block'. To test for a laterality effect on the time window expressing an emotion by spatial frequency interaction we entered the mean

difference scores across this time window for each emotion contrast, collapsed across broad and low spatial frequencies, into a Kruskal-Wallis test comparing right *vs.* left amygdalae.

Of 10 patients with amygdala electrodes who met inclusion criteria on the basis of performance on the gender judgment task, also had electrodes in visual areas. Identical data pre-processing steps were employed for these iEEG data as for amygdala contacts, with one patient rejected for not meeting criterion for spike-free trial number. Of these 5 patients, two had two different electrodes in the area of interest, yielding in total seven groups of fusiform contacts.

In a first analysis, we provide an index of face-selectivity for these fusiform contacts by comparing responses to broadband neutral faces relative to neutral scenes (presented in Exp. 1b described above). Of the 7 contact groups in the fusiform one was excluded from analyses due to signal artifact in Exp. 1b, thus iERPs from six contact groups were compared at the group level using cluster-based permutation analysis statistics with a cluster threshold of $P < 0.01$ ($n = 6$ groups of contacts). Note that some neutral IAPS pictures (18%) contained human faces embedded within the scenes, which were removed from this analysis.

Then, iERP of Exp. 1a: faces from the 7 groups of fusiform contacts were entered into the same cluster-based permutations statistics as applied to amygdala contact data (again with cluster threshold of $P < 0.01$ followed by $P < 0.05$). Also in the same fashion, post-hoc tests were performed were necessary employing the average value during each particular time window. To test for latency effects of BSF and LSF fearful faces employing non-corrected statistics, we compared iERPs for each stimulus type relative to zero in *two-tailed* one-sample t-tests. Only time clusters with more than 4 adjacent data points (i.e. at least 10 ms) are considered significant.

Further analyses were performed to compare amygdala and fusiform iERPs. For the 4 patients who completed Exp. 1a task with implanted electrodes in both the amygdala and fusiform cortex, we compared emotional face responses between these two areas in the time window expressing an early fearful emotion by SF interaction with the following non-parametric tests: we calculated the mean amplitude difference between emotions (fear *vs.*

happy, fear *vs.* neutral and happy *vs.* neutral) across the window, collapsing over broad and low spatial frequency. This was done for both the amygdala and fusiform gyrus, separately. These six difference values (three emotion differences for the amygdala and fusiform contacts, respectively) for each of the 4 patients were entered into a Friedman test Emotion by Region. The three differences of each site were also entered in two separate Friedman tests exploring Emotion.

3.4.7.2 Experiment 1b: scenes

Of 12 patients who completed the task, 8 met all inclusion criteria. Two patients were excluded due to poor push-button response rate (36% and 28% trials in which responses were omitted compared to 1.15% mean omissions for the 8 patients included in the analysis). A further 2 patients did not meet our criteria for spike-free trials (75%). Despite borderline and extremely low range IQs of Patients 05 and 08, these patients' RTs on the indoor/outdoor task are comparable to other patients' (Table 3.5). After spike and artifact rejection, data preprocessing was as for Exp. 1a: faces; epochs of unfiltered data were detrended and baseline corrected (100 ms pre-stimulus baseline). For statistical comparison of evoked responses, we applied the same cluster-based permutation approach as for Exp. 1a, but a paired *t*-test was used as the initial cluster statistic to compare emotional versus neutral pictures. To calculate the time windows for which iERPs to both picture types differ significantly from zero, we employed the same procedure as in Exp. 1a.

To formally test for a difference between fast amygdala responses to fearful faces and emotional scenes, we compared mean amplitudes of iERPs from Exp. 1s *vs.* Exp. 1b in the time cluster exhibiting an early facial emotion by frequency interaction. That is, we tested for a difference between early responses to fearful relative to neutral faces *vs.* the response in the same early time window for emotional relative to neutral IAPS scenes (for this analysis we collapsed broadband and LSF face trials). In a first analysis, we entered the normalized mean amplitudes from all amygdalae in both experiments (9 from Exp. 1a and 10 Exp. 1b) into a repeated-measure ANOVA with within-subject factor emotion (negative, neutral) and between-subject factor experiment (Exp. 1a and Exp. 1b).

For the 4 patients with electrodes in the fusiform gyrus who completed both Exp. 1a and Exp. 1b evoked responses to BSF neutral faces recorded in Exp. 1a were compared

to those evoked by neutral scenes in Exp. 1b, again employing cluster-based permutations statistics with a cluster threshold of $P < 0.01$ ($n = 6$ groups of contacts). Note that some neutral IAPS pictures (18%) contained human faces embedded within the scenes, which were removed from this analysis.

3.5 Results

3.5.1 Experiment 1a: faces

Cluster-based permutation testing using multivariate analysis of variance (MANOVA) with within-subject factors of emotion (fearful, happy, neutral) and spatial frequency (broadband, HSF, LSF) was applied to all post-stimulus time points with a 0.01 and a less restrictive 0.05 cluster thresholds. The results are summarized in Table 6. Figure 6, panels A-C show different representations of the average amygdala iERPs: of fearful, happy and neutral faces collapsed across spatial frequency overlaid with the clusters of statistical significance (panel A), of only faces containing LSF frequencies (fearful, happy and neutral BSF+LSF faces; panel B) and of all the fearful faces (panel C).

A cluster expressing a significant emotion by spatial and frequency interaction was observed between 72-108 ms (cluster threshold $P < 0.01$) and between 66-118 ms (at a cluster threshold of $P < 0.05$) after face presentation (for the cluster at $P < 0.01$, summed F-value = 640.82, $P < 0.001$; for the cluster at $P < 0.05$, summed F-value = 704.09, $P < 0.001$; Figure 3.7, panel A; Table 3.6).

Figure 3.7: Experiment 1a: faces; amygdala iERPs

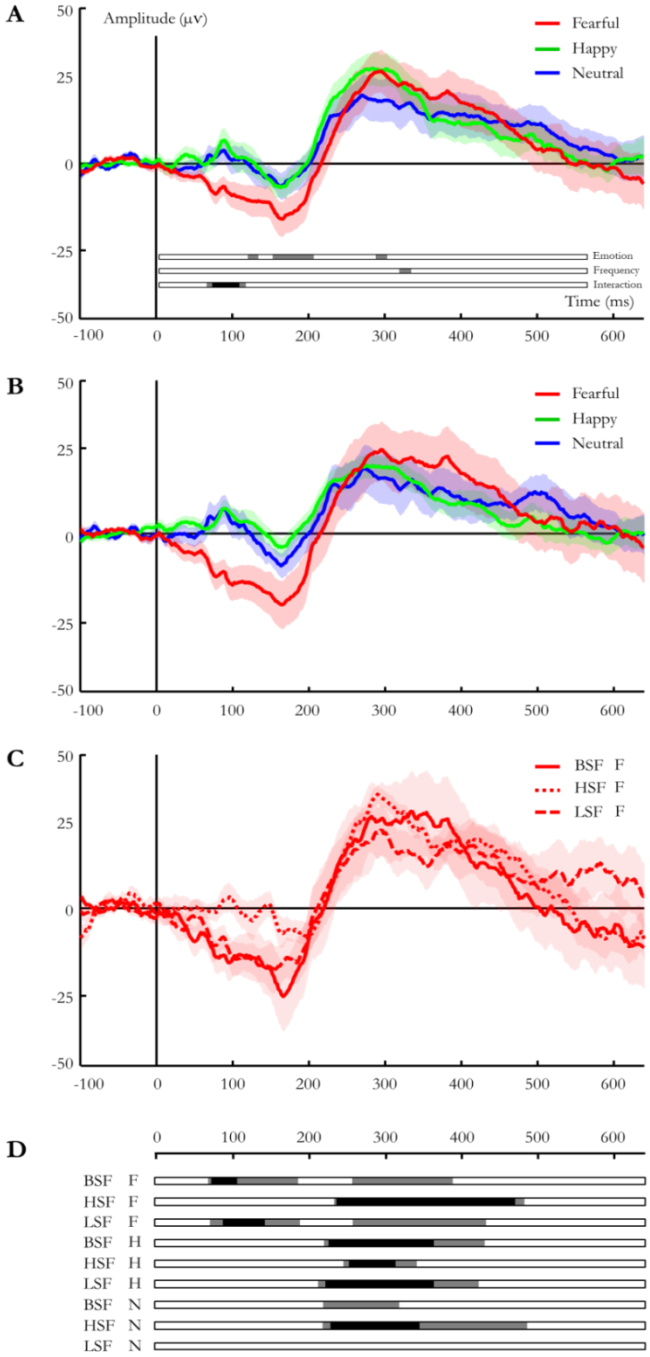

Panel A: Amygdala iERPs to fearful, happy and neutral faces, collapsed over spatial frequencies (Exp. 1a) and averaged from nine amygdalae of seven patients. Horizontal bars below depict time clusters expressing a significant main effect of emotion (top), spatial frequency (middle) or a significant interaction (bottom) using a cluster threshold of $P < 0.05$ (grey) or $P < 0.01$ (black). An emotion by spatial frequency interaction is observed from 66-118 ms post-stimulus onset (at cluster threshold $P < 0.05$; and from 72-108 ms at cluster threshold $P < 0.01$). A significant main effect of emotion is observed in time clusters from 118-132 ms, 150-204 ms and 288-302 ms, and main effect of spatial frequency from 318-334 ms (all at cluster threshold $P < 0.05$). Note that post-acquisition filtering has not been applied to the iERPs plotted here and shaded error bars indicate s.e.m. here and in all subsequent figures. Panel B **a**mygdala iERPs to emotional and neutral faces, collapsed over BSF and LSF only. Panel C amygdala iERPs to fearful broad, low and high SF faces. Panel D **h**orizontal bars depict time windows in which responses to each stimulus type are significantly different from zero with a cluster threshold of $P < 0.05$ (grey) or $P < 0.01$ (black).

Table 3.6: Experiment 1a: faces; amygdala cluster permutation statistics

Effect	Time window (ms)	Condition	Mean amplitude (μV)	
		Cluster threshold $P < 0.01$		
Emotion by Spatial Frequency Interaction	72 - 108 [F_{summed} = 640.82, P = 0.001]	BSF Fearful	-14.1	(4.7)
		HSF Fearful	0.9	(3.3)
		LSF Fearful	-11.5	(4.3)
		BSF Happy	2.5	(6.6)
		HSF Happy	-3.7	(4.2)
		LSF Happy	12.3	(4.3)
		BSF Neutral	5.5	(4.5)
		HSF Neutral	-2.7	(6.1)
		LSF Neutral	3.7	(8.1)
		Cluster threshold $P < 0.05$		
Emotion by Spatial Frequency Interaction	66 - 118 [F_{summed} = 704.09, P = 0.001]	BSF Fearful	-13.7	(4.8)
		HSF Fearful	0.3	(3.2)
		LSF Fearful	-11.8	(4.2)
		BSF Happy	1.4	(6.8)
		HSF Happy	-4.0	(4.1)
		LSF Happy	11.8	(4.4)
		BSF Neutral	5.3	(4.5)
		HSF Neutral	-2.2	(6.1)
		LSF Neutral	2.9	(7.8)
Main effect Emotion	118 – 132 [F_{summed} = 83.79, P = 0.004]	Fearful	-10.7	(2.6)
		Happy	0.6	(4.1)
		Neutral	-1.1	(3.7)
Main effect Emotion	150 – 204 [F_{summed} = 220.53, P = 0.001]	Fearful	13.0	(5.0)
		Happy	-3.9	(3.2)
		Neutral	-3.8	(3.9)
Main effect Emotion	288 – 302 [F_{summed} = 48.32, P = 0.024]	Fearful	26.2	(6.1)
		Happy	27.0	(4.7)
		Neutral	18.2	(6.1)
Main effect Spatial Frequency	318 – 334 [F_{summed} = 53.72, P = 0.014]	BSF	23.8	(7.6)
		HSF	22.2	(3.7)
		LSF	16.1	(4.7)

Mean amygdala iERP amplitudes (standard error mean in parenthesis) in Exp 1a for each condition for the time windows of the clusters showing significant effects are included in two last columns. Results of the cluster based permutation statistics are also shown. First column: type of effect tested; second column: span over time of the significant cluster and statistics. *F* and *t*-values pertaining to summed values over the significant time clusters. Note that results corresponding to both cluster thresholds ($P < 0.01$ and $P < 0.05$) are shown separately.

To determine the origin of this interaction, we performed post-hoc *t*-tests comparing iERP amplitudes across the interaction time cluster (at cluster threshold $P < 0.01$) for specific emotion and spatial frequency conditions (Table 3.7). Critically, responses to BSF and LSF fearful faces were significantly different to responses to neutral and happy faces. In addition, amygdala responses to BSF and LSF fearful faces did not differ, but, critically, were both significantly different from HSF fearful face responses (see Table 3.7).

Table 3.7: Experiment 1a: faces; amygdala early interaction window post-hocs

Time	Level	Comparison	Statistic	*P*-value
72-108 ms	BSF	**Fear *vs.* Neutral**	t_8 = -3.41	P = 0.005
		Fear *vs.* Happy	t_8 = -1.93	P = 0.045
		Happy *vs.* Neutral	t_8 = -0.36	P = 0.366
	HSF	Fear *vs.* Neutral	t_8 = 0.67	P = 0.260
		Fear *vs.* Happy	t_8 = 1.03	P = 0.166
		Happy *vs.* Neutral	t_8 = -0.15	P = 0.444
	LSF	Fear *vs.* Neutral	t_8 = -1.70	P = 0.064
		Fear *vs.* Happy	t_8 = -3.74	P = 0.009
		Happy *vs.* Neutral	t_8 = 1.01	P = 0.172
	FEAR	**BSF *vs.* HSF**	t_8 = -3.56	P = 0.004
		LSF *vs.* HSF	t_8 = -2.22	P = 0.029
		BSF *vs.* LSF	t_8 = -0.62	P = 0.276

Exp. 1a post-hoc t-tests for mean amygdala iERP amplitudes across the time-window for the early emotion by spatial frequency interaction (cluster threshold $P < 0.01$). Significant comparisons are highlighted in bold (one-tailed given *a priori* hypothesis for fear-specific amygdala responses).

To determine the onset of deflections to each face stimulus type individually, we again applied cluster-based permutation statistics to test for the onset of deflections significantly different from zero for each face stimulus type separately for the entire post-stimulus period. The results of the negative and positive going t-tests are visually represented in Figure 3.7, panel D. Particularly, significant fast latency effects beginning ~70 ms after face presentation, are limited to BSF and LSF fearful face responses. For BSF fearful faces from 72-102 ms at cluster threshold $P < 0.01$, summed t-value = -145.67; $P = 0.045$, and from 66-186 ms at cluster threshold $P < 0.05$; for LSF fearful from 92-146 ms at cluster threshold $P < 0.01$, summed t-value = -170.94; $P = 0.044$, and from 70-192 ms at cluster threshold $P < 0.05$.

Next, given that we recorded from 4 right and 5 left hemisphere amygdalae, respectively, we separated iERPs as a function of hemisphere. Figure 3.8 shows average iERPs of right and left amygdalae separately for all the spatial frequencies and for BSF and LSF faces collapsed. No significant laterality effects were observed (right *vs.* left amygdalae tests for fearful minus neutral faces $\chi^2(1) = 2.16$; $P = 0.14$; fearful minus happy $\chi^2(1) = 0.06$; $P = 0.81$; happy minus neutral $\chi^2(1) = 0.24$; $P = 0.62$).

Figure 3.8: Experiment 1a: faces; amygdala iERPs by hemisphere

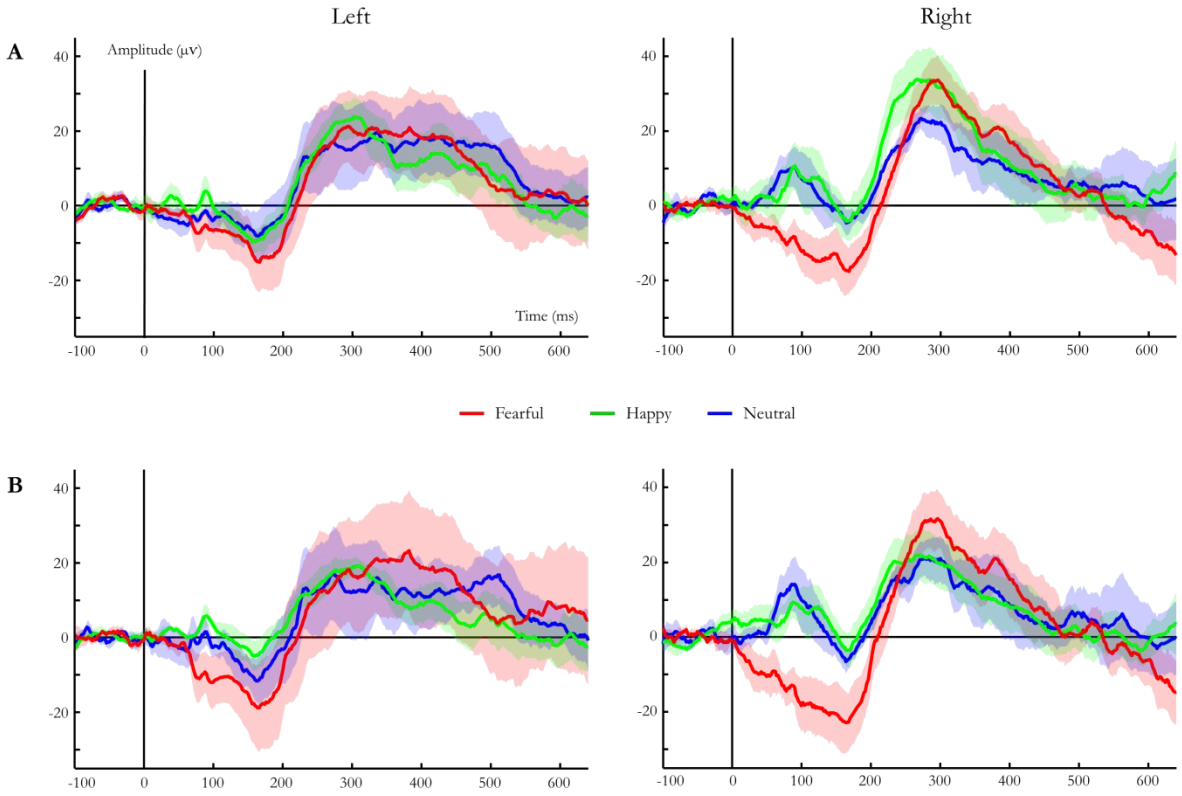

Averaged iERPs to (**a**) all spatial frequency and (**b**) broadband and LSF faces are plotted for fearful, happy, and neutral faces separately for both pools of left ($n = 5$) and right ($n = 4$) amygdala electrodes..

The emotion (fearful, happy, neutral) by spatial frequency (BSF, HSF, LSF) cluster-based permutation MANOVA test with a less conservative cluster threshold of $P < 0.05$ also reveals a relatively early main effect of emotion in two time clusters – between 118-132 ms and 150-204 ms – as well as a later effect of emotion at 288-302 and of frequency at 318-334 ms. The significant clusters are represented in Figure 3.7, panel A. The statistical results are summarized in Table 3.6. Table 3.8 summarizes the post-hoc comparisons in the emotion and frequency main effects time windows. Irrespective of frequency, responses to

fearful faces in the 118-132 and 150-204 ms time windows differed significantly from that to both neutral and happy faces, whereas happy face responses did not differ from those to neutral faces. In the later time window, 288-302 ms, responses to fearful faces were significantly different from responses to neutral faces but not from responses to happy faces, and responses to happy faces were not significantly different from responses to neutral faces. In the main frequency window, BSF faces seem to be different from LSF and HSF faces (more for the former than the later) but post-hoc comparison were not significant.

Table 3.8: Experiment 1a: faces; amygdala main effects post-hoc

Time	Level	Comparison	Statistic	Probability
118 - 132	Emotion	**Fearful *vs.* Happy**	t_8 = -2.35	P = 0.047
		Fearful *vs.* Neutral	t_8 = -3.20	P = 0.006
		Happy *vs.* Neutral	t_8 = 0.84	P = 0.424
150 - 204	Emotion	**Fearful *vs.* Happy**	t_8 = -2.46	P = 0.039
		Fearful *vs.* Neutral	t_8 = -4.21	P = 0.003
		Happy *vs.* Neutral	t_8 = -0.04	P = 0.971
288 – 302	Emotion	Fearful *vs.* Happy	t_8 = -0.16	P = 0.874
		Fearful *vs.* Neutral	t_8 = 3.68	P = 0.006
		Happy *vs.* Neutral	t_8 = 1.59	P = 0.151
318 – 334	Frequency	BSF *vs.* HSF	t_8 = 0.23	P = 0.823
		BSF *vs.* LSF	t_8 = 1.87	P = 0.098
		HSF *vs.* LSF	t_8 = 1.65	P = 0.138

Exp 1a post-hoc t-tests for amygdala iERP amplitudes in the time windows expressing significant main effects of emotion or frequency (cluster threshold $P < 0.05$). Significant comparisons are highlighted in bold (two-tailed).

For responses in the early latency interaction window, the block (one, two) by emotion (fearful, happy, neutral) by spatial frequency (BSF, HSF, LSF) MANOVA showed no emotion by spatial frequency by block interaction ($F_{4,5}$ = 0.464; P = 0.76), or a block by emotion ($F_{4,5}$ = 0.019; P = 0.982), or frequency by block ($F_{4,5}$ = 1.403; P = 0.307) interaction. Only an emotion by frequency interaction ($F_{4,5}$ = 22.89; P = 0.002) was significant. For the later time windows expressing main effects of emotion and frequency (at cluster threshold $P < 0.05$), there is also no interaction with block ($P > 0.2$ for all windows).

Regarding the visual electrode sites, the seven groups of visual contacts pertaining to five patients that performed Exp. 1a and met the inclusion criteria are represented overlaid over a ventral view of a sample brain in Figure 9, panel A. We tested the specificity to faces of the visual electrodes by comparing the responses at the group level of neutral BSF faces with the responses to those neutral stimuli of Exp. 1b that did not include any face by means of cluster-based permutation statistics. The group of contacts pertaining to Patient 05 (represented in Figure 9, panel A as Fus. 6) had a signal artifact in Exp. 1b and was excluded from this particular analysis thus iERPs from six contact groups were compared. This analysis, comparing all post-stimulus time points, revealed a significant cluster between 164-176 ms (summed *t*-values = -32.07; $P = 0.03$) indicating a selective fusiform response to faces *vs.* scenes. This time interval is consistent with the face-sensitive N170 potential (Kanwisher, McDermott and Chun, 1997). The waveforms and the resulting cluster are represented in Figure 9, panel B.

Figure 3.9, panel C represents group averaged (n=7) fusiform iERPs corresponding to fearful, happy and neutral faces in Exp. 1a collapsed across spatial frequencies. Figure 3.9, panel D shows the same average for only fearful and neutral faces. The results of the cluster-based permutation testing employing an emotion (fearful, happy, neutral) by spatial frequency (BSF, HSF, LSF) MANOVA or and emotion (fearful, neutral) by spatial frequency (BSF, HSF, LSF) MANOVA with 0.01 and 0.05 cluster thresholds are summarized in Table 3.9. The significant clusters are also represented in Figure 3.9, panels C-D in the same way it was in Figure 3.7, panel A. Post-hoc tests at each significant time window for each MANOVA (3 by 3 or 2 by 3) are summarized in Tables 3.10 and 3.11 respectively. Figure 3.9, panel E shows the group average of BSF, HSF and LSF faces collapsed across emotions, as opposed to Figure 3.8, panel C. Group averaged fusiform responses to face stimuli are characterized by a positive peak at ~120 ms post-stimulus onset, followed by a negative deflection peaking at 170 ms and then a slower positive component, and there seems to be differences between spatial frequencies at first blush. Finally, Figure 3.8, Panel F shows the fearful face response in the fusiform for BSF, HSF and LSF faces.

Figure 3.9: Experiment 1a: faces; fusiform iERPs

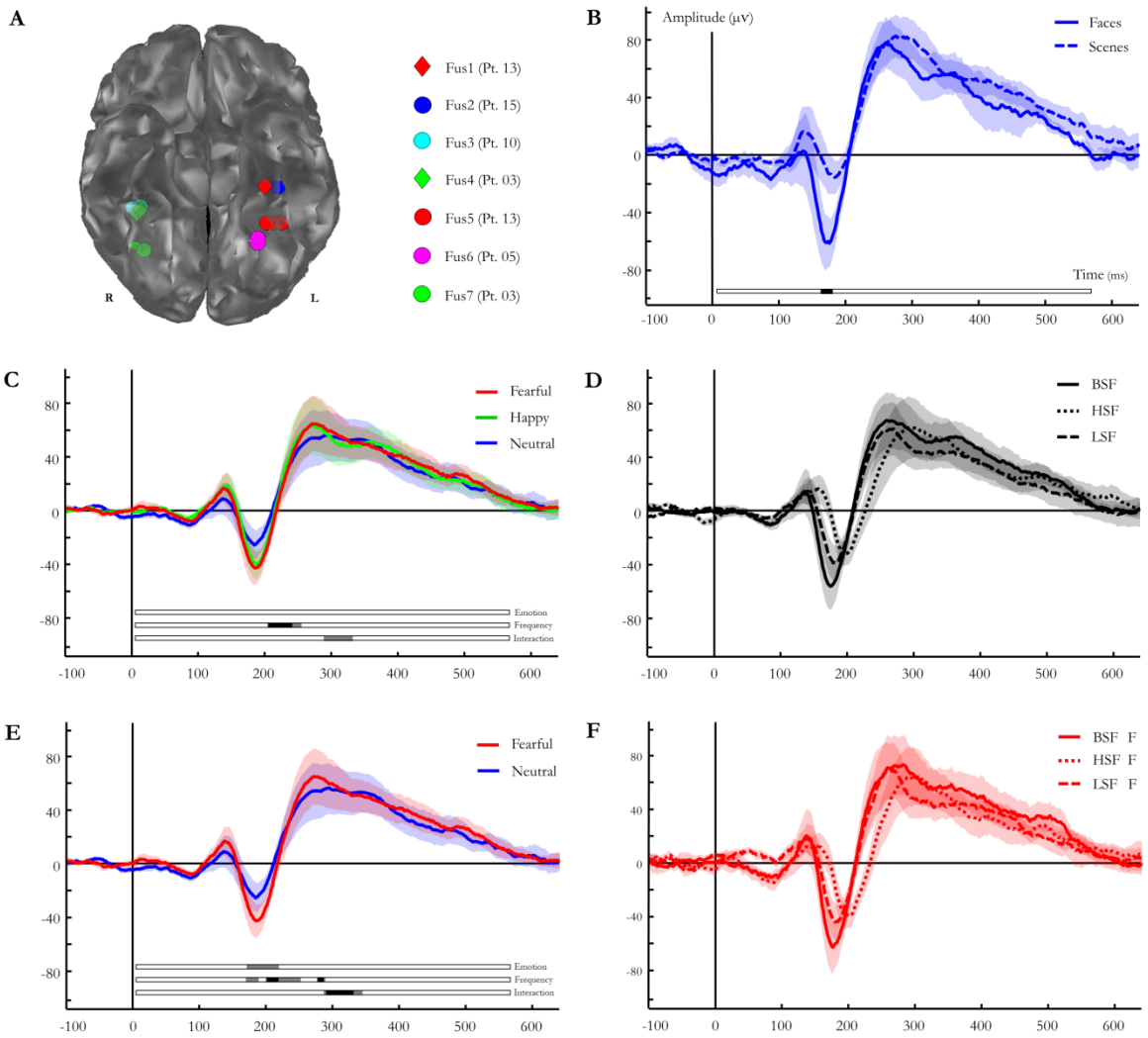

Panel A: Summary illustration of contact sites within the fusiform gyrus, depicted as colored shapes, and superimposed on semi-transparent MNI template brain. Different groups of contacts from the same patient are displayed in the same color. Panel B: Averaged iERPs to BSF neutral faces (solid line) and neutral complex scenes (dashed line) from 6 fusiform contacts. Responses to faces were significantly greater than those to scenes between 164-176 ms (cluster threshold $P < 0.01$). Panel C: Fusiform gyrus iERPs to fearful, happy, and neutral faces, collapsed across frequencies (Exp. 1). No significant main effect of emotion is observed. There is a main effect of spatial frequency from 206-240 (at cluster threshold $P < 0.01$) and an emotion by spatial frequency interaction from 290-334 ms (at cluster threshold $P < 0.05$). Panel D: Fusiform iERPs to BSF, HSF, and LSF faces, collapsed across emotion. Panel E: Fusiform gyrus iERPs to only fear and neutral faces, collapsed across spatial frequencies. Horizontal bars indicate significant time clusters of the emotion (fear and neutral) by spatial frequency (BSF, HSF and LSF) statistical analysis. A main effect of emotion is significant from 172-218 ms, as well as a main effect of frequency from 170-186 ms (both at cluster threshold $P < 0.05$). Main effects of frequency between 200 and 300 ms, as well as an emotion by spatial frequency interaction around 300 ms, are also observed. Panel F: Fusiform iERPs to BSF, HSF and LSF fearful faces only. Significant time clusters are indicated as in Figure 3.7.

Table 3.9: Experiment 1a: faces; fusiform cluster permutation statistics

Effect	Time window (ms)	Condition	Mean amplitude (μV)
Emotion (Fearful, Happy, Neutral) by Spatial Frequency (BSF, HSF, LSF)			
Cluster threshold $P < 0.01$			
Main effect Spatial Frequency	206 – 240 [$F_{summed} = 315.82$, $P = 0.003$]	BSF	37.7 (14.7)
		HSF	-9.5 (9.7)
		LSF	20.5 (12.4)
Cluster threshold $P < 0.05$			
Main effect Spatial Frequency	204 – 258 [$F_{summed} = 415.09$, $P = 0.003$]	BSF	40.4 (16.3)
		HSF	2.6 (12.2)
		LSF	29.1 (13.5)
Emotion by Spatial Frequency Interaction	290 – 334 [$F_{summed} = 537.01$, $P = 0.033$]	BSF Fearful	73.4 (16.4)
		HSF Fearful	57.8 (17.9)
		LSF Fearful	43.1 (12.9)
		BSF Happy	53.3 (16.6)
		HSF Happy	63.9 (21.7)
		LSF Happy	37.6 (14.2)
		BSF Neutral	48.8 (16.4)
		HSF Neutral	50.4 (21.1)
		LSF Neutral	47.6 (16.1)
Emotion (Fearful, Neutral) by Spatial Frequency (BSF, HSF, LSF)			
Cluster threshold $P < 0.01$			
Main effect Spatial Frequency	202 – 218 [$F_{summed} = 246.78$, $P = 0.003$]	BSF	7.9 (9.5)
		HSF	-26.3 (7.5)
		LSF	-1.0 (9.6)
Main effect Spatial Frequency	278 – 284 [$F_{summed} = 73.54$, $P = 0.032$]	BSF	66.5 (19.6)
		HSF	57.3 (23.1)
		LSF	49.5 (17.6)
Emotion by Spatial Frequency Interaction	294 – 330 [$F_{summed} = 321.90$, $P = 0.002$]	BSF Fearful	73.2 (16.4)
		HSF Fearful	58.2 (18.1)
		LSF Fearful	43.3 (12.9)
		BSF Neutral	48.2 (16.2)
		HSF Neutral	50.3 (21.2)
		LSF Neutral	47.6 (16.0)
Cluster threshold $P < 0.05$			
Main effect Emotion	172 – 218 [$F_{summed} = 229.44$, $P < 0.001$]	Fearful	-23.4 (8.5)
		Neutral	-18.5 (7.0)
Main effect Spatial Frequency	170 – 186 [$F_{summed} = 67.07$, $P = 0.043$]	BSF	-45.8 (14.1)
		HSF	-11.2 (10.4)
		LSF	-29.0 (12.0)
Main effect Spatial Frequency	200 – 258 [$F_{summed} = 467.30$, $P = 0.003$]	BSF	37.9 (16.9)
		HSF	-5.2 (10.6)
		LSF	29.4 (12.7)
Main effect Spatial Frequency	274 – 288 [$F_{summed} = 106.52$, $P = 0.012$]	BSF	68.2 (20.0)
		HSF	52.7 (24.5)
		LSF	52.7 (18.2)
Emotion by Spatial Frequency Interaction	288 – 340 [$F_{summed} = 403.05$, $P = 0.002$]	BSF Fearful	73.2 (16.2)
		HSF Fearful	57.1 (17.5)
		LSF Fearful	42.6 (12.8)
		BSF Neutral	49.1 (16.3)
		HSF Neutral	49.9 (21.0)
		LSF Neutral	47.6 (16.1)

Exp 1a mean fusiform gyrus iERP amplitudes (standard error mean in parenthesis) for significant time window resulting from the cluster-based permutation statistical testing of an emotion (fearful, happy, neutral) by spatial frequency (BSF, HSF, LSF) effect, as well as a second test using within-subject factors emotion (fearful, neutral) and spatial frequency.

Indeed, the 3x3 MANOVA cluster-based permutations at a cluster threshold of $P < 0.01$ showed only a main effect of frequency from 206-240 ms (Table 3.9). Post-hoc tests in this time window revealed that whereas responses to broad and LSF faces are greater than to HSF faces, broad and LSF responses did not differ (Table 3.10), thus reflecting the later latency negative deflection to HSF faces relative to BSF and LSF (Figure 3.9, panel E). By contrast to effects observed in the amygdala, we did not observe a significant interaction at early latencies, even after relaxing the cluster threshold to $P < 0.05$ (Table 3.9). At this lower threshold, the earliest observed effects are a main effect of frequency from 204 to 258 ms followed by an emotion by spatial frequency interaction from 290 to 334ms (see Table 3.10 for post-hoc tests).

Table 3.10: Experiment 1a: faces; fusiform three by three post-hocs

Time	Level	Comparison	Statistic	Probability
		Cluster threshold $P < 0.01$		
206 - 240	Frequency	**BSF vs. HSF**	$t_6 = 4.54$	$P = 0.004$
		BSF vs. LSF	$t_6 = 1.05$	$P = 0.333$
		HSF vs. LSF	$t_6 = -4.93$	$P = 0.003$
		Cluster threshold $P < 0.05$		
204 - 258	Frequency	**BSF vs. HSF**	$t_6 = 4.36$	$P = 0.005$
		BSF vs. LSF	$t_6 = 1.14$	$P = 0.299$
		HSF vs. LSF	$t_6 = -5.38$	$P = 0.002$
290 – 334	BSF	**Fear *vs.* Happy**	$t_6 = 2.46$	$P = 0.049$
		Fear *vs.* Neutral	$t_6 = 2.79$	$P = 0.031$
		Happy *vs.* Neutral	$t_6 = 0.92$	$P = 0.392$
	HSF	Fear *vs.* Happy	$t_6 = -0.69$	$P = 0.516$
		Fear *vs.* Neutral	$t_6 = 1.25$	$P = 0.259$
		Happy *vs.* Neutral	$t_6 = 2.08$	$P = 0.082$
	LSF	Fear *vs.* Happy	$t_6 = 1.56$	$P = 0.170$
		Fear *vs.* Neutral	$t_6 = -0.80$	$P = 0.457$
		Happy *vs.* Neutral	$t_6 = -1.36$	$P = 0.222$

Exp. 1a post-hoc t-tests for fusiform gyrus iERP for significant time window resulting from the cluster-based permutation statistical testing on an emotion (fearful, happy, neutral) by spatial frequency (BSF, HSF, LSF) MANOVA. Significant comparisons are highlighted in bold (two-tailed).

Surprisingly, no significant main effect of emotion was obtained. However, given that enhanced fusiform responses to happy faces are observed far less frequently than to fearful faces (Vuilleumier and Pourtois, 2007) we repeated this analysis, restricting our cluster-based permutation statistics to fearful and neutral stimuli (Figure 3.9, panel D; Table 3.9). This analysis yielded a significant main effect of emotion in a 172-218 ms time cluster (summed *F*-values 229.44; $P < 0.001$; at cluster threshold of $P < 0.05$) No earlier emotion or interaction effects were observed with a cluster threshold of either $P < 0.01$ or $P < 0.05$. We observed main effects of spatial frequency (2 clusters spanning 202-284 ms at a cluster threshold of $P < 0.01$ and $P < 0.05$ and a separate cluster from 170-186 at a cluster threshold of $P < 0.05$) followed by an emotion by spatial frequency interaction around 300 ms at both cluster thresholds; see Table 3.11 for post-hoc tests).

In the 4 patients with electrodes in amygdala and fusiform the Friedman tests calculated with the differences between emotions (fear *vs.* happy, fear *vs.* neutral and happy *vs.* neutral) at both sites revealed a significant interaction between emotion and brain region ($\chi^2(5) = 11.57$; $P = 0.041$). The Friedman tests separately for each region revealed a significant emotion effect within amygdala ($\chi^2(2) = 8$; $P = 0.018$) but, critically, not within fusiform contacts ($\chi^2(2) = 0.5$; $P = 0.779$).

It remains possible, however, that fast afferent input from fusiform cortex arrives at the amygdala before a differential response to fearful *vs.* neutral or happy faces is observed in this ventral visual cortical region, *i.e.*, emotion selectivity arises in the amygdala but is still dependent on up-stream activity in fusiform cortex. Given that in the amygdala, fast latency responses are observed to BSF and LSF fearful faces, we next tested for the earliest onset of any upward or downward deflection in fusiform contacts to BSF and LSF fearful faces,

The *t*-test against zero for each time point of BSF and LSF fearful face response in the fusiform (Figure 3.9, panel F) to test for the onset of any activity significantly different from zero applying an uncorrected alpha level of 0.05 showed that the first significant deflection for fearful faces is negative and spans from 174 to 192ms (174 ms: $t_6 = -2.53$; $P = 0.044$ uncorrected); for LSF fearful faces there is a significant positive deflection from 104 to 124 ms (104 ms: $t_6 = 3.68$; $P = 0.010$ uncorrected), and a negative deflection from 178-204 (178 ms: $t_6 = -2.57$; $P = 0.042$ uncorrected).

Table 3.11: Experiment 1a: faces; fusiform two by three post-hocs

Time	Level	Comparison	Statistic	Probability
		Cluster threshold $P < 0.01$		
202 - 218	FREQUENCY	**BSF vs. HSF**	$t_6 = 4.21$	$P = 0.006$
		BSF vs. LSF	$t_6 = 0.94$	$P = 0.380$
		HSF vs. LSF	$t_6 = -4.22$	$P = 0.006$
278 - 284	FREQUENCY	**BSF vs. HSF**	$t_6 = 1.96$	$P = 0.098$
		BSF vs. LSF	$t_6 = 7.01$	$P = 0.000$
		HSF vs. LSF	$t_6 = 1.25$	$P = 0.258$
294 - 330	SF	**BSF Fear *vs.* BSF Neutral**	$t_6 = 2.81$	$P = 0.031$
		HSF Fear *vs.* HSF Neutral	$t_6 = 1.27$	$P = 0.252$
		LSF Fear *vs.* LSF Neutral	$t_6 = -0.71$	$P = 0.503$
	FEAR	BSF Fear *vs.* HSF Fear	$t_6 = 1.57$	$P = 0.168$
		BSF Fear *vs.* LSF Fear	$t_6 = 5.87$	$P = 0.001$
		HSF Fear *vs.* LSF Fear	$t_6 = 1.84$	$P = 0.116$
	NEUTRAL	BSF Neutral *vs.* HSF Neutral	$t_6 = -0.26$	$P = 0.807$
		BSF Neutral *vs.* LSF Neutral	$t_6 = 0.14$	$P = 0.893$
		HSF Neutral *vs.* LSF Neutral	$t_6 = 0.52$	$P = 0.624$
		Cluster threshold $P < 0.05$		
170 - 186	FREQUENCY	**BSF vs. HSF**	$t_6 = -3.81$	$P = 0.009$
		BSF vs. LSF	$t_6 = -5.57$	$P = 0.001$
		HSF vs. LSF	$t_6 = 2.11$	$P = 0.079$
200 - 260	FREQUENCY	**BSF vs. HSF**	$t_6 = 4.17$	$P = 0.006$
		BSF vs. LSF	$t_6 = 1.00$	$P = 0.358$
		HSF vs. LSF	$t_6 = -7.35$	$P = 0.000$
274 - 288	FREQUENCY	**BSF vs. HSF**	$t_6 = 4.38$	$P = 0.005$
		BSF vs. LSF	$t_6 = 4.87$	$P = 0.003$
		HSF vs. LSF	$t_6 = 0.00$	$P = 0.999$
288 - 340	SF	**BSF Fear *vs.* BSF Neutral**	$t_6 = 2.76$	$P = 0.033$
		HSF Fear *vs.* HSF Neutral	$t_6 = 1.20$	$P = 0.276$
		LSF Fear *vs.* LSF Neutral	$t_6 = -0.91$	$P = 0.401$
	FEAR	BSF Fear *vs.* HSF Fear	$t_6 = 1.82$	$P = 0.119$
		BSF Fear *vs.* LSF Fear	$t_6 = 5.92$	$P = 0.001$
		HSF Fear *vs.* LSF Fear	$t_6 = 1.94$	$P = 0.100$
	NEUTRAL	BSF Neutral *vs.* HSF Neutral	$t_6 = -0.09$	$P = 0.931$
		BSF Neutral *vs.* LSF Neutral	$t_6 = 0.27$	$P = 0.797$
		HSF Neutral *vs.* LSF Neutral	$t_6 = 0.43$	$P = 0.684$

Exp. 1a post-hoc t-tests for fusiform gyrus iERP amplitudes in the time window for the main effects and interaction for the analysis comparing responses to only fearful and neutral faces. Significant comparisons are highlighted in bold (two-tailed).

3.5.2 Experiment 1b: scenes

Figure 3.10, panel A shows the amygdala iERPs and the significant clusters corresponding to Exp. 1b condition: negative and neutral complex pictures. Figure 3.10, panel B represents the time –points at which significant deviations from zero did occur the same way as Figure 3.7, panel D. Statistical results are summarized in Table 3.12.

Figure 3.10: Experiment 1b: scenes; amygdala iERPs

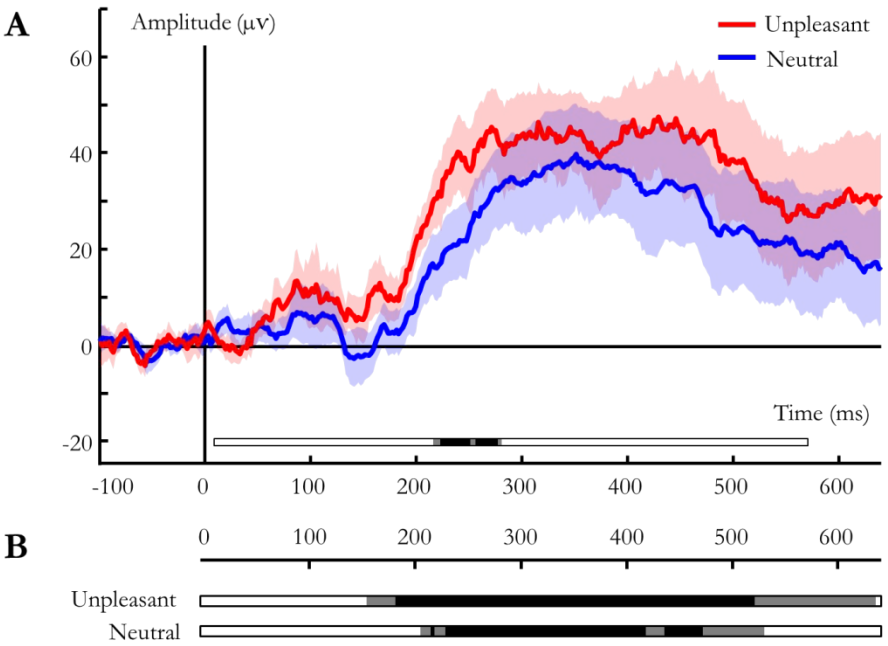

Panel A: Amygdala iERPS to experiment 1b: scenes. Significant time clusters are indicated as in Fig. 3.7. Human amygdala iERPs to unpleasant pictures are significantly different from those evoked by neutral pictures only from 220 ms (at cluster threshold $P < 0.05$). Panel B: Horizontal bars depict time windows in which responses to unpleasant (top) and neutral (bottom) pictures are significantly different from zero.

Cluster-based permutations comparing emotional and neutral pictures indicate two significant clusters, which on relaxing the cluster threshold to $P < 0.05$ collapsed into one cluster spanning 220-280 ms. With a cluster threshold of $P < 0.01$, the onset of clusters significantly different from zero baseline were observed at 188 ms and 216 ms for unpleasant and neutral pictures, respectively, which on relaxing the cluster threshold to $P < 0.05$ begin at 156 ms and 202 ms.

Table 3.12: Experiment 1b: scenes; amygdala cluster permutation statistics

Effect	Time window (ms)	Condition	Mean amplitude (μV)
	Cluster threshold $P < 0.01$		
Main effect Emotion	226 – 252 [$t_{summed} = 62.57$, $P = 0.003$]	Fearful	37.2 (7.5)
		Neutral	20.2 (3.3)
Main effect Emotion	258 – 278 [$t_{summed} = 45.01$, $P = 0.007$]	Fearful	43.1 (8.5)
		Neutral	21.0 (3.3)
	Cluster threshold $P < 0.05$		
Main effect Emotion	220 – 280 [$t_{summed} = 123.19$, $P = 0.009$]	Fearful	39.0 (7.7)
		Neutral	20.6 (3.3)

Mean amygdala iERP amplitudes (standard error mean in parenthesis.) in Exp. 1b for each condition for the time windows of the clusters showing significant effects. *F* and *t*-values pertain to summed values over the significant clusters.

The repeated-measure ANOVA employing the average value over the time window of the expressed interaction (72 – 108 ms) of neutral and unpleasant pictures on one side and negative and neutral faces corresponding to Exp. 1b (BSF and LSF collapsed) revealed a significant emotion by experiment interaction ($F_{1,17} = 12.55$; $P = 0.003$). Restricted our sample to the 5 patients completing both tasks (7 amygdalae), the ANOVA with within-subject factors emotion and task, which revealed a significant emotion by task interaction ($F_{1,6} = 10.7$; $P = 0.017$).

3.6 Discussion

A time cluster expressing a significant emotion by spatial frequency interaction is observed between 72-108 ms after face presentation (Figure 3.7, Tables 3.6 and 3.7) in the amygdala iERPs. Critically, responses to BSF and LSF fearful faces in this time window were significantly different from responses to neutral and happy faces. Amygdala responses to BSF and LSF fearful faces did not differ, but, critically, were both significantly different from HSF fearful face responses. Altogether, these data indicate a selective fast amygdala response to the low spatial frequency components of fearful faces. We note that the LSF fearful *vs.* LSF neutral comparison only reaches trend significance and suggest that this may

reflect some ambiguity in perceiving the expression of LSF neutral faces (Davis and Whalen, 2001).

The existence of a subcortical route for rapid processing of ecologically important stimuli has profoundly influenced basic and clinical research on emotional processing in the brain. However, one important limitation of this "low-road" model (Ledoux, 1996) has been an absence of support from direct electrophysiological recordings in primates, leading to an alternative account suggesting that rapid visual processing of emotional stimuli can be mediated by other visual pathways involving visual cortex (Pessoa and Adolphs, 2010). We provide direct empirical support for the "low-road" model by demonstrating human amygdala intracranial responses to fearful, but not neutral or happy, faces at very fast latency (~70 ms) that are spatial frequency-dependent. Critically, we show that this selective amygdala response precedes any evoked activity in face-sensitive ventral visual cortex to the same stimuli by more than 30 ms, and precedes the onset of a differential response to fearful faces in the same cortical region by over 100 ms. Our findings are therefore in keeping with a bottom-up amygdala response originating via a more direct subcortical magnocellular route rather than top-down influences from higher-level visual processing stages. By contrast, the later latency main effect of emotion in the amygdala (beginning from ~120 ms) is more consistent with emotional information that arrives at the amygdala having been processed in visual cortex. In support of this interpretation, this later response is also evoked by HSF fearful faces (Fig. 3.7, panel B), which also modulated fusiform cortex activity (Figure 3.9), indicating engagement of slower parvocellular pathways along visual cortical areas (Livingstone and Hubel, 1988; Merigan and Maunsell, 1993).

The few prior studies reporting field potentials (Krolak-Salmon et al., 2004; Naccache et al., 2005; Brázdil et al., 2005) or oscillatory responses (Oya et al., 2002; Sato et al., 2011) from human amygdala depth recordings failed to find the fast latency amygdala response described here. Although two previous studies (Pourtois et al., 2010; Sato et al, 2011) also presented fearful faces, they found responses around 130 ms (approximating the latency of the main effect of emotion we observe in the amygdala) and used only standard broad-band photographs. In another study (Krolak-Salmon et al., 2004) reporting late (200 ms) iERPs to fearful faces, a limited number of identities (eight) were each presented 30 times in each of 2 tasks, which may have resulted in habituation of a fast response. To safeguard against this, we presented each patient with 135 identity-unique faces, repeated

only once. We did not observe habituation effects following a single repetition. A further factor likely to have improved our ability to detect a fast latency response is that in 6 of the 7 patients included in Exp. 1a, pathology was subsequently discovered to be outside of the medial temporal lobe (Table 3.1), consistent with preserved amygdala function.

The failure of previous intracranial studies to find a rapid amygdala response to complex emotional pictures (Oya et al., 2002; Krolak-Salmon et al., 2004; Naccache et al., 2005; Brázdil et al., 2005) may reflect a fundamentally faster processing time for fearful faces, which have important motivational and communicative value among primates (Dimberg and Öhman, 1996), relative to emotional scenes with multiple objects. Using complex emotional scenes we also found only late latency iERP amplitude modulations by emotion in the human amygdala. That fast responses are limited to fearful faces provides novel support for evolutionary theories of amygdala automaticity to social threat signals (Öhman, 2002; Anderson et al., 2003). From an evolutionary perspective, stimuli associated with recurrent survival threats, such as fearful faces, require minimal neural processing for identification, a notion referred to as "preparedness" (Seligman, 1971). Moreover, the emergence of social communities and social signals of emotions during evolution presumably contributed to making amygdala-centered circuits particularly responsive to threat cues communicated by other conspecifics, such as facial expressions and perhaps other social signals (Öhman, 2002; Kling and Brothers 1992) This processing of salient emotional inputs by amygdala may be automatic in the sense that it occurs fast, efficiently, and not necessarily under voluntary control (Moors and De Houwer, 2006), hence directly elicited by presentation of the specific stimulus. In line with this notion, our data demonstrate for the first time that fast, coarse, visual inputs to the amygdala are sufficient for neuronal responses to differentially signal threat-related emotional facial expression as early as 66 ms post-stimulus presentation, but not for complex emotional pictures. Although the fast latency response we observe is selective for fearful *vs.* happy and neutral faces, fast responses may also occur to other negative facial expressions such as anger. It remains to be tested whether there is a fast human amygdala response to simple, biologically relevant stimuli, such as snakes, that provided survival threat during evolution (Seligman, 1971; Öhman and Mineka, 2001)

Accounts of automaticity in fear processing also suggest that amygdala responses to emotional stimuli occur regardless of attentional resources available or competition

between concurrent inputs (Pessoa et al., 2002; Anderson et al., 2003; Dolan and Vuilleumier, 2003). We did not explicitly manipulate attention in either Exp. 1a or Exp. 1b - amygdala responses were observed during incidental tasks of gender or indoor/outdoor judgments, respectively. Nonetheless, we note that automatic amygdala responses independent of attention would be predicted by the existence of fast, subcortical inputs (Anderson et al., 2003; Dolan and Vuilleumier, 2003), for which our data provide the first direct electrophysiological support in humans. However, it is also possible that amygdala responses to coarse inputs without attention may involve other cortical or subcortical pathways receiving privileged early access to coarse (low spatial frequency) visual information (Vuilleumier, 2005b; Kveraga, Boshyan and Bar, 2007). That is, a fast amygdala response could be driven by inputs from other cortical regions, such as emotion-sensitive ventral or orbitofrontal cortex, which also receive magnocellular pulvinar input (Barbas, 2000). This is unlikely as the 66 ms latency response observed here is considerably faster than increased neuronal firing rates previously reported (Kawasaki et al., 2001) in human ventral prefrontal cortex to emotional scenes (120-160 ms latency), and also faster than the late latency (~500 ms) responses to fearful faces observed in human orbitofrontal cortex (Krolak-Salmon et al., 2004). Without simultaneously recording from these cortical areas the data presented here cannot exclude the possibility that local short latency modulations of neural activity by SF and fear-relevance also occur in cortical regions receiving magnocellular thalamic input (Pessoa and Adolphs, 2010). Whether these brain regions indeed show the same fast LSF-dependent responses to fear relevant stimuli in humans still has to be shown. However, our findings clearly demonstrate that such a short-latency response can be observed in human amygdala.

3.7 Summary

We demonstrate for the first time, using direct electrophysiological recordings in a homogenous sample of human patients, a fast (~70 ms) and selective amygdala response to emotional information. The early amygdala response is specific to fearful, not happy, facial expressions. Furthermore, the effect is selective to socially relevant fearful facial information and is not evoked by unpleasant complex pictures. Fast responses to fear are only observed to low, not high, spatial frequency components of fearful faces, consistent

with a coarse visual input providing limited, but rapid, information via the magnocellular pathway. The latency of amygdala responses to fearful faces is significantly faster than that observed in fusiform cortex. Thus, our data provide novel support for a "low-road" circuit for fear detection in the human amygdala.

4 Experiment 2

4.1 Introduction

Classic models assume that visual processing sweeps forward in a hierarchical fashion from early perceptual areas that outline the low level features of the visual scene and rely them to domain-specific regions which in turn are able to extract categorical information finally achieving perceptual integration at higher order areas at the end of the stream (Mishkin et al., 1983). Based on several evidences like early top-down modulations of stimulus global properties (Hochstein and Ahissar, 2002) other models suggest that other non-lineal mechanisms like long-range projections and parallel or recursive processing are important characteristics of the visual system (Lamme and Roelfsema, 2000). On the other side, models of emotion understand that the limbic system and specifically the amygdala are required to provide perceptual representations with emotional properties ongoing perception. Traditional views rely on the amygdala projections with ventral and anterior temporal gyrus (Ledoux, 1996). In turn, based on conflicting evidence of early emotional modulations in posterior occipital cortex other models postulate that the circuits through which emotional aspects can affect ongoing perception are more complex and include long range projections and shortcuts between medial and low as well as high level cortical structures (Pessoa and Adolphs, 2010). Although there are proposals (Johnson, 2005; Rutman et al, 2010) that early processing is guided and/or facilitated by the LSF frequencies relying on the magnocellullar pathways it is yet to be confirmed that amygdala inputs are responsible of observed early (<100ms) modulations of cortical processing in the temporooccipital cortex.

The processing of faces is somewhat special among general visual processing. They are stimuli that convey a variety of relevant information about our peers, from identity to background, mood or intentions. Our brains had evolved to better recognize and categorize them (Dunbar, 2002) to the point that many authors talk about what is called a 'social network' (Haxby, Hoffman and Gobbini, 2002). Furthermore, facial information like expression or gaze direction provides many types of information besides social cues like communicating the presence of a nearby threat in the environment. The preference of our brains to recognize biologically relevant information is a process known as 'preparedness' (Seligman, 1971). Hence, on one side it is thought that regions of the cortex had specialized in the processing of faces, being the fusiform gyrus (McCarthy et al., 1997), and more precisely a smaller patch so called fusiform face area (FFA; Kanwisher, McDermott and Chun, 1997; Kanwisher and Yovel, 2006) the most well-known representative of this domain specific processing although other temporooccipital regions like the superior temporal sulcus (STS; Hoffman and Haxby, 2000; Allison, Puce and McCarthy, 2000) and the occipital face area (OFA; Gauthier et al., 2000; Pitcher, Walsh and Duchaine, 2011) had also been linked with face specific processing. On the other side, it is also admitted that the distributed participation of specific (O'Craven and Kanwisher, 2000) as well as general (Rossion et al., 2003b) temporooccipital perceptual areas, medial structures like the amygdala (Morris et al., 1998; Adolphs and Spezio, 2006) and higher order multimodal regions (Bruce, Desimone and Gross, 1981; Ishai, Schmidt and Boesiger, 2005) are needed for a correct processing of face information (Ishai, 2008).

The most important electrophysiological index of face processing is the N170/M170. It is a component peaking between 130-220 ms over temporo-occipital regions highly correlated with object recognition. Although it is evoked by different types of objects, it is usually bigger for faces than other objects (Bentin, Deouell and Soroker, 1999, Itier and Taylor, 2004a). It is affected by inversion (Eimer, 2000; Rossion et al, 2000a) and priming effects (Schweinberger et al., 2007; Harris and Nakayama, 2008). It is generally accepted that the N170/M170 index structural encoding processing (Itier et al 2004b; Bentin et al., 2006; Eimer et al., 2011). It has been seen that parts of faces arranged coherently or even objects resembling face configural properties (Hadjikhani et. al., 2009) evoked larger N170 amplitudes, though it is also modulated by isolated face parts per se (Harris and Nakayama, 2008). These evidences support the assumption that it reflects face selective processing. However, the debate about whether the neural mechanisms for face

perception are selectively involved in processing faces per se (Camel and Bentin, 2002; Gauthier et. al., 2003) or they also participate in the processing of any class of object is still open (Xu, Liu and Kanwisher, 2005). Expertise modulates the M170 amplitude (Rossion et. al., 2002; Bukach et al., 2006). It has been seen that non experts subjects trained to recognize a novel non face category of objects evoke larger N170 amplitudes (Rossion et. al., 2002). Furthermore, it has been seen object category intereference modulates the M170 of expert subjects (Curran, Tanaka and Weiskopf, 2002; Gauthier and Curby, 2005).

Newborns, whose neural networks are still immature, show a preference for face or face configuration like stimuli (Valenza et al., 1996; Gauthier and Nelson, 2001; Farroni et al, 2007; but see Turati 2004) and the main hypothesis is that these newborn looking preferences are generated by a subcortical route. Hence, it has been proposed that there is a subcortical face route based on LSF processing that later becomes part of the adult's social brain network (Schultz 2005; see Johnson, 2005 for a review). It has also been shown that LSF frequencies from the eyes region of the face convey the most informative information about identity and this has been proposed as a justification to why the system seems to rely more on the LSF frequencies (Keil, 2009). There are a number of studies whose results suggest that face processing relies primarily on LSF frequencies (Goffaux, Gauthier and Rossion, 2003; Holmes et al., 2005; Goffaux and Rossion, 2006). However it has been shown that HSF frequencies are also important for face recognition and face processing per se (Fiorentini, Maffei and Sandini, 1983; Goffaux et al., 2005; Halit et al., 2006; Cheung et al., 2008) as much as general object recognition and top-down feedback processing (Bar et al., 2006) while all the information from the eye region seems important for face processing (Taylor et al., 2006; Itier, Latinus and Taylor, 2006a).

Besides the M170, some authors had linked the P1/M100 with face processing. The MP100/M100 is an obligatory sensory response to visual stimulation with occipital topography and source in striate (Seki et al., 1996; Hatanaka et al., 1997) and extrastriate areas (Spinelli et al., 2000, Pins, 2003) in middle occipital cortex. It is thought to reflect domain- general early aspects of visual processing. It is sensitive to contrast, brightness and size of a picture (Schendan, Ganis and Kutas, 1998). However, a number of experiments (Liu, Harris and Kanwisher, 2002; Itier and Taylor, 2004a; Herrmann et al., 2005a; Tanskanen et al., 2005; Campanela et al., 2006; Nakashima et al., 2008; Vlamings, Goffaux and Kemner, 2009; Rutman et al., 2010) had found face specific modulations in this

component which led to conclude that at least some degree of face processing has been initiated at around ~100 ms. Indeed, it has been seen that the P100/M100 sources may also involve contribution of left and right fusiform gyrus (Di Russo et al., 2002; Herrmann et al., 2005b). The sources of the M170 are considered to be mainly face processing areas, such as the fusiform gyrus (Deffke et al., 2007) or the temporal superior sulcus (Itier and Taylor, 2004c) but its network expands beyond fusiform gyrus into occipital and parietal cortex (Herrmann et al., 2005b). Hence, temporal course wise, it is considered that *initial* face perception in the cortex is a two-step process (Liu, Harris and Kanwisher, 2002) represented by both the P100/M100 and the N170/M170, indexing a first process on which the face is categorized as a face and a second process on which individual characteristics of the face are extracted. It has been further suggested that the M170 for faces depends on two different generators more or less simultaneously active (Itier et al., 2006b) in posterior occipital cortex (M170A) and right ventral temporal cortex (M170B). Later components are also considered important in face processing, such as the M220, with sources in striate visual cortex that could be a reactivation of the aforementioned M170A generator (Itier et al., 2006b).

Regarding emotional modulations, different author had found effects in early P1/M100 (Pizzagalli, Regard and Lehmann, 1999; Schacht and Sommer, 2009; Vlamings, Goffaux and Kemner, 2009) as well as absence (Mühlberger et al., 2009) of modulations. It is assumed that emotional expression effects can be observed very early around 120ms poststimulus, prior to a full visual categorization stage indexed by the face-selective N170 component and interpreted as rapid processing of crude cues conveyed by the LSF frequencies (Vuilleumier and Pourtois, 2007; Flevaris, Robertson and Bentin, 2008). With respect to the M170, though up to date some studies had found amplitude modulations linked mostly with fearful, angry and happy expressions (Pizzagalli et al., 2002; Blau et al., 2007; Vlamings, Goffaux and Kemner, 2009) many studies had not (Krolak-Salmon et al., 2001; Herrmann et al., 2002; Eimer, Holmes and McGlone, 2003) sustaining the idea that it is insensitive to emotional manipulations or those depend on the recording technique or attention orientation (Wronka and Walentowska, 2011; Rossion and Jacques, 2011; Rellecke, Sommer and Schacht, 2013). It is a current controversy what are the conditions on which emotional effects can be expected (see Hinojosa, Mercado and Carretié, 2015 for a review of emotional dependence of the N170 in EEG studies). Importantly, studies with fMRI pinpoint that emotional modulations driven by the amygdala maybe seen not only at

the fusiform gyrus but also in visual areas of the occipital cortex and more distant regions like the superior temporal sulcus, the cingulate and the parietal cortex (Vuilleumier and Pourtois, 2007).

4.2 Objectives

Explore magnetoencephalographic data in search of a fast interaction between emotion and spatial frequency analogous or synchronous with the early interaction recorded previously with intracranial electroencephalography in Experiment 1. For this we imitated the experimental procedure of Experiment 1a: faces with some differences. First, we employed a much bigger number of identities (324 versus 135). Second, as we scanned non clinical subjects we employed the same stimulus presentation time but smaller and jittered interstimulus times (2.25/2.75 seconds versus fixed 3.5 seconds).

Localize the substrate correlate of the effects found in the magnetoencephalographic signal, if any, by means of inverse problem solution around the temporal window of interest. Early interaction effects that could be related with the activation of the magnocellullar pathway or the very amygdala may emerge at several parts of the brain other than the amygdala itself. This is the reason why we selected MEG as the acquisition technique, given it provides fine temporal resolution like iEEG but it records the overall activity of the brain at a macroscopic level unlike the later.

Explore the time course of early visual face processing on a cortical scale instead of at a localized area like in Experiment 1a: faces.

4.3 Hypothesis

For this experiment, we had a priori assumptions extracted from Experiment 1. By mimicking the same procedure, we expect to find a MEG correlate of the early interaction effect previously observed at amygdala sites. We were certain at what time window we wanted to look at: up to 100 ms post-stimulus; not only because of the previous experiment but also because emotional effects post 100 ms had already been descripted in several studies. However, both techniques differ greatly not only in the nature of the signal they record - electric potential versus magnetic fields: while LFPs are most sensible to the postsynaptic activity of the cell bodies in a volume of the brain (an spherical area about 1 cm in diameter) and stereotactic electrodes do perfuse the brain matter, able to reach subcortical, medial or ventral regions; the MEG helmet is composed of 102 pairs of sensors (called magnetometers and gradiometers) evenly distributed around and above the scalp that register the summation of postsynaptic synchronous activity of thousands of neurons over all the brain layers. Due to the additive effect, it is particularly sensible to the pyramidal cells of the cortical layers because they are arranged in parallel, like EEG. Besides, MEG is sensible to the activity of the neurons located at sulci rather than gyri due to the spread of the magnetic fields. Furthermore, the amplitude of the signal decreases with depth in both EEG and MEG. Thus we were uncertain what effects of interaction, if any, we would find. Given the scarce previous literature we were also uncertain what MEG component could show modulations. The source localisation could resolve sources in the amygdala but the characteristics of the MEG mentioned before made the possibility of localizing the effects at cortical layers more feasible. Therefore, it could happen that we could measure the indirect contribution of the amygdala outputs to the cortical layers as much as the activation of the magnocellullar projections from the thalamus to the cortex.

Secondly, we expected to disentangle to some extent the steps of early cortical face processing identifying early (before 200 ms poststimulus) components of the event related magnetic field response and performing source reconstruction. We expected striate and extrastriate regions to be the main sources of activity. Early visual striate areas should activate first and a broader occipitotemporal and occipitoparietal activations should be expected afterwards with contribution of the higher order areas related with object identification (lateral occipital complex) and specific face processing (fusiform gyrus) in the later steps, indexed by the M170 component. However, as shown before, we were aware it

could also be possible that higher order areas show peaks of activation before the M170. Critically, it has been shown that ventrotemporal cortex may activate well before contributing to the signal at around 100 ms (Di Russo et al., 2002; Herrmann et al., 2005b).

Given the heterogeneous findings concerning modulations of the M170 for faces (see Hinojosa, Mercado and Carretié, 2015) we were unsure whether our task would elicit emotional modulations on this component or if we would be able to localize the source of those differences.

Lastly, given the frequency effects found at fusiform sites in previous Experiment 1a: faces, we expected that maybe latency effects would influence the difference spatial frequency stimuli at posterior and other areas of the cortex, probably modulating the measured M170 (as occurred in Experiment 1a: faces fusiform electrodes) making the components pertaining to BSF stimuli faster than the components elicited by stimuli with only HSF frequencies.

4.4 Methods

4.4.1 Subjects

Sixteen right handed European men and women (eight women; mean age = 31.5; range = 23 - 51) participated in the recordings. They were all right handed as reported with the Edinburgh Handedness Inventory (Oldfield, 1971; mean: 97.1%; range = 89 – 100) and had normal or corrected to normal visual acuity. After ensuring they had no metallic implants they were informed about the non-invasive MEG acquisition procedure and screened for pathological mood traits with the Hamilton Anxiety Rating Scale (HARS; Hamilton, 1959) and the Hamilton Depression Rating Scale (HDRS; Hamilton, 1960). Both particular questionnaires were complemented along with the 28 items version of the General Health Questionnaire (GHQ; Goldberg, 1979). The three questionnaires have the same number of responses per item (four) and can be quantified like a Lykert's scale from 0 (absence of symptom) to 3 (the symptom is very manifest). Hence, low scores means

absence or normal presence of general problems, anxiety, or depression. The HARS and the HDRS versions employed had 14 and 17 items respectively. The original Goldstein scoring method validates also with a '0' the second choice in the GHQ items (generally the sentence "same as always") to separate better between normal and pathological health conditions. However, we used the score 1 for those items because it is the most extended method nowadays and to keep it consistent with HDR and HARD assessment. In this case, the considered normal mean values may be beyond 10 and the interpretation of the results or the establishment of a threshold is commonly contrasted with other scales like the Hamilton scale (Van Hemert et al, 1995). All the patients reported none or few anxiety (mean: 1; range 0 – 3) and depression symptoms (mean: 1.1; range: 0 – 3). General health questions layered also non-pathological ratings (mean: 5.3; range: 3 – 9). One subject received extremely large ratings in the screening (GHQ: 19; HDRS: 8; HARS: 7) that were considered too high. Thus subject's magnetoencephalographic data and behavioral performance was not further taken into account, nor was his screening scores included in the average ratings included in this section.

4.4.2 Stimuli

Like in Exp. 1a the stimuli were spatially filtered and broadband frontal portraits of actors and actresses posing neutral, happy or fearful facial expressions. We increased the number of stimuli for this experiment in comparison with Experiment 1a: faces by incorporating face portraits from five other datasets to the previously used ones, namely: the Karolinska Directed Emotional Faces database (KDEF; Karolinska, Lundqvist, Flykt and Öhman, 1998; 35 females and 35 males), the Radboud Faces database (RaFD; Langner et. al., 2010; 19 females and 20 males) and the Warsaw Set of Emotional Facial Expression Pictures (WSEFEP; Olszanowski et. al., 2015; 16 females and 14 males). The newly added pictures pertained to the following datasets: the FACES database (FACES; Ebner, Riediger and Lindenberger, 2010; 56 females and 58 males), the MacBrain Face Stimulus Set (NimStim; Tottenham et al., 2009; 8 females and 17 males), the Amsterdam Dynamic Facial Expression Set (ADFES; van der Schalk et. al., 2011; 10 females and 12 males), the Pictures of Facial Affect (POFA; Ekman and Friesen, 1976; 8 females and 6 males) and the Cohn-Kanade AU-Coded Facial Expression Database (CK+; Kanade, Cohn and Tian, 2000; Lucey et al., 2010; 10 females and 3 males). In sum, our pool was composed of 327 different identities (162 females and 165 males).

Initially, the pool included pictures with different framing, color and sizes. First, the remaining seven datasets were cropped using the same aspect ratio (4:3) to a common 'face space' based on the pictures from the dataset with the largest number of identities (FACES) taking into consideration that the eyes and the mouth of each actor/actress occupied more or less the same place in the pictures while neck and top of the head were included in the portrait. Secondly, they were resized to a convenient common size (400 pixels width x 520 pixels height) so no picture was stretched or distorted. Third, the color was changed to a grayscale and the backgrounds were set to the same value of grey, based again on the background of the dataset with the largest number of identities. Finally, brightness was adjusted so the average brightness (taken as the mean pixel value) was the same (117) for every picture.

The spatial filtering of the pictures was performed equally for all the portraits after they were homogenized. To determine the spatial filter cut-off frequencies the MEG chamber display size (45 cm) and resolution (1280 pixels) were taken into account, among the distance between the subject and the display (130 cm), the final size of the pictures in the screen (14 cm) and the visual angle (6.19 degree), albeit only the horizontal dimension was considered. Hence, the sigma values used to filter the pictures were 4.77 and 23.85 resulting in 0.77 and 3.85 cycles per degree for low (LSF) and high (HSF) spatial frequency pictures respectively.

4.4.3 Procedure

After the screening, participant sat on a wooden chair and had the Head Position Indicators (HPI) coils placed. Digitization data on the shape of the head was acquired with a Polhemus 3-D digitizer (Polhemus Incorporated, VT, USA). Then, two bipolar montages of electrodes were placed around the eyes so that horizontal and vertical electrooculogram could be recorded, and a couple of electrodes were placed between the right collar bone and over the last left ribbon to measure the heart-rate. The subjects received also verbal instructions about the task and about the importance of minimizing muscle movements while recording. They were specially asked to reduce eye-movements and blinks and to concentrate them in the period after the response and before the display of the following trial if possible. Before the acquisition started, they were guided into the isolated MEG chamber were they were familiarized with response buttons and performed to practice runs

that mimicked experimental runs with twenty different filtered and unfiltered portraits taken from the internet. The second practice run was designed to instruct them to place their blinks between trials immediately after their response. They were also instructed to remain as still as possible and minimize head movements once the experiment had begun.

Like Exp. 1a, the experiment was a factorial design of two factors with three levels (emotion: fearful happy and neutral; and frequency: BSF, HSF and LSF). Hence, there were nine conditions. For each subject 324 *different identity* portraits (162 of each gender) were randomly selected out of a total of 2943 pictures to form a single sequence. This number includes one broadband picture per actor/actress for each of the three expressions (fearful, happy and neutral) and their corresponding high and low spatial frequency filtered versions. Thus, for each emotion and spatial frequency only one identity was shown to each participant. Each condition was comprised of 36 stimuli, half women and half men. Several randomizations were done and the resulting brightness and energy values of the pictures comprising each condition were entered into an ANOVA to ensure there were no brightness differences between conditions and energy was equal within every emotion level. Those single sequences that showed significant differences were discarded. Last, the final order of presentation of the stimulus was randomized with the constraints that no more than three consecutive stimuli may pertain to the same condition.

The experimental session was divided in two runs with a ten minute gap where subjects were asked to relax. Each run was composed of the same 324 stimuli in a different random order. Subjects were asked to perform a gender judgment task pressing as fast and accurately as they could a button with one of their index finger. Left or right allocation of male or female judgments button was the same for each subject but counterbalanced across the whole sample. Each run lasted for around 15 minutes.

A single trial proceeded as follows (Figure 4.1): first a single face followed by a blank screen were displayed each for 500 ms. A blank screen with a white centered cross appeared next for a fixed time (1750 ms) plus a random jitter-time ranging between 1 and 500 ms after which the face pertaining to the next trial appeared. So, the stimulus onset asynchrony (SOA) varied between 2750 and 3250 ms. These display times were chosen to ensure there was enough time for the subjects to answer and blink while still keeping a

reasonable baseline time before the onset of the next trial and at the same time producing a pace fast enough to engage subjects attention as well as short total experimental run time.

Figure 4.1: Experimental procedure

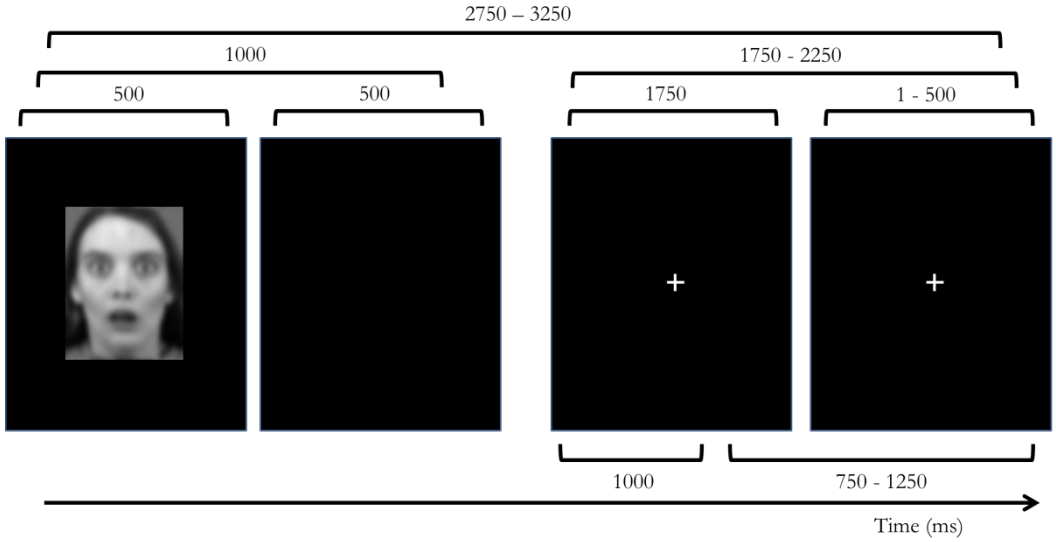

The figure illustrates Exp. 2 experimental procedure (task: gender judgment). A single trial initiated with the presentation of the stimulus for 500 ms followed by a 500 ms blank screen and a fixed cross screen that extended between 1750 and 2250 ms in a random fashion until the next trial.

4.4.4 Acquisition and preprocessing

MEG data was recorded continuously at a 1000 Hz sample acquisition rate with a 0,1 to 330 Hz online filter using an Elekta-Neuromag 306 channels system (Elekta©, VetorView). The MEG sensors in this machine consist of 102 magnetometers and additional 102 couples of orthogonal planar gradiometers pairs that can be combined into 102 axial gradiometers. For each run, the position of the subject's head below the sensors had been acquired just before the task started. Unfortunately, HPI coils registration didn't work correctly for the second run of two of the subjects (subjects 2 and 14). The data from both runs was removed from the rest of the analysis due to this issue.

External noise was removed from the MEG data using the temporal extension of Signal-Space Separation (SSS; Taulu et al., 2005) as implemented within the MaxFilter software (Elekta-Neuromag). Initial segments including 1500 ms peristimulus (1000 ms poststimulus) data were first extracted and visually inspected to discard those ones with big

artifacts product of sensor malfunction and movements. Given the spatial filter applied, few trials were removed due to these reasons. Then, the electrooculogram and the rest of the channels were visually inspected and those time segments contaminated by a blink artifact were marked. Then, peristumulus epochs of 840 ms (200 ms baseline) were extracted around each trigger, and those that overlapped with a blink were discarded. Furthermore, those trials without key presses or more than one key press were also taken aside from the rest of the analysis. As the last stage of the preprocessing, data was baseline corrected and low-pass filtered using a 40 Hz threshold. Those parameters, as opposed to the MEG preprocessing pipeline followed in Experiment 3, are fit to study the temporally fine event related / evoked field (ERF) responses.

Nine individual average ERFs (one per condition) were obtained by averaging the epochs pertaining to the same condition first within each run and then across that run average per each subject. The final grand averages were composed of fifteen individuals. All of them were the product of a mean of 64.04 trials (mean standard deviation –std- was 3.41; range between 54 and 70) without taking into account subjects 2 and 14 whose individual averages were composed of 32.3 (std was 2) and 33.9 (std was 1.8) mean trials respectively.

4.4.5 Behavioral task analysis

First, overall performance was analyzing by comparing the amount of trials on which the subject pressed the button only once in an interval between 200 and 1500 ms independently of the target's nature. After that, only correctly answered trials were selected to analyze accuracy ratings (defined as the percentage of correct responses for each individual and condition) and reaction times. Statistical analysis of behavioral data was performed first by submitting mean individual reaction times to a repeated measures analysis of variance (ANOVA) with three factors (Run: first and second; Emotion: fearful, happy and neutral; Frequency: BSF, HSF and LSF). We include these analysis in the text however given that second run data from two subjects was lacking and no effects of run were found we also performed repeated measures ANOVA with only two factors (Emotion: fearful, happy and neutral; Frequency: BSF, HSF and LSF). We report all the results of the emotion by frequency ANOVA and the run related effects (main effects and interactions) of the run by emotion by frequency ANOVA throughout the text.

4.4.6 Sensor level statistical analysis

Magnetometers were used for statistical analysis in the sensor space. Our main objective was to determine if an interaction at the sensor level recorded over the scalp with the MEG may parallel the effects of enhanced fearful processing found on the early interaction cluster (from 72 to 108 ms) that was significant at intracranial amygdala sites of Experiment 1a: faces. Thus we focused our analysis in a time segment from 50 to 110 ms. By creating new conditions (from now on called *difference waves*) subtracting the mean of happy and neutral faces from fearful faces within each spatial frequency condition and submitting them to montecarlo cluster based non-parametric statistics with 1000 permutations we were able to search the sensor space for early fear related modulations within our a priori time window of interest. Thus, the three difference waves in this analysis were: BSF fearful faces minus the average of BSF happy and BSF neutral faces; HSF fearful faces minus the average of HSF happy and HSF neutral faces and LSF fearful faces minus the average of LSF happy and LSF neutral faces. In addition to the montecarlo statistic, the values of the three difference wave within the relevant cluster were submitted into repeated measures ANOVA with factor emotion: fearful, happy and neutral. Furthermore, for each of the nine conditions the average value of the relevant sensors within the time frame of the relevant cluster were also extracted and submitted into a repeated measures ANOVA with two factors (emotion: fearful, happy and neutral; frequency: BSF, HSF and LSF). Post-hoc analyses were performed based on the nature of the effects.

However, to guide a blind exploration of the data, cluster-based non-parametric permutation statistic that would determine the temporal windows and channel locations of significant *main effects* (emotion, three levels: fearful, happy and neutral; frequency, three levels: BSF, HSF, LSF) were also performed over the whole epoch (0 – 550ms). This information and scalp plots of the temporal course of the MEG activity are provided within the Results section. Given the wide spatiotemporal span of the significant post 100 ms clusters showing main effects of frequency a more traditional analysis was performed around the M170 time window.

First, relevant sensors common to all three frequency levels (BSF, HSF and LSF) showing an M170 characteristic response were located by visual inspection of the scalp

maps. M170 representative channels in the right hemisphere were averaged from 130 to 250ms and a latency analysis was performed by searching the individual minimum value within the former time window. Mean latency differences were tested again with a repeated measures ANOVA with two factors (emotion: fearful, happy and neutral; frequency: BSF, HSF and LSF). Based on the mean latencies product of this analysis but also on observation of the scalp and the source maps (that we will talk later) three different time windows of 50 ms around the mean latency were selected for each frequency. The average amplitudes of the selected channels within this time frame was submitted into a repeated measures ANOVA identical to that performed before for the latency effects and the early interaction sensor mean values.

4.4.7 Source reconstruction and source level statistical analysis

Inverse problem was approached using a minimum norm estimate. A common surface space was constructed based on a template T1 map to which amygdala, hippocampus, accumbens and thalamus were aggregated. Individual head shape information was used to deform the default anatomy so it best fit each particular subject, and initial head position recorded at the start of each run were taking into account. An overlapping spheres head model was constructed for each run and individual. Individual mean ERF for each run were used to compute the inverse solution. Noise covariance matrix was calculated using the 200 ms pre-stimulus baseline. Signal to noise ratio was considered to be 1.5 and the diagonal of the noise covariance was used. Data from both magnetometers and gradiometers were used to compute the maps. Source maps from both runs pertaining to the same condition were averaged at the subject level (except for subject 2 and subject 14 data that belonged only to the first run) and grand average source maps were also built for visual description and component identification.

For the time windows of interest, maximum amplitude source maps were used to circumscribe surface regions (scouts) of interest. For the early interaction and given the discrepancy between the location of the channels showing an interaction effect and the scalp and source map maximum values we concluded that the effects detected by our analysis would probably not pertain to the cerebral sources showing the biggest activity within that particular time window. Thus, we lowered our threshold amplitude for the location of scouts of interest to 60%. The mean value for each of the reconstructed scouts

at a central point (82 ms) for each of the fearful faces condition were submitted into a repeated measures ANOVA with just one factor (frequency: BSF, HSF and LSF). We therefore used the same threshold to create the M170 scouts. For the M170, the values of the selected scouts were calculated as the mean activity within 10 ms around a central time point calculated ad hoc for each of the spatial frequency level (175, 180 and 205 ms for BSF, LSF and HSF respectively). Those values were submitted into a repeated measures ANOVA with two factors (emotion, three levels: fearful, happy and neutral; frequency, three levels: BSF, HSF, LSF).

4.4.8 Traditional Analysis

The data recorded for this experiment was highly complex and contained more information than the one we previously aimed to extract. The differences between spatial frequencies were evident after 100 ms making it difficult to use less standard analysis techniques like montecarlo cluster based permutation. However, our interest was to explore any interaction effects between emotion and spatial frequency that could occur at really early latencies (> 100ms). Nonetheless, we think the post 100 ms effects demanded additional further and detailed exploration. Therefore we decided to perform a traditional analysis over selected time windows and sensors of interest at the ERF components evident in the time course scalp activation (see Figure 4.2 panel B) and the grand mean ERFs (see Figure 10). This analysis was performed for the sake of completion, it is not the main objective of the current work, though we thought it was important to include it in this manuscript for a better understanding of what is happening at later stages of visual processing within our paradigm.

By visual inspection of the ERF waveforms and their spatial distribution over time we identified five different topographies between 50 and 200 ms that we propose correspond to five different components, or early steps in face processing. Figure 4.10 represents the grand average for BSF, HSF and LSF faces collapsed across emotions; the peaks corresponding to each component and the topography of each of the components can be seen. We decided to name our first three components with the approximate latency of their peak: M60, M90 and M120. We think the last two components represent two different sources of the so called M170 (see Itier et al., 2006b). Hence, we labeled the

earliest one as M170A and the later as M170B, although their actual latencies are around 150 and between 160-190 respectively.

For each of the five components, we selected five groups of sensors at locations with maximum absolute amplitudes within the time window of interest. Initially, this time window was subjectively chosen observing the temporal changes in activity over the scalp. The sensors of interest were four for each of the first three components -M60, M90 and M120- at occipital, temporal and temporooccipital locations, respectively. Given its shortness on time and space M170A was represented by a group of three parietooccipital magnetometers, while broader M170B was represented by a group of seven parietotemporal sensors. The sensors chosen for each component are highlighted in Figure 4.10 scalp plots.

The latency of each component was calculated searching for the absolute maximum value within the corresponding group of electrodes at 40-80 ms for the M60; 60-92 ms for the M90; 100-140 for the M120; 135-175 for the M170A and 150-220 for the M170B. Mean latency peaks for each subject and condition were statistically analyzed by a repeated measures ANOVA similar to the ones employed before with factors frequency (BSF, HSF and LSF) and emotion (fearful, happy and neutral). Then, based on the mean average peaks and the results of the latency statistics, we calculated the average amplitude value of each condition for all the sensors in the group of interest for each component. The M60 was averaged between 60-70; the M90 between 80-90; the M120 between 108-133; the M170A between 137-157 for the BSF faces, 143-163 for the LSF faces and between 147-167 for the HSF faces; the M170B between 155-175 for the BSF faces, 160-180 for the LSF faces and 185-205 for the HSF faces.

4.5 Results

4.5.1 Behavioral results

Regarding subject's performance, summing all the trials on which one and only one button press was given independently of the correct answer, the subjects performed quite well. The mean number of valid responses per subject was 99.2% (range: 96.2-100, s.e.m.: 0.32). The mean valid trials per condition were 96.5% (range: 90.3-100, s.e.m.: 0.42). There were no significant effects of emotion ($F_{2,28} = 0.254$; $p = 0.704$) or frequency ($F_{2,28} = 2.301$; $p = 0.148$) or an interaction emotion by frequency ($F_{4,56} = 0.577$; $p = 0.591$) either. Considering only the subjects that performed both runs (15 versus 13) the ANOVA including factor run (two levels: first and second) showed there were no main effects of run ($F_{1,12} = 0.623$; $p = 0.445$) or interaction effects between run and emotion ($F_{2,24} = 0.575$; $p = 0.520$), run and frequency ($F_{2,24} = 1.311$; $p = 0.278$) or run, emotion and frequency ($F_{4,48} = 0.466$; $p = 0.654$).

Regarding the accuracy, there were no significant effects of run ($F_{1,12} = 0.359$; $p = 0.56$) or interaction effects between run and emotion ($F_{2,24} = 0.869$; $p = 0.417$), run and frequency ($F_{2,24} = 1.627$; $p = 0.224$) or run, emotion and frequency ($F_{4,48} = 1.207$; $p = 0.091$). Nonetheless, there were significant main effects of emotion ($F_{2,28} = 8.631$; $p = 0.001$) as well as frequency (and $F_{2,28} = 24.29$; $p < 0.001$). Fearful faces provoked significantly more errors (87.32% accuracy rate) than happy (90.65% hits; $p = 0.015$) and neutral faces (90.64% hits; $p = 0.007$) while there were no differences between the later. On the other hand, the frequency effects were more complex: broadband pictures were correctly identified 94,17% of the time, significantly more than HSF (84.88%; $p < 0.001$) and LSF faces (90.56%; $p = 0.001$). The greater accuracy for LSF faces as compared with HSF faces was significant too ($p = 0.007$). Note that interaction effects were not significant but below $P = 0.1$ ($F_{4,56} = 2.245$; $p = 0.098$).

With respect to the reaction times, there were no significant main effects of run or significant interaction effects between run and frequency ($F_{2,24} = 0.016$; $p = 0.981$), run and emotion ($F_{2,24} = 0.917$; $p = 0.402$) or run, emotion and frequency ($F_{4,48} = 0.542$; $p = 0.626$). Only the effects of frequency were significant ($F_{2,28} = 82.594$; $p < 0.001$).

Broadband faces were answered faster (mean: 579.70 ms; std: 30.01) than HSF (mean: 650.45 ms; std: 30.99; $p < 0.001$) and LSF faces (mean: 590.06 ms; std: 29.42; $p = 0.001$). The difference between these later conditions was also significant (LSF faces faster than HSF faces $p < 0.001$). The effects of emotion were not significant but at trend ($F_{2,28} = 3.009$; $p = 0.08$). Fearful pictures reaction times were the longest (mean: 611.64 ms; std: 31.19), significantly smaller than those of neutral pictures (mean: 602.66; std: 29.65; $p = 0.03$) but not than those from happy faces (mean: 605.91; std: 31.18; $p = 0.218$). The interaction emotion by frequency was not significant in this comparison ($F_{4,56} = 1.582$; $p = 0.10$).

Table 4.1: Reaction times and accuracy ratings

Condition			Mean	s.e.m	Test	Statistic	Probability	Post-Hoc Comparison	
Accuracy (percentage)									
BSF	Fearful	=	91.3	(1.3)	Emotion	$F_{2,28} = 8.631$	$P = 0.001$*	Fearful < Happy	$P = 0.015$
	Happy	=	95.5	(0.9)				Fearful < Neutral	$P = 0.007$
	Neutral	=	95.7	(0.9)					
LSF	Fearful	=	89.3	(1.0)	Frequency	$F_{2,28} = 24.290$	$P = 0.000$*	BSF > HSF	$P = 0.000$
	Happy	=	91.9	(1.4)				BSF > LSF	$P = 0.001$
	Neutral	=	90.6	(1.5)				LSF > HSF	$P = 0.007$
HSF	Fearful	=	81.4	(2.5)	Interaction	$F_{2,28} = 2.244$	$P = 0.098$		
	Happy	=	84.6	(2.3)					
	Neutral	=	88.6	(1.6)					
Reaction Times (ms)									
BSF	Fearful	=	589.5	(31.9)	Emotion	$F_{2,28} = 3.009$	$P = 0.080$		
	Happy	=	577.9	(29.3)					
	Neutral	=	571.7	(29.4)					
LSF	Fearful	=	589.4	(29.9)	Frequency	$F_{2,28} = 82.594$	$P = 0.000$*	BSF > HSF	$P = 0.000$
	Happy	=	591.4	(29.5)				BSF > LSF	$P = 0.001$
	Neutral	=	589.4	(29.4)				LSF > HSF	$P = 0.000$
HSF	Fearful	=	656.1	(32.7)	Interaction	$F_{2,28} = 1.582$	$P = 0.206$		
	Happy	=	648.4	(29.8)					
	Neutral	=	646.9	(31.1)					

Global behavioral results separated by accuracy ratings (top rows) and reaction time (bottom rows). Accuracy ratings were measured as the percentage of correct responses. Reaction times are measured in milliseconds. Standard error means for both measures are in parenthesis.

Table 4.1 summarizes the results of the behavioral analyses including the mean reaction time and accuracy rates considering only the correct trials and an emotion by frequency repeated measures ANOVA without factor run. Though the interaction and emotion effects were not significant (also with factor run, see above paragraph) it is worth noting that the pattern of the emotional differences (longer reaction times for fearful faces

than for happy and neutral) seems absent for LSF and more evident for BSF and HSF faces. Uncorrected t-tests within each frequency level show that the difference between fearful and neutral faces was significant for BSF faces (t14 = 3.288; p = 0.005), not significant for HSF faces (t14 = 1.27; p = 0.225) and far from significant for LSF faces (t14 = -0.013; p = 0.990) whose mean were indeed very similar (LFS fearful faces mean: 589.35 ms; std: 115.64 ; LSF neutral faces mean: 589,41 ms; std: 113.71) and smaller than those from happy faces (LSF happy faces: 591.41 ms; std: 114.34).

4.5.2 Sensor level results

In experiment 1, using cluster based permutation statistics we found an early (between 70 and 108 ms) modulation specific tor fearful faces with low spatial frequencies at the amygdala. In experiment 3, given this a priori temporal constraint to our hypothesis, we performed a similar test by subtracting the average of happy and neutral faces from fearful faces at each frequency level. The difference between both statistics is the clusters are formed spatially (between neighboring electrodes) in addition to temporally. Montecarlo statistics with the three difference waves (fearful minus happy and neutral faces from BSF, HSF or LSF pictures) were run between 50 and 110 ms.

4.5.2.1 Cluster based permutation statistics: early interaction window

In contrast with the post 100 ms permutation effects at the sensor level there were almost no significant clusters in the interaction test time window. Seven spatio/temporal clusters were formed and though remaining six clusters has significant values above P = 0.8) the most statistically powerful cluster was slightly below alpha threshold (summed F value: 3140.8; p = 0.047). Interestingly it spanned from 72 to 92 ms over eleven central right magnetometers. (from 70 to 100 ms over thirteen sensors without minimum neighboring channel constraints to the permutation). Furthermore, it was related with increased amplitudes for LSF fearful faces. Figure 4.2, panel A shows the scalp plot of the *difference waves* indicating the channels were there was a significant interaction. Post-hoc comparisons between the average of the difference waves from 72 to 92ms showed that the amplitudes of the LSF difference wave (mean: 20.94 fT; std: 24.4) were bigger than the amplitudes of the HSF difference wave (mean: -13.26 fT; std: 26.0; P < 0.001) but also significantly bigger than the amplitudes of the BSF difference wave (mean: -3.58; std: 29.57;

p = 0.005). There were no significant differences between the BSF and HSF difference waves (BSF = HSF; P = 0.398). Given the nature of the effect and its spatiotemporal distribution we decided it was necessary to further explore it, so we observed the ERFs of the nine conditions at the sensors and temporal window of interest. The cluster corresponds with a positive going component over right hemisphere sensors peaking at around 82ms. Scalp plots for all the fearful face conditions within this time are shown in Figure 4.2 panel B, while panel C shows the ERF at a representative electrode (around C2 in the 10-20 system). We can see how LSF fearful faces elicit higher amplitude responses

than the other conditions, peaking at around 82 ms.

It is important to note that the significant cluster is not within the electrodes with the biggest amplitudes but in the gradient. Individual averages at sites of interest for all nine conditions over 72 and 92 ms were computed and submitted into a repeated measures ANOVA with factors emotion (three levels: fearful, happy and neutral) and frequency (three levels: BSF, HSF and LSF). Importantly, interaction effects turned to be significant ($F_{4,56}$ = 3.349; P = 0.029). There was also a trend for frequency effects ($F_{2,28}$ = 3.752; *P* = 0.053) and no significant emotion main effects ($F_{2,28}$ = 0.238; P = 0.741). We conducted

Figure 4.2: Early interaction: cluster permutation statistics and eRMF

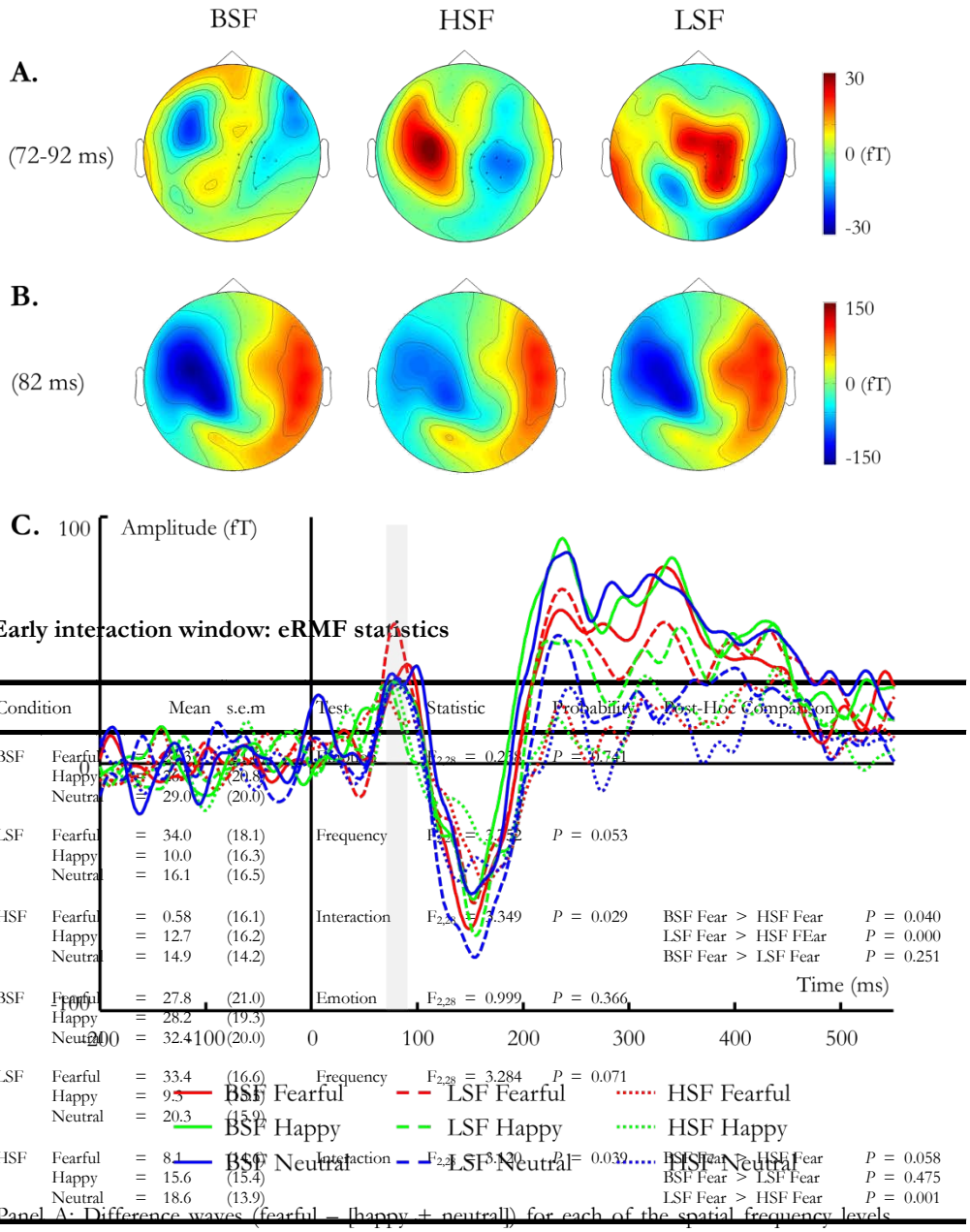

Panel A: Difference waves (fearful – [happy + neutral]) for each of the spatial frequency levels (first column: BSF; second column: HSF; third column: LSF) averaged across the significant cluster time window represented in a scalp plot. Significant sensors are highlighted. Panel B: An additional topographic representation of just fearful faces separated across spatial frequencies in a similar fashion as Panel A. Panel C: eRMF response for the nine conditions at a representative electrode (~C2). The time window of the significant cluster is represented by the shadowed gray area.

Table 4.2: Early interaction window: eRMF statistics

Time	Condition		Mean	s.e.m	Test	Statistic	Probability	Post-Hoc Comparison	
72-92	BSF	Fearful	= 31.2	(20.2)	Emotion	$F_{2,28}$ = 0.238	*P* = 0.741		
		Happy	= 29.2	(20.8)					
		Neutral	= 29.0	(20.0)					
	LSF	Fearful	= 34.0	(18.1)	Frequency	$F_{2,28}$ = 3.752	*P* = 0.053		
		Happy	= 10.0	(16.3)					
		Neutral	= 16.1	(16.5)					
	HSF	Fearful	= 0.58	(16.1)	Interaction	$F_{4,56}$ = 3.349	*P* = 0.029	BSF Fear > HSF Fear	*P* = 0.040
		Happy	= 12.7	(16.2)				LSF Fear > HSF FEar	*P* = 0.000
		Neutral	= 14.9	(14.2)				BSF Fear > LSF Fear	*P* = 0.251
72-100	BSF	Fearful	= 27.8	(21.0)	Emotion	$F_{2,28}$ = 0.999	*P* = 0.366		
		Happy	= 28.2	(19.3)					
		Neutral	= 32.4	(20.0)					
	LSF	Fearful	= 33.4	(16.6)	Frequency	$F_{2,28}$ = 3.284	*P* = 0.071		
		Happy	= 9.5	(15.9)					
		Neutral	= 20.3	(15.9)					
	HSF	Fearful	= 8.1	(14.6)	Interaction	$F_{4,56}$ = 3.120	*P* = 0.039	BSF Fear > HSF Fear	*P* = 0.058
		Happy	= 15.6	(15.4)				BSF Fear > LSF Fear	*P* = 0.475
		Neutral	= 18.6	(13.9)				LSF Fear > HSF Fear	*P* = 0.001

The table shows the mean amplitude values of the eRMF responses for the sensors (averaged across sensors) and time points (averaged across time) pertaining to the significant interaction cluster group the permutation statistics with threshold $P < 0.01$ (top rows) and $P < 0.05$ (bottom rows). Standard error means are in parenthesis. The fourth to eight columns shows the results of a three by three ANOVA performed for both time windows (regions of interest) separated between main effects and the interaction. Last (eight) column: pertinent post-hoc comparisons.

post-hoc test at each factor level to breakdown the interaction. This is; we compared the mean of all the fearful, happy or neutral faces and all the BSF, HSF and LSF faces. We observed there were only significant differences within all the LSF faces ($F_{2,28}$ = 5.073; P = 0.022) and all the fearful faces ($F_{2,28}$ = 7.878; P = 0.009). Within the fearful faces, there were no significant differences (*P* = 0.251) between the amplitudes of BSF (mean: 24.3 fT; std: 21.1) or LSF (mean: 34.0 fT; std: 18.1) faces, but both the former (*P* = 0.040) and the later (*P* = 0.000) were significantly bigger than the amplitudes of HSF fearful faces (mean: 0.58 fT; std: 16.1). On the other side, between the LSF faces, the amplitudes of the fearful faces (mean: 34.0 fT; std: 70.3) were significantly bigger (*P* = 0.001) than the amplitudes of the happy (mean: 10.0 fT; std: 63.0) and neutral faces (mean: 16.1 fT; std: 64.0) just at trend (*P* = 0.074). While at the same time there were no differences between the amplitudes of happy and neutral LSF faces (*P* = 0.477). Table 4.2 shows the mean amplitudes for each of the nine conditions in this time window.

As we mentioned before, the temporal window of the significant cluster gets bigger (from 70 to 100ms) if we don't put constraints to the number of minimum neighboring channels during the cluster based permutations. It seems in fact that HSF and BSF faces are more positive toward 100 ms. If we take this window more positive going amplitudes for the HSF faces in general are measured (for example HSF fearful faces mean: 8.1 fT; std: 5.6) but the results of the statistics are very similar to the ones disclosed before, with the exception that the differences between BSF and HSF fearful faces are no longer significant

but at trend (P = 0.058). Table 4.2 shows the mean amplitudes and the results of the statics for both windows.

4.5.2.2 Cluster based permutation statistics: Later effects

In addition to the interaction test within the time frame of our a priori hypothesis (pre 100 ms) we performed cluster based permutation statistics from 0 to 400 ms (most of the epoch) for the sake of completion. From the results of this analysis, it become evident that a different approach other than the montecarlo statistics applied in Exp. 1 would be required in the case of more complex spatio-temporal MEG data.

The test between BSF, HSF and LSF faces results in two big clusters showing significant main effects of frequency. Both clusters comprised a huge amount of channels from both hemispheres and spanned throughout the whole epoch. The first one (summed F value: 549120; P < 0.001) started at 180 ms until the end of our epoch and grouped 90 channels. The second cluster (summed F value: 102450; P = 0.007) grouped 81 channels from 94 ms to 173 ms. There were also two significant clusters in the comparison between fearful, happy and neutral faces showing main effects of emotion. The first cluster (summed F value: 116530; P < 0.001) comprised 66 channels and spanned from 318 ms to 551 ms. The second significant cluster (summed F value: 84501; P < 0.001) grouped 84 channels and extended from 145 ms to 303 ms. Figure 4.3 panel A shows what magnetometers were grouped within each mentioned cluster (upper panel)

The main effect of frequency cluster permutation results reflect the fact that the different spatial frequencies had components with different latencies, and their temporal course is shifted around 100 ms. This is evident if we look at the ERFs. Given that in the next section we show the average of a large group of magnetometers in the right

hemisphere to illustrate the M170 recorded in the experiment, in this section we provide the scalp plots of BSF, HSF and LSF from 50 ms post stimulus in steps of 10 ms (Figure 4.3, panel B) for the sake of completion. It can be appreciated that at around 100 ms the scalp plots start to differ and show different spatial distributions as reflected by the

Figure 4.3: Cluster permutation statistics (main effects): eRMF temporal course

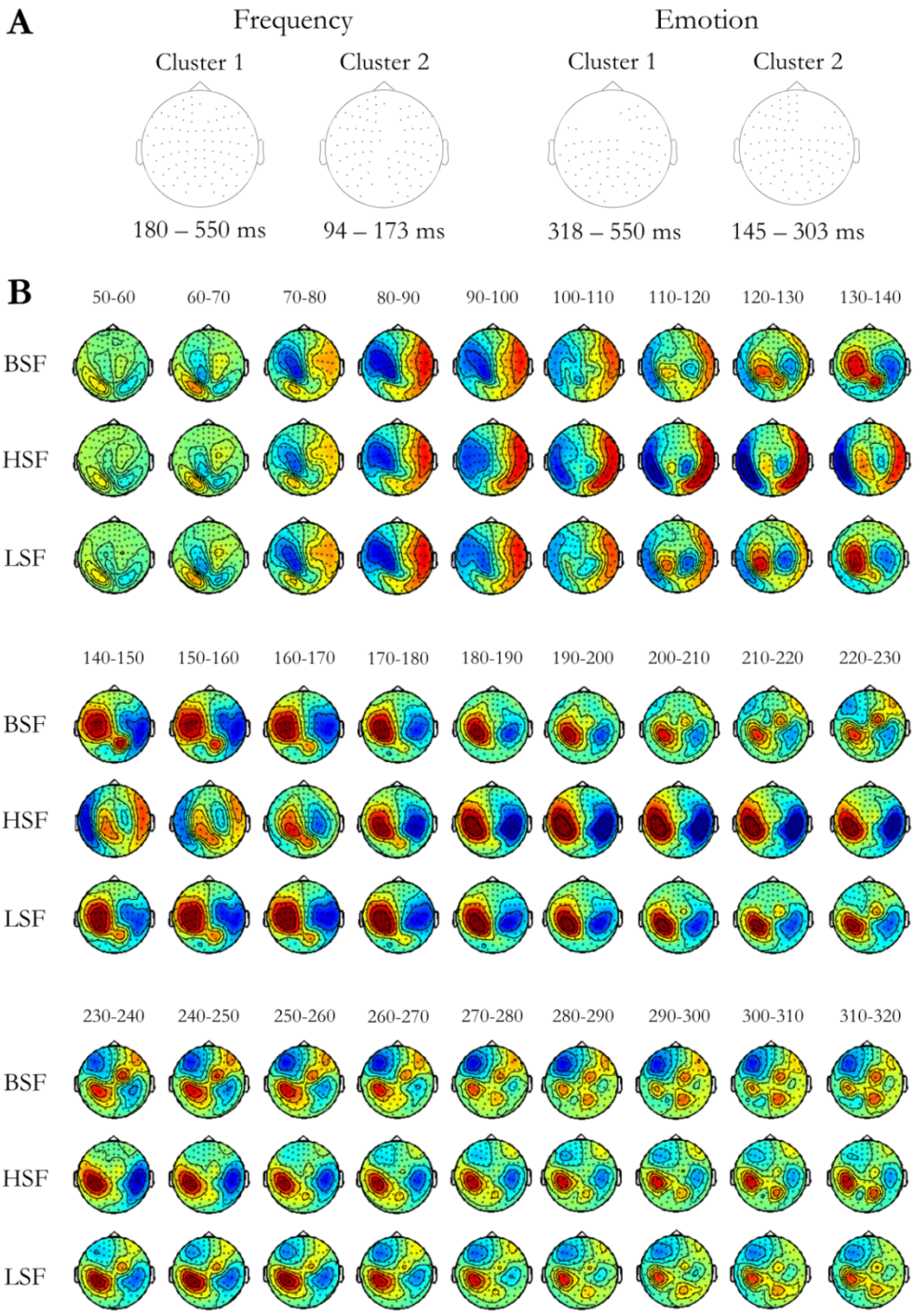

Panel A: representation of the two significant clusters for the emotion and frequency main effects product of the cluster based permutation statistics (see this section text for the statistical values). A huge number of sensors are significant within large windows of interest. Panel B: scalp plots across time. eRMFs are averaged across spatial frequency levels for the sake of simplicity. Each column is the average along 10 ms starting from 50 ms until 320 ms poststimulus. Differences between BSF or LSF and HSF faces are visibly from 100 ms onwards.

previous analysis. The fact that the spatial distribution of the ERF from the different spatial frequencies shows temporal course differences is a problem for the analysis and thus we decided to focus on the component of interest (M170) with a more traditional method.

4.5.2.3 M170

The M170 typical spatial distribution denotes two sources at occipito-temporal locations and may appear at around 140 – 230 ms poststimulus. Figure 4.4 shows the averaged topography for BSF, HSF or LSF faces M170 component in Experiment 2 based on our traditional analysis.

Figure 4.4: Cluster permutation statistics (main effects): eRMF temporal course

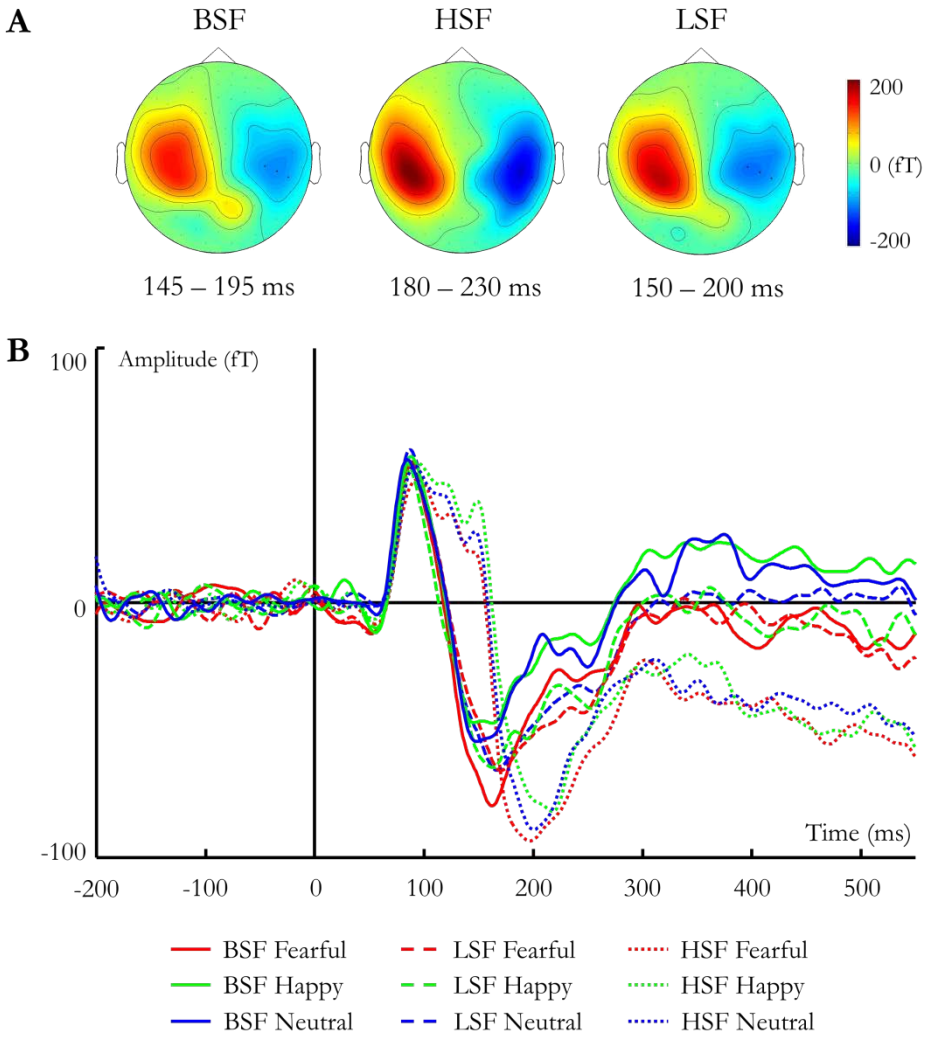

Panel A: scalp topography of eRMF averaged across spatial frequencies and time of interest according to the M170 latency windows calculations (annotated in the bottom row). Sensors employed in the analysis are highlighted. Panel B: eRMF averaged across sensors of interest for the nine conditions.

Observing the changes in the topography over time we manually selected eight channels (shown in the figure) in the right hemisphere that were within the lowest values for all the frequencies despite the slightly different spatial distributions while sufficiently sparse across the scalp. Figure 4.4 shows the average ERF at these sensors for all nine conditions.

First, we calculated the mean latency of the M170 for each condition by finding the peak (as the minimum value from 130 to 250 ms) for the average of the selected sensors at the individual level. The latencies obtained were submitted into a repeated measures with factors emotion (three levels: fearful, happy and neutral) and frequency (three levels: BSF, HSF and LSF). There were not main effects of emotion ($F_{2,28}$ = 1.067; P = 0.354) but there were main effects of frequency as expected ($F_{2,28}$ = 7.574; P = 0.003). Post-hoc comparisons showed that HSF faces (mean: 204 ms; std: 6.7) had significantly longer latencies than BSF (mean: 174 ms; std: 8.3; P = 0.001) and LSF faces (mean: 180 ms; std: 7.8; P = 0.019) while there were no significant differences between the latters (P = 0.460). The interaction effects were not significant and too far above the threshold to be further considered ($F_{4,56}$ = 1.968; P = 0.153), though it seemed that fearful and neutral faces had generally smaller latencies but in the case of HSF faces where happy faces seem to elicit longer latencies. Table 4.3 resumes the mean latencies for each condition. These values and the fact that there are main frequency effects also support our decision to choose different time windows for each spatial frequency to average the M170 amplitude.

The mean amplitude values for each condition and individual ERF were therefore computed over different time windows depending on the level of the factor frequency. M170 amplitude values were computed as the average amplitude from 150 to 200 ms for the BSF faces; from 155 to 205 ms for LSF faces; and from 180 to 230 ms for HSF faces. They are shown in Table 3 along the latency values and statistics explained in the above paragraph.

The selection of the time windows was first guided by visual observation of the changes in the scalp topography, the waves, and the inverse models (that will be discussed later). These amplitudes were submitted into repeated measures ANOVA the same way as the peaks were in the latency analysis. The repeated measures ANOVA on the amplitudes showed significant main effects of emotion ($F_{2,28}$ = 15.037; *P* = 0.000) and frequency ($F_{2,28}$

= 6.145; $P = 0.013$) but also a significant interaction ($F_{4,56} = 3.418$; $P = 0.024$). In order to better understand the interaction, we first focused on the direction of the main effects. Fearful faces (mean: -112.4; std: 22.8) elicited higher amplitude M170 than happy (mean: -89.6; std: 22.4; $P = 0.000$) and neutral faces (mean: -95.1; std: 22.7; $P = 0.001$), while there was no difference between happy and neutral faces ($P = 0.307$). At the same time, HSF faces (mean: -129.3 fT; std: 23.0) elicited higher amplitude than BSF (mean: -76.1 fT; std: 26.1; $P = 0.009$) faces but not higher than LSF faces (mean: -91.7 fT; std: 23.5; $P = 0.149$).

Table 4.3: M170: eRMF statistics

Condition				Mean	s.e.m	Test	Statistic	Probability	Post-Hoc Comparison	
Latency (ms)										
130-250	BSF	Fearful	=	174.0	(9.7)	Emotion	$F_{2,28} = 1.067$	$P = 0.354$		
		Happy	=	165.3	(8.5)					
		Neutral	=	184.3	(11.5)					
	LSF	Fearful	=	183.9	(8.4)	Frequency	$F_{2,28} = 7.574$	$P = 0.003$	BSF < HSF	$P = 0.001$
		Happy	=	174.8	(8.5)				LSF < HSF	$P = 0.019$
		Neutral	=	182.3	(9.1)					
	HSF	Fearful	=	204.0	(7.7)	Interaction	$F_{2,28} = 1.968$	$P = 0.153$		
		Happy	=	208.0	(6.7)					
		Neutral	=	200.3	(7.2)					
Amplitude (fT)										
150-200	BSF	Fearful	=	-102.8	(28.1)	Emotion	$F_{2,28} = 15.037$	$P = 0.000$	Fearful > Happy	$P = 0.000$
		Happy	=	-60.7	(25.4)				Fearful > Neutral	$P = 0.001$
		Neutral	=	-64.8	(26.2)					
155-205	LSF	Fearful	=	-93.7	(24.7)	Frequency	$F_{2,28} = 6.145$	$P = 0.013$	BSF < HSF	$P = 0.009$
		Happy	=	-89.5	(23.9)					
		Neutral	=	-91.8	(24.8)					
180-230	HSF	Fearful	=	-140.7	(21.1)	Interaction	$F_{2,28} = 3.418$	$P = 0.024$	BSF Fear > BSF Happy	$P = 0.000$
		Happy	=	-118.8	(24.6)				BSF Fear > BSF Neutral	$P = 0.001$
		Neutral	=	-128.6	(22.8)				HSF Fear > HSF Happy	$P = 0.006$
									HSF Fear > LSF Fear	$P = 0.016^{+}$
									BSF Happy < HSF Happy	$P = 0.009^{+}$
									BSF Happy < LSF Happy	$P = 0.020^{+}$
									BSF Neul < HSF Neu	$P = 0.005$
									BSF Neul < LSF Neu	$P = 0.036^{+}$

The top rows of the table show the results of the latency statistic and the M170 time window (first column). The global latency peak is shown for the nine conditions along with the results of the three by three repeated measures ANOVA and pertinent post-hoc comparison. The bottom rows of the table show the average amplitudes for each condition across its corresponding time window (first column) and the results of the three by three ANOVA over the amplitude values (and corresponding post-hoc). Standard error means are represented between parentheses for both analysis

The interaction seemed to point to the fact the emotion effects are more evident for BSF and HSF faces but seem absent in the case of LSF faces. Comparing fearful, happy and neutral faces within each level of the factor frequency showed significant effects for BSF faces ($F_{2,28} = 13.106$; P = 0.000), a trend in the case of HSF faces ($F_{2,28} = 3.34$; P =

0.059) and far from significance statistics for LSF faces ($F_{2,28}$ = 0.218; P = 0.795). Post-hoc tests showed that BSF fearful faces (mean: -102.8 fT; std: 108.7) had bigger amplitudes than BSF happy (mean: -60.7 fT; std: 98.4; P = 0.000) and BSF neutral (mean: -64.8 fT; std: 101.6; P = 0.001). At the same time, HSF fearful faces (mean: -140.7; std: 81.7) amplitudes were also bigger than HSF happy faces (mean: -118.8; std: 95.4; P = 0.006) but not significantly bigger than HSF neutral faces (mean: -128.6; std: 95.9; P = 0.187). Furthermore, comparisons within the level of emotion showed that HSF faces amplitudes were bigger than their BSF counterparts (*P* = 0.009 and *P* = 0.005 in the case of Happy and Neutral faces respectively) except for fearful faces (*P* = 0.071).

4.5.3 Source level results

4.5.3.1 Early interaction window

The MNE maps along the time window of the early interaction show an occipital source for the component. Figure 4.5 panel A represents the created scouts and the activation maps for the three fearful face conditions. Figure 4.5 panel B shows the average source activation map for all the fearful faces from 70 to 92 ms. The origin of the main activity at this time expands from extrastriate areas into lateral occipital cortex and ventrally into posterior fusiform and lingual gyrus. There are also sources in central parietal cortex and precuneus in addition to temporal pole sources.

Figure 4.5: Early interaction: source localization scouts and average

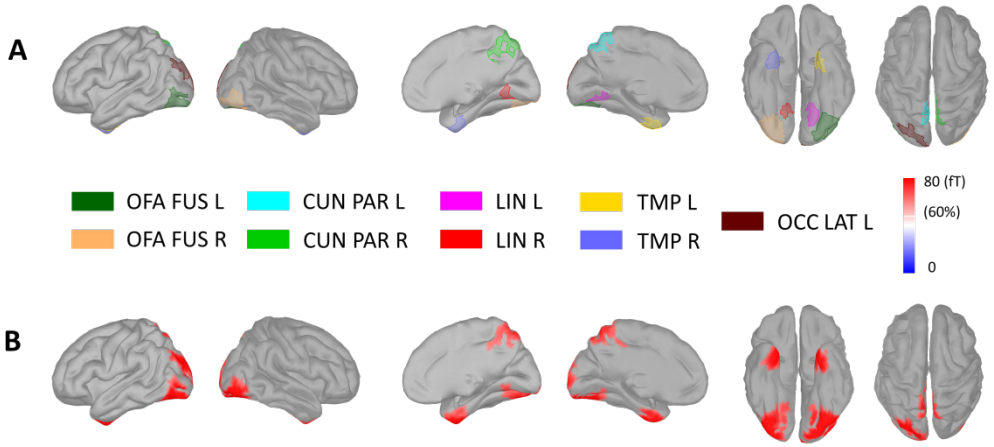

Panel A: 6-view model brain where the created nine scouts are shown in different colours. Panel B: 6-view average source map of BSF, HSF and LSF fearful faces. Areas of maximum activation are shown in red (threshold over 60 %).

This inverse solution is consistent with the topography observed in the sensor space. However, the magnetomers that showed the interaction effect (higher amplitudes for fearful faces with LSF frequencies when compared with HSF fearful faces) had a central location over the right hemisphere. We assumed that the differences in source space may not be at the locus of maximum activation but on other active areas not so prominent in terms of amplitude. Thus, in order to select regions of interest (*scouts*) over the surface of the MNE brain, we were guided by the activity map corresponding to LSF fearful faces (that had previously shown the maximum amplitude values in the sensor space) at the moment of the peak of the component (82 ms). Keeping in mind what we said before, we set the amplitude threshold to 60% and constrained the scouts to the surfaces whose activation surpassed that threshold at that time point. The resulting scouts were nine. Bilaterally, we circumscribed four regions: one at the Lingual cortex (*LIN L* and *LIN R*); another one between the cuneus and the parietal cortex (*CUN PAR L* and *CUN PAR R*); a third one involving the Occipital Face Area and the Fusiform (*OFA FUS L* and *OFA FUS R*) and a fourth one at the Temporal poles (*TMP L* and *TMP R*). In the Right hemisphere, but not in the Left hemisphere, we created also a scout between in the lateral occipital cortex (*OCC LAT R*).

The mean scout value for each fearful face condition at 82 ms was introduced in a repeated measures ANOVA with factor frequency (three levels: BSF, HSF and LSF). Figure 4.6 shows the solutions for BSF, HSF and LSF fearful faces separately.

Figure 4.6: Early interaction: scouts average maps

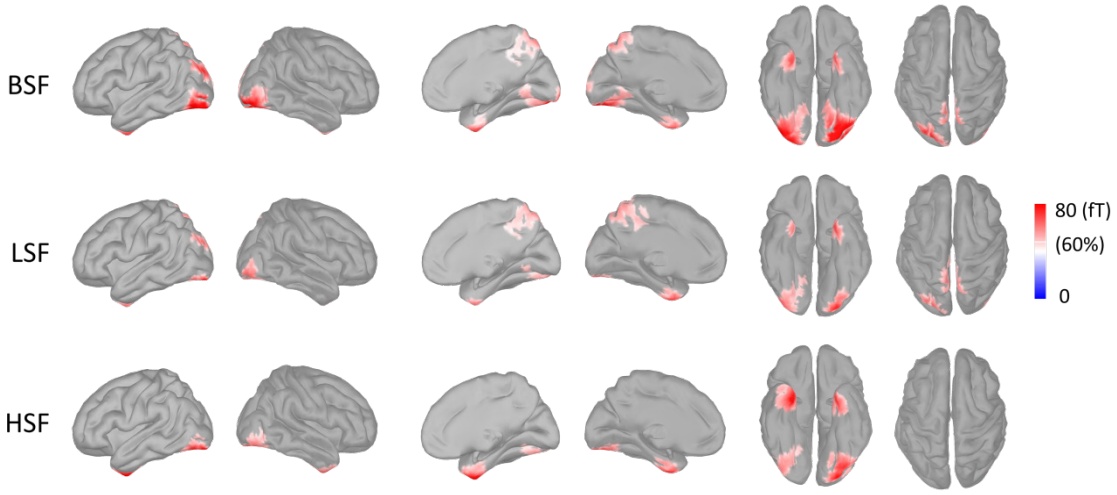

Six-view source maps for fearful faces (top row: BSF; middle row: LSF; bottom row: HSF). Areas with maximum activity are shown in red (threshold 60%)

The main effect of frequency was significant at parietal regions (*CUN PAR L*; $F_{2,28}$ = 5.58; P = 0.014; *CUN PAR R*; $F_{2,28}$ = 5.09; P = 0.013). These scouts included dorsal areas in the parietal cortex as well as medial regions pertaining to the cuneus. Post-hoc comparisons showed that there were no differences between BSF and LSF fearful faces activations (*CUN PAR L*; P = 0.347; *CUN PAR R*: 0.307) but both were significantly bigger than HSF faces in the left scout (*CUN PAR L*; BSF > HSF, P = 0.011; LSF > HSF, P = 0.047) as well as the right scout (*CUN PAR L*; BSF > HSF, P = 0.013; LSF > HSF, P = 0.04). The ANOVA on the rest of the scouts showed no significant effects of frequency. Table 4.4 shows the results of all the tests.

Table 4.4: Early interaction window: source statistics

Scout	Amplitude		s.e.m.	Statistic	Probability	Post-Hoc Comparison	
TMP L	BSF = 74.1		(9.2)	$F_{2,28}$ = 0.069	*P* = 0.916		
	LSF = 70.7		(8.1)				
	HSF = 72.7		(9.1)				
TMP R	BSF = 67.8		(7.1)	$F_{2,28}$ = 0.395	*P* = 0.635		
	LSF = 62.9		(5.9)				
	HSF = 71.0		(8.8)				
OFA FUS L	BSF = 80.9		(12.3)	$F_{2,28}$ = 1.127	*P* = 0.330		
	LSF = 67.9		(11.1)				
	HSF = 71.0		(12.3)				
OFA FUS R	BSF = 94.2		(18.5)	$F_{2,28}$ = 1.551	*P* = 0.231		
	LSF = 87.6		(15.1)				
	HSF = 79.2		(14.7)				
LIN L	BSF = 69.3		(8.9)	$F_{2,28}$ = 1.146	*P* = 0.329		
	LSF = 61.5		(6.5)				
	HSF = 58.4		(8.5)				
LIN R	BSF = 68.4		(9.2)	$F_{2,28}$ = 1.685	*P* = 0.212		
	LSF = 62.2		(7.1)				
	HSF = 55.9		(7.8)				
CUN PAR L	BSF = 69.3		(14.3)	$F_{2,28}$ = 5.158	*P* = 0.014*	BSF Fear > HSF Fear	*P* = 0.013
	LSF = 63.7		(12.4)			BSF Fear = HSF Fear	*P* = 0.347
	HSF = 49.3		(9.7)			LSF Fear > HSF Fear	*P* = 0.040
CUN PAR R	BSF = 66.8		(13.7)	$F_{2,28}$ = 5.088	*P* = 0.013*	BSF Fear > HSF Fear	*P* = 0.011
	LSF = 59.3		(13.3)			BSF Fear = HSF Fear	*P* = 0.307
	HSF = 44.2		(9.9)			LSF Fear > HSF Fear	*P* = 0.047
LAT OCC L	BSF = 70.9		(12.8)	$F_{2,28}$ = 0.413	*P* = 0.566		
	LSF = 66.3		(11.3)				
	HSF = 63.7		(9.9)				

Average activity at each of the nine scouts created for the early interaction effect. Standard error means are shown in parenthesis. Third and fourth column show respectively the statistic of the one-way repeated measures ANOVA comparing the three fearful faces at each scout and the assigned probability. Post-hoc comparisons are shown where pertinent

4.5.3.2 M170

The inverse solution maps for each spatial frequency condition were averaged across different time windows representing the M170 component (BSF faces: 150-200ms; HSF faces: 180-230ms; LSF faces: 155-205 ms) as suggested by the sensor space analysis and our exploration of the ERFs. Despite the different time windows chosen we confirmed that during the 50 ms time window the same source configurations appeared, starting with activation on ventral and occipital areas that moved ventrally into the inferior temporal cortex and lateral into parietal cortex finishing with activation over the temporal poles. Based on the averaged time window we composed ten regions of interest, or scouts, and for the statistic we calculated the average activity at each of these scouts at the time of the peak of the M170 for each spatial frequency. The scouts created were located in lateral occipital cortex (*OCC LAT L* and *OCC LAT R*), ventral occipital cortex (*LIN L* and *LIN R*), inferior temporal cortex (*FUS L* and *FUS R*), temporal pole (*TMP R* and *TMP L*) and parietal cortex (*PAR L* and *PAR R*) Figure 4.7 shows the scouts that were created plus an averaged activity map of the nine conditions.

Figure 4.7 M170: source localization averages and scouts

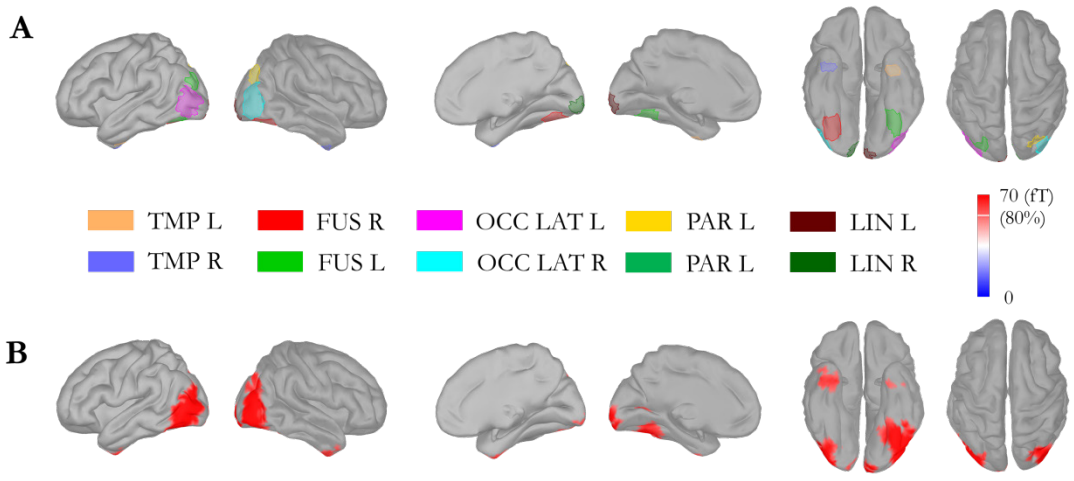

Panel A: 6-view model brain where the created nine scouts are shown in different colours. Panel B: 6-view average source map of all the faces. Areas of maximum activation are shown in red

Figure 4.8 shows the average activity map of each of the nine conditions during the M170 time window. The mean activation from each scout 10 ms around the peak of each frequency was extracted and submitted into a repeated measures ANOVA with factor emotion (fearful, happy and neutral) and frequency (BSF, HSF and LSF)

Figure 4.8 M170: scouts average maps

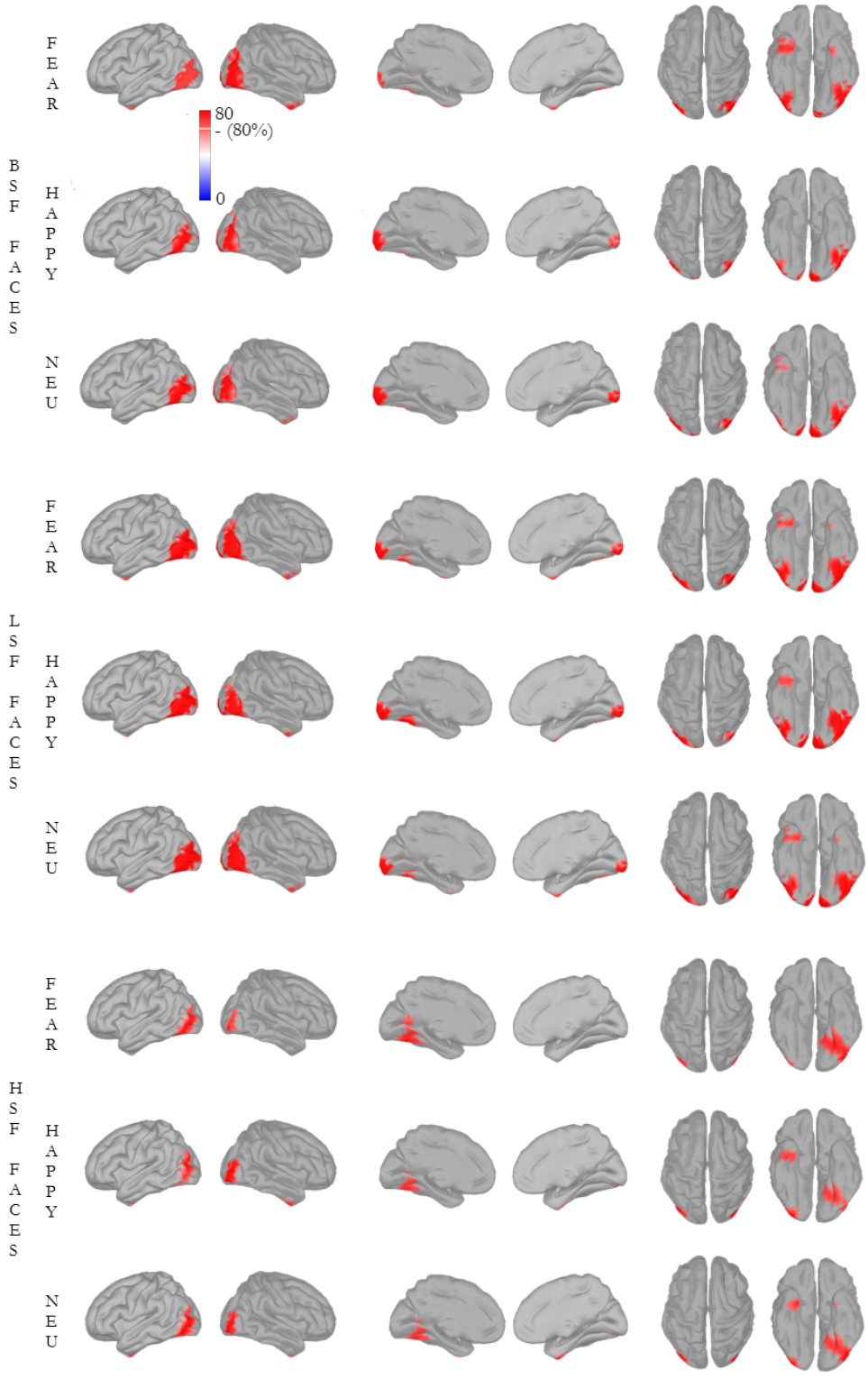

Six-view source maps of the M170 for the nine conditions. Areas with maximum activity are shown in red

Given the temporal width of the time window and the temporal differences between frequencies, we used the mean latency value obtained in the sensor analysis to compute the average activity for each of the nine conditions within the twelve scouts. The average value of all the surfaces in a scout was computed within ten ms around each frequency latency peak. This is: around 175 ms for BSF faces, 180 ms for LSF faces and 205 ms for HSF faces. For each of the scouts, those values were submitted into a repeated measures ANOVA with factors emotion (three levels: fearful, happy and neutral) and We performed statistics employing the nine conditions because we found an interaction effect in the sensor space but unlike the early interaction time window analysis we had no clear a priori though the mentioned interaction seem to point the emotion effects were more prominent for BSF and LSF faces as compared with HSF. First of all, the comparison at

Table 4.5 M170: source statistics

Scout	Test	Statistic	Probability	Post-Hoc Comparison	Probability
FUS L	Emotion	$F_{2,28} = 1.591$	$P = 0.220$		
	Frequency	$F_{2,28} = 1.539$	$P = 0.232$		
	Interaction	$F_{4,56} = 1.326$	$P = 0.276$		
FUS R	Emotion	$F_{2,28} = 0.316$	$P = 0.694$		
	Frequency	$F_{2,28} = 1.817$	$P = 0.180$		
	Interaction	$F_{4,56} = 1.013$	$P = 0.398$		
TMP L	Emotion	$F_{2,28} = 0.240$	$P = 0.779$		
	Frequency	$F_{2,28} = 1.533$	$P = 0.235$		
	Interaction	$F_{4,56} = 0.451$	$P = 0.752$		
TMP R	Emotion	$F_{2,28} = 0.752$	$P = 0.470$		
	Frequency	$F_{2,28} = 0.020$	$P = 0.931$		
	Interaction	$F_{4,56} = 1.646$	$P = 0.197$		
OCC	Emotion	$F_{2,28} = 1.855$	$P = 0.175$		
LAT L	Frequency	$F_{2,28} = 3.668$	$P = 0.052$	BSF > HSF	P = 0.058
				LSF > HSF	P = 0.049
	Interaction	$F_{4,56} = 0.354$	$P = 0.763$		
OCC	Emotion	$F_{2,28} = 0.034$	$P = 0.961$		
LAT R	Frequency	$F_{2,28} = 2.523$	$P = 0.098$		
	Interaction	$F_{4,56} = 1.315$	$P = 0.279$		
LIN L	Emotion	$F_{2,28} = 0.216$	$P = 0.216$		
	Frequency	$F_{2,28} = 4.077$	$P = 0.029$	BSF > HSF	P = 0.022
				LSF > HSF	P = 0.017
	Interaction	$F_{4,56} = 1.106$	$P = 0.356$		
LIN R	Emotion	$F_{2,28} = 0.387$	$P = 0.673$		
	Frequency	$F_{2,28} = 2.826$	$P = 0.085$		
	Interaction	$F_{4,56} = 1.145$	$P = 0.342$		
PAR L	Emotion	$F_{2,28} = 0.237$	$P = 0.237$		
	Frequency	$F_{2,28} = 0.632$	$P = 0.632$		
	Interaction	$F_{4,56} = 0.872$	$P = 0.872$		
PAR R	Emotion	$F_{2,28} = 0.085$	$P = 0.870$		
	Frequency	$F_{2,28} = 5.900$	$P = 0.007$	BSF > HSF	P = 0.006
				LSF > HSF	P = 0.065
	Interaction	$F_{4,56} = 2.444$	$P = 0.067$		

Average activity at each of the scouts created for the M170 BSF, HSF and LSF faces averaged across emotional expressions for the sake of simplicity: note that the only significant statistics were those corresponding to the main effects of frequency. Standard error means are shown in parenthesis. Third and fourth column show respectively the statistic of the three by three repeated measures ANOVA comparing the three fearful faces at each scout and the assigned probability. Post-hoc comparisons are shown where pertinent

the Right Fusiform scout left a significant interaction effect ($F_{4,56}$ = 2.768; P =0.044) while there were no effects within the Left Fusiform scout. The Table 4.6 shows the mean value for each condition at the Right Fusiform scout. Comparisons within each level (emotion: fearful, happy and neutral; frequency: BSF, LSF and HSF) showed that there were significant differences within BSF faces (BSF fearful faces had more activity than BSF neutral faces, P = 0.023) and a trend within HSF faces (HSF neutral faces bigger amplitudes than HSF fearful faces, P = 0.066) but no differences between LSF faces. Between frequencies, the only significant difference was between BSF and HSF Neutral faces (the later bigger than the former, P = 0.029). Figure 4.9 covers all the mean values at each scout for each condition.

Figure 4.9 M170: scouts average chart

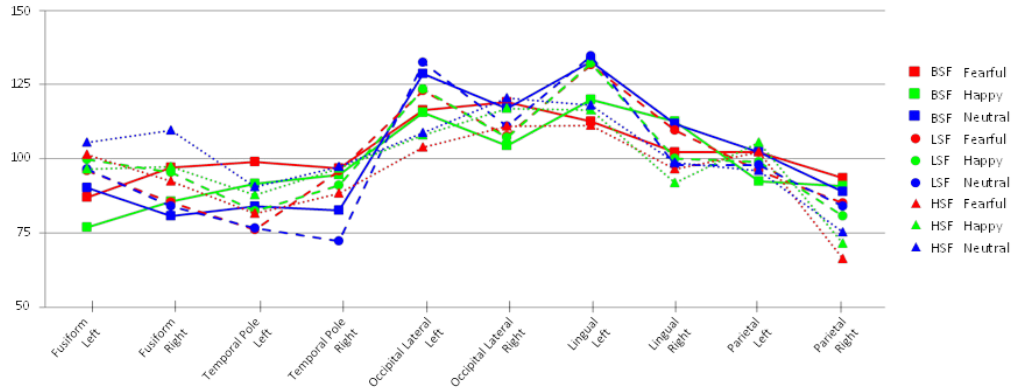

Average activity at each of the scouts created for the nine conditions. Just absolute values are displayed.

4.5.4 Traditional analysis

From observation, it can be seen that there are at least four important components before 200 ms. Figure 4.10 shows a butterfly plot including all the magnetometers for BSF, HSF and LSF frequencies and scalp plots of the activity averaged across the time window chosen for each of the first three components. Table 4.6 summarizes the results of the statistics between the mean amplitude values and Table 4.7 summarizes the statistics between mean latencies.

Figure 4.10 Traditional analysis: grand average and eRMF components topography

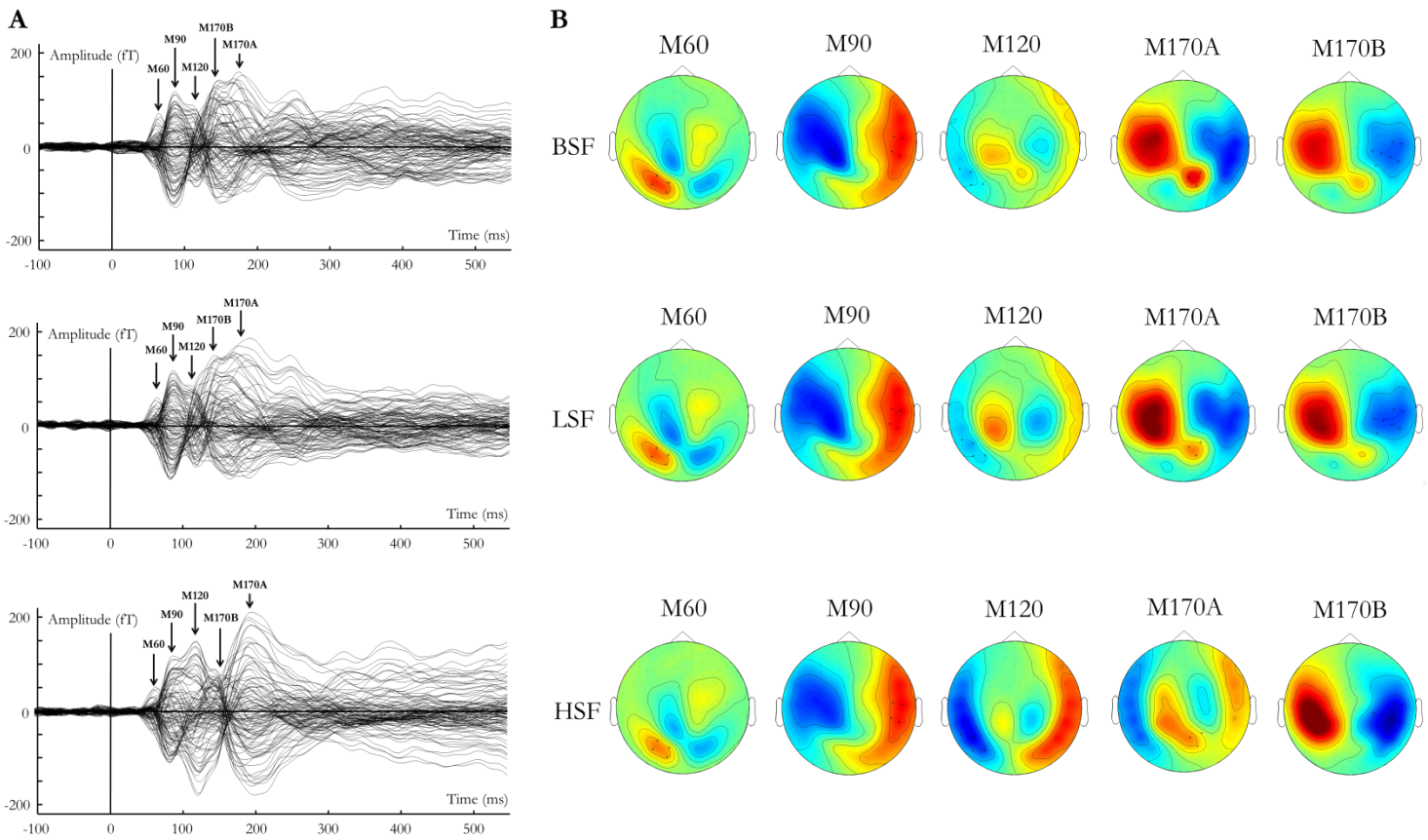

Panel A: Grand average eRMF shown for all sensors (magnetometers) for BSF (top row), LSF (middle row) and HSF (bottom row) averaged across emotions. The identified five first components are depicted with an arrow pointing toward the visually observed peak. Panel B: scalp maps at the five time marks assigned visually: 60 ms; 90 ms; 120 ms; 150 ms and 170 ms.

Table 4.6 Traditional analysis: Latency

Component	Time (ms)	Condition		Latency (ms)	s.e.m.	Test	Statistic	Probability
M60	40-80	BSF	Fearful	= 67.9	(2.5)	Emotion	$F_{2,28}$ = 0.716	P = 0.447
			Happy	= 65.6	(3.0)			
			Neutral	= 63.1	(2.9)			
		LSF	Fearful	= 65.6	(3.1)	Frequency	$F_{2,28}$ = 0.329	P = 0.654
			Happy	= 63.1	(3.6)			
			Neutral	= 67.9	(2.5)			
		HSF	Fearful	= 67.3	(3.2)	Interaction	$F_{4,56}$ = 1.835	P = 0.162
			Happy	= 67.0	(3.4)			
			Neutral	= 65.8	(3.3)			
M90	60-92	BSF	Fearful	= 86.2	(1.7)	Emotion	$F_{2,28}$ = 0.171	P = 0.838
			Happy	= 87.5	(1.5)			
			Neutral	= 85.1	(1.6)			
		LSF	Fearful	= 87.1	(1.5)	Frequency	$F_{2,28}$ = 3.399	P = 0.345
			Happy	= 85.5	(1.6)			
			Neutral	= 86.2	(1.6)			
		HSF	Fearful	= 85.9	(2.0)	Interaction	$F_{4,56}$ = 2.706	P = 0.204
			Happy	= 88.7	(1.2)			
			Neutral	= 86.5	(1.9)			
M120	100-140	BSF	Fearful	= 119.4	(3.7)	Emotion	$F_{2,28}$ = 0.637	P = 0.509
			Happy	= 119.1	(2.5)			
			Neutral	= 118.1	(2.6)			
		LSF	Fearful	= 121.6	(2.9)	Frequency	$F_{2,28}$ = 3.276	P = 0.053^{+}
			Happy	= 122.9	(2.6)			
			Neutral	= 118.9	(2.6)			
		HSF	Fearful	= 123.5	(3.3)	Interaction	$F_{4,56}$ = 0.290	P = 0.820
			Happy	= 124.6	(2.8)			
			Neutral	= 123.7	(3.0)			
M170A	130-175	BSF	Fearful	= 148.0	(2.6)	Emotion	$F_{2,28}$ = 0.247	P = 0.761
			Happy	= 145.5	(2.0)			
			Neutral	= 147.9	(2.5)			
		LSF	Fearful	= 153.8	(2.9)	Frequency	$F_{2,28}$ = 6.291	P = 0.014*
			Happy	= 152.1	(2.8)			
			Neutral	= 151.2	(2.9)			
		HSF	Fearful	= 155.6	(3.8)	Interaction	$F_{4,56}$ = 0.355	P = 0.726
			Happy	= 156.4	(3.5)			
			Neutral	= 156.9	(3.1)			
M170B	130-200	BSF	Fearful	= 166.5	(5.5)	Emotion	$F_{2,28}$ = 2.474	P = 0.125
			Happy	= 160.1	(6.6)			
			Neutral	= 167.5	(5.6)			
	150-220	LSF	Fearful	= 179.1	(5.5)	Frequency	$F_{2,28}$ = 18.422	P = 0.000*
			Happy	= 165.8	(6.2)			
			Neutral	= 171.0	(6.3)			
	130-200	HSF	Fearful	= 197.3	(4.8)	Interaction	$F_{4,56}$ = 0.539	P = 0.628
			Happy	= 193.9	(6.4)			
			Neutral	= 197.0	(4.5)			

Results of the latency traditional analysis. Global peak latencies are shown for each of the five components and the nine conditions. Standard error means are shown in parenthesis. The components are sorted in temporal order. Time is in milliseconds. The right-most rows (from sixth to seventh) show the result of each three by three repeated measures ANOVAs performed over latency.

Table 4.7 Traditional analysis: Amplitude

Component	Time (ms)	Condition		Latency (ms)	s.e.m.	Test	Statistic	Probability
M60	55-65	BSF	Fearful	= 59.5	(12.4)	Emotion	$F_{2,28}$ = 1.007	P = 0.375
			Happy	= 62.4	(17.0)			
			Neutral	= 46.8	(10.6)			
		LSF	Fearful	= 46.3	(11.3)	Frequency	$F_{2,28}$ = 1.888	P = 0.176
			Happy	= 41.2	(14.2)			
			Neutral	= 53.5	(14.1)			
		HSF	Fearful	= 40.0	(12.4)	Interaction	$F_{2,28}$ = 1.627	P = 0.204
			Happy	= 53.2	(14.8)			
			Neutral	= 34.0	(13.5)			
M90	80-92	BSF	Fearful	= 97.9	(25.1)	Emotion	$F_{2,28}$ = 0.818	P = 0.434
			Happy	= 102.6	(23.1)			
			Neutral	= 102.8	(25.1)			
		LSF	Fearful	= 97.0	(23.1)	Frequency	$F_{2,28}$ = 0.899	P = 0.409
			Happy	= 102.4	(25.1)			
			Neutral	= 113.9	(24.9)			
		HSF	Fearful	= 89.2	(19.7)	Interaction	$F_{2,28}$ = 0.246	P = 0.871
			Happy	= 98.7	(23.4)			
			Neutral	= 95.7	(20.0)			
M120	108-133	BSF	Fearful	= -50.6	(20.1)	Emotion	$F_{2,28}$ = 0.405	P = 0.650
			Happy	= -56.0	(17.7)			
			Neutral	= -64.8	(19.9)			
		LSF	Fearful	= -61.4	(18.4)	Frequency	$F_{2,28}$ = 28.828	P = 0.000*
			Happy	= -64.9	(23.1)			
			Neutral	= -68.2	(21.2)			
		HSF	Fearful	= -128.3	(21.3)	Interaction	$F_{2,28}$ = 0.846	P = 0.460
			Happy	= -124.2	(19.9)			
			Neutral	= -118.9	(20.1)			
M170A	137-157	BSF	Fearful	= 72.9	(17.6)	Emotion	$F_{2,28}$ = 3.746	P = 0.037*
			Happy	= 105.3	(23.9)			
			Neutral	= 100.4	(20.0)			
	143-163	LSF	Fearful	= 62.8	(18.7)	Frequency	$F_{2,28}$ = 1.795	P = 0.195
			Happy	= 50.6	(18.4)			
			Neutral	= 51.6	(20.2)			
	147-167	HSF	Fearful	= 30.2	(24.4)	Interaction	$F_{2,28}$ = 3.690	P = 0.019*
			Happy	= 58.5	(23.6)			
			Neutral	= 64.6	(26.7)			
M170B	155-175	BSF	Fearful	= -126.5	(32.6)	Emotion	$F_{2,28}$ = 14.782	P = 0.000*
			Happy	= -72.1	(32.2)			
			Neutral	= -78.9	(30.1)			
	185-205	LSF	Fearful	= -103.7	(28.5)	Frequency	$F_{2,28}$ = 2.962	P = 0.090+
			Happy	= -98.7	(28.5)			
			Neutral	= -106.6	(26.9)			
	160-180	HSF	Fearful	= -154.8	(24.5)	Interaction	$F_{2,28}$ = 6.206	P = 0.002*
			Happy	= -121.3	(28.2)			
			Neutral	= -142.2	(26.0)			

Results of the traditional analysis amplitude comparison between conditions. Global averages are shown per con4dition- Second column indicates the time window employed to calculate the average (may vary across spatial frequencies according to the Latency analysis, see Table 4.6). Standard error means are shown in parenthesis. The components are sorted in temporal order. Time is in milliseconds. The right-most rows (from sixth to seventh) show the result of each three by three repeated measures ANOVAs performed over amplitudes.

4.5.4.1 M60

This component was best represented by a group of occipital sensors in the left hemisphere. There were no significant main effects of emotion ($F_{2,28}$ = 1.007; P = 0.375) or frequency ($F_{2,28}$ = 1.888; P = 0.176). There was no significant interaction either ($F_{4,56}$ = 1.627; P = 0.204). Regarding the latencies the results were similar. All the peaks were around 65 ms. There were no main effects of emotion ($F_{2,28}$ = 0.716; P = 0.447) or frequency ($F_{2,28}$ = 0.329; P = 0.654) and there was not a significant interaction ($F_{4,56}$ = 1.835; P = 0.162). Figure 4.11 panel A shows the average ERF at the selected group of magnetometers (n = 4).

Figure 4.11 Traditional analysis: eRMF components waveform

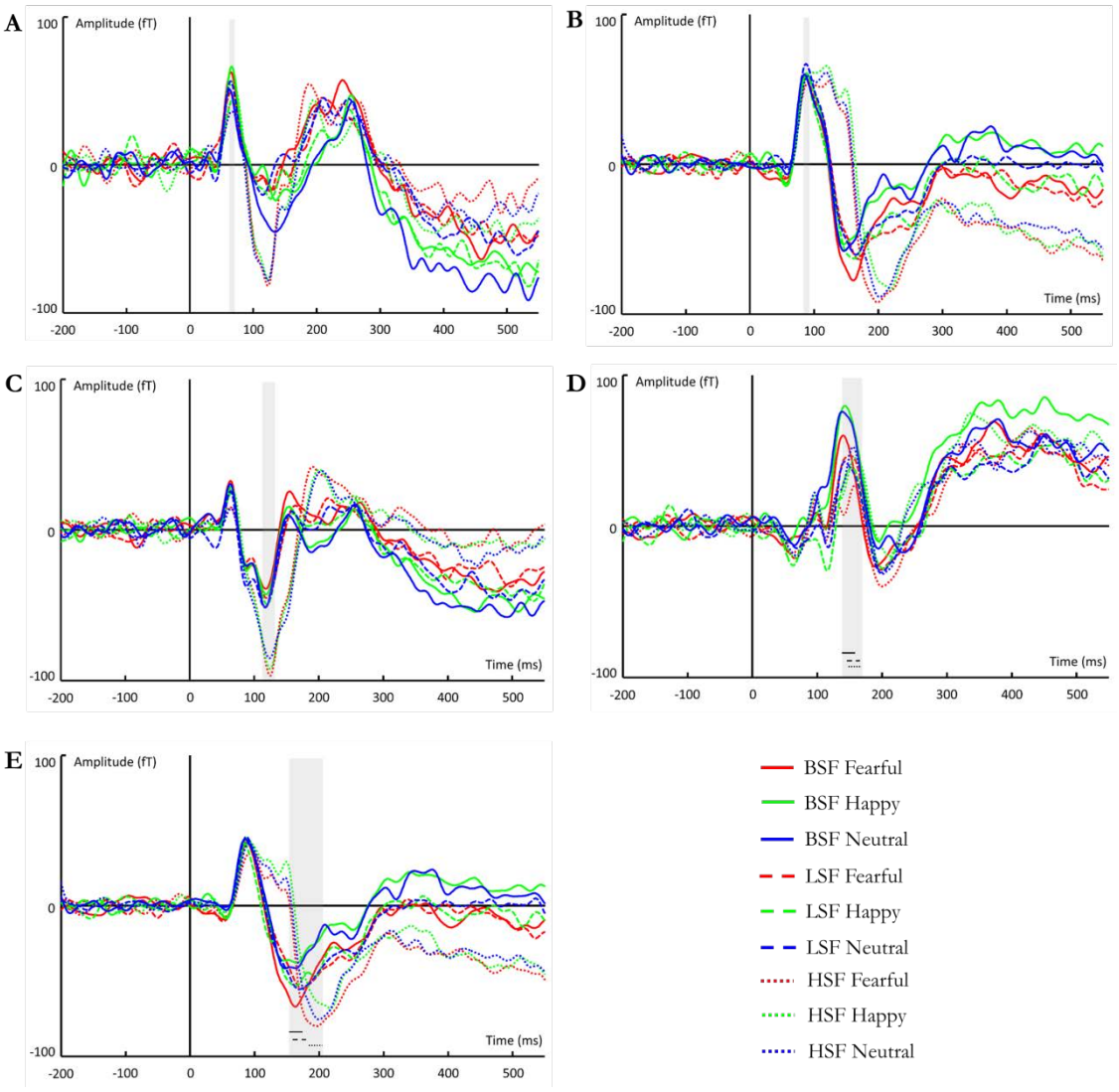

Waveforms corresponding to the average of the sensors of interest chosen to study each of the five identified eRMF components. Panel A: M60; Panel B: M90; Panel C: M120; Panel D: M170A; Panel E: M170B. Shadowed grey areas indicate the time window of interest employed in subsequent analysis. In the case of M170A and M170B the three different time windows employed are further detailed with one line. Straight line: BSF; dashed line: LSF; dotted line: HSF.

4.5.4.2 M90

This component was best represented by a group of temporal sensors in the right hemisphere. There were no significant main effects of emotion ($F_{2,28}$ = 0.818; P = 0.434) or frequency ($F_{2,28}$ = 0.899; P = 0.409). There was no significant interaction either ($F_{4,56}$ = 0.246; P = 0.871). Regarding latencies, there were no main effects of emotion ($F_{2,28}$ = 0.171; P = 0.838) or main effects of frequency ($F_{2,28}$ = 3.399; P = 0.345) and there was not an interaction ($F_{2,28}$ = 2.706; P = 0.204) either. Figure 4.11 panel B shows the average ERF at the selected group of magnetometers (n = 4).

4.5.4.3 M120

This component was best represented by a group of temporooccipital sensors in the left hemisphere. There were significant main effects of frequency ($F_{2,28}$ = 28.828; P = 0.000). There were no significant main effects of emotion ($F_{2,28}$ = 0.405; P = 0.650) or an interaction ($F_{4,56}$ = 0.846; P = 0.460). Post-hoc comparisons indicated that HSF (mean: -129.9 fT; std: 21.7) faces had bigger amplitudes than BSF (mean: -59.6 fT; std: 19.7; P = 0.000) and LSF (mean: -67.5 fT; std: 21.8; P = 0.000) faces while there were no significant differences between BSF and LSF (P = 0.368). There were no significant difference between HSF fearful, happy and neutral faces within this time window ($F_{2,28}$ = 1.510; P = 0.238). Regarding latencies, all the peaks were There were no main effects of emotion ($F_{2,28}$ = 0.637; P = 0.509) or frequency ($F_{2,28}$ = 3.276; P = 0.053). There was no significant interaction either ($F_{4,56}$ = 0.290; P = 0.820). Figure 4.11 panel C shows the average ERF at the selected group of magnetometers (n = 4).

4.5.4.4 M170A

This component was best represented by a group of parietoocipital sensors in the right hemisphere. Regarding latencies, there were no effects of emotion ($F_{2,28}$ = 0.247; P = 0.761) or an interaction ($F_{4,56}$ = 0.355; P = 0.726) but there were significant effects of frequency ($F_{2,28}$ = 6.291; P = 0.014). Post-hoc comparison indicated that BSF faces (mean: 147 ms; std: 1.9) had smaller latencies than LSF (mean: 152 ms; std: 2.2; P = 0.011) and

HSF faces (mean: 156; std: 2.9; P = 0.004). However, latencies of LSF faces were no significantly faster than latencies of HSF faces (P = 0.191).

With respect to amplitudes, there were significant main effects of emotion ($F_{2,28}$ = 3.782; P = 0.037) and interaction effects as well ($F_{2,28}$ = 3.812; P = 0.017) but no significant effects of frequency ($F_{4,56}$ = 1.928; P = 0.176). Post-hoc comparisons showed that amplitude of the fearful faces were smaller than the amplitude of happy or neutral faces within BSF (P = 0.028 and P = 0.017 compared with happy and neutral BSF faces respectively) or HSF faces (P = 0.015 and P = 0.008 compared with happy and neutral BSF faces respectively) but not within LSF faces. Between fearful faces, there were no differences between any of the frequency levels. Within the happy and neutral faces, there were no differences between BSF and HSF faces or LSF and HSF faces. However, LSF happy and neutral faces had smaller amplitudes than their BSF counterparts (P = 0.013 and P = 0.047 respectively). Figure 4.11 panel D shows the average ERF at the selected group of magnetometers (n = 3).

4.5.4.5 M170B

This component was best represented by a group of parietotemporal sensors in the right hemisphere. With respect to the latencies, there were significant main effects of frequency ($F_{2,28}$ = 14.782; P = 0.000) but no effects of emotion ($F_{2,28}$ = 2.474; P = 0.125) or an interaction ($F_{4,56}$ = 0.539; P = 0.628). Post-hoc comparison showed that HSF faces (mean:196.1 ms ; std: 4.1) had longer latencies than BSF (mean: 164.7 ms; std: 4.8; P = 0.000) or LSF (mean: 171.9 ms; std: 4.9; P = 0.001) faces. Also, the latency of BSF faces was smaller than latency of LSF faces (P = 0.039).

Regarding the amplitudes, there was a main effect of emotion ($F_{2,28}$ = 14.782; P = 0.000) as well as a significant interaction ($F_{4,556}$ = 6.206; P = 0.002) and no significant effects of frequency ($F_{2,28}$ = 2.962; P = 0.090). BSF fearful faces (mean: -126.5 fT; std: 126.2) had bigger amplitudes than their happy (mean: -121.3 fT; std: 124.5; P = 0.000) and neutral BSF counterparts (mean: -78.9; std: 116.4; P = 0.000). HSF fearful faces (mean: -126.5 fT; std: 126.2) amplitudes were bigger than HSF happy faces (mean: -126.5 fT; std: 126.2; P = 0.006) but not bigger than HSF neutral faces. There were no differences between emotions at the LSF frequency level. Within the fearful level, HSF faces had

bigger amplitudes than their LSF counterpart (P = 0.037). Within the happy faces level, BSF faces had bigger amplitudes than their LSF counterpart (P = 0.028). Within neutral faces, HSF faces had bigger amplitudes than BSF faces (P = 0.024). Figure 4.11 panel E shows the average ERF at the selected group of magnetometers (n = 3).

4.5.4.6 Temporal course source reconstruction

Our main interest was to explore for early interactions between emotion and frequency. In addition, we statistically analyzed the sources of the most important component of face processing, the M170, based on a first analysis at the source level of the activity recorded at standard temporal sensors. However, our data showed a great complexity after 100 ms that demand further exploration and analysis. The permutation statistics over the whole epoch showed there were differences between our main conditions starting at around 100 ms and spanning until the end of the window that ultimately reflect differences in the active sources and their temporal contribution to the ERFs. Although very interesting and worth exploring, driving conclusions about this part of the results extends beyond the objectives of this chapter. Nonetheless, we will describe the temporal course of activation of the neural sources as reconstructed around critical time marks identified within our traditional analysis of the sensor level. Figure 4.12 summarizes the source reconstruction of BSF, HSF and LSF faces (averaged across emotions) at five moments between 50-200 ms. From 55 to 70 ms; from 82 to 92 ms; from 114 to 134 ms; from 154 to 174 ms and from 184 to 204 ms. The first three time marks correspond to the M60, M90 and M120 components as mentioned in the sensor level traditional analysis. The fourth time was chosen to include the M170A peak of the three conditions and the early M170B peak (corresponding to BSF and LSF faces). The fifth time corresponds to the M170B of the HSF faces that effectively differed from the M170B peak of the former conditions. The color was adjusted to depict the surfaces with higher activation values than the 80 percent of a common scale (from 0 to 8 pAm) with the exception of HSF faces M120. In the case of the M120 time window, HSF faces elicited activity values considerably higher than BSF and LSF faces; hence, we also include an activity map with a different scale (from 0 to 12 pAm) just for this component for the sake of visibility.

Cortical processing began early at around 60ms. The initial highest sources were located bilaterally at striate and also extrastriate areas of the posterior occipital cortex, roughly corresponding to V1 and V2. Approximately 20-30 ms later, the maximum peaks of activation were located out of the most posterior part of the occipital cortex, occupying regions of the lingual as well as areas between lateral occipital cortex and temporal lobe (the posterior fusiform gyrus ventrally and the posterior inferotemporal cortex laterally) and parietal lobe. Activity in the temporal poles was also salient within this time-frame.

Figure 4.12 Traditional analysis: components source localization

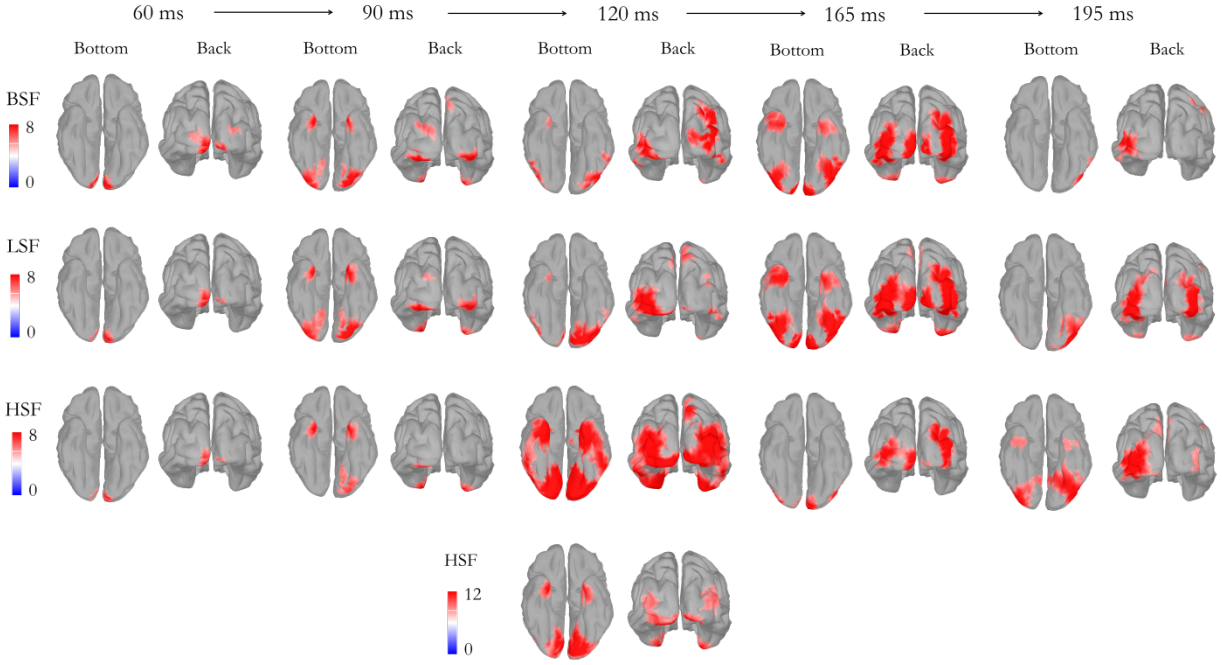

2-view source reconstruction maps of BSF, LSF and HSF faces for each of the five eRMF components identified in the traditional analysis. The solutions correspond to single time points around 60, 90, 120, 165 and 195 ms. The first three time choices roughly correspond with the latency peaks obtained in the analysis (see table 4.6) . The selection of the fourth (165 ms) and the fifth (195 ms) time choices aims to explain as much as possible the differences in activation between HSF and BSF/LSF M170. Given that the M170A and the M170B occurred almost at the same time for BSF and LSF faces (and should be considered one component labelled M170) the selected time point shows activity corresponding to both components while for HSF it only shows activity corresponding to M170A. The last time was chosen so that it would fit the HSF M170 tie window

At around 120 ms, there is a massive difference in the absolute values of activation between HSF and both BSF and LSF faces but seemingly there is not a big difference in the nature of the activated sources. The sensor analysis also showed there was no difference in latency attributable to the frequency while there were big differences in

amplitude. Parallel to this, the activated sources within this time window show very high activity when compared with the activity elicited by BSF or LSF faces. For this reason we also include in Figure 4.12 an alternative representation of the HSF activity map at this time with a locally adjusted scale of 0 to 12. The loci of activity are within the lateral occipital cortex, inferior and middle temporal gyrus, lingual gyrus and temporal poles.

Within the 155 to 175 ms time window, we can observe the sources of the M170A and the M170B concurring synchronously for BSF and HLSF faces: early visual areas corresponding to V1 and lingual gyrus in addition with regions of posterior, middle and anterior fusiform gyrus, lateral occipito temporal and occipito parietal regions. At the same time the areas of maximum activity of the HSF faces are circumscribed to the early visual / lingual region and the lateral portions of the occipital cortex. Hence, the activity of HSF faces within this time window is similar to that of BSF and LSF faces with the exception of the activation of the fusiform gyrus.

The activity map corresponding to the 185 to 205 time window is shown for the three conditions although it was selected to better show the sources of the M170B of HSF faces. Within this time window we can observe similar sources at the fusiform gyrus to the ones we observed ~30 ms earlier for BSF and LSF faces. Also, we do not observe activity at early visual at all nor activity within the lingual gyrus with the same intensity and extension than the one we observe in the previous time window for BSF or LSF faces. Ultimately, activation of the HSF faces in the lateral occipital cortex and occipitotemporal/occipitoparietal regions is similar to the activation observed for the same type of faces in the previous time window. BSF faces do not show high activations at these regions within this time frame while LSF faces still do, but it is worth note that the M170B latency peaks of BSF faces were smaller than the latency peaks corresponding to the LSF faces.

The difference between the peak of the M170A and the peak of the M170B was calculated for each subject and condition. The ANOVA returned main effects of frequency ($F_{2,28}$ = 1.089; P = 0.337) and no effects of emotion ($F_{2,28}$ = 10.340; P = 0.003) or interaction ($F_{4,56}$ = 0.248; P = 0.818). Post-hoc comparisons showed that the difference between the peaks of the M170B and the M170A for BSF and LSF faces (mean: 17.6 ms and mean: 19.6 ms respectively) was significantly smaller than the difference of the HSF

faces (mean: 39.8 ms; P = 0.003 and P = 0.007 when compared with BSF or LSF respectively).

4.6 Discussion

The main objective of this experiment was trying to know if it could be measured with magnetoencephalography something similar to the early interaction found at the amygdala with intracranial electrodes in Experiment 1a: faces. This is; enhanced processing for fearful faces specific to the images that convey low spatial frequency components. Some emotional models of visual processing (Ledoux, 1996) and face processing (Johnson, 2005) had proposed that there is a functional projection from the lateral geniculate nucleus of the thalamus with the limbic system, more specifically via dorsal pulvinar nuclei to the basolateral nuclei of the amygdala (Day-Brown et al., 2010). It is argued that this thalamo-cortical projection is able to carry low spatial frequency information of the visual scene rendering the circuit able to determine the emotional relevance of the perceived stimulus bypassing slower cortical processing at occipital and temporal visual areas. This property would make this system an ideal candidate for rapid detection of threat related stimuli. On the other side, non-traditional models of visual processing had questioned the idea that visual representation is achieved via serial and hierarchical processing, highlighting the existence of parallel and recursive processing (Lamme and Roelfsema, 2000; Pessoa and Adolphs, 2010) within the visual system as well as the existence of shortcuts between supposedly high and low level visual processing areas such as the existent connections from V2 and V4 to inferior and anterior temporal cortex (Shipp, 2003) or long range magnocellullar projection that links the lateral geniculate nucleus and the amygdala with parietal, temporal and frontal cortex (Bar, 2003).

Thus, a technique with good temporal resolution like MEG that can measure the activity of the whole brain as opposed to intracranial recordings which instead is able to give temporal information about deep structures is a very good complement to the later. Visual processing requires the integrated activity of many different areas, and MEG can provide information about most of them. Furthermore, employing source reconstruction

we can detect the origin within the cortex of the activity measured in the scalp through the sensors at a temporal window of interest defined either by the exploration of the data or by a priori hypothesis. Although it is difficult to localize MEG activation in deep medial structures like the amygdala (Attal et al., 2007) some studies had detected emotional modulations in the amygdala during perception of various types of items (Garolera et al., 2007; Maratos et al., 2009; Bayle, Henaff and Krolak-Salmon, 2009; Dumas et al., 2010). However, all the experiments seem to report late or sustained activity

Indeed we had some a priori hypothesis coming from the literature and moreover from previous Experiment I. Regarding the former, we expected that an interaction between emotion and frequency reflecting a fast threat related response would need to arise before 100 ms post stimulus. Around this time, visual processing at cortical areas had already started and magnetic/electroencephalographic components with cortical sources such as the M100 (P1) or the M170 (or N170) reflecting early visual processing had already been described in the literature showing emotion specific differences in some experiment depending on the task and the stimulus employed (Blau et al., 2007, Pizzagalli et al., 2002; Pizzagalli, Regard and Lehmann, 1999; Schacht and Sommer, 2009; Vlamings, Goffaux and Kemner, 2009). Furthermore, we had previously identified a temporal window of interest on which we show an interaction effect at amygdala sites in Exp. 1a, from 72 to 108 ms.

In contrast with Exp.1, we recorded magnetoencephalographic data from several different locations above the scalp. This posed a problem to our permutation cluster based statistical approach because the spatial dimension of our data set had increased from 1 amygdala site to 102 magnetometers and we were only able to test for lineal or quadratic effects between conditions. Therefore, we combined happy and neutral faces from each of the spatial frequency levels of our factors and subtracted them from their homologous frequency fearful faces, composing three *difference waves*. This representation of the data mimics the a priori assumption of our hypothesis; that threat related (fearful) stimuli may benefit from enhanced processing, and testing for differences between the three *difference waves* indeed allow us to test if that enhancement is spatial frequency dependent.

4.6.1 Early interaction time window

We found significant differences between the three difference waves at a group (*cluster*) of central magnetomers over the right hemisphere. Within this cluster, the direction of the effects mimics that from Experiment I: no differences between BSF and LSF fearful faces but both different from HSF fearful faces (see Table 4.2). The ERFs showed a positive going peak for all conditions, albeit more positive for LSF fearful faces, peaking around 80ms (see Figure 4.2 panel C). But the groups of sensors within the interaction cluster (see Figure 4.2 panel A) were not at the locations with maximal activity at that temporal window (see Figure 4.2 panel B).

The various on-going brain sources contributing to the scalp signal add linearly. Hence the locations of maximum activity indicate just the locus that maximally contributes to the recorded signal in the scalp. Indeed, the measured ERF indicates occipital sources consistent with the stages of visual processing that are carried out around 90-120 ms (Seki et al., 1996; Hatanaka et al., 1997; Rutman et al., 2010). Nonetheless, the source reconstruction showed with a threshold of 60 % that the areas exhibiting more activity than the rest of the brain over the whole interaction time window were more sparse than just occipital (see Figures 4.5 and 4.6). Apart from lingual regions V1 and V2, parietal cortex and cuneus, regions of the lateral inferior occipital cortex near the occipital face area, part of the fusiform gyrus and the temporal poles also contributed to the recorded activity. It was the parietal and cuneus regions (see Table 4.4) that showed a similar pattern of effects than the ERFs and Exp.1.

Though we knew the temporal window we wanted to look at, we did not expect that the effects found with this technique should mandatorily be within medial structures. Several processing steps can happen between 70 and 100 ms, not only the thalamo-amygdalar processing but also amygdalo-cortical and more classic thalamo-cortical processing as we have seen (Pessoa and Adolphs, 2010). It could be possible to measure not the modulations of the amygdala but also of other areas in the visual hierarchy related to low spatial frequency processing or with emotional relevance in the visual hierarchy as a result of the preferential processing of threat related stimulus. Furthermore, MEG records the activity of the whole brain, preferentially of cortical pyramidal cells within the sulci, and while its spatial resolution is good at cortical structures, it is poor when it comes to medial

structures such as the amygdala whose cells are orientated in many others ways but perpendicular to the sensors. However, we included in the employed head models the amygdalae and other medial structures like the hippocampi and the accumbens nuclei, despite we were uncertain if effects could be found on other than cortical sources.

Parietal and cuneus scouts show a significantly higher activity for LSF fearful faces. Magnocellullar projection had been linked with top-down facilitation of recognition (Kveraga, Boshyan and Bar, 2007), selective attention in visual search (Vidyasagar and Pammer, 1999), As seen in animal studies, magnocellullar projection from the basal ganglia are subcortical as well as neocortical, innervating cortical structures from anterior to posterior but with a high preference for frontal and parietal neocortex (Luiten et. al., 1999). At the same time animal studies have shown there are a number of amygdalo-cortical, with preference for cortical and temporal structures through the bed striatum but parietal and occipital neocortex do receive amygdalar projections too. How could it be that emotional content in the scene already modulates the processing at this stage? It has been suggested that each stage of processing adds up to 10 ms to the overall processing time in the visual system (Reid and Alonso, 1995; Pessoa and Adolphs, 2010). Though this is just a suggested 'rule of thumb' we may speculate thalamo-pulvinar inputs starting at around 50 ms (Ortuño et al., 2014) may have already made it into parietal cortex at ~80ms directly as well as via amygdaloid complex. It is important to note that in our experiment both LSF and BSF fearful faces elicit higher contribution than their HSF counterpart in the cuneus / parietal scout (see Table 4.4 and Figure 4.6), as would be suggested by a model relying on magnocellullar pathways to detect potentially threatening events fast. But, is the processing we measured in the source space just frequency dependent or also emotion dependent?

Although the interaction effects were significant at the sensor level and LSF fearful faces amplitudes were significantly higher than their happy (P = 0.001) and neutral counterparts just at trend (P = 0.074) there are no differences between emotional relevance when it comes to BSF stimuli. The differences between BSF and LSF happy or neutral faces is not significant either (P = 0.168; P = 0.142) This would suggest an underlying system showing preference for LSF frequencies probably receiving an input that already has been labeled as relevant at a previous stage. To test this, we conducted a post hoc analysis specifically at the Cuneus / Parietal scout between the two levels of our

experimental procedure (including happy and neutral stimuli). The repeated measures ANOVA showed there were only main effects of frequency in both right ($F_{2,28}$ = 6.750 ; *P* = 0.008) and left Cuneus/Parietal scouts ($F_{2,28}$ = 8.494 ; *P* = 0.002), indicating a lineal effect ($F_{1,14}$ = 7.360; P = 0.017 in the right hemisphere and $F_{1,14}$ = 11.256; P = 0.005 in the left hemisphere) were BSF faces elicited bigger activation, followed by LSF faces and HSF faces showing the smallest amplitudes. It is evident from the sensor level results that there is a specific enhancement for LSF frequencies that convey threat related cues in contrast when they do not. However, the assumption that the Cuneus and Parietal region identified in our source analysis is part of a fast detection mechanism relying on LSF should be taken with care due to this result. More likely these regions are *also* preferentially activated by just LSF components, via magnocellullar pathway (Bar, 2003; Vuilleumier et al., 2003; Vuilleumier, 2005b; Vuilleumier and Pourtois, 2007). Each node in the visual processing does not perform an isolated function but maybe serves in different specific systems and steps that are part of the bigger visual system. Sensor space analysis shows the overall summation of activity of several cortical and subcortical structures. There are several studies showing that magnocellullar projections arrive to the parietal cortex and the cuneus from the thalamus as well as from the amygdala. So the results with the ERFs can reflect a system able to detect biological relevance based on low spatial frequency information while the source analysis was not able to disentangle all the structures that take part in the process. Also, it is not known at all what is the cut-off frequency of the magnocellullar visual system (see Xu et al., 2001 for study in non-human primates) and thresholds below 0.5 and 1 cycles per degree had been employed in different experiments (see for example Winston et al., 2003; Vuilleumier, 2003; Pourtois et al., 2005). In our experimental design, we took special care measuring the amount of cycles per degree of each image, the subject distance to the display and the real size of each picture to set this threshold at 0.8 cycles per degree. A threshold we speculate is liberal enough to allow sufficient spatial complexity to convey essential information. Indeed, subjects had no special problems satisfactorily completing the gender judgment task they were involved with.

4.6.2 Frequency effects

Our data also shows there are frequency effects during the whole epoch starting very early at ~100ms. It is important to note that even if the effects in the main effect of Frequency cluster-based permutation analysis were so wide we did include the whole epoch

in the analysis and no main effects of frequencies were detected before 94 ms (from 94 to 170 ms), later than the early interaction time window. Also, until 100 ms no channels from the early interaction cluster were grouped into the cluster exhibiting main effects of frequency from 94 to 170 ms. Figure 4.3 shows the time-course of the scalp activity. It can be seen that the spatial distribution present for the three spatial frequencies categories is the same up to 100 ms. At this time, the HSF faces show a sustained increase over Lateral and Occipital sensors that peaks later and last longer than the same activity for BSF and LSF faces. From this point towards ~300ms, the spatial configuration of the recorded activity is similar for the three frequencies but its temporal course is shifted, HSF frequencies showing the longest latencies. This was a problem for our statistical permutation approach and thus we analyzed the M170, our secondary focus of interest, adapting the employed time windows to the temporal course of each spatial frequency ERF.

Although our interest was centered on the brain activity that we would measure ~80 ms post stimulus, we think that it is interesting to study what our design could say about the M170, a component that reflects a later and *higher* step in the visual processing hierarchy, integrative up to some point, as shown by category specific/dependent modulations of its activity in the literature (Camel and Bentin, 2002; Gauthier et. al., 2003); that has been linked preferentially to face processing besides other object categories (Bentin, Deouell and Soroker, 1999, Itier and Taylor, 2004a); but for which there are still conflictive results showing emotional modulations as much as absence of them (Hinojosa, Mercado and Carretié, 2015 for a review based on EEG experiments) and there is little to none literature regarding its dependence on the spatial frequencies present in the visual scene.

Indeed, spatial frequency modulated M170 latency and amplitude in the present design. When we analyzed the M170 in a traditional fashion (see results 4.3.2 section) the set of stimuli without low spatial frequency components evoked M170 with longer latencies and bigger amplitudes than the stimuli that conveyed information in the LSF bands. In one study (Vlamings, Goffaux and Kemner, 2009) HSF and LSF fearful and neutral faces were used to investigate the interaction between spatial frequencies and emotional content in face processing with EEG. They found the latency of the M170 to be faster for LSF faces than HSF faces irrespective of the emotional content. Although we used bigger cut-off

frequencies for the LSF and HSF faces (0.8 and 24 cycles per degree against 2 and 6 cycles per degree in their study) this is consistent with our results. They also studied the effect of luminance and contrast by creating two sets of HSF and LSF fearful and neutral stimuli with equated and non-equated luminance and contrast. However non-equated HSF and LSF faces evoked significantly different M170 latencies (longer for the HSF) the difference was much smaller than between equated HSF and LSF faces. Most of the studies had employed few original pictures (e.g.; Vlamings, Goffaux and Kemner, 2009, n = 16) for the creation of their stimulus pool, while we did employ one original picture for each of the 324 stimuli perceived by the subjects along the nine conditions. After processing the whole set of pictures, the HSF pictures were more heterogeneous and had lower luminance values (average: 111 for BSF and LSF and 123 for HSF pictures; measured as the mean value of all the pixels) than BSF and LSF stimuli because of the different nature of each type of image. This is related to the fact that the frequency power in natural stimuli is maximal at low SF and almost exponentially decays at higher SF (see Loftus and Harley, 2005 for a review). We homogenized our set in luminance by equating the mean value of all the pictures irrespective of the spatial frequencies to a common value of 117. However, we did not control for the Energy of the stimulus - that is measured as the root mean square value of all the pixels, instead of the average. Hence, the pictures composing the BSF, HSF and LSF sets in our study irrespective of emotional expression, differed overall in measured energy; but not in luminance. It is important to note though that the average energy between fearful, happy and neutral emotional expression stimuli from the same spatial frequency level was equated with an ANOVA on the pseudo randomization created for each participant. However, we can't discard that the cause of the HSF stimuli longer latencies in our study is due to the fact that we not properly equated the stimulus energies. Nonetheless, the differences in latency in Vlamings et al. experiment and our study start post 100 ms, after the early interaction window that was our focus of interest.

4.6.3 M170 emotional effects

In line with some studies we report an emotional modulation at the sensor level on the time window of the M170 (from 150 ms poststimulus onwards) represented by higher amplitudes of fearful faces as compared with neutral or happy ones (see Table 4.3). This modulation occurred only for faces with HSF components (BSF and HSF) while LSF fearful faces did not provoke higher amplitudes than their happy and neutral counterparts.

However, the source space analysis could not detect a suitable correlate for this effect. Sources of the M170 were localized to inferotemporal and lateraloccipital regions as expected but no emotional differences were evident between conditions within any of the created scouts.

The only emotional modulation detected in the early stages of visual processing other than the LSF fearful face enhancement found in the early interaction time window occurred 80-100 ms later, at the time of the M170 component, thought to index at least structural integration of the percept (Eimer and Holmes, 2002) and sensitive to object category - such as faces. Unlike the later, the M170 emotional modulation comes after the first feed-forward push along the ventral visual system; hence we cannot attribute this emotional modulation to a similar shortcut or automatic processing of special features likewise the former modulation. There is a wide controversy in the literature whether emotional features can modulate M170. Indeed, they were elusive at first (Krolak-Salmon et al., 2001; Herrmann et al., 2002; Eimer, Holmes and McGlone, 2003). To the present date there is no clear agreement why they arise (Pizzagalli et al., 2002; Blau et al., 2007; Vlamings, Goffaux and Kemner, 2009) or are absent likewise often occur (see Hinojosa, Mercado and Carretié, 2015 for a meta-analysis on M170 emotional modulations with electrophysiology).

One of the keys may lay on the assumption (Bruce and Young, 1986) that M170 not only reflects perceptual encoding at a holistic level but also construction of abstract structural representations. One of the standard models (Bruce and Young, 1986) proposes that the mechanisms that identify structural and abstract face features like identity, expressions or facial speech (see Atkinson and Adolphs, 2011 for a review on the different face features modulations of the component) run parallel but are functionally independent. This proposal is evidenced by clinical cases and reports of different neural substrates between identity and expression recognition tasks (Winston et al., 2004). However, there is evidence of partial neural overlap employing the same tasks (LaBar et al., 2003) as much as emotional modulations on implicit identity recognition tasks (Kauffman and Schweinberger, 2003). Hence, it may be that while we were able to detect emotional modulations on the sensor level analyzing the magnetoencephalographic activation during the M170 time window the neural correlate of these effects is not evident at the source

level because several functional activations take place at the same time and the source reconstruction does not accurately separate them.

The fact that only BSF and HSF fearful faces shown greater amplitudes while on the other side all the LSF faces elicited similar amplitudes across emotional levels (see Table 4.3) suggest that high spatial frequency components are important for the visual processing taking place at the time of the M170. First, it should be noted that the task employed was implicit so it would be interesting to compare this effects employing a task such as emotional discrimination where the subject's attention is engaged by these particular facial features instead of the supposedly automatic processing taking place with the current paradigm. Indeed, whether voluntary attention is directed to expressions or not has been proposed to influence N170/M170 modulations by facial expression (Wronka and Walentowska, 2011; Rossion, 2014, see Hinojosa, Mercado and Carretié, 2015 for a meta-analysis that takes this aspect, among others, into account). There are studies that propose that the M170 is independent of attention though (e.g.: Furey et. al., 2006) Secondly, the emotional effects we are discussing should be put in context of the overall frequency effects that modulated the M170; as BSF and LSF showed similar peak latencies 30-35 ms faster than HSF faces latency across *all* emotional levels. Thus, LSF frequencies would have been more important for normal or facilitated visual processing in general of the structural properties and configuration of the stimulus (face) than HSF frequencies. This is reflected also in the behavioral results, as both BSF and LSF stimuli were correctly discriminated faster and with more accuracy than HSF faces – that presented longer reaction times and lower correct discrimination ratios (see Table 4.1).

Also, LSF faces elicited the M170 smallest amplitudes (see Table 4.3) in our study, as compared with either BSF or HSF faces. Actually, HSF faces elicit greater amplitudes compared with all the LSF faces. There are experiments in agreement with these results showing smaller amplitudes for LSF as compared with HSF faces (Hsiao et al., 2005; Haliet et al., 2006). Halit and colleagues for example found that HSF frequencies provoked greater amplitudes in the N170 while at the same time LSF frequencies were important for the correct performance in the task. It has been said that HSF frequencies add redundant information to the one conveyed by LSF and middle frequencies. The fact that LSF faces had smaller M170 amplitudes but better behavioral performance results suggest that LSF stimuli visual processing is facilitated in contrast with those stimuli –HSF- that lack these

frequencies and whose bigger amplitudes in the current experiment may reflect difficulties at structural encoding or enhanced processing due to their bigger complexity.

4.6.4 Processing steps reconstruction

In addition to the main objectives of the experiment –studying the early interaction time window with MEG sensors and the effect of the spatial frequency on the M170- we performed lastly a traditional analysis of the evoked magnetic response. This action was motivated by the evident differences in the temporal development of the waveforms between BSF, HSF and LSF spatial frequencies (as mentioned in the above paragraph Results: Frequency effects) that restricted the use of a cluster based permutation approach like the one applied to Experiment 1 data ncluding a seemingly unique to HSF faces component around 120 ms in addition to latency shifts (Figure 4.11).

First of all, we would like to summarize the most important visual evoked potentials (VEP, Spehlmann, 1965) discussed in visual processing literature that may be related with the eRMF components that we isolated in the current study. Known visual evoked potentials such as C1 (Jeffreys and Axford, 1972), P1 (Cobb and Dawson, 1960) and N1. Respectively, C1 is the earliest known VEP, peaking at around 60-90 ms and its sources are localised within striate visual cortex (Clark, Fan and Hillyard, 1995; Di Russo, Martinez, Hillyard, 2003), in consonance with our M60. It has been found to be quite robust, invariable to attention manipulations (Mangun, Hillyard and Luck, 1993). On the other hand, it is accepted that sources of the so known P1 (peaking at around 100 ms) extend beyond striate cortex into extrastriate regions and along the ventral pathway. Some authors locate them also in dorsal occipital areas (Woldorff et al., 1998) and posterior fusiform gyrus like we do (Mangun et al., 1997). Research on P1 has shown that it may be modulated by spatial attention, this is, the orientation of the visual focus (Mangun, Hillyard and Luck, 1993), and it is affected by stimulus low-level features like luminance. The third know VEP (latency wise) is called the N1, and it would correspond in our study with the M170 (and N1 for faces; Itier and Taylor, 2004b). It occurs between 150 and 200 ms. Likewise P1, it may be modulated by attention but it is more striking its relationship with selective rather than spatial attention (Haider, Spong and Lindsley, 1964). In addition to attention discriminating tasks (Rugg et al., 1987; Luck et al., 2000), brightness and luminance had been also linked with N1 amplitude (Ito et al., 1999; Johannes et al., 2003).

Critically, N1 is unaffected when subjects are just asked to press a button as soon as they see the stimulus (Mangun and Hillyard, 1991). N1 latency is affected conversely with the difficulty of the task. (Callaway and Halliday, 1982; Fort et al., 2005), hence, the component may reflect increased efforts in processing the stimulus. Given these evidences, it is widely accepted that the N1 indexes sorts of visual discrimination process. It is suggested that higher amplitudes of the N1 reflect spatial reallocation of visual attention resources, amplifying the processing of stimulus parts/features in order to perform the task.

The traditional analysis was performed selecting channels of interest and temporal windows for each component. The identification of the components was made prior based on the study of the topography maps changes over time (Figure 4.4 panel B) to isolate characteristic and seemingly independent spatial configurations of the magnetic signal combined with the observation of the peaks or moments of maximum amplitude in the grand average of all the channels as represented in Figure 4.10 panel A up to 200ms poststimulus

The resulting five different topographies along with the Meg sensors employed in the subsequent latency/amplitude analysis are depicted in Figure 4.10, panel B, and were labeled based mainly on their temporal appearance as M60, M90, M120 and M170A/B. The first two components, prior to the 100 ms poststimulus mark suggest occipital and occipital plus lateral sources respectively (Figure 10, panel B) and the source reconstruction performed indicated accordingly that the main contributions to the first component –M60- were located in visual striate areas while the later –M90- had sources in lateral and ventrooccipital areas as well as the temporal pole and dorsoparietal cortex. As expected, there were no latency differences between emotions or spatial frequency categories for any of both components (see Table 4.6). The average amplitude was not significantly different for any condition either (see Table 4.7). As can be seen in Table 4.7, it is important to note that the we need to narrow the time window employed to calculate the average amplitude of the M90 due to the next component –M120- that had bigger amplitudes for HSF stimuli and whose initial upward slope, recorded also on the channels employed to target the M90, could have altered inconsistently the results of the statistical analysis. Hence, the width of the time window was 12 ms, instead of a minimum of 20 around the peaks (Table 4.6) employed for the rest of the components (Table 4.7, second column).

Regarding the source localisation the striate cortex is where we first expected a neural response related with the visual processing of faces as early visual cortex is the starting point for the feedforward push processing along the cerebral cortex after thalamic relay of the information according to the most extended models of visual processing (Mishkin, 1983). The lateral and ventral occipital cortex correlates found for the M90 are consistent with the distinct topography of the component but may be striking given its promptness and proximity to the fusiform gyrus. However, it has been suggested (Liu, Harris and Kanwisher, 2002) that there is a stage of processing ~100 ms previous to the M170 that the authors label M100 that correlate with categorization of faces (but not with recognition, unlike the M170). Another study (Tanskanen et al., 2005) did source localize face specific responses in the middle occipital cortex between 70 and 120 ms also previous to the M170. A third study (Itier et al., 2005) had also found face specific responses in bilateral occipital cortex at around 100 ms and 220 ms in addition to the M170. Given that these example studies describe face specific modulations occurring around the 100 ms mark in areas similar to the ones localized in our study it is expected that higher order areas are active during this time frame and we believe this is what we captured by disentangling the components with our traditional analysis. However, although we cannot state whether this response is face specific or not emotional and spatial frequency manipulations employed in our paradigm did not provoke any differences between conditions for any of the first two components; M60 or M90

Peaking at around 120 ms there is a negative going (over the left hemisphere) slope with lateral and posterior distribution. The component related with this particular topography was labeled M120 and it shows the first significant effects on the traditional analysis. Crucially, HSF faces independent of their emotional expressions elicited appreciable bigger amplitudes than their BSF or LSF counterparts. The difference in amplitude is so big that at first glance it seems the component is only present for HSF faces (see for example Figure 4.3, panel B, second row columns 6 to 9) but the same peak is also present for BSF and LSF faces, only much smaller. Indeed, the only significant differences between HSF and BSF or LSF faces was found in the analysis of the amplitudes while there were still no differences in latency between spatial frequencies or emotional expression whatsoever. However, the magnetic evoked response at most of the channels start being different between HSF and BSF or LSF faces at this time. The source reconstruction also showed that HSF faces elicited overall increased brain activity. The fifth and sixth columns

of Figure 4.12 show the average source activation at this time point. All the maps show the maximum of activity with a threshold of 80 percent between 0 and 80 pAm but given the amplitude increase in the case of HSF faces, we include additional representation with a wider scale (from 0 to 12 pAm, see Figure 4.12). Interestingly, the cortical areas expressing the highest M120 related activations for HSF faces are very similar to the ones that were active ~30 ms before for BSF and LSF faces during the M90 component. We consider this evidence to be of big interest even though it was not one of our main objectives but however we cannot but speculate what is the cause of this difference. It may be because we did not build equally luminescent stimuli in term of energy but brightness, as physical properties such as luminance had been linked with amplitude and latency differences of early components related with perceptual processing of low level features of the stimulus (Ito et al., 1999; Johannes et al., 2003). It is important to note again that latency differences were not significant at this point in time yet (see Table 4.6).

Comparing our M60 and M90/M120 responses with traditional VEPs we speculate that they may represent the so called C1 and P1 respectively. Our M60 was unaffected by our experimental manipulations and was localized to neural sources coherent with that VEP. On the other side, the components we labeled M90 and M120 do occur in the time window of the so-called P1 VEP. The reconstruction of the sources at this time window expand beyond striate areas to extrastriate, ventral and temporal cortex, consistent with the data summarized at the beginning of this section. Interestingly, it appears that HSF faces M90 and M120 are bound (see Figure 4.11). We speculate that the enhanced M120 shown for HSF faces represents the increased reallocation of spatial attention sources given the need for visual discrimination to correctly perform our attention-to gender task. Also, the higher brightness energy of the HSF faces as compared to BSF and LSF faces may be responsible too for the latency and amplitude increases of the M120 evoked by the former set of stimuli. In the current work, N1 VEP should be represented by the M170, as we will see now.

The last two components were labeled M170A and M170B. As expected from fusiform gyrus sources, the topography of the M170 measured with magnetometers consist on bilateral dipoles between two occipital and temporal maximum/minimums (see Figure 4.4 or Figure 4.3). Indeed, to explore the classic M170 most experiments select temporooccipital sensors in a time window that may vary between 130 and 220 ms. We

took this approach and discussed the M170 in terms of a single component before the currently discussed step-by-step analysis. However, by looking at the temporal development of the topography we identified two issues we wanted to address (follow Figure 4.3). First, the most posterior maximums of activity are present for a smaller time than the main temporal maximums that last longer after the former had already decreased. Secondly, in the case of HSF faces the mentioned posterior maximums seem to be smaller but almost contemporary to the posterior maximums of BSF and LSF faces, while the temporal maximum of the former frequency clearly onset at later latencies than the temporal maximum of the latters. Thus, we labeled the activity measured in the posterior and temporal sensors as M170A and M170B respectively temporal wise. By disentangling both topographic features we do not expect to measure two different components but probably different contributors to the M170 overall signal. Importantly to our research, in a MEG study by Itier and colleagues (Itier et al., 2006) addressing face processing authors conclude that the M170 is actually generated by two distinct sources, M170A and M170B, with sources in occipital extrastriate areas and around the fusiform gyrus respectively. It is important to note that in the current study both the M170 source reconstruction data and the step-by-step source localisation suggest that the areas responsible of the activity within the classic M170 window expand from fusiform gyrus and ventral occipital areas to ventrotemporal, posterior and lateral occipital cortex.

That fact we found significantly shorter-to-smaller latencies in the order BSF-LSF-HSF seems to reflect the different difficulties for structural encoding of global face features when the stimuli are intact as compared with modified stimuli lacking some type of information (HSF or LSF frequencies). Indeed, the latency of the M170 (measured as a single component) has been shown to increase with task difficulty (Rossion et al., 2000a; Latinus and Taylor, 2006) likewise the N1. In the present analysis, importantly, there were no latency differences between LSF and HSF faces regarding the M170A. If our M170A indexes brain processing of visual features carried at posterior occipital cortex instead of integration of abstract perceptual features like the classic observations of M170 propose it is possible that different spatial frequencies do not modulate distinctively such a visual process in the way they would affect a more abstract kind of representation construction because of the different type of information each band of frequency conveys: information relevant to the task would be accessible from an holistic representation in the case that LSF are present in the picture, while HSF images would require increased attention to details

and specific parts of the picture, perhaps making the construction of an integrated representation more costly in terms of cognitive resources. Within our data this is feasible, besides the aforementioned fact that two different contributors –one occipital and one ventrotemporal- had been described previously (Itier et al., 2006), because we observe different temporal spans for the M170A and the M170B in the sensor space (see Figure 4.3) and the step-by-step source reconstruction analysis shows different neural substrates of the activity corresponding to these areas but with different onsets particularly in the case of HSF faces (see Figure 4.12). Some studies focusing on visual perception, separate between an occipital and a parietal N1 (Johannes et al., 2003). Unfortunately, the step-by-step source reconstruction does not exactly match the latencies measured in the sensor space and made it difficult to disentangle M170A and M170B contributors, albeit their distribution in the sensor space would be consistent with such a spatial division. This is possibly due to the fact that M170A topographical maximum covered a very narrow area for a short span of time, especially in the case of HSF faces and probably derived by the fact that the ventrotemporal sources of the component (indexed in the step-by-step analysis as M170B) are stronger and last for a longer time. In such circumstances without statistical evidence we must refrain from extracting conclusions about differences in the source space. Thus, it seems all we can conclude boils down to the differences between M170A/B component peaks within each condition at the sensor level. We could determine that the lapse between M170A and M170B peaks was significantly smaller for BSF and LSF faces compared with HSF faces M170A and M170B time lapse (~18 ms versus 39 ms respectively). This and the observation of the source reconstruction solutions that shows how ventral and posterior sources are almost synchronous in the case of BSF and LSF but asynchronous in the case of HSF faces leads us to speculate that the lack of LSF frequencies modulates the activity of ventral higher order areas like the fusiform gyrus but has less effect on occipital bilateral posterior cortex while both underlay processes indexed classically by the M170. Indeed, if there were not an apparent dissociation between posterior and ventral sources of the M170 for HSF faces we may not have divided the M170 in two *components* in the first place.

Despite the latency effects and the fact that LSF faces showed smaller M170B amplitudes than BSF and HSF faces overall, spatial frequency did not consistently modulate the amplitude of either the M170A or the M170B, . There were rather interactive effects. The sensors and time windows employed in the analysis of the M170 (see Results

4.3.2) and the component that we identified in the step-by-step analysis and labeled M170B greatly overlaid (see Figure 4.4 versus Figure 4.11 and Table 4.3 versus Tables 4.6 and 4.7) and thus, emotion and spatial frequency modulations were homologous. There was also increased activity for fearful BSF and HSF and neutral HSF faces as compared to the rest of the conditions. As discussed above, though, the analysis in the source space did not mimic these differences with higher activations in, for example, the fusiform gyrus for fearful BSF faces and fearful and neutral HSF faces. The amplitude analysis of the M170A was done over different (more posterior) sensors and at earlier latencies (~around 150 ms) and thus gives us additional information. Fearful BSF and HSF faces were again significantly different than their happy and neutral counterparts but in this case they showed smaller amplitudes. On the other side, LSF fearful faces were not different from BSF and HSF faces, though they did not differ either from their happy and neutral counterparts as BSF or HSF fearful faces did (see Table 4.7). In addition, LSF fearful faces had smaller amplitudes than BSF or HSF faces in general. Given these results and the assumption that this component reflects processing at posterior –not ventral- visual areas that may correspond to a new or a reappraisal analysis of perceptual features of the stimulus, smaller amplitudes may indicate facilitated processing. However, given the short span of the M170A component and its narrow topography the selection of the sensors of interest is complicated and we are uncertain about the relevance of these results. If the component reflects analysis of higher-order physical attributes of the stimulus, the smaller amplitudes for LSF faces in general as compared with BSF and HSF faces would be consistent with the absence of higher-order information not redundant with the information conveyed by lower frequencies.

4.7 Summary

We found an amplitude enhancement in central-right sensors specific for LSF fearful faces in a time window (~80 ms) similar but later than Exp. 1a early interaction effect (~70ms). Among the localised sources for that magnetoencephalographic component following minimum norm reconstruction of the eRMF subsequent statistical analysis unveiled an area on the right parietal cortex were the activation was greater for LSF

fearful compared with BSF and HSF fearful faces - linearly. We believe this enhancement may be due to magnocellullar projections coming to visual parietal cortices either from the amygdalar or the pulvinar nuclei of the thalamus.

In contrast, we found no emotional modulations of the M170 at all for LSF fearful faces. Rather, only BSF and HSF fearful faces provoked significantly greater amplitudes than their happy or neutral counterparts over temporooccipital sensors. Behavioral responses imitated this pattern with lower accuracy ratings and slower reaction times for fearful faces (albeit not significant) seemingly **restricted** to BSF and HSF faces. Keeping in mind that the reason why some experiments find M170 emotional modulations where others do not are still unknown, and given the functional significance of this component, we speculate that the different type of information conveyed by LSF and HSF frequencies regarding expression and gender may lay behind these results. Information about the scene from LSF pictures can be extracted holistically from global features while HSF pictures require analysis of structural details. It would be interesting to know what would happen had we employed an explicit instead of an attention to gender task. Unfortunately, statistical analysis of the source space data did not highlight any M170 source were such an interaction occurred.

HSF faces elicited more errors and longer reaction times as well as bigger/longer M170 amplitudes/latencies than BSF and LSF faces independently of their expression. However, we reconstructed the temporal course of the first steps of visual face processing and found no actual latency differences between components until ~160 ms. We also propose that the use of high-pass filters provoked the disentanglement of two sources behind the M170 component.

5 Experiment 3

5.1 Introduction

Despite the ease with which we perceive coherent objects in our environment even under poor stimulus conditions, the integration of only partly available visual information into whole percepts is a challenge for the visual system. This integration process has been referred to as perceptual completion or closure. Gestalt psychology considers perceptual completion to arise from processing of a stimulus as a whole, via choosing the simplest interpretation from the interactions of stimulus parts as opposed to the simple summation of single parts themselves (Wertheimer, 1923). Although the Gestalt theoretical framework describes this process at the level of stimulus part interactions, how the brain achieves perceptual completion from a mechanistic point of view is less understood.

Neuroimaging studies highlight a role for ventral visual areas and parietal cortex during perceptual completion of bi-stable (e.g. Rubin vases) and degraded figures (Dolan et al., 1997; Kleinschmidt et al., 1998; Andrews et al., 2002; Sehatpour et al., 2006). Perceptual closure of two-tone Mooney faces (Mooney, 1957) elicits increased hemodynamic responses in face sensitive visual ventral brain regions such as the fusiform face area (Andres and Schluppeck, 2004; Kanwisher et al., 1998; McKeeff and Tong, 2007). Electroencephalogram studies have demonstrated a perceptual closure specific event related potential occurring in a time window between 230 ms and 400 ms peaking around 320 ms post-stimulus time (Doniger et al., 2000, 2001; Sehatpour et al., 2006). Source localisation of this component also revealed that ventral visual cortex (part of the lateral occipital cortex) and parietal cortex are active at this latency (Sehatpour et al., 2006). Taken

together, these findings accord with the suggestion that not only brain regions for cue invariant object/face recognition such as ventral visual cortex (Malach et al., 1995; Haxby et al., 1999; Kanwisher and Yovel, 2006) but also spatial attention relevant parietal brain regions (Corbetta et al., 1998; Fernandez-Duque and Posner, 2001) are crucial for perceptual closure and that his process occurs about 230 ms to 400 ms after stimulus onset.

Within the classical view of visual system hierarchy, simple geometric lines and shapes that form complex objects are processed in lower order visual cortex, whereas higher order areas within the ventral visual stream (Mishkin et al., 1983) code invariant object and category information (e.g. Vogels and Orban, 1996) based on feedforward communication from early visual cortex (for a review of these models see Hochstein and Ahissar, 2002). However, recent models of conscious visual perception suggest reverse hierarchical processing (for a review see Hochstein and Ahissar, 2002) whereby higher order visual areas in the ventral and dorsal streams provide top-down feedback to early visual cortex (e.g. predictive coding - Friston, 2003a; Rao and Ballard, 1999). In the case of perceptual completion, this top-down feedback is suggested to carry global information to local processing units in early visual cortex (Lamme and Roelfsema, 2000; Bullier, 2001b; Hochstein and Ahissar, 2002; Campana and Tallon-Baudry, 2013), which accords with Gestalt theory in that global visual information interacts with local stimulus part processing (Wagemans et al., 2012s, 2012b).

The neuroimaging studies of perceptual completion described above do not report engagement of lower order visual cortex. However, one event-related fMRI study (Altmann et al., 2003) reported both primary and higher order visual cortex activation during global shape integration of collinear contours. Although these observations were interpreted as potential reflecting top-down modulation in global shape perception (Altman et al., 2003), a measure of interaction between these levels of hierarchy was not provided. Transcranial magnetic stimulation (TMS) studies in humans demonstrate that interrupting recurrent interactions between early and higher visual cortices in the ventral visual stream impairs perception of natural scenes (Koivisto et al., 2011) and perceptual completion of illusionary Kanizsa-type figures (Wokke et al., 2013). However, perceptual impairment by TMS-evoked disruption of early visual areas (Wokke et al., 2013) does not directly demonstrate feedback coupling of neuronal activity; an alternative explanation is simply that early visual cortex activates at later latencies independently from any feedback from higher order areas.

Thus, although recent evidence suggests that coherent perception relies on feedback from higher to lower order visual cortex. Paralleling the global-to-local concept of Gestalt psychology, a characterization of this process in terms of effective connectivity is currently lacking.

To address this, we measured induced Neuromagnetic oscillatory brain responses to two-tone Mooney faces that consist of white patches that have to be spatially integrated to perceive a face (Mooney, 1957). We employ the Mooney face paradigm for two reasons: first, it represents a classical measure of perceptual completion (Mooney, 1957) and brain areas involved in Mooney face perception are well characterized (Andres and Schluppeck, 2004; Grutzner et al., 2010; Kanwisher et al., 1998; McKeeff and Tong, 2007). Second, Mooney face perception consistently elicits neuronal oscillations in the gamma frequency band (>30 Hz) in the EEG (Rodriguez et al., 1999; Trujillo et al., 2005), intracranial EEG (Lachaux et al., 2005), and MEG (Grutzner et al., 2010). Synchronized oscillatory neuronal gamma band responses can be observed during coherent perception of a wide range of visual stimuli (Müller et al., 1996; Tallon-Baudry et al., 1996, 1997; Keil et al., 1999; Gruber and Muller, 2005; Gruber et al., 2008; Martinovic et al., 2008;) and are thought to reflect dynamic neuronal interactions between brain areas critical for perceptual synthesis (Singer and Gray, 1995; Müller et al., 1996; Engel et al., 2001; Martinovic et al., 2008; Hipp e al., 2011).

5.2 Objectives

The main objective of Experiment III is studying the process of perceptual completion (Wertheimer, 1923). To do this we employed a face-non face discrimination task with intact and scrambled Mooney faces (Mooney, 1957) during MEG acquisition. We intend to employ the gamma response as an index of perceptual completion. Based on source reconstruction and the cross spectral density of gamma band responses, we will invert biophysical neuronal models that estimate the underlying effective connectivity between the identified brain areas and submit them to Dynamic Causal Modeling. This will

test whether feedback/recurrent processing between low- and higher order areas is need in addition to classic feedforward processing.

5.3 Hypothesis

We predict that Mooney face perceptual completion will increase gamma band responses in face sensitive fusiform face area (Kanwisher and Yovel, 2006), spatial attention relevant parietal (Corbetta, 1998; Fernandez-Duque and Posner, 2001) and lower order visual cortex (Wokke et al., 2013). Based on the reverse hierarchy-processing hypothesis we also predict that inversion of effective connectivity models reveals feedback coupling of gamma oscillations from fusiform and parietal to early visual cortex during perceptual completion.

5.4 Methods

5.4.1 Subjects

The subjects were eighteen right-handed volunteers (9 females, mean age: 31.8 years; s.e.m: 1.3). They participated in our study after having given written informed consent. All subjects had no history of neurological or psychiatric disease and had normal or corrected to normal vision.

5.4.2 Stimuli

Stimuli comprised 40 Mooney (Mooney, 1957) and 40 scrambled Mooney faces. Scrambled faces were derived by rotating (45-90°) the originals and randomly rearranging stimulus features. Stimuli were presented by a video projector (Panasonic PT-D7700E) via a mirror system to the center of a screen in a magnetically shielded MEG room (visual angle 7° by 10°). Example stimuli can be seen in Figure 5.1.

Figure 5.1 Experiment 3 stimuli

Examples of Mooney (left) and scrambled Mooney faces employed as stimuli. 40 different Mooney faces were employed.

5.4.3 Procedure

In two experimental runs, 40 Mooney and 40 scrambled faces were presented in random order (total 80 trials per picture category). Stimuli were presented for 200 ms with inter-stimulus interval randomly varying between 2000 and 2500 ms. Participants indicated by button press after stimulus offset when they had perceived a face or not (right and left response buttons counterbalanced across subjects). A visual representation of the procedure is shown in Figure 5.2.

Figure 5.2 Experimental procedure

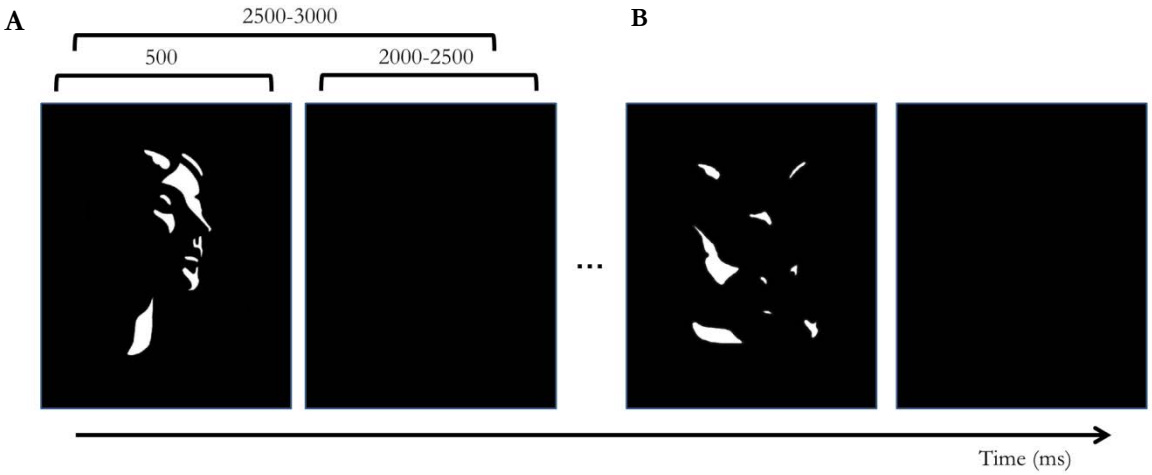

Both panels resemble a typical trial for each of the possible outputs of the face discrimination task: face (A) or non-face (B).

5.4.4 Behavioral data analysis

Accuracy was measured as the percentage of correct identification of Mooney *vs.* scrambled faces. Both accuracy and mean reaction times were compared employing a t-student statistics.

5.4.5 Acquisition and preprocessing

MEG data were recorded continuously (1000 Hz sample rate, 0.1-330 Hz online filter) using a 306-channel system (Elekta©, VectorView). The MEG sensors consisted of 102 magnetometers and 102 pairs of orthogonal planar gradiometer pairs. Both type of sensors were used for the analysis, as opposed to Experiment 2 whose MEG recordings were acquired with the same machine but only magnetometer information was analyzed.

Peri-stimulus epochs of 2000 ms (1000 ms baseline) were extracted for each MEG channel and stimulus category. Epochs were discarded from analyses when containing eye artifacts, movement artifacts identified by visual inspection, high amplitudes (3 pT and 1 pT in magneto- or gradiometers, respectively), and pertaining to incorrect trials (a

scrambled picture was perceived as a face or vice versa). The number of trials per picture category was equalized by randomly choosing a subset of trials of the picture category that contained more artifact free epochs., This was done in order not to bias experimental conditions with respect to their signal to noise rations., For statistical comparisons, beamformer power estimations, and connectivity analysis (that we will discuss later), it has been recommended that experimental conditions should contain the same number of trials (Gross et al., 2013)

Given our interest in oscillatory gamma, we calculated the spectral power changes measured at magnetometers and gradiometers. We conducted a multitaper time frequency analysis with fixed length time windows in the range between 30 and 100 Hz from -800 ms to 600 ms peri-stimulus based on previous reports of induced oscillatory power changes elicited by Mooney faces (Grutzner et al., 2010; Lachaux et al., 2005; Rodriguez et al., 1999; Trujillo et al., 2005). Time frequency decomposition was performed using sliding time windows of 200 ms length in 40 ms steps. We applied 3 tapers (Slepian sequences) obtaining a frequency smoothing of ± 10 Hz (for a similar approach see Capilla et al., 2012). Then, time frequency decompositions of epochs for each experimental condition and subject were averaged and relative power changes with respect to baseline (-800 ms to -200 ms pre-stimulus time) were determined. Note that orthogonal gradiometer data were combined by calculating the modulus of the horizontal and vertical gradients of their relative power changes. Finally, power changes for each MEGG channel (magneto- and combined gradiometers) and stimulus category were employed in subsequent to statistical analysis.

Multitaper-, as opposed to single-taper decompositions are used to achieve better control over the frequency smoothing: more tapers results in greater smoothing. Importantly, high frequency smoothing has been shown to be particularly advantageous when dealing with electrophysiological brain signals above 30 Hz like oscillatory gamma activity, while a single taper approach may fit best lower, narrower signals (Percival and Walden, 1993, Mitra and Pesaran, 1999). In addition, fixed time windows approach has been recommended for later statistical comparisons, as the number of time-frequency bins is equal across the time-frequency range (Gross et al., 2013). Finally, the Slepian tapers are sets of multiple (orthogonal) tapers that optimize the frequency resolution and minimize the intrusion of signal from distant frequencies (Walden, 2000). Hence, Slepian are better

than Hanning tapers when performing multitaper time frequency analysis. All preprocessing steps were done using the Fieldtrip toolbox (http://fieldtrip.fcdonders.nl/).

5.4.6 Sensor level statistical analysis

We applied -to the magnetometer and combined planar gradiometers separately- cluster-based nonparametric statistics with one thousand permutation steps to determine the time-frequency windows (that had a length of 200 ms, as explained above) and channel locations of significant relative power differences between Mooney and scrambled faces within a 30 to 100 Hz frequency band. Unlike Experiments 1a: faces or Experiment 2 and much like Experiment 1b: scenes the statistic selected were paired t-test (initial threshold of $p < 0.01$) given our two experimental conditions. Clusters were formed by temporal, spectral, and spatial adjacency (a cluster threshold contained at least two significant neighbors along the three dimensions). Unlike Experiment 2 were magnetic signals were also acquired but ERM fields were analyzed, in the current experiment clusters were spatiotemporal and spectral, comprising time points and sensors as well as frequency bins. The summed of t-values that were greater or smaller than the 97.5^{th} percentile ($p < 0.025$ two tailed test) within the permutation distribution were considered as significant clusters of a picture category effect. All permutations statistics were done using the FieldTrip toolbox.

Additionally, we calculated the phase locking factor (PLV) with respect to picture onset for each subject, picture category, and MEG sensor. Thereby, the complex Fourier components of each time and frequency bin (see Methods section of the main text for the description of the spectral analysis) where divided by their corresponding complex modulus (magnitude) for each trial, resulting in a normalized phase vector. Finally, the absolute value of the mean normalized phase vectors across trials served as PLV estimating the phase alignment with respect to stimulus onset. The PLV is zero if phase vectors are randomly distributed and one if uniformly distributed across trials. For visualization the PLVs were averaged across subjects for each picture category. The same cluster based permutation statistics were applied to assess if PLVs were significantly different from baseline.

5.4.7 Source reconstruction

The underlying cortical sources of the time-frequency window of interest showing different relative power changes between Mooney and scrambled faces were estimated using a beamformer approach (Van Veen et al., 1997) implemented in FieldTrip. The head and sensor positions of each subject were first co-registered with a MNI canonical template brain (Collins et al-. 1998) by realigning it with the individual's fiducials and head shape points. The triangulated skull surface of the template brain served as a single shell volume conduction model (Nolte, 2003). The leadfields for orthogonal dipole pairs tangentially oriented to the scalp surface placed on a three dimensional regular spaced source grid (8 mm distance) were calculated using the method described in Nolte (2003). The source grid was spatially restricted to the gray matter of the template brain.

First, based on sensor space data, cortical responses for the broadband gamma responses (50-100 Hz) were estimated by using a linearly constrained minimum variance (LCMV) beamformer (Van Veen et al., 1997). MEG time series were band-pass filtered between 50 and 100 Hz for each trial. Then, time windows of 100 ms steps beginning at 100 ms and ending at 600 ms post-stimulus time were extracted from the MEG data for each participant and experimental condition (see Figure 5.4). Pre-stimulus segments of the same length were extracted. For every 100 ms time window pre- and post-stimulus time segments of both experimental conditions were concatenated and the covariance matrix was calculated to determine the spatial filter coefficients of the LCMV beamformer (Van Veen et al., 1997). A regularization factor was applied by adding 10% of the mean across the eigenvalues of the covariance matrix to each element of the covariance matrix. Then, each band-pass filtered sensor level MEG epoch was projected into source space through the common spatial filter for each 100 ms time window and the pre-stimulus interval. For each experimental condition, participant, 100 ms time window, and source grid location, power along the optimal dipole orientation as determined by the first eigenvector of the covariance matrix of the two tangentially oriented dipoles was averaged across epochs. For each subject, experimental condition and 100 ms time window relative power changes with respect to the baseline were calculated at each source grid location like this: (post-stimulus power – pre-stimulus power) / pre-stimulus power.

Second, based on the results (see Results 5.5.1) of the statistical comparison between the time frequency decompositions of Mooney and scrambled face epochs, MEG time series were band-pass filtered between 55 and 71 Hz for each trial. Then, post-stimulus time windows of interest (333 to 538 ms ± 100 ms, see Results) and pre-stimulus segments of the same length were extracted. Pre- and post-stimulus time segments of both experimental conditions were concatenated and the covariance matrix was calculated to determine the spatial filter coefficients of the LCMV beamformer (Van Veen et al., 1997). As for the broadband gamma response (see above) each band-pass filtered sensor level MEG epoch was projected into a source space through the common spatial filter and a regularization factor of 10% was applied. For each experimental condition, participant and source grid location, power along the optimal dipole orientation as determined by the first eigenvector of the covariance matrix of the two tangentially oriented dipoles was averaged across epochs. Cortical power source grid volumes for the Mooney and scrambled face conditions were the submitted to statistical analysis.

Third, we recalculated the beamformer results with respect of the time and frequency ranges based again upon the comparison between the time frequency decompositions of Mooney and scrambled face epochs, but dividing he time window in an early (333-433 ms ± 100 ms) and late (433-538 ± 100 ms) time segment. At each source grid location the relative power changes for the Mooney with respect to scrambled faces were calculated. Finally, based on these relative activity maps relative power changes for the late vs. early time segments were determined.

5.4.8 Statistical analysis at source level

Oscillatory gamma power projected into cortical source space for Mooney and scrambled faces was compared using the same non-parametric cluster based permutation statistics as described for the time frequency sensor level data (see Methods 5.4.5 section). However, as the beamformer solutions (3 dimensional dipole grids in MNI space) already reflect relative power changes within a certain time frequency window, clusters were formed along the spatial dimension only.

5.4.9 Dynamic Causal Modeling of Effective Cortical Network Connectivity

To examine effective coupling between gamma power sources, we applied DCM to the cross-spectral densities (CSD) of the sources in the time-frequency range of interest (Friston et al., 2012). Cross-spectral density is the Fourier Transform of the signal cross-correlations, thus, it can tell the level of power shared by a two signals at a given frequency. There were 3 cortical sources (one source in early visual cortex in the right occipital lobe, one in the right fusiform and parietal cortices, respectively (see Table 5.1) based on the non-parametric cluster based permutation statistics of oscillatory gamma power differences between Mooney and scrambled faces (see Figure 5.6). The coordinates of these sources were selected by identifying the peak *t* values ($t_{17} > 2.89$; $P < 0.01$) within the significant source cluster - spanning early visual, inferotemporal and parietal cortices.

In order to extract the time series of the three sources of interest, unfiltered MEG epochs were projected from the sensor level to source space through the spatial beamformer filter. All three source waveforms were baseline corrected using the same baseline as described before (see Methods 5.4.8 Source reconstruction section) and normalized by their standard deviations to eschew confounding of DCM results by amplitude differences. Finally, the three cortical source time series were submitted to CSD-based DCM analysis, as mentioned before. This analysis was limited to a latency of 233 to 638 ms and a frequency range of 55 to 71 Hz, later range chosen based on significant gamma power differences between Mooney and scrambled faces within the former particular temporo-spectral window.

Nine possible DCM models resembling the different gamma connectivity directions, in addition to a null model were submitted to the DCM. The modeling of the connections between the three selected sources connectivity was done in light of the reverse hierarchical processing model of the visual system (Hochstein and Ahissar, 2002). Strength modulations between early visual cortex and fusiform or parietal cortex were modeled as purely forward, backward or both forwards and backwards. On the other side, coupling between fusiform and parietal cortices was modeled in a forward, backward or bi-directional manner. This permutation result in nine different models. Finally, as gamma power synchronization may occur locally, an additional model was created without

modulation of connectivity between any areas. Hence, ten different DCMs (Figure 5.3) were inverted to estimate the connectivity strength modulations between the three sources by picture category (Mooney vs. scrambled). Model parameters were estimated using a variational Bayesian scheme as implemented in SPM12b, with the parameter of interest here being the connectivity modulations between cortical sources by picture category.

Figure 5.3 Models inverted in the DCM

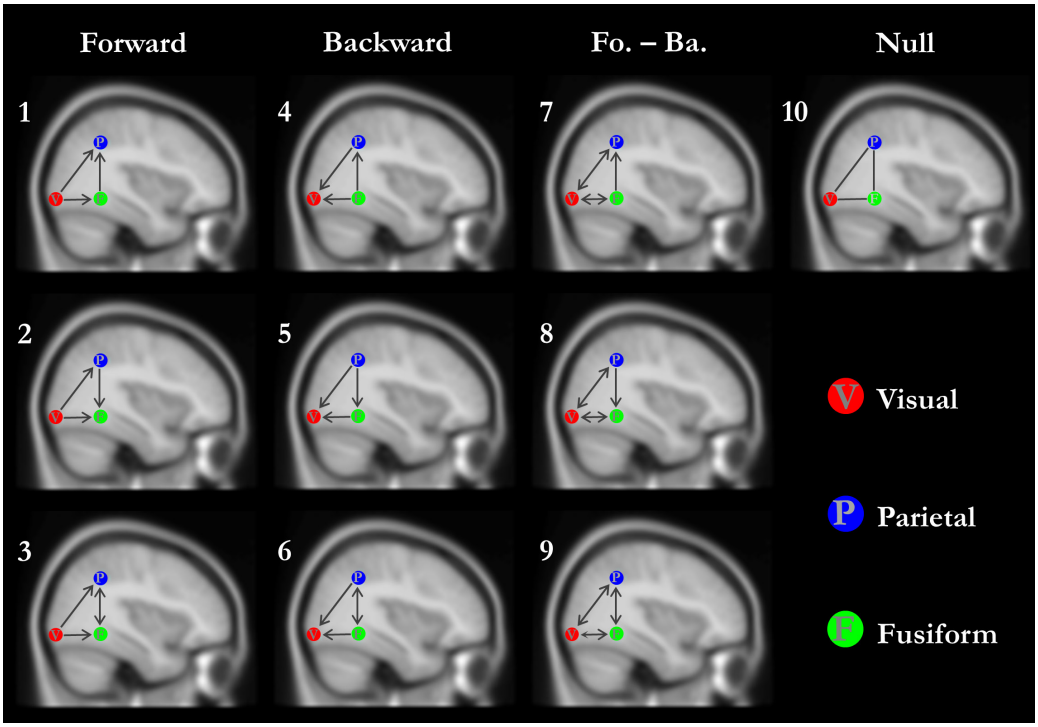

The figure shows the ten different putative effective connectivity modulations by Mooney face perception. The three circles represent the cortical sources: visual, parietal and fusiform. Arrows represent the direction of the connectivity modulations: one-way, bi-directional, or absent (dashed line). Columns organize the models based on the directionality of early (visual) and higher-order cortical sources (parietal and fusiform): forward, backward or both (Fo. – Ba.: forward and backward).

All models were tested against each other employing Bayesian model selection with fixed effects (see Garrido et al., 2007 for details). Each model log evidence, which is a measure indicating the probability of the data given the model, was used to estimate the model evidence per subject, Next, for each DCM model the log evidences were added across subjects (equivalent to multiplying the marginal likelihoods of the models, assuming independence between subjects). The winning model was defined as the model with the log

evidence greater than at least a value of 3 relative to all other models (relative likelihood is greater than 20:1). This difference threshold is considered as indicating strong evidence for the winning model reflected in the model posterior probability (Garrido et al., 2007)

Connectivity modulation by picture category (the parameter of interest) was estimated by calculating the conditional density of the parameters at the group level, a method named Bayesian parameter averaging. Briefly (for details see Garrido et al., 2007), the individual parameters and precision matrices are multiplied and summed across participants. The sum of products is then multiplied by the overall precision matrix as defined by the sum across all individual precision matrices. This procedure was applied to the winning model only, yielding mean coupling parameters and their associated conditional probabilities across subjects. Note that conditional probability expresses how likely the coupling parameter is different from zero change with respect to the baseline conditions (scrambled faces).

Finally, In order to estimate how the best DCM model's data fit we calculated the rest variance between the model prediction and actual data for the auto- and cross spectra as estimated by the DCM algorithm for cross-spectral densities implemented in SPM12b.. The rest variance was estimated by dividing the sum of squares of the residuals by the sum of squares of the data multiplied by 100 across the frequency bins within our frequency range of interest (55 – 71Hz).

5.5 Results

5.5.1 Behavioral results

Performance, indexed by correct identification of Mooney and scrambled faces, was high. The mean (s.e.m) accuracy ratings and reaction times were 85.8% (1.7) and 712 ms (22.3) for Mooney faces and 90.9% (1.6) and 772 ms (22.2) for scrambled stimuli.

5.5.2 Sensor level results

Both stimulus types induced broadband gamma power (50-100 Hz ± 10 Hz) in posterior MEG sensors with onset latency around 100 ms (see Figure 5.4). Critically, however, Mooney faces elicited prolonged oscillatory gamma band power changes. Mooney faces significantly increase gamma band activity, relative to scrambled faces, in a frequency range from 55 to 71 Hz (± 10 H<) and from 333 to 538 ms (± 100 ms) after

Figure 5.4 Sensor level results

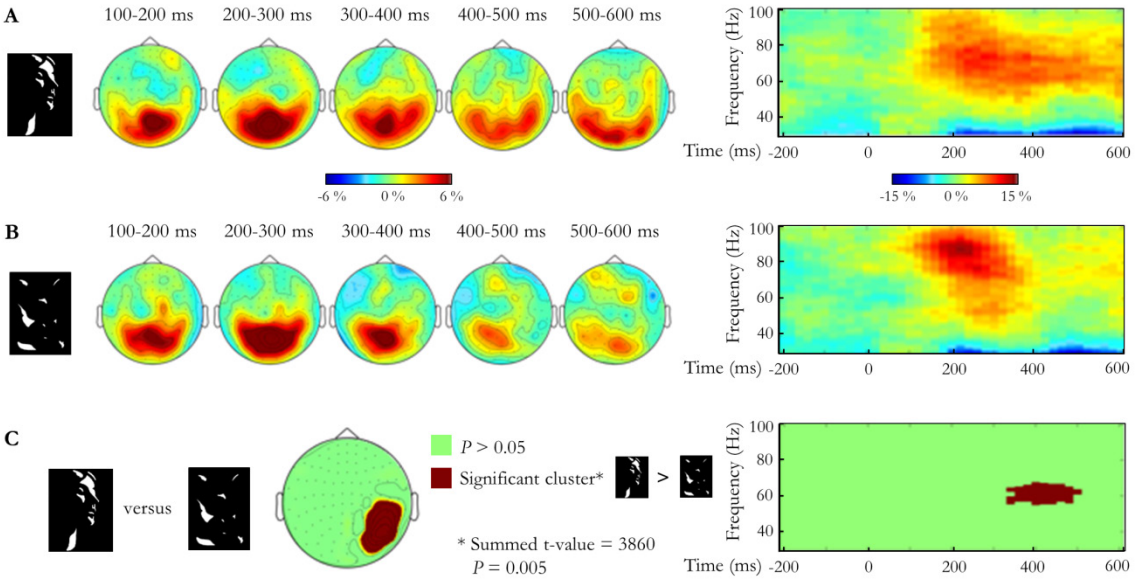

Upper panels represent gamma power changes with respect to the baseline for Mooneys (panel A) and Scrambled (Panel B) faces. Main section of the panels depicts the topography of said changes from 50 to 100 Hz in steps of 100 ms from 100 ms to 500 ms poststimulus. Right side of the panels represents broadband (40 – 100 Hz) power changes with respect to the baseline across the whole epoch. Panel C shows the results of the significant statistical comparison upon the cluster based permutation analysis. The spatial extension of the significant cluster is represented in the topoplots while it sspectral and temporal span is depicted in the right.

stimulus onset.

Note that although our statistical analysis indicates that gamma power differences started at 333 ms after stimulus onset, due to fixed 200 ms time windows (time resolution ± 100ms) utilized for the time frequency decomposition (Gross et al., 2013), the time interval in which gamma band activity can be said to be increased is therefore between 233 and 638 ms post-stimulus onset. This effect is restricted to a right occipito-parietal sensor cluster (cluster-based permutation testing Mooney > scrambled: summed t-value = 3860, p = 0.005). Mean power changes relative to baseline (± s.e.m.) across the significant sensor-

time-frequency cluster are 7.3% ± 1.2 for Mooney and -2.2% ± 1.2 for scrambled faces, respectively. No sensor-time-frequency cluster indicated increased gamma activity for scrambled, relative to Mooney faces (cluster-based permutation testing scrambled > Mooney: summed t-value = -189; $P = 0.78$).

The result of the phase-locking value analysis (Figure 5.5) clearly demonstrated that the gamma power modulation employed in the previous analysis was not phase-locked but induced.

Figure 5.5 PLVs and statistical analysis

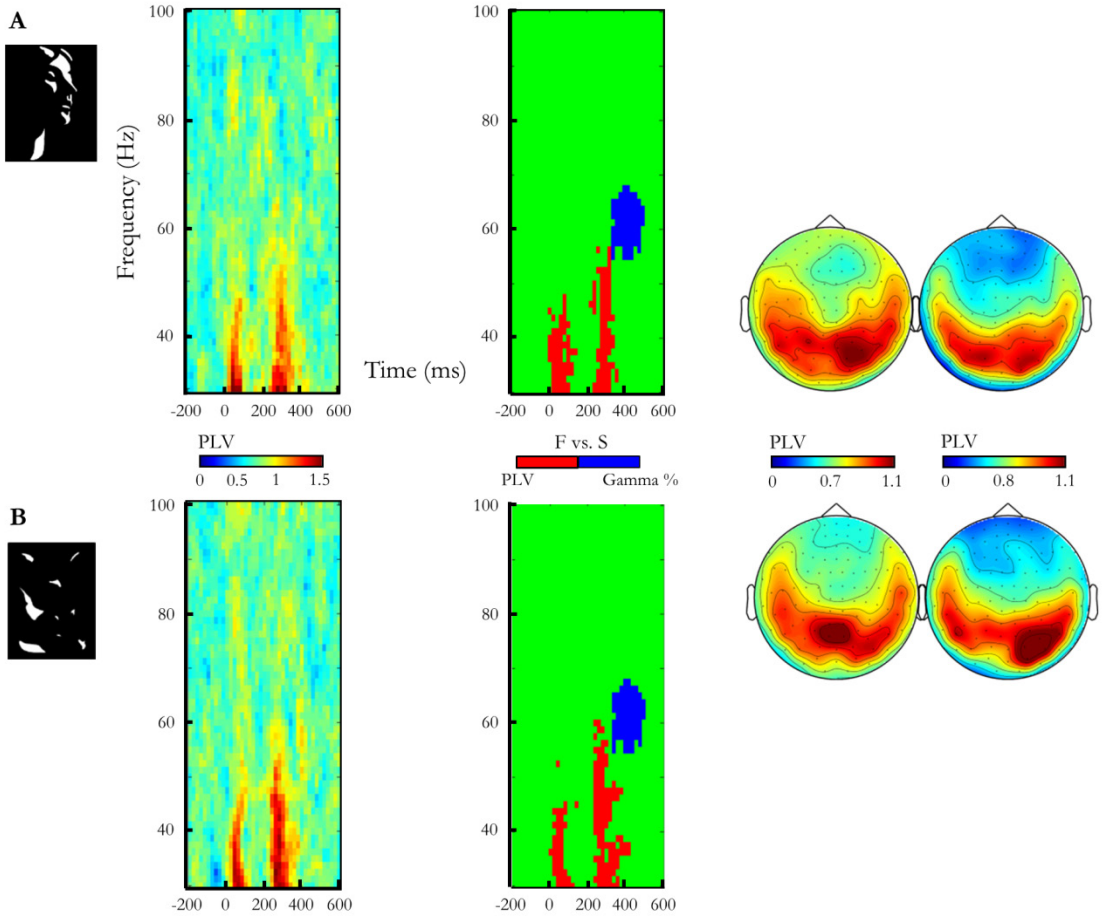

Left side of both panels represents the grand averages (N = 18) of phase locking values (PLVs) with respect to stimulus onset for Mooney (panel A) and scrambled Mooney faces (panel B) across time and spectra for a representative posterior MEG sensor. The colorbar indicates average PLVs. Middle side of the panels shows the same time-frequency representation of phase locking as but significant clusters are coded (shown in red; $p < 0.05$, corrected for multiple comparisons). For the sake of clarity, significant clusters representing increases in gamma power for Mooney faces (as described previously in this section) are also shown in blue. The right side of the panels shows the mean topographies across the corresponding significant temporal-spectral time range for the early and late time segment (both conditions had two significant clusters) F = Mooney faces; S = scrambled Faces.

Cluster based permutation statistics indicated two spatio-temporal-spectral clusters different from baseline in the lower gamma frequency band for Mooney faces (0 to 150ms ± 100ms, 30 to 48 Hz ± 10 Hz: summed t-value: 1757, $p < 0.0001$; 211 to 371ms ± 100ms, 30 to 57Hz ± 10 Hz: summed t-value 550, $p = 0.048$). Cluster based permutation statistics indicated two spatio-temporal-spectral clusters different from baseline in the lower gamma frequency band for scrambled faces (0 to 150ms ± 100ms, 30 to 53Hz ± 10Hz: summed t-value: 12090, $p < 0.001$; 230 to 450ms ± 100ms, 30 to 61Hz ± 10Hz: summed t-value: 6801, $p < 0.001$). Figure 6.7 middle panel shows the significant PLVs clusters in red and the induced gamma change significant cluster in blue to demonstrate that gamma power modulations during perceptual completion were induced and not phase locked. However, due to time frequency uncertainties inherent to spectral analysis some overlap cannot be ruled out. Nevertheless, the peak effects do not overlap.

5.5.3 Source level results

Brain sources of gamma power were estimated by LCMV beamformer (see Methods 5.4.8 Source reconstruction section). Figure 5.6 shows the result of said sources reconstruction as well as subsequent statistical analyses. Cluster based permutation statistic in the source space show that Mooney faces elicited higher gamma power than scrambled Mooney faces (Mooney > Scrambled; summed t-value = 1229; $P = 0.04$) between 333 and 538 ms. Importantly, such cortical source cluster extended from early visual to inferotemporal (fusiform) and parietal cortices (Figure 5.6 panel C left). Mean power changes relative to baseline (± s.e.m.) across all voxels within the significant cluster are 2.3% ± 0.5 for Mooney and 0.4% ± 0.4 for scrambled faces. Fusiform and parietal cortex activities started at earlier latencies, whereas early visual cortex activation occurred al later stages (Figure 5.6 panel C middle-right and -left).

Figure 5.6 Source localisation results

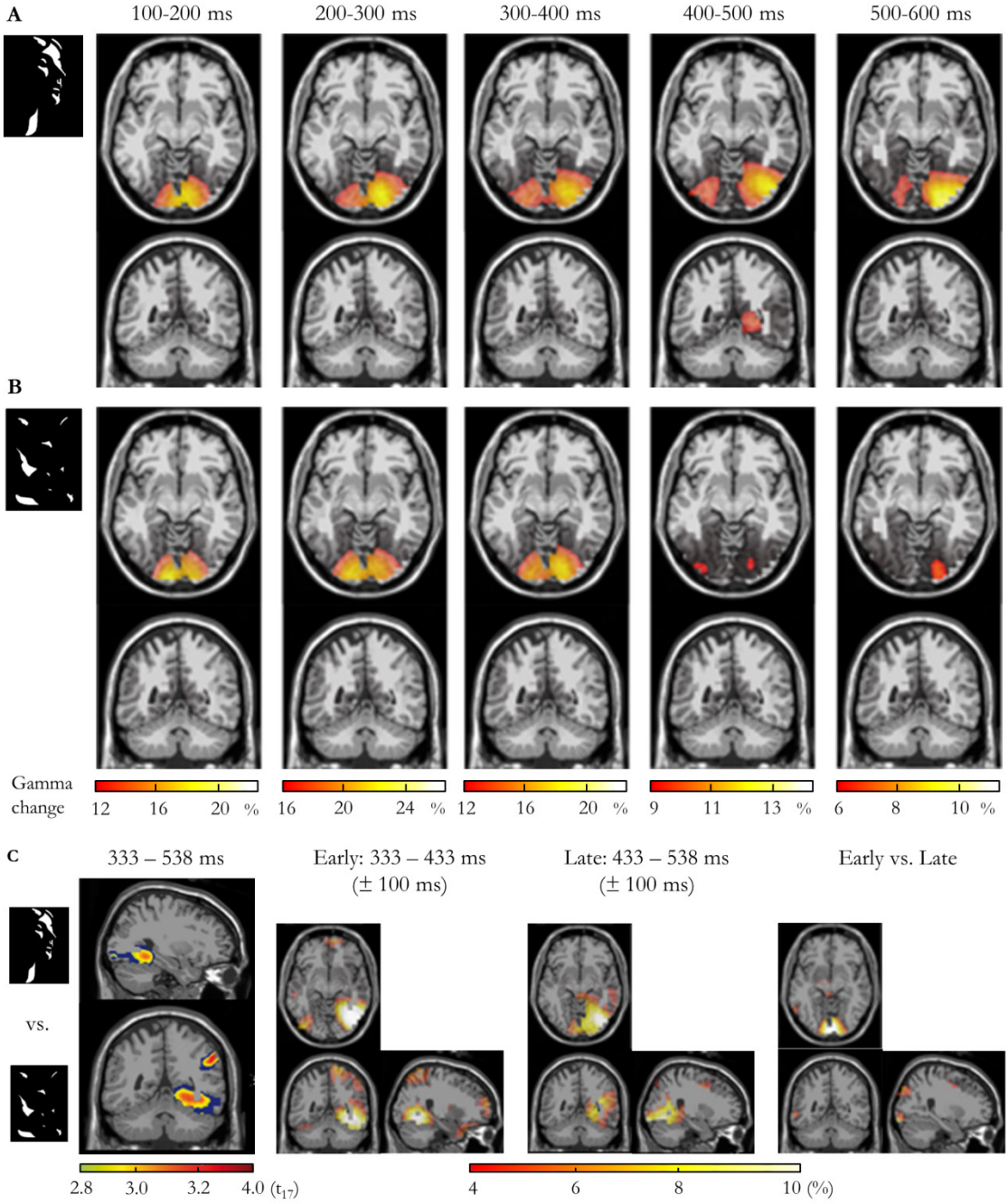

Upper panels show the results of the gamma power sources reconstruction in steps of 100 ms for both Mooney (panel A) and scrambled Mooney faces (panel B). Left side of Panel C shows the location of the source cluster were Mooney faces elicited significantly higher gamma power between 333 and 538 ms, comprising visual, inferotemporal and parietal cortices. Middle figures of panel C show the relative power changes for Money with respect to scrambled faces for an early (333-433 ms ± 100 ms) and late (433-538 ms ±100 ms) time subdivisions of the main time window of interest. Right figure shows the result of subtracting the activity elicited in the later segment from the earlier segment making more evident the increased activity at visual cortex at later latencies.

Three peak voxels (t_{17} = 2.8; P < 0.01) within this cluster can be localized to early visual, fusiform and parietal cortices of the right cerebral hemisphere (see Table 5.1 for MNI coordinates and relative power changes for the peak voxels) and, as mentioned before, these source locations served as reference sources for the DCM models.

Table 5.1 MNI coordinates of the three peak voxels

Region	x	y	z	t_{17}	P	Relative Power Change	
						Mooneys	Scrambled
Parietal	56	-49	40	3.3	0.004	1.5 % (0.4)	-0.3 % (0.4)
Fusiform	25	-50	-10	3.1	0.007	2.5 % (0.6)	0.4 % (0.5)
Occipital	30	-89	-11	2.8	0.01	3.6 % (0.8)	1.4 % (0.7)

The table shows the coordinates of the peak voxel corresponding to each of the three sources derived from the LCMV Beamformer analysis and cluster permutation statistic in source space, along with their statistical value and associated *P* value (two-tailed) and the power changes relative to each voxel.

5.5.4 Dynamic causal modeling results

To test biological plausible, effective connectivity models of coupled gamma oscillator in early visual, fusiform and parietal cortices at time frequency bins of significant induced gamma power differences between picture categories (Mooney vs. scrambled faces) ten DCM models (Figure 5.5) were inverted. Regarding the results of the modelling, the model assuming no modulation of connectivity by Mooney face perception between the three cortical brain areas is the least likely in the case of the observed data (Figure 5.8). On the contrary, the effective connectivity model of bi-directional coupling between fusiform and parietal cortices and feedback connectivity modulation from these areas to early visual cortex is the one that best explains observed gamma power modulations by Mooney faces (Figure 5.9 panel A). The best and the second nest performing models differed by 5846 with respect to log evidences, suggesting very strong support for the best fitting model (model posterior probability 100%; Figure 5.9 panel B). A difference of 3 is

considered as evidence favoring one model. The percentage changes of effective connectivity between cortical sources induced by Mooney faces together with their corresponding conditional probabilities are shown in Figure 5.9 panel C.

The auto- and cross spectra with respect to occipital, fusiform, and parietal cortical sources employed in the analysis of a representative participant (see Methods section 5.4.10 for a brief explanation of the DCM analysis steps) are represented in Figure 5.10. Some deviations between predicted and empirical data can be seen. However, the differences are quite small (note the scale) as indicated by small rest variance for the best model (faces: 0.13%, scrambled: 0.15%). For the whole sample rest variances were in the range of 0.06% to 0.62% for faces and 0.05% to 1.33% for scrambled faces, respectively.

Figure 5.7 Bayesian model selection and connectivity estimation:

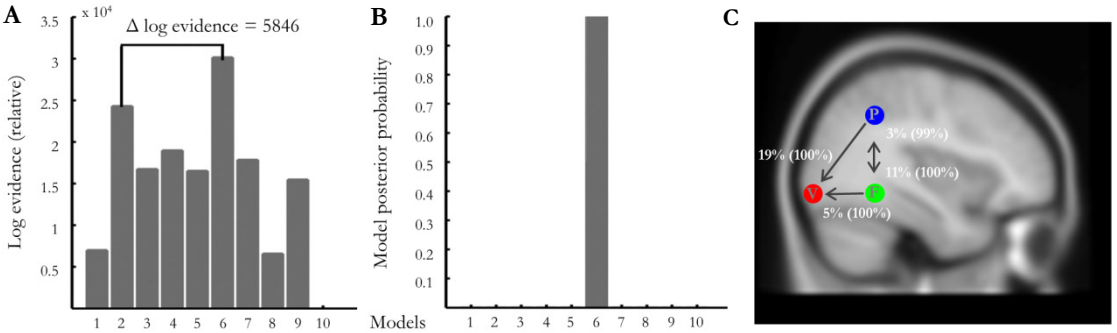

Differences between log evidences of all inverted DCMs and the least likely model (model 10) are shown in panel A. Model 6 assuming bi-directional connectivity modulations between fusiform and parietal cortices and feedback coupling from these regions to early visual cortex outperforms all other models (posterior probability 100%) is shown in panel B. The winning DCM with its estimated coupling parameters between brain regions is shown in panel C. White arrows indicate coupling directions. Numbers indicate percentage change of gamma frequency coupling between Mooney and scrambled face picture categories. Posterior probabilities of coupling parameters indicating picture category differences are shown (scrambled face condition served as baseline condition in all DCMs). All posterior probabilities were greater than 95%. (show in white around the arrows)

Figure 5.8 Representative subject best fit model spectra

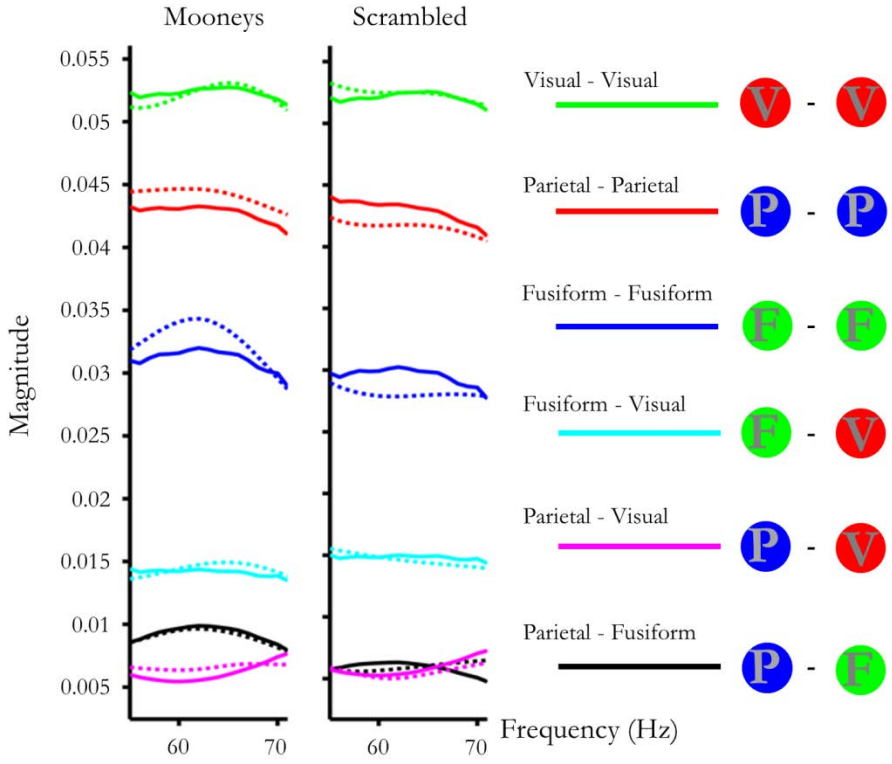

The auto- and cross-spectra for all cortical sources derived from the best fit model are shown for a representative participant. Solid lines represent predicted spectra from the best DCM model, whereas dashed lines show the real data.

5.6 Discussion

We observe increased gamma power for Mooney *vs.* scrambled faces in the right early visual, fusiform, and parietal cortices, in keeping with gamma power increases previously reported during perceptual completion in humans (Keil et al., 1999; Rodriguez et al., 1999; Tallon-Baudry and Bertrand, 1999; Trujillo et al., 2005; Grutzner et al., 2010). Increased gamma band activity occurs between 233 and 638 ms post-stimulus time, consistent with the latency of perceptual closure-related event-related potentials (Doniger et al., 2000, 2001; Sehatpour et al., 2006), and MEG gamma power modulations during perceptual closure of Mooney faces (Grutzner et al., 2010) and perception of complex objects (Gruber et al., 2008). Further, gamma band modulations by Mooney faces were

induced and not phase locked (see Methods 6.4.7. Sensor level statistical analysis section and Results 6.5.2. Sensor level results section) as has been reported before for holistic Gestalt perception (Tallon-Baudry et al., 1997; Jensen et al., 2001). In direct support of the anatomical and temporal precision of the effects we report, intracranial data from electrodes in occipital, fusiform and parietal sites during Mooney face perception Lachaux et al., 200%) overlap with the time interval and anatomical locations observed in the present study.

Critically, we demonstrate that Mooney face perception is associated with feedback coupling of gamma band oscillators from fusiform and parietal to early visual cortex. Importantly, our results indicate that the consistently reported gamma band activity during Mooney face perception (Grutzner et al., 2010; Lachaux et al., 2005; Rodriguez et al., 1999; Trujillo et all., 2005) reflects dynamic neuronal feedback interactions between higher and lower order visual cortices. Thus, our data unite previous findings of gamma power modulations and the concept of reverse hierarchical processing during perceptual completion (Bullier, 2001b; Hochstein and Ahissar, 2002; Altmann et al., 2003; Campana and Tallon-Baudry, 2013; Wokke et al., 2013). Feedback coupling downstream to early visual cortex as detected by our DCM analysis is in line with low level visual cortex activation at later latencies during perceptual completion after fusiform cortex engagement (Figure 5.8). Similar reactivation patterns in coherent percept formation for early visual cortex have been reported before (e.g., Jiang et al., 2008).

Gamma band activity is considered a fundamental activity mode for information processing not only for perception but also for higher cognitive functions such as attention and memory (Fries et al., 2007; Jensen et al., 2007). One proposal is that the amplitude of pyramidal cell excitation is re-coded as the time of occurrence of output spikes relative to the inhibitory gamma cycle, stronger inputs leading to earlier responses (Olufsen et al., 2003). Within this framework the gamma cycle is viewed as a temporal reference frame for sharing spike-phase coded information in neuronal networks (Fries et al., 2007; Singer and Gray, 1995). Thus, one interpretation of the top-down feedback coupling from fusiform and parietal to early visual cortex we observe is that neuronal populations in lower sensory cortex are tuned to temporal reference codes of neuronal activity patterns pertaining to face-selective and attention-relevant brain areas. The fusiform face area is a higher order brain region for processing facial stimulus features (Kanwisher et al., 1998; Caldara and

Seghier, 2009), whereas the parietal cortex is part of a cortical spatial attention network (Corbetta, 1998; Robertson, 2003; Slagter et al., 2007). Gamma frequency feedback coupling from these areas could be viewed as conveying global aspects of a Mooney face, such as facial features and spatial relationships between face parts, to local processing units in early visual cortex by sharing the temporal scheme of neuronal activity throughout a cortical network relevant for perceptual completion.- Such a mechanism would indeed parallel the classic Gestalt idea that local stimulus parts are processed as a function of global aspects of the stimulus (Wagemans et al., 2012b).

Further, coherent perception of Mooney faces depends on reciprocal forward and backward connectivity modulation of gamma activity between fusiform face area and parietal cortex. In view of the parietal role in spatial attention (Corbetta, 1998; Robertson, 2003; Slagter et al., 2007), we suggest that gamma frequency coupling between fusiform face area and parietal cortex reflects the detection and integration of facial spatial regularities (Caldara and Seghier, 2009) into a whole Gestalt.

Some limitations should be considered in interpreting our results. First, the precision of cortical source localisation is limited due to the inverse problem underlying any electromagnetic source modeling (Hau, 2004). However, our source data are consistent with localisation from fMRI (Dolan et al., 1997; Kanwisher et al., 1998; Kleinschmidt et al., 1998; Andres et al., 2002; Andres and Schluppeck, 2004; Sehatpour et al., 2006; McKeeff and Tong, 2007), EEG source localisation (Sehatpour et al., 2006) and intracranial recordings (Lachaux et al., 2005) in perceptual completion tasks. Furthermore, that Mooney face perception-induced gamma power modulations are restricted to the right hemisphere is consistent with evidence that face perception in humans is right lateralized (Hillger and Koenig, 1991; Rossion et al., 2000; Ramon and Rossion, 2012) as demonstrated by behavioral visual hemi-field (e.g. Heller and Levy, 1982; Parkin and Williamson, 1987), brain lesion (e.g. Sergent and Signoret, 1992b; Wada and Yamamoto, 2001) and functional brain imaging studies (e.g. Kanwisher et al., 1997; Rossion et al., 2012).

A second limitation with respect to the DCM connectivity analysis arises from the beamformer approach for cortical source localisation. Conventional beamformers have problems in separating correlated sources. However, simulation studies have shown that

the LCMV beamformer utilized in our study can separate sources that are correlated by 50-55% (Van Veen et al., 1997; Belardinelli et al., 2102). Therefore, the LCMV beamformer is a valid method for connectivity analysis. However, highly correlated sources (e.g. 100% correlation) cannot be co-localized by this method.

A third limitation is that Bayesian model selection indicates the probability of the data given a model from a model pool chosen a-priori based on plausible connectivity configurations, E.G. not all possible models are tested. However, we selected our model in line with reverse hierarchical processing in visual perception and its alternatives. Further, we specifically tested a null model that assumed no connectivity modulation between relevant brain areas as it has been argued that gamma band oscillations are better suited for local than for long-distance synchronization (Kopell et al., 2000). Our data are not consistent with this notion, as Bayesian model selection clearly identified the connectivity model without gamma band coupling between early visual, fusiform and parietal cortices as the least likely model given the data. Thus, our DCM results are in line with long distance gamma band synchronization previously reported in animal (Engel et al., 1991a, 1991b; Konig et al., 1995; von Stein et al., 2000; Saalmann et al., 2007) and humans (Rodriguez et al., 1999; Schoffelen et al., 2005, 2011; Siegel et al., 2008; Hipp et al., 2011).

We note a recent suggestion that feedforward and feedback cortical connectivity may not occur at the same frequencies due to asymmetric intrinsic properties of neurons in superficial and deeper cortical layers (Bastos et al., 2012). Specifically, feedforward connections originate predominately from superficial layers, which typically show neuronal synchronization predominantly in the gamma range, whereas feedback connections arise from deep layers, which prefer lower (alpha or eta) frequencies (Roopun et al., 2006, 2008; Maier et al., 2010; Buffalo et al., 2011). We acknowledge that the class of dynamic causal model employed here (based on cross-spectral density) is agnostic to layer-specific parameters. Although thus was the best DCM routine available at the time of analysis, we note that a novel routine within the SPM DCM framework, canonical microcircuits (CMC), has recently been implemented which specifically takes these parameters into account. Thus, although we show top-down coupling in the gamma range during perceptual completions, the CMC framework will enable the relative contributions of different frequency bands to feedforward vs. feedback coupling to be elucidated. However, in non-human primates performing a visual attention task, directed granger causal connectivity in

the gamma range has been also observed in the backward direction (V4 to V1), although the forward gamma coupling was stronger (Bosman et al., 2012)

Bayesian computational views of perception stress that purely forward architectures of the visual system are no sufficient for perception and that top-down feedback connections from higher order regions are necessary (Friston. 2003a). Reverse hierarchical processing in the visual system extends beyond perceptual completion. For example, movement perception is abolished when feedback from higher order area MT to primary visual cortex is disrupted by Transcranial magnetic stimulation (Pascual-Leone and Walsh, 2001; Silvanto et al., 2005; Koivisto et al., 2010). In fact, neuronal interactions between association and lower order sensory cortices are probably a prerequisite for conscious perception in general (Boly et al., 2011). Thus, or data link current views of distributed cortical gamma power activity I perceptual synthesis with the notion that top-down feedback from higher to lower order visual cortex is required for awareness of coherent visual percepts.

5.7 Summary

Replicating previous research, Mooney face trials elicited a gamma response like scrambled Mooney face trials albeit bigger and sustained for a longer time. Statistical comparison of the signal in the source space isolated three regions with higher gamma in the fusiform gyrus, visual and parietal cortices, that we identify as the network responsible for achieving and holding perceptual closure in our paradigm, as gamma band activity usually indexes long and short range connectivity. The functional connectivity of the network established with DCM revealed bidirectional flow of information between early visual cortex and parietal and fusiform nodes, supporting a global-to-local nature of perceptual completion and the existence of recursive and/or feedback processing routes within in contrast with pure feedforward models of visual processing.

6 General Discussion

The two leading cognitive processes of the current work were affective and visual processing. The main focus was addressing whether the so-called 'Low Road' (the pulvino-amygdalar projections that bypass cortical visual processing) subserves rapid detection of threat related cues; an additional interest was defining the mechanism behind perceptual closure and object representation. Both interests reflect evaluative processes that occur at different stages of visual processing. Emotionally driven modulations at the amygdala as a consequence of the subcortical pathway would be achieved arguably faster than object recognition would via classic (hierarchical and feed-forward) cortical visual pathways (or 'High Road'). Integration of the stimulus features ('biding') and maintenance of a mental representation ('percept') would lie on the other end of the visual stream. As such, we are interested on one side in a seemingly automatic process taking place at a dedicated modular circuit probably favored by evolution (composed by the certain nuclei of the thalamus and the amygdala) and a high-level human-characteristic process probably requiring the synchronous collaboration of several areas at the end of the 'visual road' on the other. Shedding light on both issues will hopefully improve our understanding of how our brains recognize the visual scene at different stages of processing. We think we were able to achieve that goal up to some degree but among some remarks, we feel that exploring affective modulation of perceptual closure processes is the most relevant thing that our work lacks, although we would like to note the amount of work required to answering the questions risen in the objectives (specifically the difficulty of acquiring intracranial data for Experiment 1) and we sincerely hope it will be possible to perform future works like that to extend and complete this line of research

With medially implanted stereotactic electrodes we were able to record the activity of ten amygdalae and seven sites along the fusiform gyrus from several epileptic patients in Experiment 1. The main tasks employed were a gender judgment task with pictures of 135 different actors distributed without repetitions across nine different combinations of facial expression (fearful, happy and neutral) and spatial frequencies (broadband or naturalistic, high spatial frequency and low spatial frequency) and an indoor/outdoor judgment task with neutral and extremely negative pictures portraying more complex scenes. In Experiment 2 we repeated the former tasks to healthy subjects while acquiring MEG data. As we were interested in timing of fast processes we studied the recorded signals (LFPs/ERMFs) on the temporal domain. Finally, in Experiment 3 we performed a face-non face discrimination task employing ambiguous intact and scrambled Mooney faces and acquiring data with MEG from healthy subjects like in Experiment 2; though in this case, as we were interested on the collaborative work of different areas responsible for perceptual closure we explored the frequency domain of the magnetic signal because gamma band is related with integrative and long-range connectivity with different neural sources.

6.1 Summary

The fast (~70 ms) response in the amygdala to fearful faces (and not complex pictures) dependent on the presence in the scene of low spatial frequency components is the main novel finding reported in this work. Accordingly with previous studies, we also report later modulations (~200-300 ms) of the amygdalar response (independent of spatial frequencies) to emotional facial expressions and highly arousing negative pictures. Furthermore, we identified the earliest emotional modulation to fearful faces in the fusiform gyrus taking place after the early amygdala response (~170 ms).

In addition, we do report a similarly fast (~80 ms) interaction -fear dependent activation specific to LSF frequencies- going on at central sites of the scalp with magnetoencephalographic data. Source reconstruction analysis revealed higher activity at

the cuneus and parietal cortices for the LSF fearful faces as compared (linearly) with BSF and HSF fearful faces.

We report no main effects of emotion or an interaction in Experiment 1 and 2 reaction times (there was however an effect of emotion in Experiment 2 accuracy ratings given that fearful faces elicited significantly more errors). We report a main effect of frequency in both experiments –smaller reaction times for BSF faces- although in Experiment 2 HSF faces required longer reaction times and induced more errors than LSF faces too, in contrast with Experiment 1 reaction times were we found no differences between HSF and LSF faces. This concurred with an equally linear main effect of frequency on the M170. M170 was recorded 40 to 30 ms earlier for BSF and LSF than HSF faces (independent of emotion).

We report main effects of frequency in the amplitude of the M170 (bigger amplitudes for HSF faces in general) and also emotional effects (bigger amplitudes for fearful faces), in agreement with part of the literature. More novel is the fact that only fearful faces with HSF frequencies (BSF and HSF faces) provoked enhanced M170 amplitudes. We report no modulations of the M170 amplitudes due to facial expression. Activity within the M170 time window was localized to fusiform gyrus, temporal pole, and lateorooccipital, parietal and occipital (lingual) cortex. Statistics in the source space did not classify any neural source were these interactive effects could be taking place.

We include a traditional analysis of the first's steps of face visual processing: before the M170 three components were identified occurring at ~60 ms,-~90ms and ~120ms. We report a big main effect of frequency at around 120 ms. No other latency or amplitude tests at each of these components showed significant differences. In the source space, we report initial sources in striate early visual areas, followed by later activation of ventrotemporal (posterior fusiform) and lateorooccipital cortex similar to the M170 sources. This is followed (prior to the M170) by reactivation of occipital cortices in the case of BSF and LSF faces and sustained activity broadly sparse across ventral and occipital cortex in the case of HSF faces.

Motivated by the eRMF showing two overlapping topographies between 150 and 220 ms that were contemporaneous in the case of BSF and LSF faces but consecutive in

the case of HSF faces we report a decomposition of the M170 into two different components: an earlier occipital activation on one side (M170A) and a more sustained in time temporal magnetic response (M107B). We found that the latency differences affected only the second component, source localized to the fusiform gyrus and lateroоccipital complex and cuasi homologous to the previously reported M170. On the other side, no amplitude or latency differences were significant between LSF and HSF faces in the earliest of the two components.

In concordance with some previous research, we report in Experiment 3 and index of perceptual closure corresponding to an increment on the gamma band response with respect to the baseline around 200-400 ms that is longer sustained for Mooney versus scrambled Mooney faces. As a novelty, we performed source reconstruction and report three neural sources responsible of sustaining the mental representation: fusiform gyrus, visual and parietal cortices. Furthermore, from dynamic causal modelling of the different relationships (in terms of inputs and outputs) between those three areas we conclude that the most feasible model accounting for the observed variations would be one such that communication between low-level visual source and hierarchically higher fusiform and parietal sources is bidirectional. This functional connectivity approach is the novel contribution to the secondary objective of this work – as stated briefly in the introduction to this section.

6.2 General discussion

We have addressed two current controversies about visual processing pathways; whether subcortical routes are functional for discriminating biologically relevant stimuli in the scene before the contribution of projections from cortical structures and whether purely feedforward processing through the cortical route is enough to elaborate a neural representation of the perceived object or recursive and feedback connections are required.

We uniquely demonstrated functional capacity of the Low Road to trigger fast emotional responses in the amygdala by recording intracranial activity to negative, positive

and neutral facial expressions. This finding gives support to the hypothesis (Ledoux, 1999) that thalamus and amygdala, via magnocellullar fibers from the pulvinar nucleus of the superior colliculus from the former to the later constitute an automatic, rapid, neural circuit for detection of alert signals. We are able to make inferences about the mechanism of such circuit because our crucial spatial frequency experimental manipulation; that allowed us to contrast amygdalar responses with and without meaningful low spatial frequency information of the scene – assuming that mainly only LSF frequencies are carried through the subcortical route (Schiller, Malpeli and Schein, 1979; Berson, 1988; Vuilleumier, 2003; Carretié et al., 2007; Inagaki and Fujita, 2011). However, it remains possible that information processing through the cortical route is able to detect threat related signals in the scene as fast as this system (Pessoa and Adolphs, 2010). To address that matter, we synchronously recorded intracranial activity from the visual cortex, more specifically along the fusiform gyrus. The primate amygdala receives extensive input from uni- and multi-modal areas of the temporal lobe (Aggleton et al.. 1980; Amaral and Insausti, 1992; Stefanacci and Amaral, 2000) but there is no evidence of amygdala afferences from the occipital lobe (Aggleton et al., 1980; Stefanacci and Amaral, 2000).

We show that within our paradigm the first emotional modulation of the intracranial activity in the fusiform arises much later, at around 170 ms. A difference highly suggestive of a bottom-up amygdala response originating via a more direct subcortical magnocellular route. An alternative explanation is that the fast amygdala response is driven by inputs from emotion-sensitive ventral or orbitofrontal cortex, which also receives magnocellular input (Barbas, 2000). However, the 70 ms latency response observed here is considerably faster than increased neuronal firing rates previously reported (Kawasaki et al., 2001) in human ventral prefrontal cortex to emotional scenes (120-160 ms latency), and also faster than the late latency (~500 ms) responses to fearful faces observed in human orbitofrontal cortex (Krolak-Salmon et al., 2004). We are therefore confident that the early response reflects local processing of low spatial frequency components of fearful faces by amygdala neurons. By contrast, the late latency main effect of emotion in the amygdala (between 350-396 ms) is consistent with information that has been processed via visual cortex. In support of this interpretation, this later response is also evoked by HSF fearful faces, which also modulated fusiform cortex, indicating engagement of slower parvocellular pathways along visual cortical areas (Merigan and Maunsell, 1993; Livingstone and Hubel, 1988).

We cannot rule out the possibility of earlier emotional responses at lower level visual cortices, but such areas do not project to the amygdala but do so further forward (i.e.: to the fusiform) in the hierarchical high road visual scheme. Nonetheless, emotional responses in visual cortex had been reported as early as 100 ms (Schupp et al., 2003; Stolarova, Keil and Moratti, 2006; Schacht, Sommer, 2009; Bayer, Sommer and Schacht, 2012) in the electrophysiological literature. The mechanisms behind these early cortical effects are still unknown. We report indeed enhanced activity at ~82 ms in central regions of the scalp probably corresponding to the cuneus and parietal cortex, consistent with magnocellullar projections to this areas coming from the amygdala (Stepniewska and Kaas, 1999; Lyon et al, 2010) or other areas (Bar, 2003) like early visual cortex (Kveraga et al., 2007).

Another concern that may arise is why previous studies had not report such a fast response in the amygdala. We think that the employment of faces, as opposed to other studies employing complex pictures (Oya et. al., 2002; Brazdil et. al., 2009) was crucial in our design, given their important motivational and communicative value among primates (Dimberg and Öhman, 1996). Three previous studies employing faces found responses around 130 ms (Pourtois et al., 2010; Sato et al., 2011) and 200 ms (Krolak-Salmon, 2004). However, they presented a limited number of identities repeatedly, which may have resulted in rapid habituation of a fast response.

Note, however, that in the present study, we report also late emotional responses between 110-150 ms and later than 200 ms that overlap with reports in the mentioned works were irrespectively of frequency, responses to fearful faces were significantly higher. Furthermore, a later main effect of frequency showed a significant difference between BSF and LSF faces that was not present between BSF and HSF faces. Thus, unlike early amygdala responses to fear driven by LSF, the later response appeared more sensitive to HSF inputs.

The replica of Experiment 1a: faces with MEG recordings in Experiment 2 did not go completely as expected. We found that HSF stimuli, irrespectively of emotion, were answered slower, with more errors. They elicited a relatively big occipital peak of activity at ~120ms and the latency of the posterior components like the M170 is shifted. It seems probable that the former peak corresponds to an enhanced P1 visual evoked component,

because it is modulated by low stimulus features like energy. Energy is the sum of the square of the pixels. Because of their nature, HSF pictures have inherently more energy than their BSF or LSF counterparts. Other studies had created masks or superimposed stimuli of different frequency categories to avoid possible signal deviations due to this issue. We did not do so; however we made sure there were no energy differences between emotions at each frequency level. Importantly, main frequency effects did not start before the early interaction time window of the Experiment 1 (~70 ms) or the early effects found in Experiment 2 (~80 ms). This lets us drive conclusions about brain behavior before ~100 ms but we are afraid of extrapolating any other major assumptions about later stages from Experiment 2

Conciliating the Low Road hypothesis with other standard visual processing models, author Pessoa and Adolphs (Pessoa and Adolphs, 2010) had elaborated a theoretical model named multiple wave's hypothesis. This model, assuming that cortical processing can occur really fast and accounting for the aforementioned early emotional modulations that had been observed, stated that visual processing develops through more than one route at the same time, and the information reaches high level structures from many places recursively. As theoretical framework it does not exclude the possibility that thalamoamygdalar projections constitute an early threat detector system, part of the global visual processing mechanism concomitantly with other visual subsystems.

We believe that real life perception is generated by the work of the brain as whole rather than single structures. Also, visual processing occurs so fast at both subcortical and cortical levels that this disentanglement is not experienced by the individuals in a quotidian basis. The activity of most of the structures is so intermingled via shortcuts and long-range projections that the conjunctive perceptual elaboration is not so expensive in term of cognitive resources and is able to elicit the most adequate response. However, it is undeniable that from a Darwinist point of view, a fast detection circuit that would alert the system of relevant stimuli enhancing overall processing poses an evolutionary advantage and has most probably evolved in humans. Our data provides novel support for a "low road circuit" for fear detection in human amygdala. This pathway, and its functional properties, may also constitute an important neural substrate for models of non-conscious processing in anxiety disorders (Rauch et al., 2000; Öhman and Mineka, 2001; Etkin et al.,

2004) and the generalization of fear responses to coarsely defined cues in pathological conditions (Sheline et al., 2001; Anderson et al., 2003).

We would feel satisfied if this work serves at least to put into question some of the established assumptions regarding visual processing. Connecting with the conception of the visual system as a multimodular process we demonstrate in Experiment 3 that the orchestrated participation of several distant areas (fusiform, visual and parietal cortices) is required to elaborate a representation -perceptual completion- of the objects in the visual scene. We are able to extract such conclusion because we analyzed the changes in gamma power relative to the baseline. Gamma band is associated with long range connections (Tallon-Baudry and Bertrand, 1999; Fries et al., 2007, Gruber et al., 2008). We specifically measured the coherence of activity between the three areas responsible for maintaining the mental representation by employing a very novel algorithm (DCM; Friston, Harrison and Penny, 2003b) that uniquely showed us that feedback projections from high-l to low-level areas form part of the visual system. Just like our main finding, this secondary report puts into question another standard assumption of visual processing models, this is: that visual perception is achieved in a hierarchical fashion, as a feedforward bottom-up push that goes from early sensory areas to high level multimodal structures. Rather, the integrated participation of both types of structures and additional top-down communications fit best the models derived from our data. It is very important to broad our comprehension of the visual system as a one-direction ladder that grows not only as two separate highways (the low and the high roads, corresponding to the cortical and the subcortical pathways) but more like two mixed highways with several shortcuts, bypasses and U-turns.

7 References

Adolphs, R., Tranel, D., Damasio, H., Damasio, A., 1994. Impaired recognition of emotion in facial expressions following bilateral damage to the human amygdala. *Nature* 372, 669-672.

Adolphs, R., Cahill, L., Schul, R., Babinsky, R., 1997. Impaired declarative memory for emotional material following bilateral amygdala damage in humans. *Learning & Memory* 4, 291–300.

Adolphs, R., Tranel, D., Damasio, A. R., 1998. The human amygdala in social judgment. *Nature* 393, 470-474.

Adolphs, R., Tranel, D., Hamann, S., Young, A. W., Calder, A.J., Phelps, E. A., Anderson, A., Lee, G. P., Damasio, A. R., 1999. Recognition of facial emotion in nine individuals with bilateral amygdala damage. *Neuropsychologia* 37, 1111-1117.

Adolphs, R., Baron-Cohen, S., Tranel, D., 2002. Impaired recognition of human social emotions following amygdala damage. *Journal of Cognitive Neuroscience* 14, 1-11.

Adolphs, R., Tranel, D., 2003 Amygdala damage impairs emotion recognition from scenes only when they contain facial expressions. *Neuropsychologia* 41, 1281-1289.

Adolphs, R., Gosselin, F., Buchanan, T. W., Tranel, D., Schyns, P., Damasio, A. R., 2005. A mechanism for impaired fear recognition after amygdala damage. *Nature* 433, 68-72.

Adolphs, R., Spezio, M., 2006. Role of the amygdala in processing visual social stimuli. *Progress in Brain Research* 156, 363-378.

Adolphs, R., 2008. Fear, faces and the human amygdala. *Current Opinion in Neurobiology* 18, 166–172.

Aggleton, J. P., 1986. A description of the amygdalo-hippocampal interconnections in the macaque monkey. *Experimental brain research* 64, 515-526.

Aggleton, J., Burton, M., Passingham, R., 1980. Cortical and subcortical afferents to the amygdala of the rhesus monkey (Macaca mulatta). *Brain Research* 190, 347-368.

Alheid, G. F., 2003. Extended amygdala and basal forebrain. *Annals of the New York Academy of Sciences* 985, 185-205.

Allison, T., Ginter, H., McCarthy, G., Nobre, A. C., Puce, A., Luby, M., Spencer, D. D., 1994. Face recognition in human extrastriate cortex. *Journal of Neurophysiology* 71, 821-825

Allison, T., Puce, A., Spencer, D. D., McCarthy, G., 1999. Electrophysiological studies of human face perception. I: Potentials generated in occipitotemporal cortex by face and non-face stimuli. *Cerebral Cortex* 9, 415-430.

Altmann, C. F., Bulthoff, H. H., Kourtzi, Z., 2003. Perceptual organization of local elements into global shapes in the human visual cortex. *Current Biology* 13, 342–349.

Amaral, D. G., Insausti, R., 1992. Retrograde transport of D-[3H]-aspartate injected into the monkey amygdaloid complex. *Experimental Brain Research* 88, 375-388.

Amaral, D. G., Behniea, H., Kelly, J. L., 2003. Topographic organization of projections from the amygdala to the visual cortex in the macaque monkey. *Neuroscience 118*, 1099-1120.

Anderson, A. K., Phelps, E. A., 2001. Lesions of the human amygdala impair enhanced perception of emotionally salient events. *Nature* 411, 305-309.

Anderson, A. K., Christoff, K., Panitz, D., De Rosa, E., and Gabrieli, J. D. E., 2003. Neural correlates of the automatic processing of threat facial signals. *The Journal of Neuroscience* 23, 5627-5633.

Andrews, T.J., Schluppeck, D., Homfray, D., Matthews, P., Blakemore, C., 2002. Activity in the fusiform gyrus predicts conscious perception of Rubin's vase-face illusion. *Neuroimage* 17, 890–901.

Andrews, T.J., Schluppeck, D., 2004. Neural responses to Mooney images reveal a modular representation of faces in human visual cortex. *Neuroimage* 21, 91-98.

Ashley, V., Vuilleumier, P., Swick, D., 2004. Time course and specificity of event-related potentials to emotional expressions. *Neuroreport* 15, 211-216.

Atkinson, A. P., Adolphs, R., 2011. The neuropsychology of face perception: beyond simple dissociations and functional selectivity. *Philosophical Transactions of the Royal Society of London Series B: Biological Sciences* 366, 1726-1738.

Attal, Y., Bhattacharjee, M., Yelnik, J., Cottereau, B., Lefevre, J., Okada, Y., Bardinet, E., Chupin, M., Baillet, S., 2007. Modeling and detecting deep brain activity with MEG & EEG. In *Engineering in Medicine and Biology Society*. EMBS 2007. 29th Annual International Conference of the IEEE, pp. 4937-4940.

Bar, M., Tootell, R. B., Schacter, D. L., Greve, D. N., Fischl, B., Mendola, J. D., Rosen, B. D., Dale, A. M., 2001. Cortical mechanisms specific to explicit visual object recognition. *Neuron* 29, 529-535.

Bar, M., 2003. A cortical mechanism for triggering top-down facilitation in visual object recognition. *Journal of Cognitive Neuroscience* 15, 600-609.

Bar, M., Kassam, K. S., Ghuman, A. S., Boshyan, J., Schmid, A. M., Dale, A. M., Hämäläinen M.S., Halgren, E., 2006. Top-down facilitation of visual recognition. *Proceedings of the National Academy of Sciences of the United States of America*, 103, 449-454.

Barbas, H., 2000. Connections underlying the synthesis of cognition, memory, and emotion in primate prefrontal cortices. *Brain Research Bulletin*. 52, 319-330.

Bard, P., 1928. A diencephalic mechanism for the expression of rage with special reference to the central nervous system. *American Journal of Physiology* 84, 490-513.

Bastos, A. M., Usrey, W. M., Adams, R. A., Mangun, G. R., Fries, P., Friston, K. J., 2012. Canonical microcircuits for predictive coding. *Neuron* 76, 695–711.

Batty, M., Taylor, M. J., 2003. Early processing of the six basic facial emotional expressions. *Cognitive Brain Research* 17, 613-620.

Bayer, M., Sommer, W., Schacht, A., 2012. P1 and beyond: functional separation of multiple emotion effects in word recognition. *Psychophysiology* 49, 959-969.

Bayle, D. J., Henaff, M. A., Krolak-Salmon, P., 2009. Unconsciously perceived fear in peripheral vision alerts the limbic system: a MEG study. *PLoS One* 4, e8207.

Belardinelli, P., Ortiz, E., Braun, C., 2012. Source activity correlation effects on LCMV beamformers in a realistic measurement environment. *Computational and Mathematical Methods in Medicine* 2012, 190513.

Bentin, S., Allison, T., Puce, A., Perez, E., McCarthy, G.J., 1996. Electrophysiological Studies of Face Perception in Humans. *Cognitive Neuroscience* 8, 551-565.

Bentin, S., Deouell, L. Y., Soroker, N., 1999. Selective visual streaming in face recognition: Evidence from developmental prosopagnosia. *Neuroreport* 10, 823-827.

Bentin, S., Golland, Y., Flevaris, A., Robertson, L.C., Moscovitch, M., 2006. Processing the trees and the forest during initial stages of face perception: Electrophysiological evidence. *Journal of Cognitive Neuroscience* 18, 1406-1421.

Berman, R. A., Wurtz, R. H., 2008. Exploring the pulvinar path to visual cortex. Progress in *Brain Research* 171, 467–473.

Berson, D. M., 1988. Retinal and cortical inputs to cat superior colliculus: composition, convergence and laminar specificity. *Progress in Brain Research* 75, 17-26.

Blair, H. T., 2001. Synaptic Plasticity in the Lateral Amygdala: A Cellular Hypothesis of Fear Conditioning. *Learning & Memory* 8, 229-242

Blau, V. C., Maurer, U., Tottenham, N., McCandliss, B.D., 2007. The face-specific N170 component is modulated by emotional facial expression. *Behavioral and Brain Functions* 3, 1-13.

Boly, M., Garrido, M. I., Gosseries, O., Bruno, M. A., Boveroux, P., Schnakers, C., Massimini, M., Litvak, V., Laureys, S., Friston, K., 2011. Preserved feedforward but impaired top down processes in the vegetative state. *Science* 332, 858–862.

Bosman, C. A., Schoffelen, J. M., Brunet, N., Oostenveld, R., Bastos, A. M., Womelsdorf, T., Rubehn, B., Stieglitz, T., De Weerd, P., Fries, P., 2012. Attentional stimulus selection through selective synchronization between monkey visual areas. *Neuron* 75, 875–888.

Bötzel, K., Schulze, S., Stodieck, S.R., 1995. Scalp topography and analysis of intracranial sources of face-evoked potentials. *Experimental Brain Research* 104, 135-143.

Brázdil, M., Roman, R., Urbánek, T., Chládek, J., Špok, D., Mareček, R., Rektor, I., 2009. Neural correlates of affective picture processing--a depth ERP study. *NeuroImage* 47, 376-383.

Breiter, H. C., Etcoff, N. L., Whalen, P. J., Kennedy, W. A., Rauch, S. L., Buckner, R. L., Strauss, M. M., Hyman, S. E., Rosen, B. R., 1996. Response and habituation of the human amygdala during visual processing of facial expression. *Neuron* 17, 875-887.

Bruce, V., Young, A., 1986. Understanding face recognition. British Journal of Psychology 77, 305-327.

Buffalo, E.A., Fries, P., Landman, R., Buschman, T. J., Desimone, R., 2011. Laminar differences in gamma and alpha coherence in the ventral stream. Proceedings of *the National Academy of Sciences U. S. A.* 108, 11262–11267.

Bukach, C. M., Gauthier, I., Tarr, M. J., 2006. Beyond faces and modularity: the power of an expertise framework. *Trends in cognitive sciences* 10, 159-166.

Bullier, J,, Kennedy, H., 1983. Projection of the lateral geniculate nucleus onto cortical area V2 in the macaque monkey. *Experimental Brain Research* 53, 168-172.

Bullier, J., Hupé, J. M., James, A. C., Girard, P., 2001a. The role of feedback connections in shaping the responses of visual cortical neurons. *Progress in Brain Research*, 134, 193-204.

Bullier, J., 2001b. Integrated model of visual processing. *Brain Research Reviews* 36, 96-107.

Bzdok, D., Langner, R., Caspers, S., Kurth, F., Habel, U., Zilles, K., Laird, A., Eickhoff, S. B., 2010. ALE meta-analysis on facial judgments of trustworthiness and attractiveness. *Brain Structure and Function* 215, 209-223.

Cacioppo, J. T., Gardner, W. L., 1999a. "Emotion". *Annual Review of Psychology* 50, 191-214.

Cacioppo, J. T., Berntson, G. G., 1999b. The affect system architecture and operating characteristics. *Current Directions in Psychological Science* 8, 133-137.

Caharel, S., Courtay, N., Bernard, C., Lalonde, R., Rebaï, M., 2005. Familiarity and emotional expression influence an early stage of face processing: an electrophysiological study. *Brain and Cognition* 59, 96-100.

Cahill, L., Babinsky, R., Markowitsch, H. J., McGaugh, J. L., 1995. The amygdala and emotional memory. *Nature* 377. 295-296

Cahill L., Haier, R. J., Fallon, J., Alkire, M. T., Tang, C., Keator, D., Wu, J., Mcgaugh, J. L., 1996. Amygdala activity at encoding correlated with long-term, free recall of emotional information. *Proceedings of the National Academy of Sciences*, 93, 8016-8021.

Caldara, R., Seghier, M. L., 2009. The fusiform face area responds automatically to statistical regularities optimal for face categorization. *Human Brain Mapping* 30, 1615–1625.

Callaway, E., Halliday, R., 1982. The effect of attentional effort on visual evoked potential N1 latency. *Psychiatry Research* 7, 299-308.

Campana, F., Tallon-Baudry, C., 2013. Anchoring visual subjective experience in a neural model: the coarse vividness hypothesis. *Neuropsychologia* 51, 1050–1060.

Cannon, W., 1932. Wisdom of the Body. *W.W. Norton & Company*, United States.

Capilla, A., Schoffelen, J. M., Paterson, G., Thut, G., Gross, J., 2012. Dissociated alpha-band modulations in the dorsal and ventral visual pathways in visuospatial attention and perception. *Cerebral Cortex* 24, 550-561

Carlson, N. R., 2012. Physiology of Behavior. *Pearson.*

Carmel, D., Bentin, S., 2002. Domain specificity versus expertise: factors influencing distinct processing of faces. *Cognition* 83, 1-29.

Carretié, L., Mercado, F., Tapia, M., Hinojosa, J. A., 2001. Emotion, attention, and the 'negativity bias', studied through event-related potentials. *International journal of Psychophysiology* 41, 75-85.

Carretié, L., Hinojosa, J. A., López-Martín, S., Tapia, M., 2007. An electrophysiological study on the interaction between emotional content and spatial frequency of visual stimuli. *Neuropsychologia* 45, 1187-1195.

Cauchoix, M., Crouzet, S. M., 2013. How plausible is a subcortical account of rapid visual recognition? *Frontiers in Human Neuroscience* 7.

Cheung, O. S., Richler, J. J., Palmeri, T. J., Gauthier, I., 2008. Revisiting the role of spatial frequencies in the holistic processing of faces. *Journal of Experimental Psychology: Human Perception and Performance 3*4, 1327.

Chomsung, R. D., Wei, H., Day-Brown, J. D., Petry, H. M., and Bickford, M. E., 2010. Synaptic organization of connections between the temporal cortex and pulvinar nucleus of the tree shrew. *Cerebral Cortex* 20, 997–1011.

Clark, V. P., Fan, S., Hillyard, S. A., 1995. Identification of early visual evoked potential generators by retinotopic and topographic analyses. *Human Brain Mapping* 2, 170-187.

Cobb, W. A., Dawson, G. D., 1960. The latency and form in man of the occipital potentials evoked by bright flashes. *Journal of Physiology* 152, 108-121

Cohen, L., Dehaene, S., 2004. Specialization within the ventral stream: the case for the visual word form area. *Neuroimage* 22, 466-476.

Cohen, J. D., 2005. The vulcanization of the human brain: A neural perspective on interactions between cognition and emotion. *Journal of Economic Perspectives* 3-24.

Collins, D. L., Zijdenbos, A. P., Kollokian, V., Sled, J. G., Kabani, N. J., Holmes, C. J., Evans, A. C., 1998. Design and construction of a realistic digital brain phantom. *IEEE Transactions on Medical Imaging* 17, 463–468.

Cook, M., Mineka, S., 1989. Observational conditioning of fear to fear-relevant versus fear-irrelevant stimuli in rhesus monkeys. *Journal of abnormal psychology*, 98, 448.

Corbetta, M., 1998. Frontoparietal cortical networks for directing attention and the eye to visual locations: identical, independent, or overlapping neural systems? *Proceedings of the National Academy of Sciences U.S.A.* 95, 831–838.

Corbetta, M., Akbudak, E., Conturo, T. E., Snyder, A. Z., Ollinger, J. M., Drury, H. A., Linenweber, M. R., Petersen, S. E., Raichle, M. E., Van Essen, D. C., Shulman, G. L., 1998. A common network of functional areas for attention and eye movements. *Neuron* 21, 761–773.

Cowey, A., 2010. The blindsight saga. Exp. Brain Res. 200, 3–24.

Critchley, H., Daly, E., Phillips, M., Brammer, M., Bullmore, E., Williams, S., Van Amelsvoort, T., Robertson, D., David, A., Murphy, D., 2000. Explicit and implicit neural mechanisms for processing of social information from facial expressions: a functional magnetic resonance imaging study. *Human brain mapping* 9, 93-105.

Curran, T., Tanaka, J. W., Weiskopf, D. M., 2002. An electrophysiological comparison of visual categorization and recognition memory. *Cognitive, Affective, & Behavioral Neuroscience* 2, 1-18.

Damasio, A. R., Damasio, H., Van Hoesen, G. W., 1982. Prosopagnosia Anatomic basis and behavioral mechanisms. *Neurology* 32, 331-331.

Darwin, C., 1872. The expression of the emotions In man and animals. *John Murray*, Great Britain.

Darwin, C., 2002. The expression of the emotions in man and animals. *Oxford University Press*, New York.

Davis, M., Whalen, P. J., 2001. The amygdala: vigilance and emotion. *Molecular Psychiatry* 6, 13-34.

Day-Brown, J. D., Wei, H., Chomsung, R. D., Petry, H. M., Bickford, M. E., 2010. Pulvinar projections to the striatum and amygdala in the tree shrew. *Frontiers in Neuroanatomy* 4, 143.

Debiec, J., LeDoux, J. E., 2006. Noradrenergic signaling in the amygdala contributes to the reconsolidation of fear memory: treatment implications for PTSD. *Annals of the New York Academy of Sciences* 1071, 521-524.

Deffke, I., Sander, T., Heidenreich, J., Sommer, W., Curio, G., Trahms, L., Lueschow, A., 2007. MEG/EEG sources of the 170-ms response to faces are co-localized in the fusiform gyrus. *Neuroimage* 35, 1495-1501.

Dering, B., Martin, C. D., Thierry, G., 2009. Is the N170 peak of visual event-related brain potentials car-selective? *Neuroreport* 20, 902-906.

Desimone, R, Duncan, J., 1995. Neural mechanisms of selective visual attention. *Annual Review of Neuroscience* 18, 193-222.

Di Russo, F., Martínez, A., Sereno, M. I., Pitzalis, S., Hillyard, S. A., 2002. Cortical sources of the early components of the visual evoked potential. *Human Brain Mapping* 15, 95-111.

Di Russo, F., Martinez, A., Hillyard, S. A., 2003. Source analysis of event-related cortical activity during visuo-spatial attention. *Cerebral Cortex* 13, 486-499

Dimberg, U., Öhman, A., 1996. Behold the wrath: Psychophysiological responses to facial stimuli. *Motivation and Emotion* 20, 149-182.

Dolan, R. J., Fink, G. R., Rolls, E., Booth, M., Holmes, A., Frackowiak, R. S., Friston, K. J., 1997. How the brain learns to see objects and faces in an impoverished context. *Nature* 389, 596-599.

Dolan, R.J., Vuilleumier, P., 2003. Amygdala automaticity in emotional processing. *Annals of the New York Academy of Sciences* 985, 348-355.

Dolcos, F., LaBar, K. S., Cabeza, R., 2004. Interaction between the amygdala and the medial temporal lobe memory system predicts better memory for emotional events. *Neuron* 42, 855-863.

Doniger, G. M., Foxe, J. J., Murray, M. M., Higgins, B. A., Snodgrass, J. G., Schroeder, C. E., Javitt, D. C., 2000. Activation time course of ventral visual stream object-recognition areas: high density electrical mapping of perceptual closure processes. *Journal of Cognitive Neuroscience* 12, 615-621.

Doniger, G. M., Foxe, J. J., Schroeder, C. E., Murray, M. M., Higgins, B. A., Javitt, D. C., 2001. Visual perceptual learning in human object recognition areas: a repetition priming study using high-density electrical mapping. *Neuroimage* 13, 305–313.

Dumas, T., Attal, Y., Chupin, M., Jouvent, R., Dubal, S., George, N., 2010. MEG study of amygdala responses during the perception of emotional faces and gaze. In 17th *International Conference on Biomagnetism Advances in Biomagnetism*. Berlin, Biomag 2010, pp. 330-333.

Ebner, N. C., Riediger, M., Lindenberger, U., 2010. FACES - A database of facial expressions in young, middle-aged, and older women and men: Development and validation. *Behavior Research Methods* 42, 351-362.

Eimer, M., 2000. Effects of face inversion on the structural encoding and recognition of faces: Evidence from event-related brain potentials. *Cognitive Brain Research* 10, 145-158.

Eimer, M., Holmes, A., McGlone, F. P., 2003. The role of spatial attention in the processing of facial expression: an ERP study of rapid brain responses to six basic emotions. *Cognitive, Affective, & Behavioral Neuroscience* 3, 97-110.

Eimer, M., 2011. The face-sensitivity of the n170 component. *Frontiers in Human Neuroscience* 5.

Eimer, M., Gosling, A., Nicholas, S., Kiss, M., 2011. The N170 component and its links to configural face processing: a rapid neural adaptation study. *Brain Research* 1376, 76-87.

Ekman, P., Friesen, W. V., 1971. Constants across cultures in the face and emotion. *Journal of Personality and Social Psychology* 17, 124-129.

Ekman. P., Friesen, W. V., 1976. Pictures of facial affect. Palo Alto, CA: *Consulting Psychologists Press.*

Ekman, P., 1992. An argument for basic emotions. *Cognition and Emotion* 6, 169-200.

Ekman, P. E., Davidson, R. J., 1994. The nature of emotion: Fundamental questions. *Oxford University Press*, New York

Ekman, P., 2006. Darwin and facial expression: A century of research in review. *Malor books*, California.

Engel, A. K., Konig, P., Kreiter, A. K., Singer, W., 1991a. Interhemispheric synchronization of oscillatory neuronal responses in cat visual cortex. *Science* 252, 1177–1179.

Engel, A.K., Kreiter, A.K., Konig, P., Singer, W., 1991b. Synchronization of oscillatory neuronal responses between striate and extrastriate visual cortical areas of the cat. *Proceedings of the National Academy of Sciences U.S.A.* 88, 6048–6052.

Engel, S. A., Glover, G. H., Wandell, B. A., 1997. Retinotopic organization in human visual cortex and the spatial precision of functional MRI. *Cerebral cortex* 7, 181-192.

Engel, A. K., Fries, P., Singer, W., 2001. Dynamic predictions: oscillations and synchrony in top-down processing. *Nature Reviews Neuroscience* 2, 704–716.

Ernst, M. O., Bülthoff, H. H., 2004. Merging the senses into a robust percept. *Trends in cognitive sciences*, 8, 162-169.

Farah, M.J., McMullen, P.A., Meyer, M.M., 1991. Can recognition of living things be selectively impaired? *Neuropsychologia* 29, 185-193.

Farroni, T., Menon, E., Rigato, S., Johnson, M. H., 2007. The perception of facial expressions in newborns. *European Journal of Developmental Psychology* 4, 2-13.

Feinberg, T. E., Schindler, R. J., Ochoa, E., Kwan, P. C., Farah, M. J., 1994. Associative visual agnosia and alexia without prosopagnosia. *Cortex* 30, 395-411.

Feinstein, J. S., Adolphs, R., Damasio, A., Tranel, D., 2011. The human amygdala and the induction and experience of fear. *Current Biology* 21, 34-38.

Felleman, D. J., Xiao, Y., McClendon, E., 1997. Modular organization of occipito-temporal pathways: cortical connections between visual area 4 and visual area 2 and posterior inferotemporal ventral area in macaque monkeys. *The Journal of Neuroscience* 17, 3185-3200.

Fernández-Duque, D., Posner, M.I., 2001. Brain imaging of attentional networks in normal and pathological states. *Journal of Clinical and Experimental Neuropsychology* 23, 74–93.

Fiorentini, A., Maffei, L., Sandini, G., 1983. The role of high spatial frequencies in face perception. *Perception* 12, 195-201.

Fischer, H., Wright, C. I., Whalen, P. J., McInerney, S. C., Shin, L. M., Rauch, S. L., 2003. Brain habituation during repeated exposure to fearful and neutral faces: a functional MRI study. *Brain research bulletin* 59, 387-392.

Flevaris, A. V., Robertson, L.C., Bentin, S., 2008. Using spatial frequency scales for processing face features and face configuration: An ERP analysis. *Brain Research* 1194, 100-109.

Fort, A., Besle, J., Giard, M., Pernier, J., 2005. Task-dependent activation latency in human visual extrastriate cortex. *Neuroscience Letters* 379: 144-148

Fries, P., Nikolic, D., Singer, W., 2007. The gamma cycle. *Trends in Neurosciences*. 30, 309-316.

Friston, K. J., Büchel, C., 2000. Attentional modulation of effective connectivity from V2 to V5/MT in humans. *Proceedings of the National Academy of Sciences* 97, 7591-7596.

Friston, K., 2003a. Learning and inference in the brain. *Neural Networks* 16, 1325-1352.

Friston, K. J., Harrison, L., Penny, W., 2003b. Dynamic causal modelling, *Neuroimage 19*, 1273-1302.

Friston, K. J., Bastos, A., Litvak, V., Stephan, K. E., Fries, P., Moran, R. J., 2012. DCM for complex-valued data: cross-spectra, coherence and phase-delays. *Neuroimage* 59, 439–455.

Garolera, M., Coppola, R., Muñoz, K. E., Elvevåg, B., Carver, F. W., Weinberger, D. R., Goldberg, T. E., 2007. Amygdala activation in affective priming: a magnetoencephalogram study. *Neuroreport* 18, 1449-1453.

Garrido, M. I., Kilner, J. M., Kiebel, S. J., Stephan, K. E., Friston, K. J., 2007. Dynamic causal modelling of evoked potentials: a reproducibility study. *Neuroimage* 36, 571–580.

Garrido, M. I., Barnes, G. R., Sahani, M., Dolan, R. J., 2012. Functional evidence for a dual route to amygdala. *Current Biology* 22, 129-134.

Gauthier, I., Anderson, A. W., Tarr, M. J., Skudlarski, P. Gore, J. C., 1997. Levels of categorization in visual recognition studied using functional magnetic resonance imaging. *Current Biology* 7, 645–651.

Gauthier, I., Tarr, M. J., Anderson, A. W., Skudlarski, P., Gore, J. C., 1999. Activation of the middle fusiform 'face area' increases with expertise in recognizing novel objects. *Nature* N*euroscience* 2, 568-573.

Gauthier, I., Nelson, C.A., 2001. The development of face expertise. *Current Opinion in Neurobiology* 11, 219-224.

Gauthier, I., Curran, T., Curby, K. M., Collins, D., 2003. Perceptual interference supports a non-modular account of face processing. *Nature Neuroscience* 6, 428-432.

Gauthier, I., Curby, K. M., 2005. A Perceptual Traffic Jam on Highway N170 Interference Between Face and Car Expertise. *Current Directions in Psychological Science* 14, 30-33.

GhashghaeiI, H. T., Barbas, H., 2002. Pathways for emotion: interactions of prefrontal and anterior temporal pathways in the amygdala of the rhesus monkey. *Neuroscience* 115, 1261-1279.

Glickstein, M., 2000. How are visual areas of the brain connected to motor areas for the sensory guidance of movement? *Trends in Neurosciences* 23, 613-617.

Goffaux, V., Gauthier, I., Rossion, B., 2003. Spatial scale contribution to early visual differences between face and object processing. *Cognitive Brain Research* 16, 416-424.

Goffaux, V., Hault, B., Michel, C., Vuong, Q. C., Rossion, B., 2005. The respective role of low and high spatial frequencies in supporting configural and featural processing of faces. *Perception* 34, 77-86.

Goffaux, V., Rossion, B., 2006. Faces are "spatial" - holistic face perception is supported by low spatial frequencies. *Journal of Experimental Psychology: Human Perception and Performance* 32, 1023.

Goldberg, D. P., Hiller, V. F., 1979. A scaled version of the general health questionnaire. *Psychological Medicine* 9, 139-45.

Goodale, M. A., Milner, A. D., 1992. Separate visual pathways for perception and action. *Trends in Neurosciences* 15, 20-25.

Gosselin, N., Peretz, I., Johnsen, E., Adolphs, R., 2007. Amygdala damage impairs emotion recognition from music. *Neuropsychologia* 45, 236-244.

Gothard, K. M., Battaglia, F. P., Erickson, C. A., Spitler, K. M., Amaral, D. G., 2007. Neural responses to facial expression and face identity in the monkey amygdala. *Journal of Neurophysiology* 97, 1671-1683.

Grieve, K. L., Acuna, C., Cudeiro, J., 2000. The primate pulvinar nuclei: vision and action. *Trends in Neurosciences*. 23, 35–39.

Grill-Spector, K., Kushnir, T., Edelman, S., Avidan-Carmel, G., Itzchak, Y., Malach, R., 1999. Differential processing of objects under various viewing conditions in the human lateral occipital complex. *Neuron* 24, pp. 187–203.

Grill-Spector, K., Kourtzi, Z., Kanwisher, N., 2001. The lateral occipital complex and its role in object recognition. *Vision Research* 41, 1409-1422.

Grill-Spector, K., 2003. The neural basis of object perception. *Current opinion in neurobiology* 13, 159-166.

Grill-Spector, K., Malach, R., 2004a. The human visual cortex. Annual Review of Neuroscience 27, 649-677.

Grill-Spector, K., Knouf, N., Kanwisher, N., 2004b. The fusiform face area subserves face perception, not generic within-category identification. *Nature Neuroscience* 7, 555-562.

Gross, J., Baillet, S., Barnes, G. R., Henson, R. N., Hillebrand, A., Jensen, O., Jerbi, K., Litvak, V., Maess, B., Oostenveld, R., Parkkonen, L., Taylor, J.R., van Wassenhove, V., Wibral, M., Schoffelen, J.M., 2013. Good practice for conducting and reporting MEG research. *Neuroimage* 65, 349–363.

Gruber, T., Muller, M. M., 2005. Oscillatory brain activity dissociates between associative stimulus content in a repetition priming task in the human EEG. *Cerebral Cortex* 15, 109–116.

Gruber, T., Maess, B., Trujillo-Barreto, N. J., Muller, M. M., 2008. Sources of synchronized induced gamma-band responses during a simple object recognition task: a replication study in human MEG. *Brain Research* 1196, 74–84.

Grutzner, C., Uhlhaas, P. J., Genc, E., Kohler, A., Singer, W., Wibral, M., 2010. Neuroelectromagnetic correlates of perceptual closure processes. *The Journal of Neurosciences* 30, 8342–8352.

Gur, R. C., Schroeder, L., Turner, T., McGrath, C., Chan, R. M., Turetsky, B. I., Alsop, D., Maldijan, J., Gur, R. E., 2002. Brain activation during facial emotion processing. *Neuroimage* 16, 651-662.

Habel, U., Windischberger, C., Derntl, B., Robinson, S., Kryspin-Exner, I., Gur, R. C., Moser, E., 2007. Amygdala activation and facial expressions: explicit emotion discrimination versus implicit emotion processing. *Neuropsychologia* 45, 2369-2377.

Hadjikhani, N., Kveraga, K., Naik, P., Ahlfors, S.P., 2009. Early (N170) activation of face-specific cortex by face-like objects. *Neuroreport* 20, 403-407.

Haider, M., Spong, P., Lindsley, D. B., 1964. Attention, vigilance, and cortical evoked-potentials in humans. *Science* 145, 180-182.

Halit, H., De Haan, M., Schyns, P. G., Johnson, M. H., 2006. Is high-spatial frequency information used in the early stages of face detection? *Brain Research* 1117, 154-161.

Hamann, S. B., Ely, T. D., Grafton, S. T., Kilts, C. D., 1999a. Amygdala activity related to enhanced memory for pleasant and aversive stimuli. *Nature neuroscience* 2, 289-293.

Hamann, S., Adolphs, R., 1999b. Normal recognition of emotional similarity between facial expressions following bilateral amygdala damage. *Neuropsychologia* 37. 1135-1141.

Hamilton, M., 1959. The assessment of anxiety states by rating. *British Journal of Medical Psychology* 32, 50-55.

Hamilton, M., 1960. A rating scale for depression. *Journal of Neurology, Neurosurgery, and Psychiatry* 23, 56.

Harris, A., Nakayama, K., 2008. Rapid adaptation of the M170 response: importance of face parts. *Cerebral Cortex* 18, 467-476.

Harting, J. K., Updyke, B. V., Van Lieshout, D. P., 2001. The visualoculomotor striatum of the cat: functional relationship to the superior colliculus. *Experimental Brain Research* 136, 138–142.

Harting, J. K., Updyke, B. V., 2006. Oculomotor-related pathways of the basal ganglia. *Progress in Brain Research* 151, 441–460.

Hatanaka, K., Nakasato, N., Seki, K., Kanno, A., Mizoi, K., Yoshimoto, T., 1997. Striate cortical generators of the N75, P100 and N145 components localized by pattern reversal visual evoked magnetic fields. *The Tohoku Journal of Experimental Medicine* 182, 9-14.

Hauk, O., 2004. Keep it simple: a case for using classical minimum norm estimation in the analysis of EEG and MEG data. *Neuroimage* 21, 1612–1621.

Haxby, J. V., Ungerleider, L. G., Clark, V. P., Schouten, J. L., Hoffman, E. A., Martin, A., 1999. The effect of face inversion on activity in human neural systems for face and object perception. *Neuron* 22, 189–199.

Haxby, J. V., Hoffman, E. A., Gobbini, M. I., 2002. Human neural systems for face recognition and social communication. *Biological Psychiatry* 51, 59-67.

Hegdé, J., Van Essen, D. C., 2000. Selectivity for complex shapes in primate visual area V2. *The Journal of Neuroscience* 20, 61-66.

Heller ,W., Levy, J., 1981. Perception and expression of emotion in right-handers and left handers. *Neuropsychologia* 19, 263–272.

Herrmann, M. J., Aranda, D., Ellgring, H., Mueller, T. J., Strik, W. K., Heidrich, A., Fallgatter, A., 2002. Face-specific event-related potential in humans is independent from facial expression. *International Journal of Psychophysiology* 45, 241-244.

Herrmann, M. J., Ehlis, A. C., Ellgring, H., Fallgatter, A. J., 2005a. Early stages (P100) of face perception in humans as measured with event-related potentials (ERPs). *Journal of Neural Transmission* 112, 1073-1081.

Herrmann, M. J., Ehlis, A. C., Muehlberger, A., Fallgatter, A.J., 2005b. Source localisation of early stages of face processing. *Brain topography* 18, 77-85.

Hess, U., Thibault, P., 2009. Darwin and emotion expression. *American Psychologist*, 64, 120.

Hillger, L. A., Koenig, O., 1991. Separable mechanisms in face processing: evidence from hemispheric specialization. *Journal of Cognitive Neuroscience* 3, 42–58.

Hinojosa, J. A., Mercado, F., Carretié, L., 2015. N170 sensitivity to facial expression: a meta-analysis. *Neuroscience and Biobehavioral Reviews* 55, 498-509.

Hipp, J. F., Engel, A. K., Siegel, M., 2011. Oscillatory synchronization in large-scale cortical networks predicts perception. *Neuron* 69, 387–396.

Hochstein, S., Ahissar, M., 2002. View from the top: hierarchies and reverse hierarchies in the visual system. *Neuron* 36, 791-804.

Holmes, A., Winston, J. S., Eimer, M., 2005. The role of spatial frequency information for ERP components sensitive to faces and emotional facial expression. *Cognitive Brain Research* 25, 508-520.

Hooker, C. I., Germine, L. T., Knight, R. T., D'Esposito, M., 2006. Amygdala response to facial expressions reflects emotional learning. *The Journal of Neuroscience* 26, 8915-8922.

Huang, Y. X., Luo, Y. J., 2006. Temporal course of emotional negativity bias: an ERP study. *Neuroscience letters* 398, 91-96.

Hubel, D. H., Wiesel, T. N., 1977. Ferrier lecture: Functional architecture of macaque monkey visual cortex. *Philosophical Transactions of the Royal Society of London Series B: Biological Sciences* 198, 1-59.

Inagaki, M., Fujita, I., 2011. Reference frames for spatial frequency in face representation differ in the temporal visual cortex and amygdala. *The Journal of Neuroscience* 31, 10371-10379.

Ishai, A., 2008. Let's face it: it's a cortical network. *Neuroimage* 40, 415-419.

Itier, R. J., Taylor, M. J., 2004a. Source analysis of the N170 to faces and objects. *Neuroreport* 15, 1261-1265.

Itier, R. J., Taylor, M. J., 2004b. N170 or N1? Spatiotemporal differences between object and face processing using ERPs. *Cerebral Cortex* 14, 132-142.

Itier, R.J., Taylor, M.J., 2004c. Face recognition memory and configural processing: a developmental ERP study using upright, inverted, and contrast-reversed faces. *Journal of Cognitive Neuroscience* 16, 487-502.

Itier, R. J., Latinus, M., Taylor, M. J., 2006a. Face, eye and object early processing: what is the face specificity? *Neuroimage* 29, 667-676.

Itier, R. J., Herdman, A. T., George, N., Cheyne, D., Taylor, M. J., 2006b. Inversion and contrast-reversal effects on face processing assessed by MEG. *Brain Research* 1115, 108-120.

Ito, M., Tamura, H., Fujita, I., Tanaka, K., 1995. Size and position invariance of neuronal responses in monkey inferotemporal cortex. *Journal of Neurophysiology* 73, 218-226.

Ito, M., Sugata, T., Kuwabara, H., Wu, C., Kojima, K., 1999. Effects of angularity of the figures with sharp and round corners on visual evoked potentials. *Japanese Psychological Research* 41, 91-101.

Jeffreys, D. A. Axford, J. G., 1972. Source locations of pattern-specific components of human visual evoked potentials. II. Component of extrastriate cortical origin. *Experimental Brain Research* 16, 1-21.

Jensen, O., Kaiser, J., Lachaux, J. P., 2007. Human gamma-frequency oscillations associated with attention and memory. *Trends in Neurosciences* 30, 317-324.

Jiang, Y., Boehler, C. N., Nonnig, N., Duzel, E., Hopf, J. M., Heinze, H. J., Schoenfeld, M. A., 2008. Binding 3-D object perception in the human visual cortex. *Journal of Cognitive Neuroscience* 20, 553–562.

Johannes, S., Munte, T. F., Heinze, H. J., Mangun, G. R., 2003. Luminance and spatial attention effects on early visual processing. *Cognitive Brain Research* 2, 189-205.

Johnson, M. H., 2005. Subcortical face processing. *Nature Reviews Neuroscience* 6, 766-774.

Kanade, T., Cohn, J. F., Tian, Y., 2000. Comprehensive database for facial expression analysis. Proceedings of the Fourth IEEE *International Conference on Automatic Face and Gesture Recognition* (FG'00), Grenoble, France, 46-53.

Kanwisher, N., McDermott, J., Chun, M. M., 1997. The fusiform face area: a module in human extrastriate cortex specialized for face perception. *The Journal of Neuroscience* 17, 4302-4311.

Kanwisher, N., Tong, F., Nakayama, K., 1998. The effect of face inversion on the human fusiform face area. *Cognition* 68, B1-B11.

Kanwisher, N., Stanley, D., Harris, A., 1999. The fusiform face area is selective for faces not animals. *Neuroreport* 10, 183-187.

Kanwisher, N., 2000. Domain specificity in face perception. *Nature neuroscience* 3, 759-763.

Kanwisher, N., Yovel, G., 2006. The fusiform face area: a cortical region specialized for the perception of faces. *Philosophical Transactions of the Royal Society of London Series B: Biological Sciences*. 361, 2109–2128.

Kawasaki, H., Adolphs, R., Kaufman, O., Damasio, H., Damasio, A. R., Granner, M., Bakken, H., Hori, T., Howard M. A., 2001. Single-neuron responses to emotional visual stimuli recorded in human ventral prefrontal cortex. *Nature Neuroscience*. 4, 15-16.

Keil, A., Muller, M. M., Ray, W. J., Gruber, T., Elbert, T., 1999. Human gamma band activity and perception of a gestalt. *The Journal of Neurosciences* 19, 7152–7161.

Keil, M. S., 2009. "I look in your eyes, honey": Internal face features induce spatial frequency preference for human face processing. *PLoS Computational Biology* 5, 1-13.

Kennedy, D. P., Gläscher, J., Tyszka, J. M., Adolphs, R., 2009. Personal space regulation by the human amygdala. Nature Neuroscience 12, 1226-1227.

Kleinschmidt, A., Buchel, C., Zeki, S., Frackowiak, R.S., 1998. Human brain activity during spontaneously reversing perception of ambiguous figures. *Proceedings of the Royal Society Biological Sciences* 265, 2427-2433.

Klemenhagen, K. C., Dudman, J. T., Rogan, M. T., Hen, R., Kandel, E. R., Hirsch, J., 2004. Individual differences in trait anxiety predict the response of the basolateral amygdala to unconsciously processed fearful faces. *Neuron* 44, 1043-1055.

Kling, A.S., Brothers, L.A., 1992. The amygdala and social behavior, in The amygdala: Neurobiological aspects of emotion, memory, and mental dysfunction. *Wiley-Liss*, New York, 353-377.

Kluver, H., Bucy, P.C., 1937. 'Psychic blindness' and other symptoms following bilateral temporal lobectomy. *American Journal of Physiology* 119, 254-284.

Knapska, E., Nikolaev, E., Boguszewski, P., Walasek, G., Blaszczyk, J., Kaczmarek, L., Werka, T., 2006. Between-subject transfer of emotional information evokes specific pattern of amygdala activation. *Proceedings of the National Academy of Sciences* 103, 3858–3862.

Koivisto, M., Mantyla, T., Silvanto, J., 2010. The role of early visual cortex (V1/V2) in conscious and unconscious visual perception. *Neuroimage* 51, 828–834.

Koivisto, M., Railo, H., Revonsuo, A., Vanni, S., Salminen-Vaparanta, N., 2011. Recurrent processing in V1/V2 contributes to categorization of natural scenes. *The Journal of Neuroscience* 31, 2488–2492.

Konig, P., Engel, A. K., Singer, W., 1995. Relation between oscillatory activity and long range synchronization in cat visual cortex. *Proceedings of the National Academy of Sciences* U. S. A. 92, 290–294.

Kopell, N., Ermentrout, G. B., Whittington, M. A., Traub, R. D., 2000. Gamma rhythms and beta rhythms have different synchronization properties. *Proceedings of the National Academy of Sciences* U. S. A. 97, 1867–1872.

Krolak-Salmon, P., Fischer, C., Vighetto, A., Mauguière, F., 2001. Processing of facial emotional expression: spatio-temporal data as assessed by scalp event-related potentials. *European Journal of Neuroscience* 13, 987-994.

Krolak-Salmon, P., Henaff, M.A., Vighetto, A., Bertrand, O., Mauguiere, F., 2004. Early amygdala reaction to fear spreading in occipital, temporal, and frontal cortex: a depth electrode ERP study in human. *Neuron* 42, 665-676.

Kunzle, H., 2006. Thalamo-striatal projections in the hedgehog tenrec. *Brain Research* 1100, 78–92.

Kuraoka, K., Nakamura, K., 2007. Responses of single neurons in monkey amygdala to facial and vocal emotions. *Journal of Neurophysiology* 97, 1379–1387.

Kveraga, K., Boshyan, J., Bar, M., 2007. Magnocellullar projections as the trigger of top-down facilitation in recognition. *The Journal of Neuroscience* 27, 13232-13240.

LaBar, K. S., Crupain, M. J., Voyvodic, J. T., McMCarthy, G., 2003. Dynamic perception of facial affect and identity in the human brain. *Cerebral Cortex* 13, 1023-1033.

Lachaux, J. P., George, N., Tallon-Baudry, C., Martinerie, J., Hugueville, L., Menottia, L., Kahane, P., Renault, B., 2005. The many faces of the gamma band response to complex visual stimuli. *Neuroimage* 25, 491–501.

Lamme, V. A., Roelfsema, P.R., 2000. The distinct modes of vision offered by feedforward and recurrent processing. *Trends in Neurosciences* 23, 571-579.

Lang, P. J., Bradley, M. M., Cuthbert, B. N., 2005. International affective picture system (IAPS): affective ratings of pictures and instruction manual (Technical Report A-6). Un*iversity of Florida*, Gainesville, Florida.

Langner, O., Dotsch, R., Bijlstra, G., Wigboldus, D. H. J., Hawk, S. T., van Knippenberg, A., 2010. Presentation and validation of the Radboud Faces Database. *Cognition & Emotion* 24, 1377-1388.

Latinus, M., Taylor, M. J., 2006. Face processing stages: impact of difficulty and the separation of effects. *Brain research* 1123, 179-187.

LeDoux, J. E., Cicchetti, P., Xagoraris, A., Romanski, L. M., 1990. The lateral amygdaloid nucleus: sensory interface of the amygdala in fear conditioning. *The Journal of neuroscience* 10, 1062-1069.

LeDoux, J. E., 1992. Brain mechanisms of emotion and emotional learning. *Current opinion in neurobiology* 2, 191-197.

LeDoux, J. E., 1994. Emotion, memory and the brain. *Scientific American* 270, 50-57.

LeDoux, J. E., 1996. The Emotional Brain. *Simon & Schuster,* New York.

Leonard, C. M., Rolls, E. T., Wilson, F. A., Baylis, G. C., 1985. Neurons in the amygdala of the monkey with responses selective for faces. *Behavioural Brain Research* 15, 159-176.

Liddell, B. J., Williams, L. M., Rathjen, J., Shevrin, H., Gordon, E., 2004. A temporal dissociation of subliminal versus supraliminal fear perception: an event-related potential study. *Journal of Cognitive Neuroscience* 16, 479–486.

Liddell, B. J., Brown, K. J., Kemp, A. H., Barton, M. J., Das, P., Peduto, A., Gordon, E., Williams, L. M., 2005. A direct brainstem-amygdala-cortical 'alarm' system for subliminal signals of fear. *Neuroimage* 24, 235–243.

Linke, R., De Lima, A. D., Schwegler, H., Pape, H.C., 1999. Direct synaptic connections of axons from superior colliculus with identified thalamoamygdaloid projection neurons in the rat: possible substrates of a subcortical visual pathway to the amygdala. *Journal of Comparative Neurology* 403, 158–170.

Linkenkaer-Hansen, K., Palva, J. M., Sams, M., Hietanen, J. K., Aronen, H. J., Ilmoniemi, R. J., 1998. Face-selective processing in human extrastriate cortex around 120 ms after stimulus onset revealed by magneto-and electroencephalography. *Neuroscience Letters* 253, 147-150.

Liu, J., Harris, A., Kanwisher, N., 2002. Stages of processing in face perception: an MEG study. *Nature Neuroscience* 5, 910-916.

Livingstone, M., Hubel, D., 1988. Segregation of form, color, movement, and depth: anatomy, physiology, and perception. *Science* 240, 740-749.

Loftus, G. R. Harley, E. M., 2005. Why is it easier to identify someone close than far away? *Psychonomic Bulletin & Review* 12, 43–65.

Lucey, P., Cohn, J. F., Kanade, T., Saragih, J., Ambadar, Z., Matthews, I. 2010. The Extended Cohn-Kanade Dataset (CK+): A complete expression dataset for action unit and emotion-specified expression. *Proceedings of the Third International Workshop on CVPR for Human Communicative Behavior Analysis* (CVPR4HB 2010), San Francisco, USA, 94-101.

Luck, S. J., Woodman, G. E., Vogel, E. K., 2000. Event-related potential studies of attention. *Trends in Cognitive Sciences* 4, 432-440.

Luiten, P. G. M., Gaykema, R. P. A., Traber, J., Spencer, D. G., 1987. Cortical projection patterns of magnocellular basal nucleus subdivisions as revealed by anterogradely transported Phaseolus vulgaris leucoagglutinin. *Brain Research* 413, 229-250.

Lundqvist, D., Flykt, A., Öhman, A., 1998. The Karolinska Directed Emotional Faces – KDEF, CD ROM from Department of Clinical Neuroscience, Psychology section, Karolinska Institutet, ISBN 91-630-7164-9.

Luria, A. R., 1966. Higher cortical functions in man. Basic Books, Oxford.

Lyon, D. C., Nassi, J. J., Callaway, E.M., 2010. A disynaptic relay from superior colliculus to dorsal stream visual cortex in macaque monkey. *Neuron* 65, 270–279.

MacLean, P. D., 1949. Psychosomatic disease and the "visceral brain": Recent developments bearing on the Papez theory of emotion. *Psychosomatic Medicine* 11, 338-353.

Maier, A., Adams, G.K., Aura, C., Leopold, D.A., 2010. Distinct superficial and deep laminar domains of activity in the visual cortex during rest and stimulation. *Frontiers in Systems Neuroscience* 4. 100.

Malach, R., Reppas, J. B., Benson, R. R., Kwong, K. K., Jiang, H., Kennedy, W. A., Ledden, P. J., Brady, T. J., Rosen, B. R., Tootell, R. B., 1995. Object-related activity revealed by functional magnetic resonance imaging in human occipital cortex. *Proceedings of the Natural Academy of Science* 92, 8135-8139.

Mangun, G. R., Hillyard, S. A, 1991. Modulations of sensory-evoked brain potentials indicate changes in perceptual processing during visual-spatial priming. *Journal of Experimental Psychology: Human perception and performance* 17, 1057-1074.

Mangun, G. R., Hillyard, S. A., Luck, S. J., 1993. Electrocortical substrates of visual selective attention. In D. Meyer & S. Kornblum (Eds.), Attention and Performance XIV 219-243. Cambridge, Massachusetts: MIT Press.

Mangun, G. R., Hopfinger, J. B., Kussmaul, C. L., Fletcher, E. M., Heinze, H. J., 1997. Covariations in ERP and PET measures of spatial selective attention in human extrastriate visual cortex. *Human Brain Mapping*, 5, 273-279.

Maratos, F. A., Mogg, K., Bradley, B. P., Rippon, G., Senior, C., 2009. Coarse threat images reveal theta oscillations in the amygdala: a magnetoencephalography study. *Cognitive, Affective, & Behavioral Neuroscience* 9, 133-143.

Maren, S., 1999. Long-term potentiation in the amygdala: a mechanism for emotional learning and memory. *Trends in Neurosciences* 22, 561-567

Maris, E., Oostenveld, R., 2007. Nonparametric statistical testing of EEG-and MEG-data. *Journal of Neuroscience Methods* 164, 177-190.

Martinovic, J., Gruber, T., Hantsch, A., Muller, M. M., 2008. Induced gamma-band activity is related to the time point of object identification. *Brain Research* 1198, 93–106.

McCarthy, G., Puce, A., Gore, J. C., Allison, T., 1997. Face-specific processing in the human fusiform gyrus. *Journal of Cognitive Neuroscience* 9, 605-610.

McKeeff, T. J., Tong, F., 2007. The timing of perceptual decisions for ambiguous face stimuli in the human ventral visual cortex. *Cerebral Cortex* 17, 669-678.

Merigan, W. H., Maunsell, J. H. R., 1993. How parallel are the primate visual pathways? *Annual Review of Neuroscience*. 16, 369-402.

Mineka, S., Davidson, M., Cook, M., Keir, R., 1984. Observational conditioning of snake fear in rhesus monkeys. *Journal of Abnormal Psychology* 93, 355.

Miserendino, M. J., Sananes, C. B., Melia, K. R., Davis, M., 1990. Blocking of acquisition but not expression of conditioned fear-potentiated startle by NMDA antagonists in the amygdala. *Nature* 345, 716-718.

Mishkin, M., Ungerleider, L. G., Macko, K., 1983. Object vision and spatial vision: two cortical pathways. *Trends in Neurosciences* 6, 414-417.

Mooney, C. M., 1957. Age in the development of closure ability in children. *Canadian Journal of Experimental Psychology* 11, 219–226.

Moors, A. De Houwer, J., 2006. Automaticity: a theoretical and conceptual analysis. *Psychological Bulletin* 132, 297.

Moran, J., Desimone, R., 1985. Selective Attention Gates Visual Processing in the Extrastriate *Cortex*. Science 229, 782-784.

Morecraft, R. J., McNeal, D. W., Stilwell-Morecraft, K. S., Gedney, M., Ge, J., Schroeder, C. M., Van Hoesen, G. W., 2007. Amygdala interconnections with the cingulate motor cortex in the rhesus monkey. *Journal of Comparative Neurology* 500, 134-165.

Morris, J. S., Frith, C. D., Perrett, D. I., Rowland, D., Young, A. W., Calder, A. J., Dolan, R. J., 1996. A differential neural response in the human amygdala to fearful and happy facial expressions. *Nature* 383, 812-815.

Morris, J. S., Ohman, A., Dolan, R. J., 1998. Conscious and unconscious emotional learning in the human amygdala. *Nature* 393, 467-470.

Morris, J. S., DeGelder, B., Weiskrantz, L., Dolan, R. J., 2001. Differential extrageniculostriate and amygdala responses to presentation of emotional faces in a cortically blind field. *Brain* 124, 1241-1252.

Morris, J. S., deBonis, M., Dolan, R. J., 2002. Human amygdala responses to fearful eyes. *Neuroimage* 17, 214-22.

Moscovitch, M., Winocur, G., Behrmann, M., 1999. What is special about face recognition? Nineteen experiments on a person with visual object agnosia and dyslexia but normal face recognition. *Journal of Cognitive Neuroscience* 9, 555-604.

Movshon, J.A., Thompson, I. D., Tolhurst, D. J., 1978. Spatial summation in the receptive fields of simple cells in the cat's striate cortex. *The Journal of Physiology* 283, 53-77.

Mufson, E. J., Mesulam, M. M., Pandya, D. N., 1981. Insular interconnections with the amygdala in the rhesus monkey. *Neuroscience 6*, 1231-1248.

Mühlberger, A., Wieser, M.J., Herrmann, M.J., Weyers, P., Tröger, C., Pauli, P., 2009. Early cortical processing of natural and artificial emotional faces differs between lower and higher socially anxious persons. *Journal of Neural Transmission* 116, 735-746.

Müller, M. M., Bosch, J., Elbert, T., Kreiter, A., Sosa, M.V., Sosa, P.V., Rockstroh, B., 1996. Visually induced gamma-band responses in human electroencephalographic activity—a link to animal studies. *Experimental Brain Research*. 112, 96–102.

Naccache, L., Gaillard, R., Adam, C., Hasboun, D., Clémenceau, S., Baulac, M., Dehaene, S., Cohen, L., 2005. A direct intracranial record of emotions evoked by subliminal words. *Proceedings of the National Academy of Sciences of the United States of America* 102, 7713-7717.

Nakamura, K., Mikami, A., Kubota, K., 1992. Activity of single neurons in the monkey amygdala during performance of a visual discrimination task. *Journal of Neurophysiology* 67, 1447-1463

Nakashima, T., Kaneko, K., Goto, Y., Abe, T., Mitsudo, T., Ogata, K., Makinouchi, A., Tobimatsu, S., 2008. Early ERP components differentially extract facial features: Evidence for spatial frequency-and-contrast detectors. *Neuroscience Research* 62, 225-235.

Nauhaus, I., Nielsen, K. J., Disney, A. A., Callaway, E. M., 2012. Orthogonal micro-organization of orientation and spatial frequency in primate primary visual cortex. *Nature Neuroscience* 15, 1683-1690.

Nolte, G., 2003. The magnetic lead field theorem in the quasi-static approximation and its use for magnetoencephalography forward calculation in realistic volume conductors. *Physics in Medicine and Biology* 48, 3637–3652.

Nowak, L. G., Bullier, J., 1997. In: Cerebral Cortex: Extrastriate Cortex in Primate. *Plenum*, New York. pp. 205–241.

Öhman, A., Mineka, S., 2001. Fears, phobias, and preparedness: toward an evolved module of fear and fear learning. *Psychological Review* 108, 483-522.

Öhman, A., 2002. Automaticity and the amygdala: Nonconscious responses to emotional faces. *Current Directions in Psychological Science* 11, 62-66.

Oldfield, R.C., 1971. The assessment and analysis of handedness: the Edinburgh inventory. *Neuropsychologia* 9, 97-113.

Olsson, A., Nearing, K. I., Phelps, E. A., 2007. Learning fears by observing others: the neural systems of social fear transmission. *Social Cognitive and Affective Neuroscience* 2, 3–11.

Olszanowski, M., Pochwatko, G., Kukliński, K., Ścibor-Rylski, M., Lewinski, P., Ohme, R., 2015. Warsaw set of emotional facial expression pictures: a validation study of facial display photographs. *Frontiers in Psychology* 5, 1516.

Olufsen, M. S., Whittington, M. A., Camperi, M., Kopell, N., 2003. New roles for the gamma rhythm: population tuning and preprocessing for the Beta rhythm. *Journal of Computational Neuroscience* 14, 33–54.

Ortuño, T., Grieve, K. L., Cao, R., Cudeiro, J., Rivadulla, C., 2014. Bursting thalamic responses in awake monkey contribute to visual detection and are modulated by corticofugal feedback. *Frontiers in Behavioral Neuroscience* 8, 198.

Ouellette, B. G., Casanova, C., 2006. Overlapping visual response latency distributions in visual cortices and LP-pulvinar complex of the cat. *Experimental Brain Research* 175, 332-341.

Oya, H., Kawasaki, H., Howard, M. A., III, Adolphs, R., 2002. Electrophysiological responses in the human amygdala discriminate emotion categories of complex visual stimuli. *The Journal of Neuroscience*. 22, 9502-9512.

Papez, J. W., 1937. A proposed mechanism of emotion. *Archives of Neurology and Psychiatry* 38, 725-743.

Parkin, A. J., Williamson, P., 1987. Cerebral lateralisation at different stages of facial processing. *Cortex* 23, 99–110.

Pascual-Leone, A., Walsh, V., 2001. Fast back projections from the motion to the primary visual area necessary for visual awareness. *Science* 292, 510–512.

Pasley, B. N., Mayes, L. C., Schultz, R.T., 2004. Subcortical discrimination of unperceived objects during binocular rivalry. *Neuron* 42, 163-172.

Peeters, G., Czapinski, J., 1990. Positive-negative asymmetry in evaluations: the distinction between affective and informational negativity effects. *European Review of Social Psychology* 1, 33_60.

Pessoa, L., McKenna, M., Gutierrez, E., Ungerleider, L., 2002. Neural processing of emotional faces requires attention. *Proceedings of the National Academy of Sciences* 99, 11458-11463.

Pessoa, L., Adolphs, R., 2010. Emotion processing and the amygdala: from a 'low road' to 'many roads' of evaluating biological significance. *Nature Reviews Neuroscience* 11, 773-783.

Pessoa, L., 2013. The cognitive-emotional brain: from interactions to integration. *The Mit Press*, Cambridge.

Peyrin, C., Musel, B., 2012. *On the Specific Role of the Occipital Cortex in Scene Perception*. INTECH Open Access Publisher.

Phelps, E. A., Ledoux, J. E., 2005. Contributions of the amygdala to emotion processing: from animal models to human behavior. *Neuron* 48, 175-187.

Phillips, R. G., LeDoux, J. E., 1992. Differential contribution of amygdala and hippocampus to cued and contextual fear conditioning. *Behavioral neuroscience* 106, 274-285.

Pins, D., 2003. The neural correlates of conscious vision. *Cerebral Cortex*, 13, 461-474.

Pizzagalli, D. A., Lehmann, D., Hendrick, A.M., Regard, M., Pascual-Marqui, R.D., Davidson, R.J., 2002. Affective judgments of faces modulate early activity (~ 160 ms) within the fusiform gyri. *Neuroimage* 16, 663-677.

Pizzagalli, D., Regard, M., Lehmann, D., 1999. Rapid emotional face processing in the human right and left brain hemispheres: an ERP study. *Neuroreport*, 10, 2691-2698.

Pizzagalli, D. A., Lehmann, D., Hendrick, A. M., Regard, M., Pascual-Marqui, R. D., Davidson, R. J., 2002. Affective judgments of faces modulate early activity (~ 160 ms) within the fusiform gyri. *Neuroimage* 16, 663-677.

Porrino, L. J., Crane, A. M., Goldman-Rakic, P. S., 1981. Direct and indirect pathways from the amygdala to the frontal lobe in rhesus monkeys. *Journal of Comparative Neurology* 198, 121-136.

Pourtois, G., Dan, E. S., Grandjean, D., Sander, D., Vuilleumier, P., 2005. Enhanced extrastriate visual response to bandpass spatial frequency filtered fearful faces: Time course and topographic evoked-potentials mapping. *Human Brain Mapping* 26, 65-79.

Pourtois, G., Spinelli, L., Seeck, M., Vuilleumier, P., 2010 Temporal precedence of emotion over attention modulations in the lateral amygdala: Intracranial ERP evidence from a patient with temporal lobe epilepsy. *Cognitive, Affective and Behavioral Neuroscience* 10, 83-93.

Qiu, F. T., Von Der Heydt, R., 2005. Figure and ground in the visual cortex: V2 combines stereoscopic cues with Gestalt rules. *Neuron* 47, 155-166.

Ramon, M., Rossion, B., 2012. Hemisphere-dependent holistic processing of familiar faces. *Brain and cognition* 78, 7–13.

Rao, R. P., Ballard, D. H., 1999. Predictive coding in the visual cortex: a functional interpretation of some extra-classical receptive-field effects. *Nature Neuroscience* 2, 79-87.

Rauch, S. L., Whalen, P. J., Shin, L. M., McInerney, S. C., Macklin, M. L., Lasko, N. B., Orr, S. P., Pitman R. K., 2000. Exaggerated amygdala response to masked facial stimuli in posttraumatic stress disorder: a functional MRI study. *Biological Psychiatry* 47, 769-776.

Reid, R. C., Alonso, J. M., 1995. Specificity of monosynaptic connections from thalamus to visual cortex. *Nature* 378, 281-283.

Reinders, A., Gläscher, J., De Jong, J. R., Willemsen, A., Den Boer, J. A., Büchel, C., 2006. Detecting fearful and neutral faces: BOLD latency differences in amygdala–hippocampal junction. *Neuroimage* 33, 805-814.

Rellecke, J., Sommer, W., Schacht, A., 2013. Emotion effects on the N170: a question of reference? *Brain Topography* 26, 62-71.

Richardson, M. P., Strange, B. A., Dolan, R. J., 2004. Encoding of emotional memories depends on amygdala and hippocampus and their interactions. *Nature neuroscience* 7, 278-285.

Robertson, L. C., 2003. Binding, spatial attention and perceptual awareness. *Nature Reviews Neuroscience* 4, 93–102.

Rodriguez, E., George, N., Lachaux, J. P., Martinerie, J., Renault, B., Varela, F. J., 1999. Perception's shadow: long-distance synchronization of human brain activity. *Nature* 397, 430–433.

Roopun, A.K., Middleton, S. J., Cunningham, M. O., LeBeau, F. E., Bibbig, A., Whittington, M. A., Traub, R. D., 2006. A beta2-frequency (20–30 Hz) oscillation in nonsynaptic networks of somatosensory cortex. *Proceedings of the National Academy of Sciences U. S. A.* 103, 15646–15650.

Roopun, A. K., Kramer, M. A., Carracedo, L. M., Kaiser, M., Davies, C. H., Traub, R. D., Kopell, N. J., Whittington, M. A., 2008. Period concatenation underlies interactions between gamma and beta rhythms in neocortex. *Frontiers in Cellular Neuroscience* 2, 1.

Rossion, B., Gauthier, I., Tarr, M. J., Despland, P., Bruyer, R., Linotte, S., Crommelinck, M., 2000a. The N170 occipito-temporal component is delayed and enhanced to inverted faces but not to inverted objects: an electrophysiological account of face-specific processes in the human brain. *Neuroreport* 11, 69-72.

Rossion, B., Dricot, L., Devolder, A., Bodart, J. M., Crommelinck, M., De Gelder, B., Zoontjes, R., 2000b. Hemispheric asymmetries for whole-based and part-based face processing in the human fusiform gyrus. *Journal of Cognitive Neuroscience* 12, 793–802.

Rossion, B., Gauthier, I., Goffaux, V., Tarr, M. J., Crommelinck, M., 2002. Expertise training with novel objects leads to left-lateralized facelike electrophysiological responses. *Psychological Science* 13, 250-257.

Rossion, B., Caldara, R., Seghier, M., Schuller, A.M., Lazeyras, F., Mayer, E., 2003b. A network of occipito-temporal face-sensitive areas besides the right middle fusiform gyrus is necessary for normal face processing. *Brain*, 126, 2381-2395.

Rossion, B., Joyce, C. A., Cottrell, G. W., Tarr, M. J., 2003a. Early lateralization and orientation tuning for face, word, and object processing in the visual cortex. *Neuroimage* 20, 1609-1624.

Rossion, B., Jacques, C., 2008. Does physical interstimulus variance account for early electrophysiological face sensitive responses in the human brain? Ten lessons on the N170. *Neuroimage* 39, 1959-1979.

Rossion, B., Jacques, C., 2011. The N170: understanding the time-course of face perception in the human brain. In: Luck, S., Kappenman, E. (Eds.), The Oxford Handbook of ERP Components. *Oxford University Press*, New York, 115–142.

Rossion, B., Hanseeuw, B., Dricot, L., 2012. Defining face perception areas in the human brain: a large-scale factorial fMRI face localizer analysis. *Brain and Cognition*. 79, 138–157.

Rossion, B., 2014. Understanding face perception by means of human electrophysiology. *Trends in cognitive Sciences* 18, 310–318

Rozin, P., Royzman, E. B., 2001. Negativity bias, negativity dominance, and contagion. *Personality and Social Psychology Review* 5, 296-320.

Rugg, M. D., Milner, A. D., Lines, C. R., Phalp, R., 1987. Modulations of visual event-related potentials by spatial and non-spatial visual selective attention. *Neuropsychologia* 25, 85-96.

Rutman, A. M., Clapp, W. C., Chadick, J. Z., Gazzaley, A., 2010. Early top–down control of visual processing predicts working memory performance. *Journal of Cognitive Neuroscience* 22, 1224-1234.

Saalmann, Y. B., Pigarev, I. N., Vidyasagar, T. R., 2007. Neural mechanisms of visual attention: how top-down feedback highlights relevant locations. *Science* 316, 1612–1615.

Sato, W., Kochiyama, T., Uono, S., Matsuda, K., Usui, K., Inoue, Y., Toichi, M., 2011. Rapid amygdala gamma oscillations in response to fearful facial expressions. *Neuropsychologia* 49, 612-617.

Schacht, A., Sommer, W., 2009. Emotions in word and face processing: early and late cortical responses. *Brain and Cognition* 69, 538-550.

Schendan, H. E., Ganis, G., Kutas, M., 1998. Neurophysiological evidence for visual perceptual categorization of words and faces within 150 ms. *Psychophysiology* 35, 240-251.

Schiller, P. H., Malpeli, J. G., Schein, S. J., 1979. Composition of geniculostriate input at superior colliculus of the rhesus monkey. *Journal of Neurophysiology* 42, 1124-1133.

Schmid, M. C., Panagiotaropoulos, T., Augath, M. A., Logothetis, N. K., Smirnakis, S.M.., 2009. Visually driven activation in macaque areas V2 and V3 without input from the primary visual cortex. *PLoS One* 4, e5527.

Schmolesky, M. T., Wang, Y., Hanes, D. P., Thompson, K. G., Leutgeb, S., Schall, J. D., Leventhal, A.G., 1998. Signal timing across the macaque visual system. *Journal of Neurophysiology* 79, 3272-3278

Schoffelen, J. M., Oostenveld, R., Fries, P., 2005. Neuronal coherence as a mechanism of effective corticospinal interaction. *Science* 308, 111–113.

Schoffelen, J. M., Poort, J., Oostenveld, R., Fries, P., 2011. Selective movement preparation is subserved by selective increases in corticomuscular gamma-band coherence. *The Journal of Neurosciences* 31, 6750–6758.

Schultz, R. T., 2005. Developmental deficits in social perception in autism: the role of the amygdala and fusiform face area. *International Journal of Developmental Neuroscience* 23, 125-141.

Schupp, H. Y., Junghöfer, M., Weike, A. I., Hamm, A. O, 2003. Emotional facilitation of sensory processing in the visual cortex. *Psychological Science* 14, 7-13.

Schweinberger, S. R., Kaufmann, J. M., Moratti, S., Keil, A., Burton, A. M., 2007. Brain responses to repetitions of human and animal faces, inverted faces, and objects - an MEG study. *Brain Research* 1184, 226-233.

Schyns, P. G., Petro, L. S., Smith, M. L., 2007. Dynamics of visual information integration in the brain for categorization facial expressions. *Current Biology* 17, 1580–1585.

Sehatpour, P., Molholm, S., Javitt, D.C., Foxe, J.J., 2006. Spatiotemporal dynamics of human object recognition processing: an integrated high-density electrical mapping and functional imaging study of "closure" processes. *Neuroimage* 29, 605-618.

Seki, K., Nakasato, N., Fujita, S., Hatanaka, K., Kawamura, T., Kanno, A., Yoshimoto, T., 1996. Neuromagnetic evidence that the P100 component of the pattern reversal visual evoked response originates in the bottom of the calcarine fissure. *Electroencephalography and Clinical Neurophysiology/Evoked Potentials Section* 100, 436-442.

Seligman, M. E., 1971. Phobias and preparedness. *Behavior Therapy* 2, 307-320.

Sergent, J., Ohta, S., MacDonald, B., 1992a. Functional neuroanatomy of face and object processing. A positron emission tomography study. *Brain* 115, 15–36.

Sergent, J., Signoret, J. L., 1992b. Varieties of functional deficits in prosopagnosia. *Cerebral Cortex* 2, 375–388.

Serre, T., Kouh, M., Cadieu, C., Knoblich, U., Kreiman, G., Poggio, T., 2005. A theory of object recognition: computations and circuits in the feedforward path of the ventral stream in primate visual cortex AI memo 2005-036. *Massachusetts Institute of Technology*, Cambridge.

Sheline, Y. I., Deanna M. B., Donnelly, J. M. Ollinger, J. M., Snyder, A. Z., Mintun, M. A., 2001. Increased amygdala response to masked emotional faces in depressed subjects resolves with antidepressant treatment: an fMRI study. *Biological Psychiatry* 50, 651-658.

Shi, C., Davis, M., 2001. Visual pathways involved in fear conditioning measured with fear-potentiated startle: behavioral and anatomic studies. *The Journal of Neuroscience* 21, 9844–9855.

Shipp S, 2003. The functional logic of cortico-pulvinar connections. *Philosophical Transactions of the Royal Society of London Series B: Biological Sciences* 358, 1605-1624.

Siegel, M., Donner, T. H., Oostenveld, R., Fries, P., Engel, A. K., 2008. Neuronal synchronization along the dorsal visual pathway reflects the focus of spatial attention. *Neuron* 60, 709–719.

Silvanto, J., Lavie, N., Walsh, V., 2005. Double dissociation of V1 and V5/MT activity in visual awareness. *Cerebral Cortex* 15, 1736–1741.

Singer, W., Gray, C. M., 1995. Visual feature integration and the temporal correlation hypothesis. *Annual Review of Neuroscience* 18, 555–586.

Slagter, H. A., Giesbrecht, B., Kok, A., Weissman, D. H., Kenemans, J. L., Woldorff, M. G., Mangun, G. R., 2007. fMRI evidence for both generalized and specialized components of attentional control. *Brain Research* 1177, 90–102.

Smith, S. D., Most, S. B., Newsome, L. A., Zald, D. H., 2006. An emotion-induced attentional blink elicited by aversively conditioned stimuli. *Emotion* 6, 523-527.

Snow, J. C., Allen, H. A., Rafal, R. D., Humphreys, G. W., 2009. Impaired attentional selection following lesions to human pulvinar: evidence for homology between human and monkey. *Proceedings of the National Academy of Sciences* 106, 4054-4059

Solomon, R. C., 2002. Back to basics: On the very idea of "basic emotions*". Journal for the Theory of Social Behaviour,* 32, 115-144.

Solano-Castiella, E., Anwander, A., Lohmann, G., Weiss, M., Docherty, C., Geyer, S., Reimer, E., Friederici, A.D., Turner, R., 2010. Diffusion tensor imaging segments the human amygdala in vivo. *Neuroimage* 49, 2958–2965.

Spehlmann, R., 1965. The average electrical responses to diffuse and to patterned light in the human. *Electroencephalography and Clinical Neuropsychology* 19, 560-569

Speziom, M. L., Huang, P. -Y. S., Castelli F., Adolphs, R., 2007. Amygdala damage impairs eye contact during conversations with real people. *The Journal of Neuroscience* 27, 3994–3997.

Spinelli, L., Andino, S.G., Lantz, G., Seeck, M., Michel, C.M., 2000. Electromagnetic inverse solutions in anatomically constrained spherical head models. *Brain Topography* 13, 115-125.

Stefanacci, L., Amaral, D.G., 2000. Topographic organization of cortical inputs to the lateral nucleus of the macaque monkey amygdala: a retrograde tracing study. *Journal of Comparative Neurology* 421, 52-79.

Stepniewska, I., Qi, H. X., Kaas, J. H., 1999. Do superior colliculus projection zones in the inferior pulvinar project to MT in primates? *European Journal of Neuroscience* 11, 469–480.

Stepniewska, I., Qi, H. X., Kaas, J. H., 2000. Projections of the superior colliculus to subdivisions of the inferior pulvinar in New World and Old World monkeys. *Visual Neuroscience* 17, 529–549.

Stepniewska, I., 2004. In: The Primate Visual System. *CRC Press,* Florida, 53–80.

Stolarova, M., Keil, A., Moratti, S., 2006. Modulation of the C1 Visual event-related component by conditions stimuli: evidence for sensory plasticity in early affective perception. *Cerebral Cortex* 16, 87-887.

Strange, B. A., Dolan, R. J., 2004. β-Adrenergic modulation of emotional memory-evoked human amygdala and hippocampal responses. *Proceedings of the National Academy of Sciences of the United States of America* 101, 11454-11458.

Strange, B. A., Kroes, M. C., Fan, J., Dolan, R. J., 2010. Emotion causes targeted forgetting of established memories. *Frontiers in behavioral neuroscience* 4, 175.

Suzuki, W. A., 1996. Neuroanatomy of the monkey entorhinal, perirhinal and parahippocampal cortices: organization of cortical inputs and interconnections with amygdala and striatum. *Seminars in Neuroscience* 8. 3-12.

Takada, M., Itoh, K., Yasui, Y., Sugimoto, T., Mizuno, N., 1985. Topographical projections from the posterior thalamic regions to the striatum in the cat, with reference to possible tecto-thalamo-striatal connections. *Experimental Brain Research* 60, 385–396.

Tallon-Baudry, C., Bertrand, O., Delpuech, C., Pernier, J., 1996. Stimulus specificity of phase-locked and non-phase-locked 40 Hz visual responses in human. *The Journal of Neurosciences* 16, 4240–4249.

Tallon-Baudry, C., Bertrand, O., Delpuech, C., Pernier, J., 1997. Oscillatory gamma-band (30–70 Hz) activity induced by a visual search task in humans. *The Journal of Neurosciences* 17, 722–734.

Tallon-Baudry, C., Bertrand, O., 1999. Oscillatory gamma activity in humans and its role in object representation. *Trends in Cognitive Sciences* 3, 151–162.

Tamietto, M., de Gelder, B., 2010. Neural bases of the non-conscious perception of emotional signals *Nature Reviews Neuroscience* 11, 697-709.

Tamietto, M., Pullens, P., de Gelder, B., Weiskrantz, L., Goebel, R., 2012. Subcortical connections to human amygdala and changes following destruction of the visual cortex. *Current Biology* 22, 1449-1445.

Tanaka, J. W., Curran, T., 2001. A neural basis for expert object recognition. *Psychological Science* 12, 43-47.

Tanskanen, T., Näsänen, R., Montez, T., Päällysaho, J., Hari, R., 2005. Face recognition and cortical responses show similar sensitivity to noise spatial frequency. *Cerebral Cortex* 15, 526-534.

Tarr, M. J., Gauthier, I., 2000. FFA: a flexible fusiform area for subordinate-level visual processing automatized by expertise. *Nature Neuroscience* 3, 764-770.

Taulu, S., Simola, J., Kajola, M., 2005. Applications of the signal space separation method. *IEEE Transactions on Signal Processing* 53, 3359-3372.

Taylor, S. E., 1991. Asymmetrical effects of positive and negative events. The mobilization minimization hypothesis. *Psychological Bulletin* 110, 67-85.

Taylor, M. J., Edmonds, G. E., McCarthy, G., Allison, T., 2001. Eyes first! Eye processing develops before face processing in children. *Neuroreport* 12, 1671-1676.

Thierry G., Martin, C. D., Downing, P., Pegna, A. J. 2007. Controlling for interstimulus perceptual variance abolishes N170 face selectivity. *Nature Neuroscience* 10, 505–11.

Tong, F., Nakayama, N., Moscovitch, M., Weinrib, O., Kanwisher, N., 2000. Response properties of the human fusiform face area. *Cognitive Neuropsychology*, 257-280.

Tootell, R. B., Hadjikhani, N. K., Vanduffel, W., Liu, A. K., Mendola, J. D., Sereno, M. I., Dale, A. M., 1998. Functional analysis of primary visual cortex (V1) in humans. *Proceedings of the National Academy of Sciences* 95, 811-817.

Tottenham, N., Tanaka, J. W., Leon, A. C., McCarry, T., Nurse, M., Hare, T. A., Marcus, D.J., Westerlund, A., Casey B.J., Nelson, C., 2009. The NimStim set of facial

expressions: Judgments from untrained research participants. *Psychiatry Research*, 168, 242-249.

Treisman, A., 1998. Feature binding, attention and object perception. *Philosophical Transactions of the Royal Society B: Biological Sciences* 353, 1295-1306.

Trujillo, L. T., Peterson, M. A., Kaszniak, A. W., Allen, J. J., 2005. EEG phase synchrony differences across visual perception conditions may depend on recording and analysis methods. *Clinical Neurophysiology*. 116, 172–189.

Turati, C., 2004. Why Faces Are Not Special to Newborns An Alternative Account of the Face Preference. *Current Directions in Psychological Science* 13, 5-8.

Vaish, A., Grossmann, T., Woodward, A., 2008. Not all emotions are created equal: the negativity bias in social-emotional development. *Psychological Bulletin* 134, 383.

Valenza, E., Simion, F., Cassia, V. M., Umiltà, C., 1996. Face preference at birth. *Journal of Experimental Psychology: Human Perception and Performance* 22, 892.

Vallar, G., 2001. Extrapersonal visual unilateral spatial neglect and its Neuroanatomy. *Neuroimage* 14, 52-58.

van der Schalk, J., Hawk, S. T.; Fischer, A. H., Doosje, B., 2011. Moving faces, looking places: Validation of the Amsterdam Dynamic Facial Expression Set (ADFES). *Emotion* 11, 907-920.

Van Essoni, D.G., Mcclendoni, E., 1994. Multiple processing streams in occipitotemporal visual cortex. *Nature* 371, 151.

Van Hemert, A. M., Den Heijer, M., Vorstenbosch, M., Bolk, J. H., 1995. Detecting psychiatric disorders in medical practice using the General Health Questionnaire. Why do cut-off scores vary? *Psychological Medicine* 25, 165-170.

Van Veen, B. D., van Drongelen, W., Yuchtman, M., Suzuki, A., 1997. Localisation of brain electrical activity via linearly constrained minimum variance spatial filtering. *IEEE Transactions on Biomedical Engineering* 44, 867–880.

Verdon, V., Schwartz, S., Lovblad, K. O., Hauert, C. A., Vuilleumier, P., 2010. Neuroanatomy of hemispatial neglect and its functional components: a study using voxel-based lesion-symptom mapping. *Brain* 133, 880–894.

Vidyasagar, T. R., Pammer, K., 1999. Impaired visual search in dyslexia relates to the role of the magnocellular pathway in attention. *Neuroreport* 10, 1283-1287.

Vincent, J. L., Patel, G. H., Fox, M. D., Snyder, A. Z., Baker, J. T., Van Essen, D. C., Zempel, J. M., Snyder, L. H., Corbetta, M., Raichle, M.E., 2007. Intrinsic functional architecture in the anaesthetized monkey brain. *Nature* 447, 83-86.

Vlamings, P. H., Goffaux, V., Kemner, C., 2009. Is the early modulation of brain activity by fearful facial expressions primarily mediated by coarse low spatial frequency information? *Journal of Vision* 9, 12.

Vogels, R., Orban, G. A., 1996. Coding of stimulus invariances by inferior temporal neurons. *Progress in Brain Research* 112, 195–211.

von Stein, A., Chiang, C., Konig, P., 2000. Top-down processing mediated by interareal synchronization. *Proceedings of the National Academy of Sciences U. S. A.* 97, 14748–14753.

Vuilleumier, P., Schwartz, S., 2001. Emotional facial expressions capture attention. *Neurology* 56,153-158.

Vuilleumier, P., Armony, J. L., Driver, J., Dolan, R. J., 2003. Distinct spatial frequency sensitivities for processing faces and emotional expressions. *Nature Neuroscience* 6, 624-631.

Vuilleumier, P., 2005a. Cognitive science: Staring fear in the face. *Nature* 433, 22-23.

Vuilleumier, P., 2005b. How brains beware: neural mechanisms of emotional attention. *Trends in Cognitive Sciences* 9, 585-594.

Vuilleumier, P., Pourtois, G., 2007. Distributed and interactive brain mechanisms during emotion face perception: evidence from functional neuroimaging. *Neuropsychologia* 45, 174-194.

Wada, Y., Yamamoto, T., 2001. Selective impairment of facial recognition due to a haematoma restricted to the right fusiform and lateral occipital region. *Journal of Neurology, Neurosurgery and Psychiatry* 71, 254–257.

Wagemans, J., Elder, J. H., Kubovy, M., Palmer, S.E., Peterson, M. A., Singh, M., von der Heydt, R., 2012a. A century of Gestalt psychology in visual perception: I. Perceptual grouping and figure-ground organization. *Psychological Bulletin* 138, 1172-1217.

Wagemans, J., Feldman, J., Gepshtein, S., Kimchi, R., Pomerantz, J.R., van der Helm, P.A., van Leeuwen, C., 2012b. A century of Gestalt psychology in visual perception: II. Conceptual and theoretical foundations. *Psychological Bulletin* 138, 1218-1252.

Ward, R., Danziger, S., Bamford, S., 2005. Response to visual threat following damage to the pulvinar. *Current Biology* 15, 571–573.

Weiner, K. S., Grill-Spector, K., 2010. Sparsely-distributed organization of face and limb activations in human ventral temporal cortex. *Neuroimage* 52, 1559–1573

Weiskrantz, L., 1956. Behavioral changes associated with ablation of the amygdaloid complex in monkeys. *Journal of Comparative and Physiological Psychology* 49, 381-391.

Wertheimer, M., 1923. Untersuchungen zur Lehre von der Gestalt, II. *Psychologische Forschung*. 4, 301-350.

Wertheimer, M., Sarris, V., Sekuler, R., 2012. On perceived motion and figural organization. *MIT Press*.

Whalen, P. J., Rauch, S. L., Etcoff, N. L., McInerney, S. C., Lee, M. B., Jenike, M. A., 1998. Masked presentations of emotional facial expressions modulate amygdala activity without explicit knowledge. *The Journal of Neuroscience* 18, 411-418.

Whalen, P. J., Shin, L. M., McInerney, S. C., Fischer, H., Wright, C. I., Rauch, S. L., 2001. A functional MRI study of human amygdala responses to facial expressions of fear versus anger. *Emotion* 1, 70.

Wilke, M., Turchi, J., Smith, K., Mishkin, M., Leopold, D. A., 2010. Pulvinar inactivation disrupts selection of movement plans. *The Journal of Neuroscience* 30, 8650–8659.

Williams, L. M., Liddell, B. J., Kemp, A. H., Bryant, R. A., Meares, R. A., Peduto, A. S., Gordon, E., 2006. Amygdala prefrontal dissociation of subliminal and supraliminal fear. *Human Brain Mapping* 27, 652–661.

Williams, L. M., Gatt, J. M., Schofield, P. R., Olivieri, G., Peduto, A., Gordon, E., 2009. 'Negativity bias' in risk for depression and anxiety: brain–body fear circuitry correlates, 5-HTT-LPR and early life stress. *Neuroimage*, 47, 804-814.

Winston, J. S., Vuilleumier, P., Dolan, R. J., 2003. Effects of low-spatial frequency components of fearful faces on fusiform cortex activity. Current Biology 13, 1824-1829.

Winston, J. S., Henson, R. N. A., Fine-Goulden, M. R., Dolan, R. J., 2004. fMRI-adaptation reveals dissociable neural representations of identity and expression in face perception. *Journal of Neurophysiology* 92, 1830-1839.

Wokke, M. E., Vandenbroucke, A. R., Scholte, H. S., Lamme, V. A., 2013. Confuse your illusion: feedback to early visual cortex contributes to perceptual completion. *Psychological Science* 24, 63–71.

Woldorff, P. T., Matzke, M., Lancaster, J. L., Veeraswarmy, S., Zamarripa, F., Seabolt, M., Glass, T. Gao, J. H., Martin, C. C., Jerabek, P., 1998. Retinotopic organization of early visual spatial attention effects as revealed by PET and ERPs. *Human Brain Mapping* 5, 280-286.

Wong, P., Collins, C. E., Baldwin, M. K., Kaas, J. H., 2009. Cortical connections of the visual pulvinar complex in prosimian galagos (Otolemur garnetti). *Journal of Comparative Neurology* 517, 493–511.

Wright, C. I., Fischer, H., Whalen, P. J., McInerney, S. C., Shin, L. M., Rauch, S. L., 2001. Differential prefrontal cortex and amygdala habituation to repeatedly presented emotional stimuli. *Neuroreport* 12, 379-383.

Wronka, E., Walentowska, W., 2011. Attention modulates emotional expression processing. *Psychophysiology* 48, 10471056.

Xu, X., Ichida, J. M., Allison, J. D., Boyd, J. D., Bonds, A. B., Casagrande, V. A., 2001. A comparison of koniocellular, magnocellular and parvocellular receptive field properties in the lateral geniculate nucleus of the owl monkey (Aotus trivirgatus). *The Journal of Physiology* 531, 203-218.

Xu, Y., Liu, J., Kanwisher, N., 2005. The M170 is selective for faces, not for expertise. *Neuropsychologia* 43, 588-597.

Yukie, M., Iwai, E., 1981. Direct projection from the dorsal lateral geniculate nucleus to the prestriate cortex in macaque monkeys. Journal of Comparative *Neurology* 201, 81-97.

Zald, D.H., 2003. The human amygdala and the emotional evaluation of sensory stimuli. *Brain Research Reviews* 41, 88-123.

Zeki, S., Watson, J. D., Lueck, C. J., Friston, K. J., Kennard, C., Frackowiak, R.S., 1991. A direct demonstration of functional specialization in human visual cortex. *The Journal of neuroscience* 11, 641-649.

Zeki, S., 1996. Brain activity related to the perception of illusory contours. *Neuroimage* 3, 104-108.